COMBUSTION MODELLING OF PULVERISED COAL BOILER FURNACES FUELLED WITH ESKOM COALS

Niels Wilhelm Eichhorn

A dissertation submitted to the Faculty of Engineering, University of the Witwatersrand, Johannesburg, in fulfilment of the requirements for the degree of Master in Science in Engineering

Johannesburg

September 1998

DECLARATION

This dissertation is the original and independent work of the author except where acknowledged otherwise in the text. It is being submitted for the degree of Master of Science in Engineering at the University of the Witwatersrand, Johannesburg. It has not been submitted before for any degree or examination to any other University.

Niels Wilhelm Eichhorn

September 1998

ABSTRACT

Combustion modelling of utility furnace chambers provides a cost efficient means to extrapolate the combustion behaviour of pulverised fuel (pf) as determined from drop tube furnace (DTF) experiments to full scale plant by making use of computational fluid dynamics (CFD). The combustion model will be used to assimilate essential information for the evaluation and prediction of the effect of

- changing coal feedstocks
- proposed operational changes
- boiler modifications.

TRI commissioned a DTF in 1989 which has to date been primarily used for the comparative characterisation of coals in terms of combustion behaviour. An analysis of the DTF results allows the determination of certain combustion parameters used to define a mathematical model describing the rate at which the combustion reaction takes place. This model has been incorporated into a reactor model which can simulate the processes occurring in the furnace region of a boiler, thereby allowing the extrapolation of the DTF determined combustion assessment to the full scale. This provides information about combustion conditions in the boiler which in turn are used in the evaluation of the furnace performance.

Extensive furnace testwork of one of Eskom's wall fired plant (Hendrina Unit 9) during 1996, intended to validate the model for the applications outlined above, included the measurement of :

- gas temperatures
- O_2, CO_2, CO, NO_x and SO_2 concentrations
- residence time distributions
- combustible matter in combustion residues extracted from the furnace
- furnace heat fluxes.

The coal used during the tests was sampled and subjected to a series of chemical and other lab-scale analyses to determine the following :

- physical properties
- composition
- devolatilisation properties
- combustion properties

The same furnace was modelled using the University of Stuttgart's AIOLOS combustion code, the results of which are compared with the measured data.

A DTF derived combustion assessment of a coal sampled from the same site but from a different part of the beneficiation plant, which was found to burn differently, was subsequently used in a further simulation to assess the sensitivity of the model to char combustion rate data. The results of these predictions are compared to the predictions of the validation simulation.

It was found that the model produces results that compare well with the measured data. Furthermore, the model was found to be sufficiently sensitive to reactivity parameters of the coal. The model has thereby demonstrated that it can be used in the envisaged application of extrapolating DTF reactivity assessments to full scale plant. In using the model, it has become apparent that the evaluations of furnace modifications and assessments of boiler operation lie well within the capabilities of the model.

ACKNOWLEDGEMENTS

The author wishes to express his sincere appreciation to all Eskom staff at Hendrina Power Station (viz. Pieter Paynter, Leon van Wyk, Louis Buckle, the staff from Performance and Testing, the operating staff as well as Hendrina Management) for providing Hendrina as a test site, for contributing to the funding required for these tests and for helping to run them.

The author wishes further to thank the University of Stuttgart's *Institut für Verfahrenstechnik und Dampfkesselwesen (IVD)* - viz. Dr.-Ing. Uwe Schnell and Dipl.-Ing. Benedetto Risio for the extensive support in setting up and running the model of the Hendrina furnace and the staff of Eskom TRI, Energy Technologies (viz. the DTF team, Priven Rajoo, Dr Mark Van der Riet, Chad Botha, Dave Fong and Mike Blenkinsop) for helping making this work possible.

Many thanks also to Brian Pitman (GED), the Coal Combustion Steering Committee and Technical Focus Area Working Group and Eskom Research Management as well as Prof. David Glasser and Dr Dianne Hildebrandt of the University of the Witwatersrand for their support and guidance in this project.

I would like to dedicate this thesis to my family and fiancé, Véronique, whose patience and moral support made this work possible.

CONTENTS page

LIST OF FIGURES

	FIGURE *(continued)*	page

LIST OF TABLES

LIST OF SYMBOLS

T	: temperature
T_g	: temperature of furnace gas
T_c	: wall temperature of the suction channel
t	: time
k	: thermal conductivity
k_{devol}	: devolatilisation reaction rate coefficient
k_{char}	: char combustion reaction rate coefficient
m	: mass
dp	: assumed particle diameter
d	: diameter
x	: distance
F	: volumetric flow
P	: pressure
v	: velocity
g	: gravitational constant (9.81 m/s^2)
A	: ash content
$A_{particle}$	: assumed particle surface area
A_r	: area available for radiative heat transfer
A_c	: area available for convective heat transfer
VM	: volatile matter content of char (fractional)
V_x	: extent of devolatilisation
E_a	: activation energy
R	: Universal Gas Constant
Cp	: particle heat capacity
Nu	: Nusselt number
CE	: combustion extent
D	: diffusional coefficient
n_B	: swelling index
Δh	: enthalpy of formation
S_Φ	: source term of field variable
u	: cartesian component of velocity in the x-direction
KE_{turb}	: kinetic turbulent energy
C_μ	: turbulent viscosity model constant
X, Y	: parameters of hydrocarbon description C_XH_Y

LIST OF GREEK SYMBOLS

λ : convective heat exhange coeffiecient

ε : emissivity

α : convective heat transfer coefficient

σ : Stefan Boltzmann constant

τ_i : time constant i

τ_d : dead time

ρ : density

μ : viscosity

Φ : general field variable

σ_Φ : stress associated with field variable Φ

1. INTRODUCTION

Eskom utilised approximately 70 million tons of coal in 1995 in pulverised coal boilers. As coal usage increases and reserves are depleted, Eskom will face changing feedstocks. It is accepted that the conventional proximate analysis, calorific value, ash and petrographic analyses alone cannot adequately quantify the performance of steam raising coals[1]. It is therefore difficult to predict the combustion behaviour of a coal without some other means of combustion behaviour assessment or prior operating experience with the coal in question.

In order to assess a coal's combustion behaviour, TRI commissioned a Drop Tube Furnace (DTF) in 1989 and has to date assimilated an extensive database of physical-, chemical- and combustion behaviour information of Eskom and other steaming coals. The combustion behaviour information of a coal includes a description for the rate of char combustion which, under pulverised fuel (pf) firing conditions, is the slowest of the combustion reactions. Ignition properties are estimated from devolatilisation characteristics.

DTF coal characterisations have been mainly used for the comparative assessment of the combustion behaviour of coals, with one coal generally being considered a reference coal whose combustion performance was considered acceptable.

A number of attempts have been made to correlate the DTF to full scale plant, and while the DTF can reproduce most of the combustion conditions typical in the full scale plant, this requires detailed measurements of conditions in the boiler, which can only be obtained from experiments on full-scale plant. These are both costly and time-consuming. However, the rapid development of numerical methods, physical- and chemical sub-models and computer hardware in the last 10 to 15 years has made computational fluid dynamics (cfd) based methods valuable for the engineering assessment of furnace processes. These processes include the combustion of pf and the formation of nitrogen pollutants.

This report presents the ADVANCED SIMULATION CODE FOR FLOWS IN COMBUSTION SYTEM... ...LOS), for the analysis of the flow field, combustion, heat transfer and nitrogen pollutants in multi-burner pulverised coal furnaces to extrapolate DTF results to full scale plant to provide essential information for the evaluation of

- changing coal feedstocks
- operational changes for optimisation purposes
- boiler modifications for NOx reduction or optimised heat release.

2. METHODOLOGY AND THEORETICAL BACKGROUND

2.1 OVERVIEW

2.1.1 THEORETICAL OVERVIEW

Calculation based methods have been used in the design of fossil fuel fired combustion chambers to refine, to some extent, the design and operation optimisation experiences since the early 20th century. Particularly the advent and rapid development of computer technology has spurred the evolution of calculation based simulation tools. These are intended to help the engineer in designing and diagnosing combustion plant to improve combustor efficiencies and further, as a broader spectrum of fossil fuels is being considered, the capability of combustion plant to burn certain fuels. A number of models are available, some of which have particlular applications. An attempt has been made to broadly classify these (Khalil[43], 1982) in terms of the information they yield on their application.

ZERO Dimensional Models

These models are used to predict average combustor heat transfer, furnace efficiency and other overall averaged properties such as wall emissivity, gas emissivity, gas composition and combustor temperature .

ONE Dimensional Models

These models allow the prediction of the aforementioned combustion environment properties in length or time. This type of model is restricted to flows with little or no recirculation although some recirculation effect may be taken into account by considering a combination of plug flow and well stirred reactors.

TWO and THREE Dimensional models

These models allow the determination of the spatial distribution of fluid and energy flow through the combustion system. Most models incorporate a variety of submodels for turbulence, reaction and heat transfer. The validity of these sub-models to various furnace and combustion chamber configurations has been assessed with

comparisons with experiments. Results from the above models require critical assessment since the models and their interactions are complex and relevant experimental data is limited. The prediction of trends of the effect of operational variables on the overall combustor performance has however improved dramatically with the development of computer technology which has provided the possibility to improve certain submodels, particularly the turbulence submodel.

2.1.2 OVERVIEW OF METHODOLOGY

Extensive testing of Hendrina's Unit 9 furnace was performed during February 1998 to obtain a set of furnace condition data that could be used to validate the AIOLOS advanced three dimensional combustion model for Eskom's coal fired plant. The furnace testwork included the measurement of :

- gas temperatures
- O_2, CO_2, CO, NO_x and SO_2 concentrations
- combustible matter in combustion residues extracted from the furnace
- residence time distributions
- furnace heat fluxes

Hendrina's boiler 9 coal feedstock was extensively sampled during the furnace tests, and characterised and analysed using the DTF and TRI's coal laboratory. The results of these tests, together with furnace design and operation information, were used to set up the AIOLOS combustion model, which was then run at the University of Stuttgart. The configuration of the model for the furnace in question was used to train an Eskom staff member in the use thereof, while the model predictions were compared to the measured data.

A DTF derived combustion assessment of a coal sampled from the same site but from a different part of the beneficiation plant, which was found to burn differently, was subsequently used in a further simulation to assess the sensitivity of the model to char combustion rate data. The results of these predictions are compared to the predictions of the validation simulation.

2.2 FURNACE TESTING

2.2.1 SELECTION OF BOILER TEST SITE

The reason for selecting Hendrina power station was that the furnace is relatively small (200 MWe) compared to the furnaces of Eskom's >500 MWe boilers, and hence the furnace could be probed to sufficient depth to obtain a set of data that could validate the AIOLOS combustion code.

2.2.2 FURNACE PROBING

Probing of the boiler's combustion chamber through various observation ports, situated on the side wall of the furnace, was performed by making use of water cooled suction probes ranging in length from 6 to 12m. The probes were used to measure furnace gas temperatures, O_2-, CO-, CO_2-, NOx- and SO_2-concentrations, as well as extracting combustion residue samples at 0.5m intervals up to a furnace depth of around 6m, depending on what probe could be used at a particular access point. Figure 1 shows a schematic of the testing equipment used.

2.2.3 FURNACE GAS TEMPERATURE MEASUREMENT

Furnace gas temperatures are ideally directly measured using R-type (Platinum/Platinum -10% Rhodium) thermocouples supported by the aforementioned water cooled probes and protected at the junction from radiative heat exchange by a double ceramic sheath. Hot gas is drawn over the shielded junction at velocities high enough to render the temperature measurement independent of gas velocity (Land et al[2] (1954)). This means of measurement did however fail frequently during the testing as a result of slag deposits in the ceramic shield, which in time blocked the flow of the hot gas. This condition became evident when the measured furnace temperature suddenly dropped several hundred degrees Celsius. Once evident, measurements were discarded, fouled components removed and replaced.

An indirect gas temperature measurement method (Idiatulin[3] et al (1977)) was subsequently adopted, which uses three axially aligned K-Type (Nickel / Chrome-Nickel) thermocouples situated in the suction probe (see Figure 2).

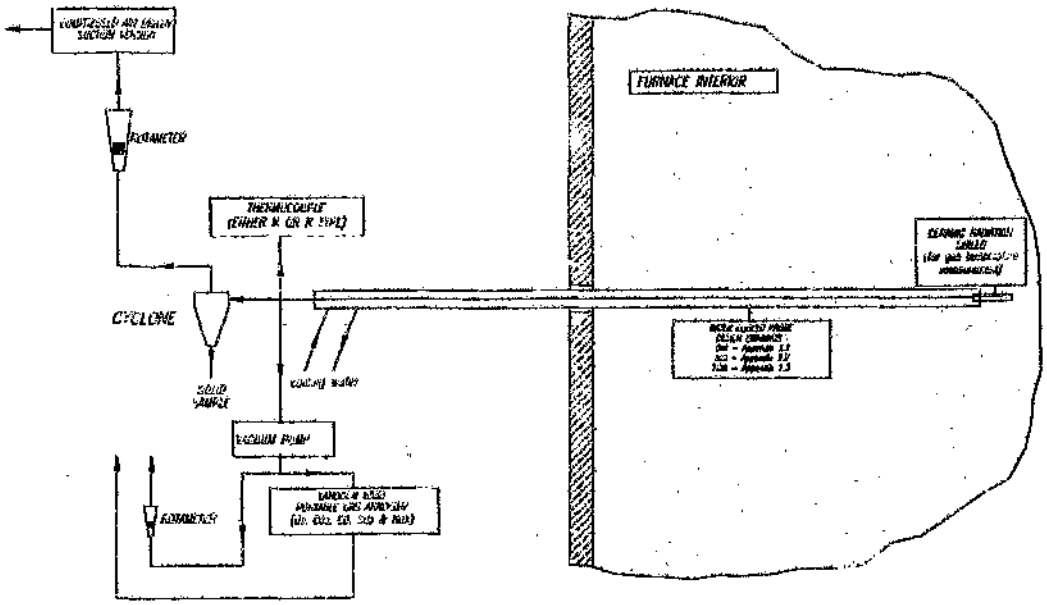

Figure 1 : ***Schematic of Furnace Probing Equipment (A4 copy of Figure 1 is attached in Appendix 1.1)***

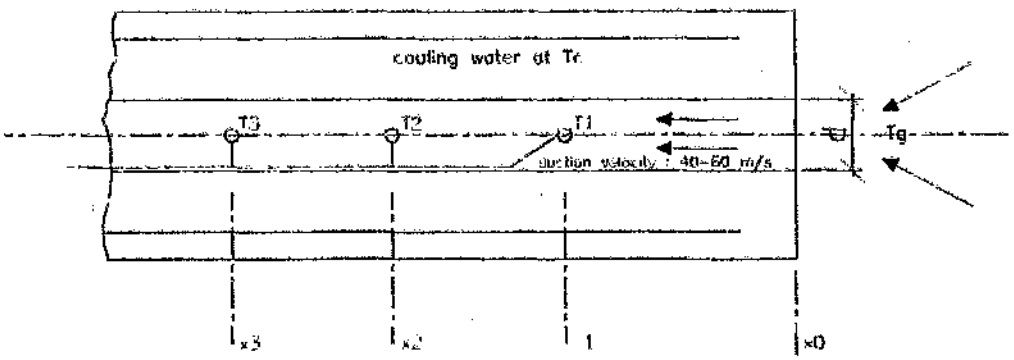

Figure 2 : ***Arrangement of Thermocouples in Suction Probe***

Because the gas sample is quenched the instant it enters the probe (resulting in molten ash particles solidifying before they adhere to any probe surfaces) and because the probe surfaces are not as conducive to slag deposits forming on them as the ceramic surfaces are, this method of temperature measurement is considerably less problematic. However, the inlet gas temperature needs to be extrapolated from the temperatures measured using the thermocouples. The extrapolated temperature is determined as follows :

$$T_g = T_{x_i} + \frac{\varepsilon \cdot \sigma}{\alpha} \cdot \left[\left(T_{x_i} \right)^4 - T_c^4 \right] \qquad (1)$$

$$i = 1,2,3$$

where

ε = emissivity of the thermocouple junction

α = convective heat transfer coefficient between the gas and the thermocouple junction

σ = Stefan-Boltzmann constant

The wall temperature of the suction channel, T_c, can be determined with sufficient accuracy by measurement with the thermocouple without suction, when the thermocouple assumes the temperature of the surrounding walls. It was further found by the developers of this method that at a distance of x = 2.5 d from the probe tip, the radiation from the furnace no longer affects the thermocouple. An extrapolated temperature can be determined by solving equation (1) simultaneously with two of the three thermocouple readings, assuming that ε remained constant, which can be reasonably assumed, as the temperature measured using the three thermocouples varied by only 200 - 400°C. The suction velocity through the probe (40-60 m/s) was sufficiently high to ensure turbent flow past the thermocouples and hence α could be considered constant.

This temperature measurement system did however only function well when the thermocouples were in equilibrium and the furnace temperature remained reasonably constant over approx. 3s. When the three extrapolated temperatures differed significantly , the measurements were discarded. For the purpose of this investigation, a temperature variance of more than 20°C between the maximum and minimum predicted value was considered significant. Further analysis would however have to be performed to identify a steady state condition of the thermocouples.

Figure 3 shows a graph of the extrapolated temperatures as a function of furnace depth and time since start of measurement. Note the fluctuations of up to 70°C in gas temperature at a single furnace depth.

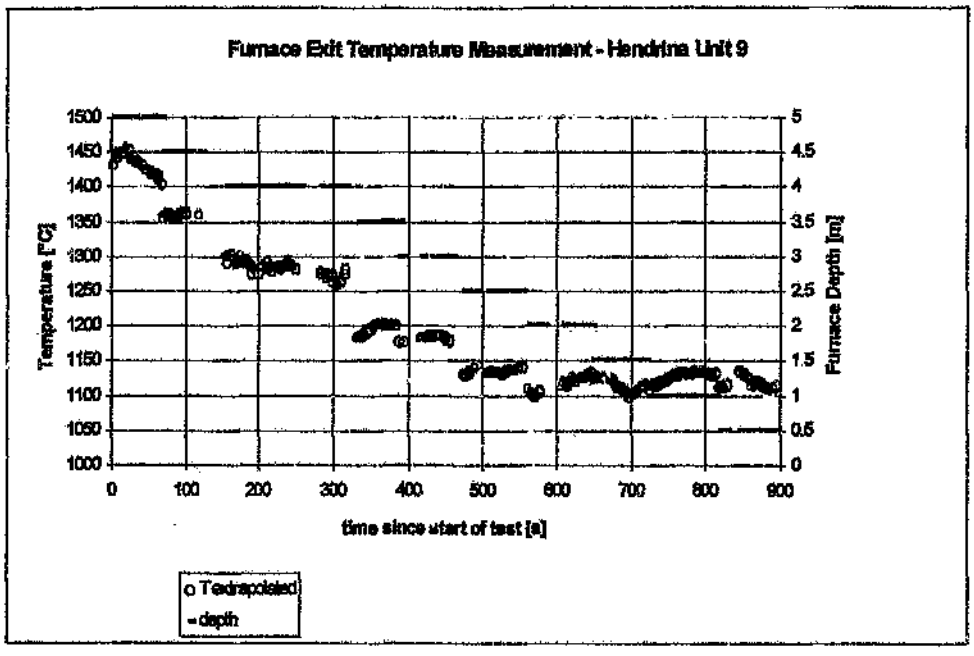

Figure 3 : *Furnace Gas Temperature Measurements*

2.2.4 GAS SPECIES CONCENTRATION MEASUREMENT

A furnace gas sample was drawn from the suction stream of the water cooled probe, as shown in Figure 1, using a suction pump. A portion of this stream was then continuously passed through a membrane dryer before entering the Landcom 6500 portable flue gas analyser. This flue gas analyser uses dedicated electrochemical cells for the determination of the following gases :

GAS	RANGE	ACCURACY	RESOLUTION
O_2	0 - 25% vol.	± 1%	± 0.1% vol.
CO (low range)	0 - 2000 ppm	± 4%	± 1 ppm
CO (high range)	0 - 40000 ppm	-	± 100 ppm
SO_2	0 - 2000 ppm	± 4%	± 1 ppm
NO	0 - 1000 ppm	± 4%	± 1 ppm
CO_2	calculated	-	-

The analyser was calibrated using prepared standard certified sample gases prior to every test. The standard gases used were as follows :

GAS	COMPOSITION
O_2	5.20%, balance N_2
CO (low range)	120 ppm, 14% CO_2, balance N_2
CO (high range)	not calibrated
SO_2	768 ppm, balance N_2
NO	474 ppm, balance N_2

2.2.5 RESIDENCE TIME DISTRIBUTION MEASUREMENTS

For the purpose of this investigation, the residence time is defined as the time a pf particle has spent in the furnace region of the boiler. Due to the complex turbulent flowfield in the furnace, particularly in the burner regions, identical pf particles may spend different times in the furnace depending on the flow path they have taken through it. The residence time distribution (RTD) is by definition the statistical distribution of residence times that pf particles entering the furnace through a particular burner may spend in the furnace. The furnace exit plane does however have the s cross section as the furnace and the flue passing through it cannot be assumed to be perfectly mixed. In view of this, the RTD's from each of the three burner rows to a number of points on the furnace exit plane were determined.

It was however not practical to measure the RTD of a batch of particles that simultaneously enter the furnace through a burner, because this would require that the particle be identifiable based on some property unique to the batch in question and furthermore, the identification would have to be made at very short time increments throughout the test.

Because of the small size of pf particles (75% <75μm), it can be reasonably assumed that the RTD of particles will not differ much from the RTD of a gas molecule. Indeed, the free fall velocity of a 50μm particle would be only about 0.05 m/s compared to the gas velocities of around 10m/s at furnace exit.

Experiments with various tracers during a previous furnace RTD investigation at Matimba Power Station (Blenkinsop et al[4]) showed that sulphur powder could be used. A 5kg charge of sulphur was injected very rapidly (using air cannons) into the primary air / pf stream just before the burner inlet of one burner. The injected sulphur was sufficient to increase the furnace exit SO_2 concentration tenfold.

The sulphur sublimes at around 440°C, and then oxidises when in the gas phase. The rate of formation of SO_2 from the sulphur powder is therefore similar to the combustion rates of volatile products from the coal (diffusion limited), and for the purpose of the RTD estimations, was considered to occur instantaneously. Figure 4 shows a schematic of the testing equipment used.

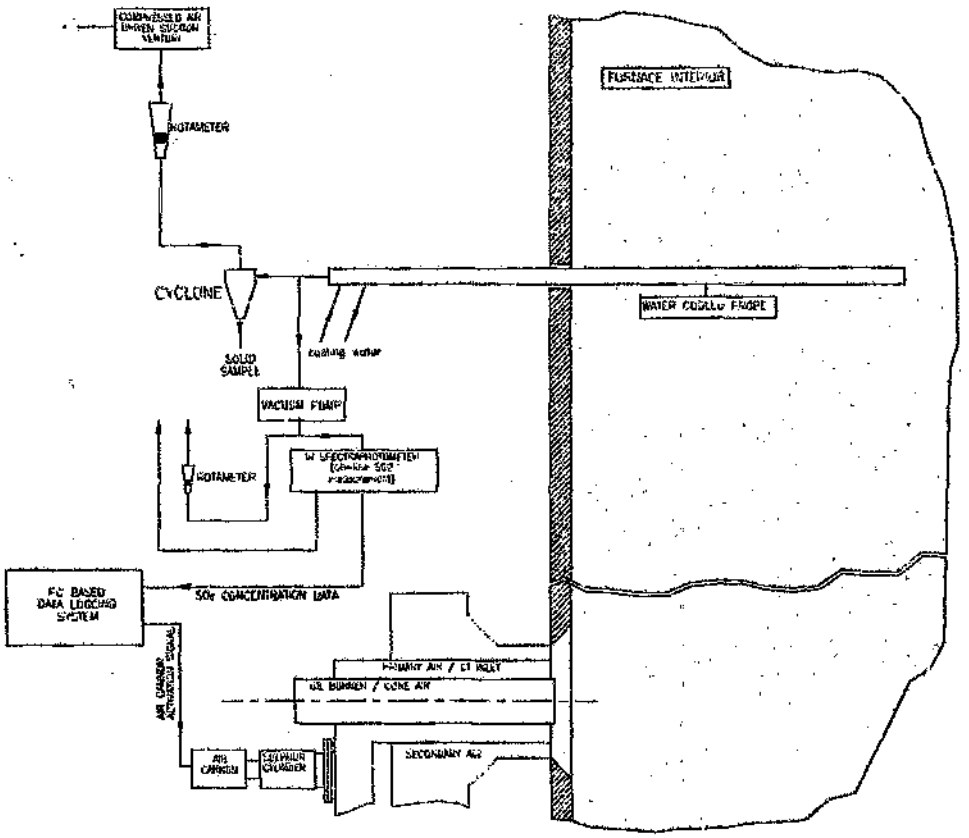

Figure 4 : ***Schematic of RTD Measurement Equipment***
(A4 copy of Figure 4 is attached in Appendix 1.1)

The SO_2 concentration vs. time profile measured at furnace exit could therefore be considered to be a RTD of the combined furnace and probing system given an instantaneous SO_2 source just in front of the burners where sulphur was being injected.

Plot of experimental overall response to sulphur tracer injection

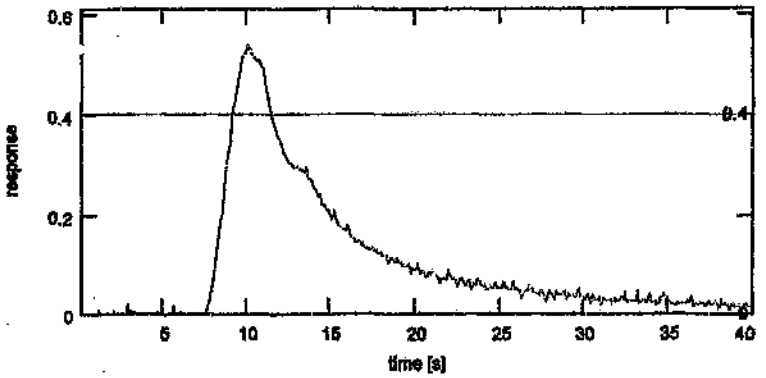

Figure 5 : ***Graph of overall RTD Response***

The suction pyrometer used to sample the furnace exit does, however, have it's own RTD (refer to Figure 6), necessitating that the overall measured RTD (refer to Figure 5) be corrected. In order to perform this correction, the RTD of the probe had to be determined. This was done measuring the SO_2 concentration vs. time profile through the probe given identical sampling conditions with a SO_2 sample being injected into the sample stream just in front of the probe using an injection device designed to disrupt the sample stream as little as possible. The design drawing of this device is presented in Appendix 1.1.5.

Plot of experimental probe response to SO_2 tracer injection

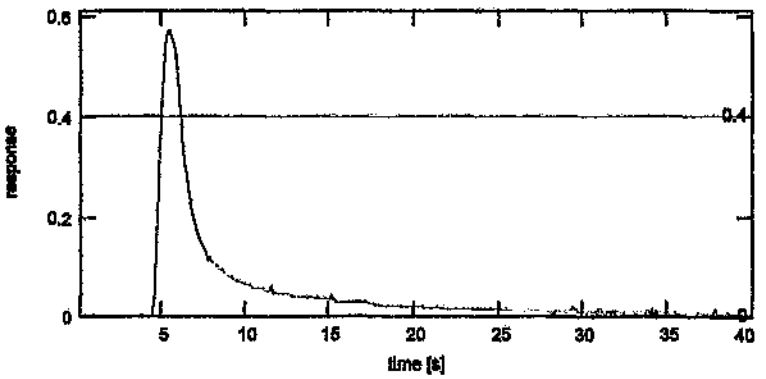

Figure 6 : ***Graph of Probe RTD Response***

It was found that the experimentally determined concentration profiles determined by the tracer experiments could be satisfactorily described by fitting the data to a curve describing the response of a second order system with a lag or dead time to an impulse disturbance. The general form of the function in the time domain is given by :

$$f(t) = C \cdot \left(\frac{1}{\tau_1 - \tau_2}\right) \cdot \left[e^{\left[\tau_1 \cdot (t - \tau_d)\right]} - e^{\left[\tau_2 \cdot (t - \tau_d)\right]} \right] \cdot \Phi\,(t - \tau_d) \qquad (2)$$

where

τ_d = dead time

τ_1 = time constant 1

τ_2 = time constant 2

C = constant required to normalise the RTD so that $\int_0^\infty f(t)\,dt = 1$

$\Phi\,(t - \tau_d)$ = Heaviside function, i.e. $\Phi = 0$ for $t < \tau_d$; $\Phi = 1$ for $t \geq \tau_d$

The effect of the RTD on any disturbance (e.g. the tracer injection) entering the otherwise steady state system (i.e. with constant inputs and outputs) can be described by the convolution integral (Levenspiel[6] (1972)).

$$C_{out}(t) = \int_0^t C_{in}(t - t') \cdot E_o(t')\,dt' \qquad (3)$$

where

$E_o(t)$ = RTD of the system (i.e. the furnace and probe combinatio

$C_{in}(t)$ = time domain description of the disturbance entering system (i.e. the sulphur injection resulting in a virtually instantaneous source of SO_2 at the burner mouth)

$C_{out}(t)$ = time domain description of a system output (e.g. SO_2) at the outlet of the system (i.e. the furnace exit)

The overall RTD, $E_o(t)$, of the furnace and probe combination can be considered as two independent systems in series, each with it's own RTD. This system is illustrated in Figure 7.

If the system input ($C_{in}(t)$) is given, the outlet concentration vs. time distribution function ($C_{out}(t)$) and the RTD of the probing system ($E_{probe}(t)$) is measured, then the RTD of the first system, i.e. the furnace ($E_{furnace}(t)$), can be determined.

Equation (4) is obtained by Laplace transforming equation (3).

$$\overline{C_{out}}(s) = \overline{C_{in}}(s) * \overline{E_o}(s) \qquad (4)$$

The reason for implying that the RTD of the probing system ($E_{probe}(t)$) can be measured is that given an instant SO_2 injection at the probe inlet, the SO_2 concentration vs. time profile at the outlet has identical distribution and dead time characteristics as the RTD of the probing system because the Laplace transform of the impulse input is unity.

Levenspiel[6] (1972) refers to C_{out} as the convolution of E_o with C_{in}. C_{out} is, however, also the convolution of the Laplace domain description of the furnace output with E_{probe}, which in turn is the convolution of $E_{furnace}$ with C_{in}.

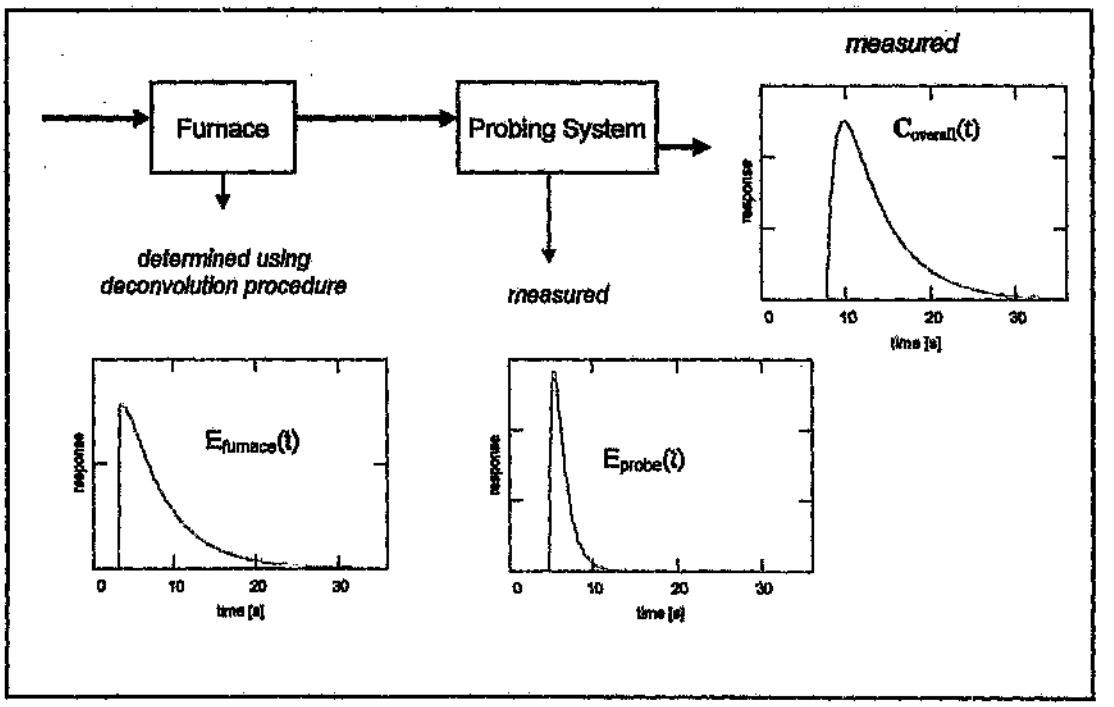

Figure 7 : *Modification of an impulse tracer signal , $C_{in}(t)$, on passing through two systems in series*

The Laplace domain description of the entire system is therefore :

$$\overline{C_{out}}(s) = \overline{C_{in}}(s) * \overline{E_{furnace}}(s) * \overline{E_{probe}}(s) \qquad (5)$$

The mathematical properties of the convolution operator allow a deconvolution to obtain a Laplace domain description of $E_{furnace}$. The convolution operation becomes a multiplication in the Laplace domain, while a deconvolution a division operation.

$$\overline{E_{furnace}}(s) = \frac{\overline{C_{out}}(s)}{\left(\overline{C_{in}}(s)\cdot\overline{E_{probe}}(s)\right)} \qquad (6)$$

In the Laplace domain, equation (2), the general form of the time domain distribution, becomes :

$$\overline{F}(s) = C\cdot\frac{e^{-\tau_d\cdot s}}{\left(1+\tau_1\cdot s\right)\cdot\left(1+\tau_2\cdot s\right)} \qquad (7)$$

Similar expressions in the Laplace domain for the time domain overall (denoted by the subscript : *overall*) and probe (denoted by the subscript : *probe*) responses can be obtained :

$$\overline{E_{probe}}(s) = C_{probe}\cdot\frac{e^{-\tau_{d\,probe}\cdot s}}{\left(1+\tau_{probe_1}\cdot s\right)\cdot\left(1+\tau_{probe_2}\cdot s\right)} \qquad (8)$$

$$\overline{C_{out}}(s) = C_{overall}\cdot\frac{e^{-\tau_{overall\ d}\cdot s}}{\left(1+\tau_{overall_1}\cdot s\right)\cdot\left(1+\tau_{overall_2}\cdot s\right)} \qquad (9)$$

The Laplace transform of the system input, which for the purpose of this investigation was considered an impulse input, is given by :

$$\overline{C_{in}}(s) = 1 \qquad (10)$$

Expressions (8), (9) and (10) can now be substituted into (6) and by taking the inverse Laplace transform of the resulting expression, the RTD of the furnace ($E_{furnace}(t)$) in the time domain can be obtained :

$$E_{furnace}(t) = \frac{C_{overall}}{C_{probe}} \cdot \left[A \cdot e^{\tau_{overall\ 1} \cdot (t - \tau_{furnace})} + B \cdot e^{\tau_{overall\ 2} \cdot (t - \tau_{furnace})} \right] \cdot \Phi\left(t - \tau_d\right) \qquad (11)$$

where

$$A = \frac{\left(\tau_{overall\ 1} - \tau_{probe\ 1}\right) \cdot \left(\tau_{overall\ 1} - \tau_{probe\ 2}\right)}{\left(\tau_{overall\ 1} - \tau_{overall\ 2}\right)}$$

$$B = \frac{\left(\tau_{overall\ 2} - \tau_{probe\ 1}\right) \cdot \left(\tau_{overall\ 2} - \tau_{probe\ 2}\right)}{\left(\tau_{overall\ 2} - \tau_{overall\ 1}\right)}$$

$$\tau_{furnace} = \tau_{overall\ d} - \tau_{probe\ d}$$

2.2.6 HEAT FLUX MEASUREMENTS

25 heat flux probes were installed into the left wall of the furnace and monitored on-line during the testing period. Figure 8 shows a schematic of a heat flux probe mounted in the furnace wall. The linearised temperature transmitters output a 4-20 mA signal to a centrally situated PC based data logger. The temperature measurements as well as the calculated heat fluxes were logged at 1 minute intervals. Figure 9 shows the positions of the heat flux probes

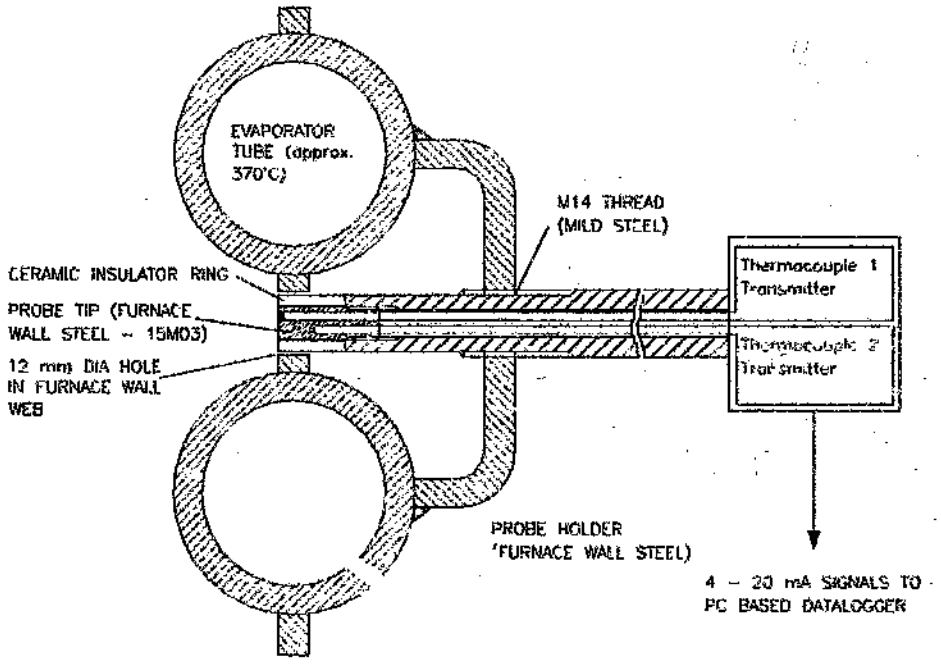

Figure 8 : *Schematic of Heat Flux Probe*

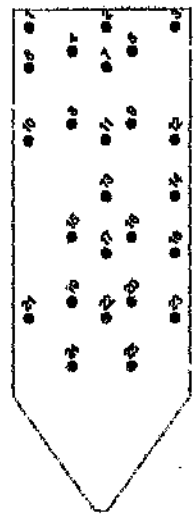

Figure 9 : *Position of Heat Flux Probes on Hendrina Unit 9's Left Furnace Wall*

The heat flux can be calculated from the temperature measurements obtained from the thermocouples. Let the temperature of the front and rear thermocouples be denoted by T_{front} and T_{rear} respectively. The heat flux through the probe tip is given by :

$$q = \frac{k}{x}\left(T_{front} - T_{rear}\right) \qquad (12)$$

where k = thermal conductivity of 15MO3 steel

x = distance between the thermocouple beads

Figure 10 shows the thermal conductivity of the furnace wall steel (15MO3) as a function of metal temperature.

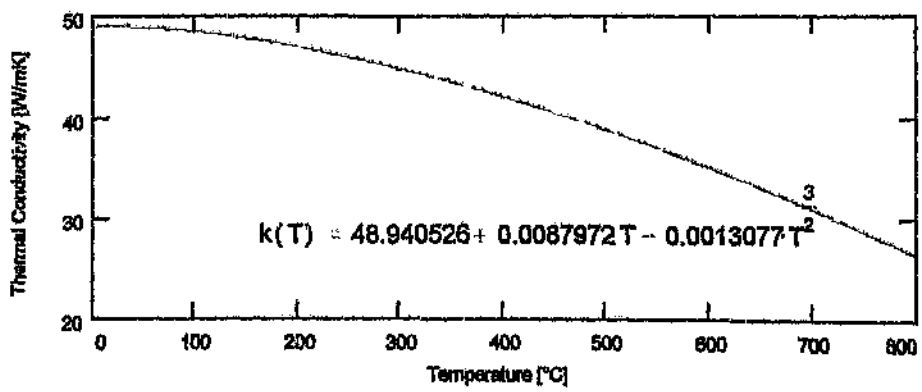

Figure 10 : *Thermal Conductivity of 15MO3*

Since the temperature difference between the thermocouples did not vary dramatically, an average thermal conductivity could be assumed. The average thermal conductivity was determined as follows :

$$k_{ave}(T_{front}, T_{rear}) = \frac{1}{T_{front} - T_{rear}} \int_{T_{rear}}^{T_{front}} k(T)\, dT \qquad (13)$$

Figure 11 shows a typical 24 hour heat flux and temperature measurement log obtained during the furnace tests. Note the effect of wall blowing just after 02h00 and load changes from about 07h00 onwards.

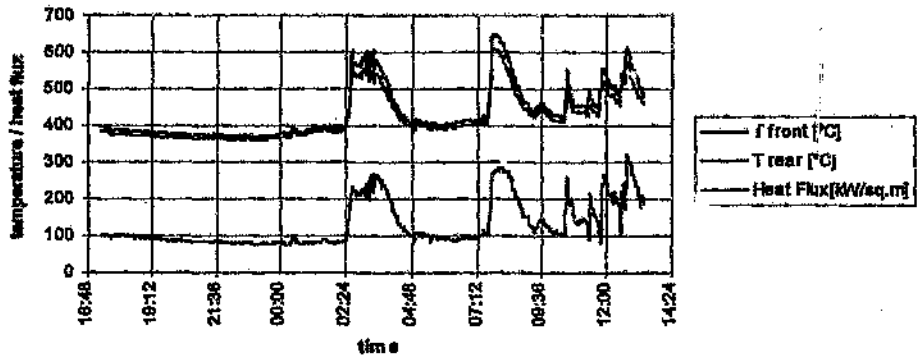

Figure 11 : ***Heat Flux / Temperature Log***

2.3 COAL CHARACTERISATION

2.3.1 COAL SAMPLING AND OVERVIEW OF BASIC ANALYSES PERFORMED

Raw coal from the mill feeder systems of all operational mills was sampled on each day that furnace testwork was performed and composited to form a daily sample. Each sample was subjected to :

- moisture analysis (total and inherent)
- proximate analysis
- ultimate analysis
- calorific value determination.

The samples were subsequently composited to form a representative sample for the entire furnace testing program. This sample, hereafter referred to as '*R.C. Composite*', was analysed as follows :

- moisture analysis (total and inherent)
- proximate analysis
- ultimate analysis
- calorific value determination
- mineral matter analysis
- Hardgrove Index
- Abrasiveness Index
- ash fusion temperature determinations
- devolatilisation tests (using DTF)
- char combustion tests (using DTF)

Pulverised coal from each operational mill was sampled isokinetically on various days during the furnace tests. The following analyses were performed :

- moisture analysis (inherent)
- proximate analysis
- ultimate analysis
- calorific value determination
- particle size analyses

All analyses were performed according to standard Eskom methods. Detailed procedures of the DTF based devolatilisation and char combustion tests are described in 2.3.3 and 2.3.4 below.

2.3.2 DESCRIPTION OF THE DROP TUBE FURNACE (DTF)

The DTF is an electrically heated vertical tube reactor, in which coal particles are exposed to a controlled temperature and oxygen concentration environment for variable time periods in a hot laminar flow gas stream. The feed gas is preheated and enters the DTF's 70 mm ID alumina ceramic tube through a ceramic honeycomb flow straightener at a flowrate of approximately 20 l/min (STP). The reactor tube is heated by silicon carbide elements, which are controlled by dual thermocouples situated at the outside of the reactor tube wall. In furnace gas temperatures typically range between 700°C and 1400°C. About 1 g of dry coal/char sample is fed into the reactor over a period of about 10 minutes through a water cooled injection probe, the tip of which is situated approximately 450 mm from the top of the reactor tube. The burning particles are carried in the combustion gas axially down the furnace, the length of the reaction zone being variable up to 122 cm. The free fall velocity of the particles ranges between 0.01m/s for a particle of approx. 25 µm to 0.04 m/s for a particle of approx. 48 µm, while the gas velocity through the reactor is about 0.4 m/s, depending on the reaction temperature. Partially reacted particles are caught in a water cooled collection probe, which quenches combustion. Field[6] (1969) found the end effects of the feeder and collector combined to be small. Combustible matter analyses on the partially combusted product allow the determination of the extents of reaction, which vary according to combustion conditions and residence times. The DTF thus allows the control of three important variables of the combustion process, namely temperature, oxygen concentration and time. Based on the extent of combustion with respect to these variables, the kinetic behaviour during combustion of a particular coal can be quantified for a typical boiler combustion environment.

A schematic of the DTF is presented in Figure 12.

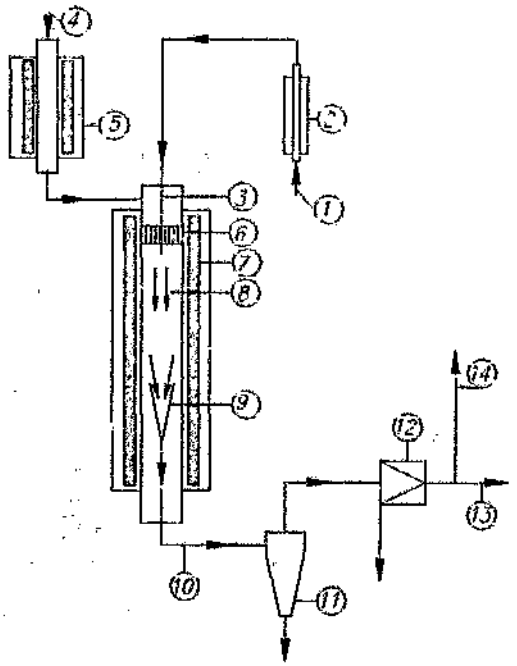

1	primary air
2	coal container and dosing hardware
3	water cooled injection probe
4	secondary air (with variable oxygen content)
5	secondary air preheater
6	honeycomb flow straightener
7	heating elements
8	70 ID alumina tube
9	movable watercooled collection probe
10	reaction product gas stream
11	cyclone
12	particulates filter
13	stream to gas analysers
14	stream to vacuum pump

Figure 12 : ***Schematic of Drop Tube Furnace***

2.3.3 DETERMINATION OF THE DTF PARTICLE RESIDENCE TIME

The calculation of the time spent by a particle in the combustion environment of the DTF, viz. the particles residence time, is outlined below. The particle residence time is required for the calculation of the combustion kinetics.

The volumetric flow (F) of the gas must be corrected (from STP, inlet conditions) to the conditions in the combustion zone of the DTF. From the ideal gas law, the following relationship can be derived.

$$F = F_o \cdot \left(\frac{P_o}{P_1}\right) \cdot \left(\frac{T_1}{T_o}\right) \qquad (14)$$

where

F = corrected volumetric flow (m^3/s)

F_o = inlet volumetric flow (m^3/s - STP)

P_o = inlet pressure, T_o = inlet temperature (STP)

P_1 = combustion zone pressure (atmospheric)

T_1 = average combustion zone gas temperature

The linear velocity of the gas (v_g) is given by the quotient of the volumetric flow and the reactor volume per unit length.

The gas density (ρ_g) may be derived from the ideal gas law, which may be simplified to the following equation.

$$\rho_g = 3.36 \cdot 10^2 \cdot \frac{P}{T} \qquad (15)$$

where

ρ_g = gas density in combustion zone (kg/m^3)

P = gas pressure (atm)

T = gas temperature (K)

The gas viscosity[41] (μ_g) has been found to be described satisfactorily by the following empirical relation.

$$\mu_g = 10^{\frac{\log T_g - 3.5019}{1.3733} + 4} \qquad (16)$$

where μ_g = gas viscosity (kg/m/s)

T_g = average gas temperature in combustion zone (K)

The free fall velocity of the particle (v_{ff}) can be determined by assuming that the velocity falls into the region governed by Stokes' Law[42], then

$$v_{ff} = \frac{g \cdot d_p^2 \cdot (\rho_p - \rho_g)}{18 \cdot \mu_g} \qquad (17)$$

where v_{ff} = free fall velocity (m/s)

g = gravitational acceleration (m/s^2)

d_p = particle diameter (m)

ρ_p , ρ_g = particle, gas density (kg/m^3)

μ_g = gas viscosity (kg/m/s)

The residence time is given by

$$t_{res} = \frac{L}{(v_{ff} + v_g)} \qquad (18)$$

where t_{res} = residence time (s)

L = Length of particle path in the combustion zone

v_{ff} , v_g = free fall, gas velocities

The gas temperature was found to vary along the length of the combustion zone by up to 30K. In order to describe the physical parameters (i.e. density and viscosity) of the gas, the average temperature in the combustion zone was used for all

calculations. In order to describe the variation, the measured temperature data was curve fitted with a 6th order polynomial (P(x)). To determine the average gas temperature, the polynomial function was integrated over the length of the combustion zone as shown below.

$$T_{ave} = \frac{1}{L} \int_0^L P(x)\, dx \qquad (19)$$

where T_{ave} = Average temperature in the combustion zone

L = length of the particle trajectory

P(x) = 6^{th} order polynomial describing the temperature distribution

2.3.4 DETERMINATION OF DEVOLATILISATION YIELDS AND RATES

The DTF is capable of reproducing particle heating rates of around 10^4 to 10^5 K/s, as found in pf combustors typical of steam raising plant and therefore can be used in the determination of devolatilisation rates and yields. For the purpose of the devolatilisation rate determination, the RC Composite sample was prepared as follows :

1. sample ground to PF consistency (viz. 75% < 75μm)
2. sample screened to remove all +150μm material, which was then reground and reintroduced into the sample
3. >75μm was reground to <75μm and reintroduced into the sample
4. sample was split into two size fractions, namely 38-75μm and <38μm
5. each size fraction underwent batch DTF testing at 5 residence times ranging between 0.05 and 1.1s for furnace setpoint temperatures of 1000, 1200 and 1400°C in N_2
6. solid residues collected from the above tests underwent proximate analyses to determine the extent of devolatilisation, from which the devolatilsation rates were determined

The volatile yield after DTF pyrolysis is determined by solving equation (20) given the ash content of a <150μm coal sample *before* and *after* it is passed throught the DTF at 1400°C for 2.2s.

$$VM_{DTF} = \frac{1}{A_1}\cdot\left[A_1\cdot(1-A_0) - A_0\cdot(1-A_1)\right] \qquad (20)$$

where A_0 = Ash content in DTF feed (dry basis) *-before*

A_1 = Ash content in sampled residue (dry basis) *-after*

This result is used in the assessment of the devolatilisation kinetics of the sample to suit the pyrolysis (i.e. devolatilisation) model of the combustion code. The combustion model uses a single step zero order Arrhenius reaction model by Badzioch and Hawksley[7] according to which the pyrolysis rate is given by

$$\frac{d}{dt}\cdot V_x = -k_{devol}\exp\left(-\frac{\Delta E_{a_{devol}}}{R\cdot Tp}\right) \qquad (21)$$

where V_x = extent of devolatilisation

k_{devol} = Arrhenius Factor for devolatilisation

$\Delta E_{a_{devol}}$ = Activation Energyfor devolatilisation

R = Universal Gas Constant

Tp = Particle Temperature

The particle temperature, Tp, is determined from a simultaneous solution of the energy and mass balance around the devolatilising particle, taking into account radiative and convective heat transfer as the particle passes through the DTF. Assuming a constant external surface area of the coal / ash particles (viz. shrinking core), the radiative heat exchange between the particle and the DTF is given by :

$$r_{T_{rad}} = \frac{\varepsilon \cdot \sigma \cdot A_{particle} \cdot \left[(T_{wall})^4 - (T_{particle})^4 \right]}{Cp_{particle} \cdot m_{particle}} \qquad (22)$$

where

ε	=	average emissivity between the particle and the wall	
σ	=	Stefan Boltzman constant	
$A_{particle}$	=	assumed external surface particle area	(m^2)
T_{wall}	=	DTF Wall Temperature	(K)
$T_{particle}$	=	Particle Temperature	(K)
$Cp_{particle}$	=	Particle Heat Capacity	$\left(\frac{J}{kg \cdot K}\right)$
$m_{particle}$	=	mass of particle	(kg)

The convective heat exchange between the hot furnace gas and the particle is given by :

$$r_{T_{conv}} = \frac{Nu \cdot A_{particle} \cdot \lambda \left(T_{particle}, T_{gas}\right) \cdot \left(T_{boundary} - T_{particle}\right)}{Cp_{particle} \cdot m_{particle} \cdot dp} \qquad (23)$$

where

Nu	=	Nusselt Number for boundary layer convective heat exchange	
$A_{particle}$	=	external particle surface area	(m^2)
$T_{boundary}$	=	Boundary Layer Temperature (assumed to be the average of the Gas and Particle Temperatures)	(K)
$T_{particle}$	=	Particle Temperature	(K)
λ	=	$2.43 \cdot 10^{-5} \cdot \left(\frac{T_{boundary}}{273}\right)^{0.82}$ convective heat exchange coefficient	$\left(\frac{W}{m \cdot K}\right)$
$Cp_{particle}$	=	Particle Heat Capacity	$\left(\frac{J}{kg \cdot K}\right)$
$m_{particle}$	=	mass of particle	(kg)
dp	=	particle diameter	(m)

The solution of the sum of the differential equations (22) and (23) gives an overall account of particle temperature with time. Figure 13 shows particle temperature vs. time plots for DTF set-point temperatures of 1000,1200 and 1400°C for a 22μm coal particle.

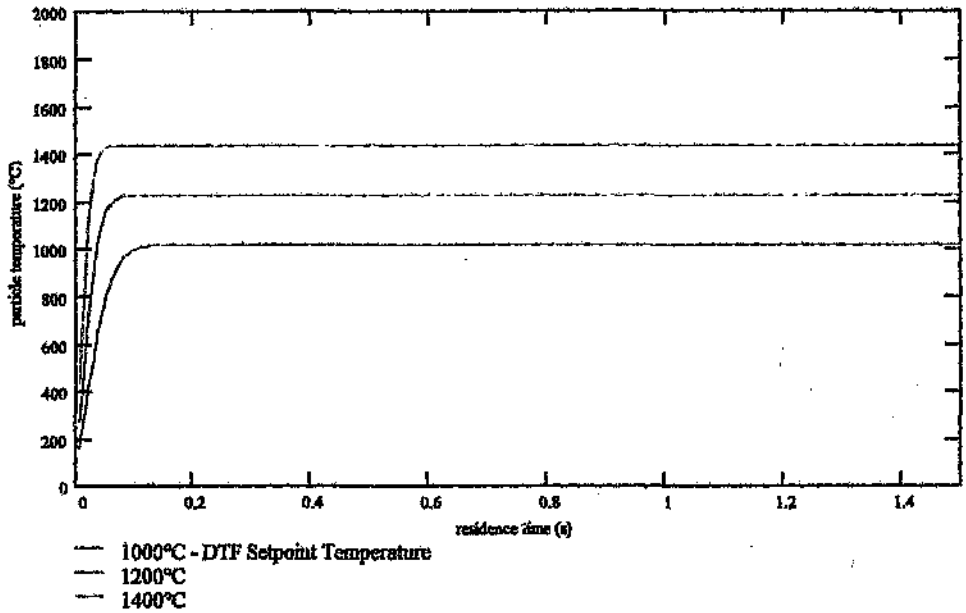

Figure 13 : *Particle Temperature vs. time during Pyrolysis in the DTF*

The corresponding devolatilisation vs. time graphs are shown in Figure 14 along with the DTF results.

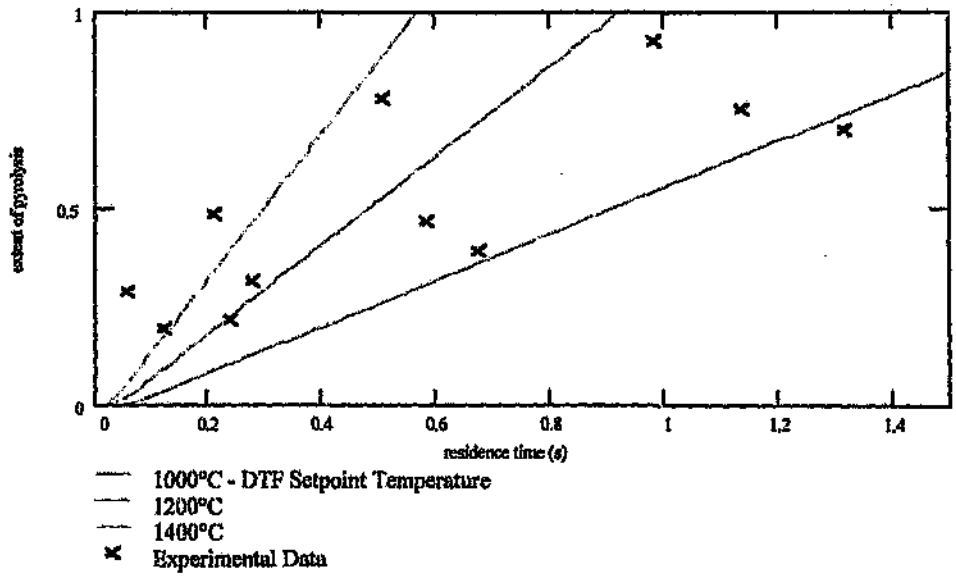

Figure 14 : *Extent of Pyrolysis vs. time in the DTF*

2.3.5 DETERMINATION OF CHAR COMBUSTION RATES

The standard ESKOM char combustion test procedure as performed on the RC Composite sample is outlined below :

1. sample ground to PF consistency (viz. 75% <75μm)
2. sample screened to remove all +150μm material, which was then reground and reintroduced into the sample
3. sample pyrolised at 1400°C in N_2 for 2.2s
4. the resulting product was screened at 75μm and all >75μm material was reground to <75μm and reintroduced into the sample
5. the sample was split into a <38μm and a 38-75μm size fraction
6. each size fraction underwent DTF testing at 5 residence times ranging between 0.4 and 3.2 s for DTF setpoint temperatures of 1000,1100,1200,1300 and 1400°C at 3 vol.% O_2 with the balance being N_2 (This particular oxygen concentration is chosen since it is similar to the depleted bulk oxygen concentration in a typical utility boiler)
7. the solid combustion residues from the above tests were analysed for combustible matter and ash content, from which the extent of the combustion reaction is determined

As the mass fraction of ash increases with increasing residence time, the extent of combustion can be determined using the ash in the combustion residue as a tracer. The fractional extent of combustion or combustion efficiency (CE) is given by (on a dry ash free basis):

$$CE = \frac{A_0}{(1-A_0)} \cdot \frac{(1-A_1)}{A_1} \qquad (24)$$

where A_0 = mass fraction of ash in the raw char (dry basis)

A_1 = mass fraction of ash in the sampled residue (dry basis)

The experimentally determined combustion extent data along with its corresponding residence time in the DTF at a given DTF set-point temperature, is used to estimate the char combustion parameters required for the combustion sub-model of the combustion code. A pseudo steady–state assumption with regard to the particle temperature is required to arrive at estimations of the char combustion parameters, which are then refined by simulating the DTF combustion process. This simulation model is described later in this section. The method of arriving at the estimations of the char combustion parameters is described below :

Depending on the particle surface temperature, the rate of combustion can be limited either by the rate of O_2 diffusion to the surface of the particle or the rate of chemical reaction at the particle surface. In either situation, the rate of combustion depends on the partial pressure of O_2, the surface area available for char combustion and the combustion characteristics of the char in question. The overall rate of char combustion is mathematically modelled by equation (25) :

$$\frac{d}{dt} m_{C_{particle}} = k_{char_{overall}} \cdot P_{O_2,\infty} \cdot A_{particle} \qquad (25)$$

where

$m_{C_{particle}}$ = mass of combustible matter in char particle

$k_{char_{overall}}$ = overall reaction rate coefficient

$P_{O_2,\infty}$ = partial pressure of Oxygen

$A_{particle}$ = apparent reactivesurface area of the particle

Field[8] (1970) proposed that the overall rate reaction coefficient comprise a rate coefficient description of oxygen diffusion to the reaction surface as well as description of the rate coefficient of chemical reaction at the surface according to equations (26) to (28). If the chemical reaction rate is fast compared to the rate of O_2 diffusion to the reacting char surface, the reaction is diffusion controlled. If the rate of chemical reaction is slow compared the rate of O_2 diffusion to the reacting surface, the reaction is chemically controlled.

$$\frac{1}{k_{char\ overall}} = \frac{1}{k_{char_{diffusion}}} + \frac{1}{k_{char_{reaction}}} \qquad (26)$$

where

$$k_{char_{diffusion}} = \frac{24 \cdot \phi_m \cdot D_{O2}(1600\,K) \cdot \left(\frac{T_{boundary}}{1600\,K}\right)^{1.75}}{R \cdot 10^{-5} \cdot d_{particle} \cdot T_{gas}} \quad \left(\frac{kg}{m^2 \cdot s \cdot bar}\right) \qquad (27)$$

$$D_{O2}(1600\,K) = 3.3 \cdot 10^{-4} \quad \left(\frac{m^2}{s}\right)$$

ϕ_m = mechanism factor (**2** if C oxidises to CO and **1** if C oxidises to CO_2)

and

$$k_{char_{reaction}} = A_{reaction} \cdot \exp\left(\frac{-\Delta E_a}{R \cdot T_{particle}}\right) \quad \left(\frac{kg}{m^2 \cdot s \cdot bar}\right) \qquad (28)$$

$A_{char_{reaction}}$ = Arrhenius factor $\quad \left(\frac{kg}{m^2 \cdot s \cdot bar}\right)$

ΔE_a = Activation Energy $\quad \left(\frac{J}{mol}\right)$

The overall rate is determined from the experimental data by integration of differential equation (25). A description of the integration results is given in equations (29) and (30).

$$\int_{\left(m\,C_{particle}\right)^{initial}}^{\left(m\,C_{particle}\right)^{final}} \frac{m\,C_{particle}}{A_{particle}}\, dm\,C_{particle} = \int_0^{t_{res}} k_{char_{overall}} \cdot P_{O_2}\, dt \qquad (29)$$

where

$$m\,C_{particle} = \left(m\,C_{particle}\right)^{initial} \cdot (1 - CE)$$

similarly

$$A_{particle} = \left(A_{particle}\right)^{initial} \cdot (1 - CE)^{n_B} \qquad (30)$$

where $\left(A_{particle}\right)^{initial}$ = initial particle surface area

n_B : swelling index

The superscripts initial and final refer to the DTF feed and product respectively while t_{res} is the corresponding residence time in the DTF. Because the DTF is operated with a considerable oxygen excess (300 - 400%), the partial pressure of oxygen (P_{O2}) remains effectively constant.

The initial particle surface area includes the active internal pore area created during the devolatilisation process and would depend primarily on the char structure and the heating rate. Laine et al[9] (1964) found that for the same coal a higher heating rate resulted in a greater surface area for reaction and an increased combustion rate. Smoot et al[10] noted that physical changes in the char structure resulted in changes in surface area and in turn changes in combustion rate. In order to account to some extent for the complex nature and structure of char forms and their transformations during the combustion process, an empirical swelling index, n_B, is used in equation (24). Table 1 summarises how this surface area model predicts the reactive surface area of char particle during the combustion process for various swelling indices.

Table 1 : ***Particle Surface Area as a function of Combustion Extent (CE)***

Description	"non swelling"	"swelling"
Swelling Index n_B	2/3	1
$\frac{A_{particle}}{\left(A_{particle}\right)^{initial}} = (1 - CE)^{n_B}$	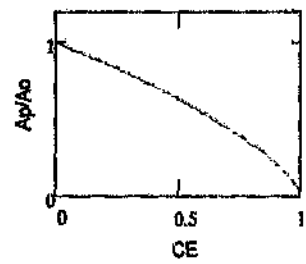	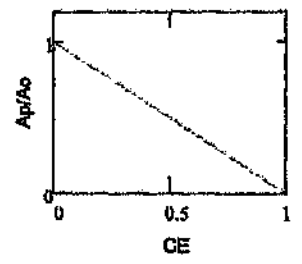

As the combusting particle passes through the DTF, it is first heated by radiation from the hot furnace walls and by convection from the preheated gases passing through the DTF. An estimation of the particle surface temperature can be made by solving an energy balance around the particle which equates the heat lost/gained by radiation and convection to the heat released at the surface due to reaction. The heat release can be calculated from the measured overall reaction rate assuming that the surface reaction mechanism is known. For the purpose of this investigation, it is assumed that the oxidation on the particle surface results in the formation of CO. The overall energy balance is given in equation (31).

$$\Delta h\left[\frac{\left(m_{C_{particle}}\right)^{final}-\left(m_{C_{particle}}\right)^{initial}}{t_{res}}\right]=\varepsilon\cdot A_r\cdot\sigma\cdot\left[\left(T_{wall}\right)^4-\left(T_{particle}\right)^4\right]+\frac{Nu\lambda}{\bar{d}}\cdot A_c\left(T_{boundary}-T_{particle}\right) \qquad (31)$$

where

Δh	=	enthalpy of formation of CO from C(s) and O(g)	$\left(\frac{J}{mol}\right)$
A_r	=	surface area available for radiative heat exchange	(m^2)
A_c	=	surface area available for convective heat transfer	(m^2)
$\bar{d}$	=	average particle diameter	(m)
Nu	=	Nusselt Number (assumed = 2)	
$T_{boundary}$	=	temperature of the gas film around the particle	(K)
T_{wall}	=	temperature of the inside wall of the Drop Tube Furnace	(K)
$T_{particle}$	=	average temperature of the particle	(K)

Figure 15 shows estimated particle temperatures for a variety of DTF residence times, wall and gas temperatures:

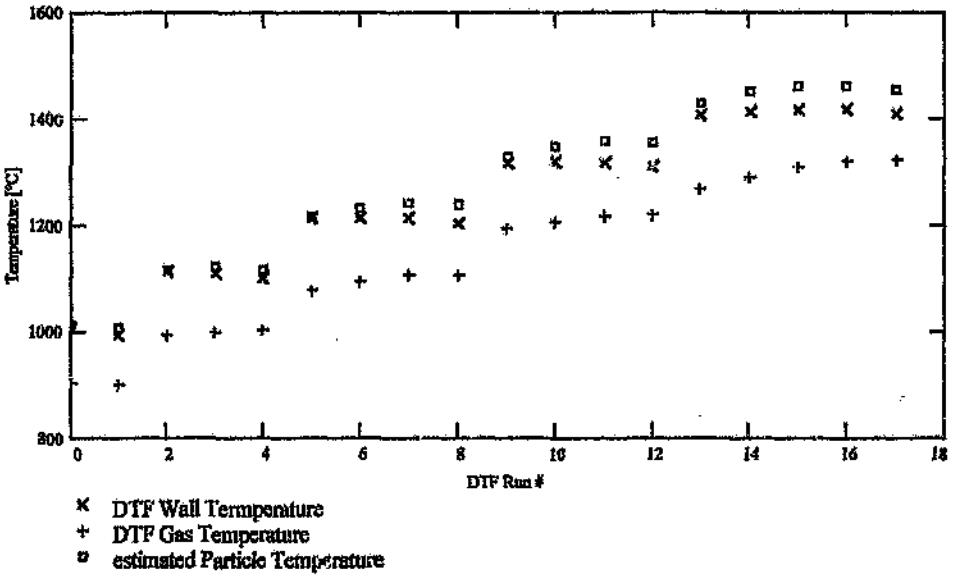

Figure 15 : ***estimated particle temperatures for various DTF experiments***

The diffusion rate can be determined by solving equation (28) given the particle temperature estimate and a particle diameter assumed to be the mean initial particle diameter. Note, however, that when the diffusion rate is similar in magnitude to the experimentally derived overall reaction rate, the reaction may be diffusion controlled. In this event the reaction rate cannot be accurately determined for that particular DTF run because the value of the mechanism factor, ϕ_m, which cannot be determined accurately, becomes significant in the analysis of the results. Field[6] (1969) suggests that only reaction rate coefficients from DTF experiments where

$$\frac{k_{char\ overall}}{k_{char\ diffusion}} < 0.5 \qquad (32)$$

be used to obtain values for the chemical reaction rate coefficients.

When the surface reaction rate coefficients are plotted against the estimated surface temperatures, and a curve fit using the function form given in equation (22) of the data as reviewed by Field et al[11] (1967) is performed, the function parameters define the kinetic parameters for the Arrhenius type reaction model. Figure 16 shows a

typical $\ln(k_{char,surface})$ vs. $10^4/T_p$ plot. The intercept and slope of the linear fit give the pre-exponential factor and activation energy respectively.

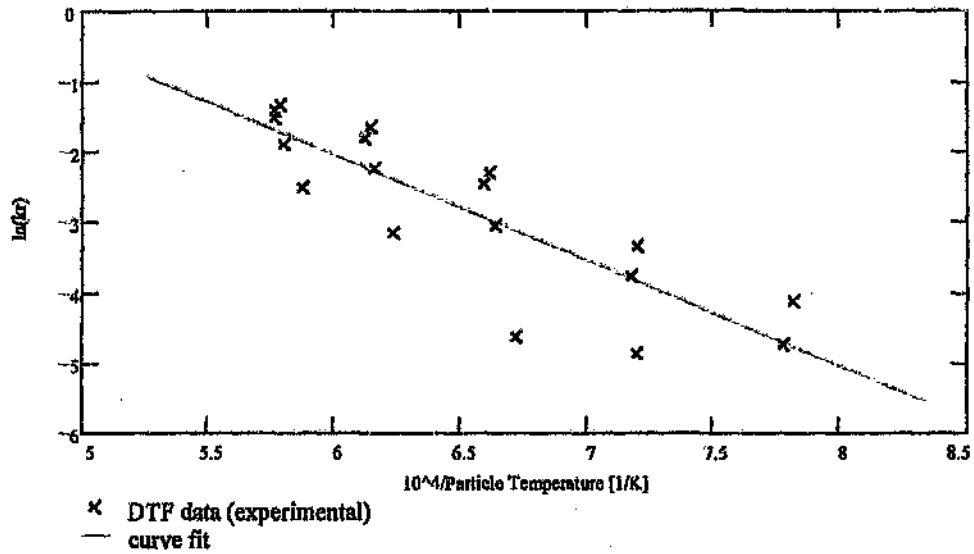

Figure 16 : ***Linear fit of DTF data to determine Arrhenius kinetic parameters***

A model of the combustion process in the DTF was derived using the above process description. The model involves solving two simultaneous differential equations, one describing the combustion at the surface of the char, and the other, the surface temperature of the reacting char particle. The differential equations are given in equations (33) and (34).

$$\frac{d}{dt}C_c = -A_{char}\cdot\exp\left(\frac{-\Delta E_a}{R\cdot T_{particle}}\right)\cdot P_{O2}\cdot A_{particle}(C_c) \qquad (33)$$

$$\frac{d}{dt}T_p = \Gamma_{T\,rad}(T_p, T_w) + \Gamma_{T\,conv}(T_p, T_g) + \Gamma_{T\,gen}(T_p, C_c, T_g) \qquad (34)$$

The change in particle temperature by radiation and convection has been outlined in equations (22) and (23), while equation (35) describes the change in particle temperature due to reaction.

$$\Gamma_{T\,gen}(T_p, C_c, T_g) = \frac{\Delta h}{(C_c + C_{ash})\cdot Cp_{char}}\frac{\delta}{\delta t}C_c \qquad (35)$$

Figure 17 shows the char particle surface temperature of a particular coal in the DTF when operated at a set-point temperature of 1400°C and 3% (Vol.) O_2 in N_2.

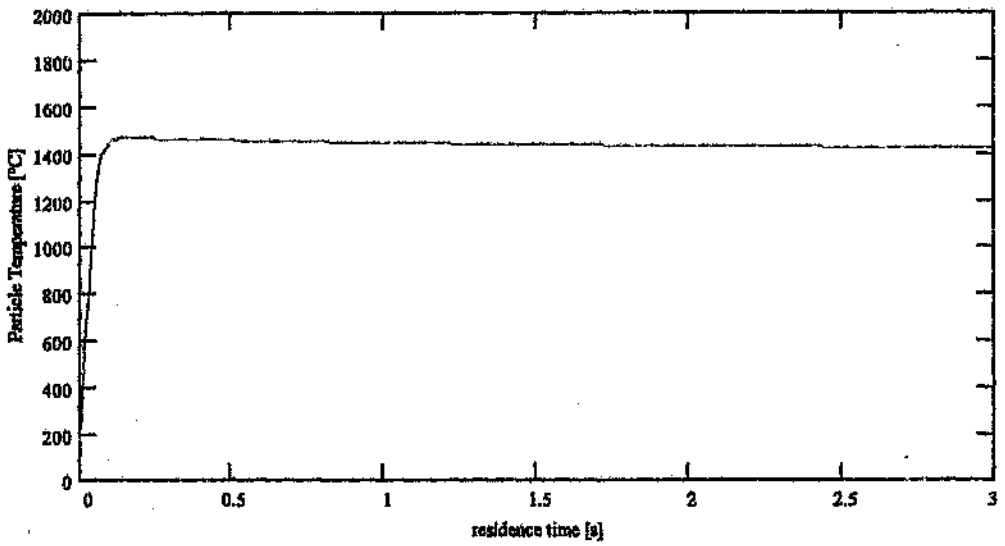

Figure 17 : ***Graph of Particle Temperature vs. time***

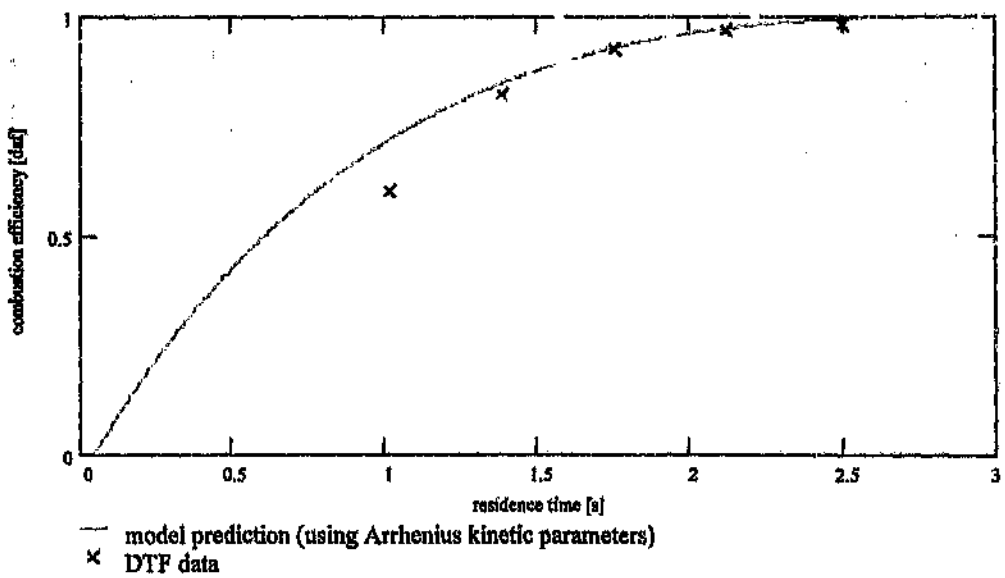

Figure 18 : ***Graph of Combustion Extent vs. time***

2.4 THE *AIOLOS* COMBUSTION MODEL

A detailed account of the model's operational engine and it's many physical, thermodynamic and chemical sub-models is available from Schnell[12] (1991), Epple[13] (1993), Epple et al[14] (1992), Epple et al[15] (1993) and Schnell et al[16] (1995). A brief outline of the model has been extracted from the aforementioned references for the purpose of a convenient review.

Turbulent flow in combustion chambers is predicted using the k-ε turbulence model formulated in partial differential equations compiled in equations (36) to (39) , where the basic equation for a general variable ϕ is specified in equation (36).

The terms in equation (36) describe the local change of ϕ due to transient, convective, diffusive and source term contributions to a particular property assigned to this general variable. Adaptation of this equation leads to the derivation of equations (37) to (39).

Transport Equation :

$$\frac{\delta}{\delta t}\cdot(\rho\cdot\Phi) + \frac{\delta}{\delta x_j}\cdot(\rho\cdot u_j\cdot\Phi) = \frac{\delta}{\delta x_j}\cdot\left(\frac{\mu_{eff}}{\sigma_\Phi}\cdot\frac{\delta\Phi}{\delta x_j}\right) + S_\Phi \qquad (36)$$

transient convective diffusive source

where

t	=	time variable
x_j	=	direction variable where j = 1,2,3
u_j	=	velocity component
Φ	=	general field variable
ρ	=	density
μ_{eff}	=	effective viscosity
σ_Φ	=	stress associated with that general field variable
S_Φ	=	source term of field variable

Time-averaged Navier-Stokes Equation :

$$\frac{\delta}{\delta t}\cdot\left(\rho\cdot u_i\right)+\frac{\delta}{\delta x_j}\cdot\left(\rho\cdot u_j\cdot u_i\right)=\frac{\delta}{\delta x_j}\cdot\left(\Gamma_{ji}\cdot\frac{\delta u_i}{\delta x_j}\right)-\frac{\delta p}{\delta x_i}+\rho\cdot g_i+S_\tau \qquad (37)$$

$$i = 1,2,3$$

where

$\Gamma_{ji} = \frac{\mu_{eff}}{\sigma_i}$

p = pressure

g_i = effectiveacceileration

Kinetic Turbulent Energy

$$\frac{\delta}{\delta t}\cdot\left(\rho\cdot KE_{turb}\right)+\frac{\delta}{\delta x_j}\cdot\left(\rho\cdot u_j\cdot k\right)=\frac{\delta}{\delta x_j}\cdot\left(\frac{\mu_{eff}}{\sigma_k}\cdot\frac{\delta k}{\delta x_j}\right)+G-\rho\varepsilon \qquad (38)$$

where

KE_{turb} = kinetic turbulent energy

Dissipation Rate of of Turbulent Energy

$$\frac{\delta}{\delta t}\cdot\left(\rho\cdot\varepsilon\right)+\frac{\delta}{\delta x_j}\cdot\left(\rho\cdot u_j\cdot\varepsilon\right)=\frac{\delta}{\delta x_j}\cdot\left(\frac{\mu_{eff}}{\sigma_\varepsilon}\cdot\frac{\delta\varepsilon}{\delta x_j}\right)+\frac{\varepsilon}{k}\cdot\left(C_{\varepsilon_1}\cdot G-C_{\varepsilon_2}\cdot\rho\cdot\varepsilon\right) \qquad (39)$$

Generation Term : $G = \frac{\delta u_i}{\delta x_j}\cdot\left[\mu_t\cdot\left(\frac{\delta u_j}{\delta x_i}+\frac{\delta u_i}{\delta x_j}\right)\right]$

Turbulent Viscosity : $\mu_t = C_\mu\cdot\rho\cdot\frac{KE_{turb}^2}{\varepsilon}$

where

ε = dissipation rate of turbulent energy

C_μ = *constant of turbulent viscosity model*

The time averaged Navier Stokes equation (also called the Reynolds equation) describes the momentum balance (velocities) around (into and out of) a control volume. The pressure, which can be considered as the source term in this momentum equation, is calculated by means of a pressure correction method by Epple et al[17] (1991). The turbulence is characterised by the kinetic turbulent energy

KE_{turb} and its dissipation rate ε. More advanced and sophisticated turbulence models, which provide improved prediction accuracy, are available for use with AIOLOS. They do however require considerably more computation time (Schnell[18], (1989)) and are therefore not generally used in three dimensional simulations. Their use in two dimensional AIOLOS applications has however been demonstrated with success.

The general variable ϕ may also stand for species that feature in the combustion of coal. Figure 19 shows how the combustion process is modelled and what species are considered. The circled numbers in Figure 19 refer to the column headed **No** of Table 2.

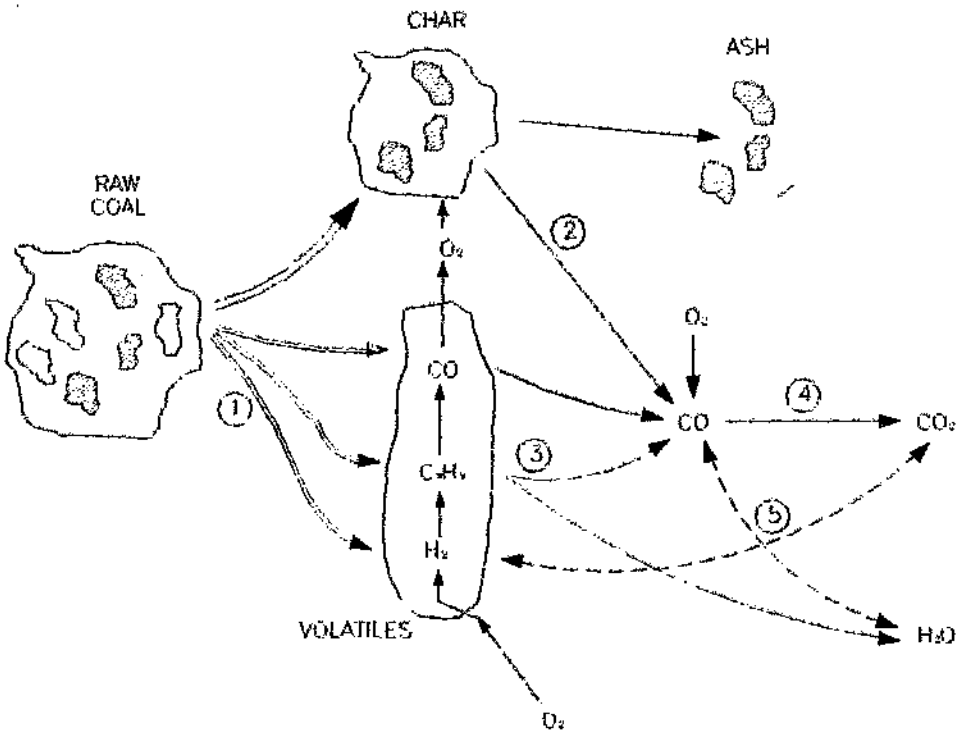

Figure 19 : ***Reaction Models of Pulverised Coal Combustion***

Table 2 : ***Reaction Models of Pulverised Coal Combustion***

No	Reaction Model	Reference
1	Devolatilisation	Section 2.3.3 of this report
2	Char Combustion	Section 2.3.4 of this report
3	Volatiles Combustion	Field et al[8] (pp 179)
4	Oxidation of CO	Field et al[8] (pp 175)
5	Water Gas Shift Reaction	Denn [21], Schilling [22] (pp 10)

The AIOLOS coal combustion model (as outlined in Figure 19) considers coal to be devolatilised in a single step to form char and volatiles (reaction 1). The rate of devolatilisation for the Hendrina R.C. Composite was investigated using the DTF and analysed according to the method and analysis procedures described in part 2.3.3 of this report. The volatiles are assumed to consist of CO, H_2 and hydrocarbons C_XH_Y. The hydrocarbon parameters X and Y are determined from the ultimate analysis of the coal. C_XH_Y is assumed to oxidise in a two-step reaction yielding CO_2 and H_2O (reactions 3 and 4). These reactions are modelled with an Eddy-Dissipation-Model (Magnussen[19] (1981) and Magnussen and Hjertager[20] (1976)). The residual char is heterogenously oxidised to CO at the surface of the char (reaction 2). The rate of char oxidation depends on the local oxygen concentration, the reactive surface area and reactivity of the char itself. The reactivity of the char is experimentally determined using the DTF according to the method and analysis procedure outlined in section 2.3.4 of this report. Additionally, the water-gas-shift reaction adjusts the concentrations of CO, H_2, CO_2, and H_2O towards equilibrium (reaction 5). Information on this reaction is available from Denn[21] 1967) and Schilling et al[22] (1981). Particle size effects are also included by considering various size classes for the solid fuel. Ash is treated as an inert substance.

Besides the heat release due to the combustion reactions, the source of enthalpy in each control volume is dominated by radiative heat exchange. In pulverised coal fired combustors, radiative heat exchange in the furnace accounts for approx. 90% of the total heat transfer. AIOLOS allows the use of a number of radiative heat exchange models.

Viskanta[23] compiled an overview of radiation models and in the area of radiative heat transfer in pulverised coal combustion applications, these can grouped into 'zone'- , 'flux'-, and statistical models.

Zone methods, such as proposed by Hottel et al[24] (1967), require a non-linear integro-differential equation for each zone, making the application of this method unsuitable for finely discretised furnace chambers in view of the computational effort required. The 'flux'-models are grouped according to the number of directions in which they model radiative heat transfer into and out of a control volume. 2-, 4- and 6-'flux' models have been proposed by Siddal and Selcuk[25,26] (1979, 1976) and Filia and Maresa[27] (1975), which are coupled to resolve radiative exchange in three dimensions via the control volume temperature alone. A 6-'flux' model by De Marco and Lockwood[28] (1975) refined the 'flux' approach by coupling the radiation exchange in three dimensions. The 'flux'-radiation models can use the numerical solution

algorithms used by the flow solver. It should however be noted at this stage the 'Monte-Carlo-' and 'Discrete-Transfer-' radiation models considerably outperform the 'flux' radiation models with regard to solution accuracy.

The 'Discrete-Transfer-' model, proposed by Lockwood and Shah[29,30] (1976), specifies a network of beams within the combustion chamber, along which radiative heat exchange occurs. An overall energy balance around the entire combustion chamber is required in the solution algorithm. The 'Discrete-Transfer-' model differs from the 'Monte-Carlo-' model in that no beam reflection from the furnace wall is considered. As the beams traverse the individual control volumes that the combustion chamber has been broken down into, a portion of the beams energy is transferred to the control volume according it's radiative properties. These properties are determined from the gas emissivity (which depends on the local gas composition) and more importantly the particulate loading. A comparison between the 'Monte-Carlo' radiation model (first proposed for cylindrical combustion chamber geometries by Stewart and Cannon[31] (1971)) and the 'Discrete-Transfer-' model has been made by Guilbert[32] (1989). A further radiation model, named the 'Discrete-Ordinates-' model as proposed by Fiveland[33,34] (1987, 1984), is available in the AIOLOS combustion model.

A detailed outline of the application of the 'Monte-Carlo-' radiation exchange model in combustion modelling applications is available from Richter[35,36] (1978, 1974). Whereas the Monte-Carlo method uses an entirely statistically determined array of beams to describe the radiative heat transfer, Richter has specified the beam numbers and directions at the source. Statistical treatment of the beam direction only takes place on beam reflections at the furnace walls. A previous Eskom combustion modelling investigation by Eichhorn et al[37] (1995) used a furnace model by Richter based on Monte-Carlo method for radiation exchange. It was found that despite having performed the simulation with a very coarse grid, reasonable predictions were made.

In order to analyse pollutant formation in pulverised coal combustion, the nitrogen oxides (NOx) formed from fuel bound nitrogen must be modelled. A fuel-NO- and thermal NO formation model are included in the AIOLOS combustion model. The thermal NO formation model is based on the well-known Zeldovich[38] mechanism, while the fuel N oxidation/reduction is assumed to occur according the mechanisms described in Figure 20.

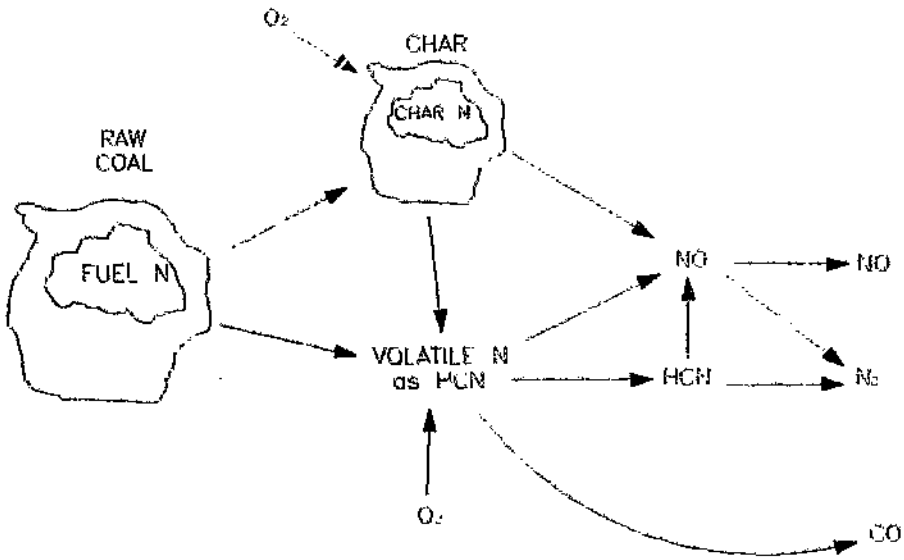

Figure 20 : *Reaction Scheme of Fuel N Conversion*

The fate of HCN and its successors is strongly dependant on the local flame conditions, particularly stoichiometry and temperature. De Soete[39] (1974) proposed a reduced scheme for NO formation from HCN, which has been adopted for use in AIOLOS. It must be noted that the reaction times of HCN in the flame are of the same order as the turbulent fluctuations in combustion conditions in the flame as is typical to many pollutant formation reactions which show high activation energies. It is assumed in the model that the species concentration fluctuations are not as marked as the temperature fluctuations in the burner regions as radiation is the dominant mechanism of heat transfer. A simplified probability density function (pdf) approach with a model for the instantaneous temperature fluctuations yields the HCN decay rate by oxidation to NO and reduction to N_2. Details of the model for the instantaneous temperature fluctuations are given by Schnell[12] (1991).

2.5 APPLICATION OF *AIOLOS* TO HENDRINA UNIT 9

2.5.1 DESCRIPTION OF THE HENDRINA UNIT 9 FURNACE

The furnace of Hendrina Unit 9 has 6 burner rows, each of which is fuelled by a dedicated vertical spindle mill of which five must be in operation at full load. Each mill supplies four burners, which are arranged in a single row on either the front or back wall of the furnace. A vertical section and view of the front wall of the furnace are shown in Figure 21.

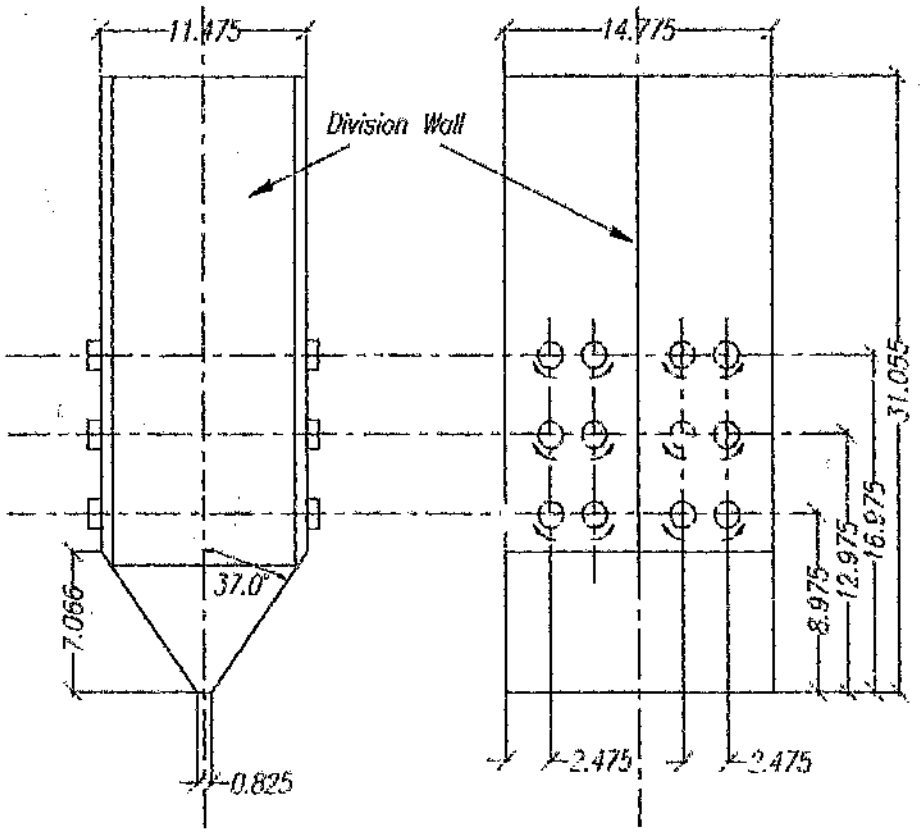

Figure 21 : *Hendrina Unit 9 Furnace : Vertical Section and View of Front Wall*

A summary of boiler specifications as required for the combustion model, sourced from the design specifications[40] by Steinmüller , the boiler's designers and manufacturers, has been compiled in Table 3. Note that the 97% maximum capacity rating (MCR) values have been obtained by linear interpolation of the 94% and 100% MCR specifications.

A section through the burner is shown in Figure 22. Note that the cylinder contained within the core air duct holds the oil burner assembly and that the primary air / pf mixture is not swirled. Swirl vanes have recently been installed into the core air ducts. Their effect on the combustion process has however not been modelled at this stage.

Table 3 : ***Furnace Specification as required for Combustion Model***

Specification	94% MCR (202 kg/s evaporation)	100% MCR (215 kg/s evaporation)	97% MCR (208.5 kg/s evaporation)
Air Temperature at Air Heater Outlet	242	247	244.5
Temperature of air/fuel mix entering burners	80	80	80
Fuel Consumption (refer to Table in footnote [1])	26.4	28.1	[illegible]25
Air supplied to furnace as			
primary air(kg/s)	45.5	54.0	49.75
secondary air (kg/s)	177.5	185	181.25
Gas Temperature at Furnace Exit (°C)	1100	1125	1112

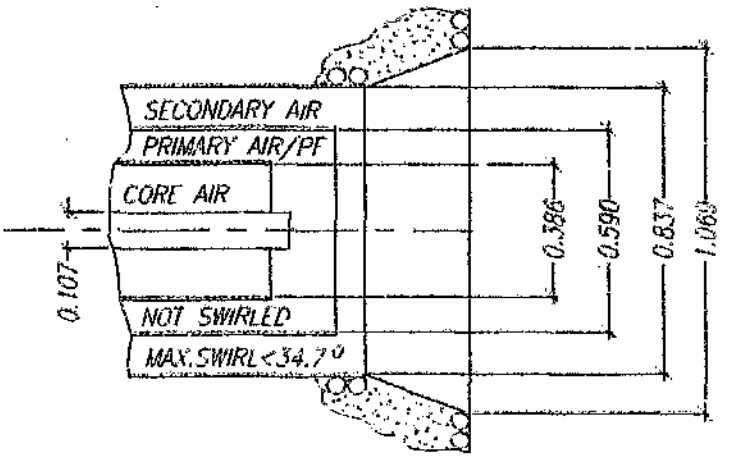

Figure 22 : ***Section through Hendrina Unit 9 Burner***

[1] for typical coal properties from design specification :

	Typical Washed Fuel
Inherent Moisture (m% air dried)	4
Ash (m% air dried)	20
Volatile Matter (m% air dried)	24
Fixed Carbon (m% air dried)	53
Calorific Value (MJ/kg air dried)	25
Surface Moisture (m% as received)	6

2.5.2 FURNACE DISCRETISATION

The furnace was discretised into 276546 Cartesian grid based finite volumes (or cells) by dividing the height, width and depth of the furnace as follows :

height :	100
width (front / rear wall) :	76
depth (left / right wall) :	45

The divisions were specified to become gradually smaller as the burner regions were approached, to improve the resolution of near burner zone regions and to reduce the gradients in local combustion conditions between adjacent cells. A finer discretisation is necessary for the simulation of the volatiles combustion and NO formation which feature predominantly in this region. Figure 23 shows the discretised furnace. The AIOLOS code containing the discretisation information is attached in Appendix 3.1.

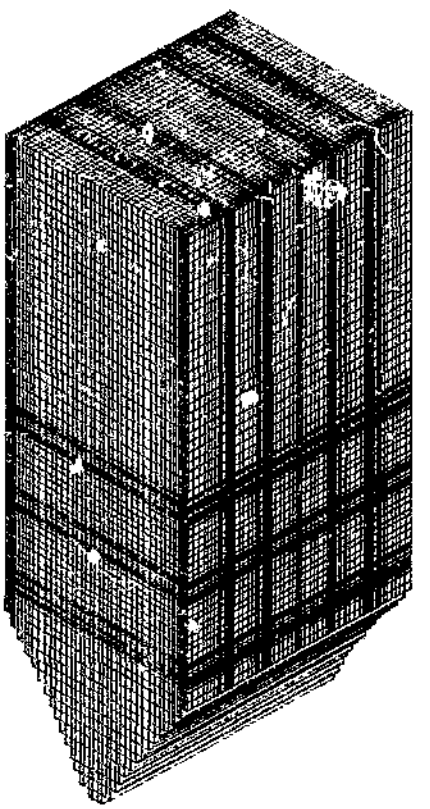

Figure 23 : ***Discretisation of Hendrina Unit 9 Furnace***

2.5.3 SPECIFICATION OF BOUNDARY CONDITIONS

The specification of boundary conditions required that every cell inlet be allocated the mass flowrates of the species entering there as well as their respective inlet velocities and directions. For the purpose of defining the inlet flow patterns of the swirl burners, the centre-points of the burners were specified, around which, depending on the angle of rotation around the bu ·r centre, the direction of flow of the inlet stream was described in terms of it's velocity components.

Furthermore, the inlet stream temperature was specified for both the flow and radiation component of the combustion model. The AIOLOS code specifying the inlet conditions has been attached in Appendix 3.2.

2.5.4 SPECIFICATION OF THE COAL COMPOSITION, DEVOLATILISATION AND COMBUSTION PROPERTIES

The coal properties outlined in Table 4 require specification. Note that the bold typeface indicates the parameter specified.

Table 4 : *Coal Specifications for AIOLOS*

Likely Volatile Hydrocarbon	C_XH_Y
Calorific Value (on dry ash free (daf) basis)	**HUDAF**
Volatile Matter (from DTF analysis, daf)	**VMDAFA**
Ultimate Anlaysis (as received basis)	**XSI**$_I$ where I = **C, O, H, S, N, A** (Ash) and **F** (inherent moisture)
Devolatilisation Kinetic Parameters	Pre-exponential factor : **RK01** Activation Energy : **E1R**
Char Combustion Kinetics	Pre-exponential factor : **RK02** Activation Energy : **E2R**
Particle Size Distribution (3 size classes)	distribution (**WSIZE**$_j$) and average particle diameter (**DPJJ**$_j$) in size class where j = 1 .. 3
Density of Coal	**RHOSO**
Swelling Index	**RN_B**

The AIOLOS input file containing the aforementioned information has been attached in Appendix 3.3.

2.5.5 AIOLOS NOx MODEL SPECIFICATIONS

The NOx model is generally used in a post-processing mode since the quantities involved in NO formations are negligible compared to the coal combustion reactions and therefore do not affect the calculated combustion conditions. The model requires that the coal nitrogen on a daf basis be provided and if possible, the fraction of coal nitrogen reporting to volatile matter and char respectively. As little is known about the oxidation of char nitrogen, an arbitrary conversion factor of char nitrogen to NO can be specified. An AIOLOS input file containing the listed specifications required for the NOx model has been attached in Appendix 3.4.

3. RESULTS AND DISCUSSION

3.1 FURNACE OPERATION ASSESSMENT

During the entire furnace testing program the operation of the furnace was logged according to standard Hendrina operation procedures. Figures 24 to 26 show logs of selected plant variables considered to be significant indicators of furnace operation.

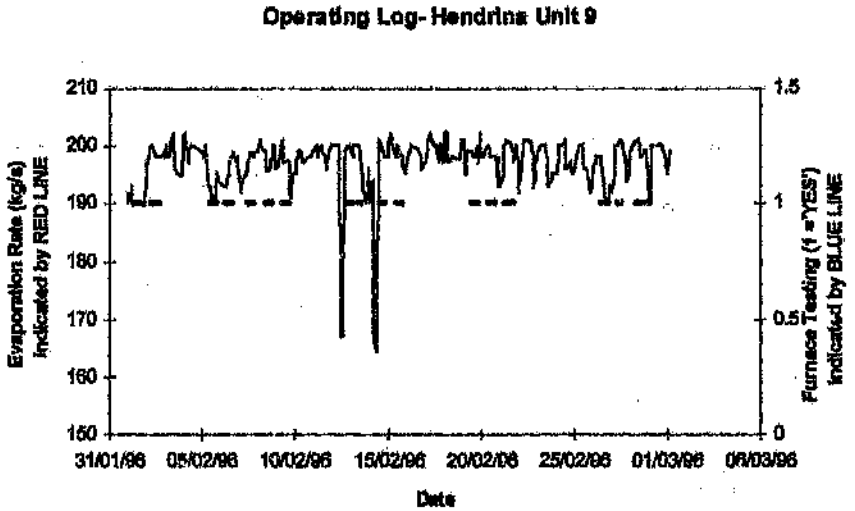

Figure 24 : ***Log of Evaporation Rate during Furnace Tests***

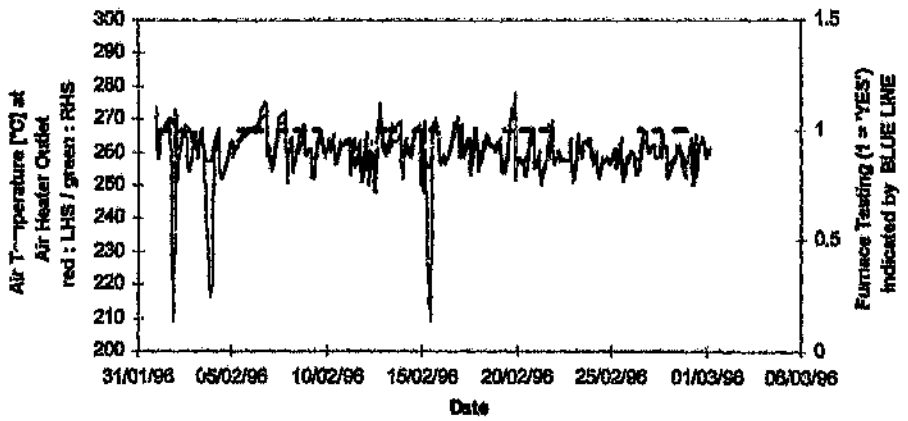

Figure 25 : ***Log of Air Temperatures (LHS/RHS) at Air Heater Outlet***

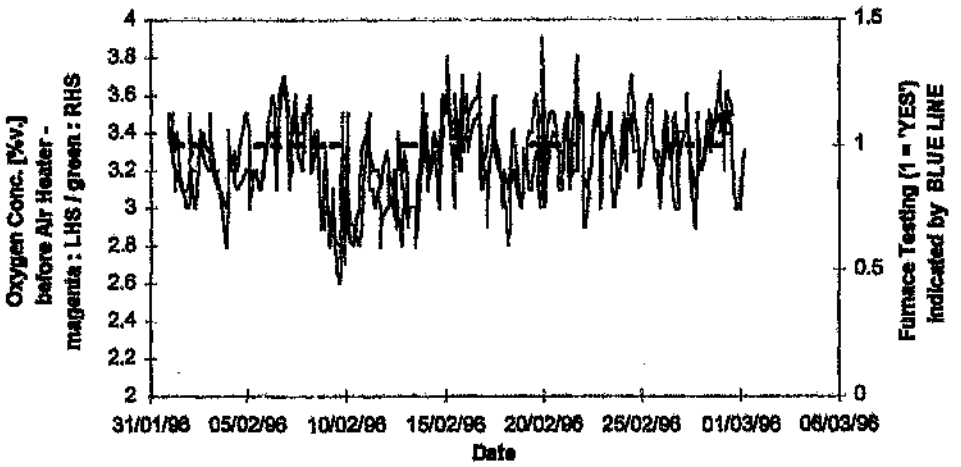

Figure 26 : *Log of Oxygen Concentrations (LHS/RHS) before Airheater*

The fluctuations in boiler operating parameters during the time of testing indicate that the furnace probing results require a critical review. It must however be noted that during the time it took to perform a furnace probing experiment, there were considerable variations in the property measured. This was particularly evident in the burner belt region of the boiler. The furnace exit conditions were considerably more stable.

The repeatability of furnace exit measurements was tested by means of furnace exit temperature measurements of boilers 9 and 10. These results of these measurements have been illustrated Figures 27 and 28.

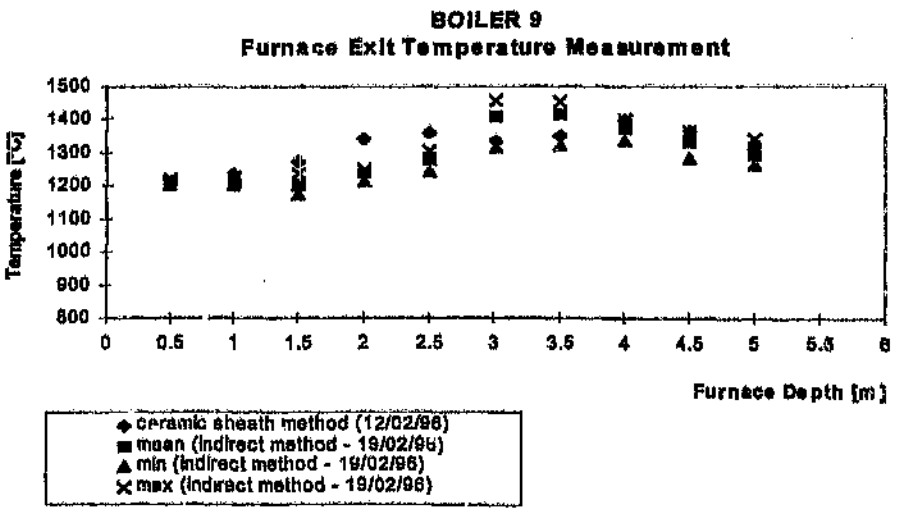

Figure 27 : *Temperature Measurement - BOILER 9*

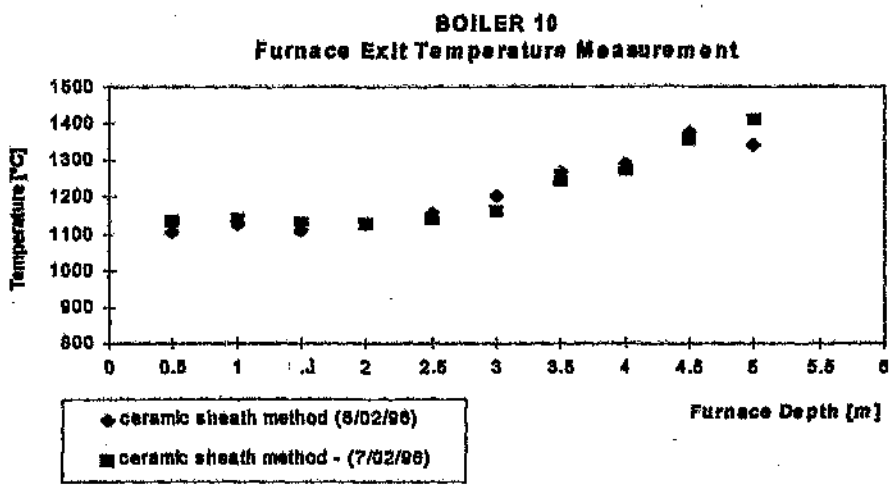

Figure 28 : *Temperature Measurement - BOILER 10*

The results depicted in Figure 27 show that most of the temperature measurements for 12/02/96 (ceramic sheath method) lie within the range observed on 19/02/96 (indirect method).

The results of the furnace tests did, however, show that furnace measurements are subject to considerable variations over short periods. This should be considered when comparing model predictions to measured data.

3.2 FURNACE RESIDENCE TIME DISTRIBUTIONS

The results of the RTD measurements have been presented in Table 5. In all RTD tests performed, all but one of the top burner rows was in operation.

Table 5 : *RTD Measurement Results*

RTD from Burner Level	Insertion Depth of Probe [m]	Dead Time [s]	Furnace RTD
top, right	2	3.1	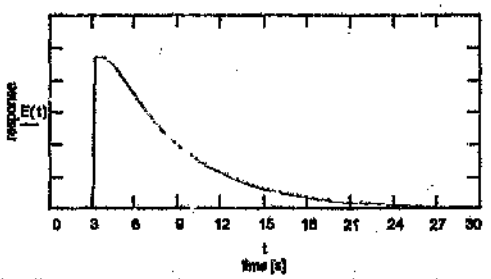
top, right	3	2.4	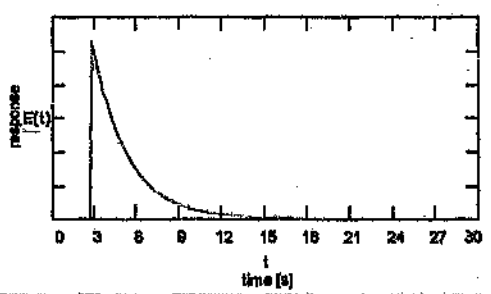
top, left	4	3.5	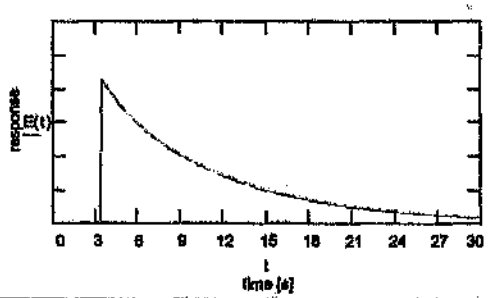
top, right	4	3.4	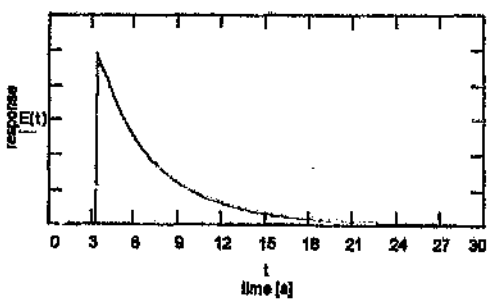

Table 5 : *continued*

RTD from Burner Level	Insertion Depth of Probe [m]	Dead Time [s]	Furnace RTD
middle, left	4	3.7	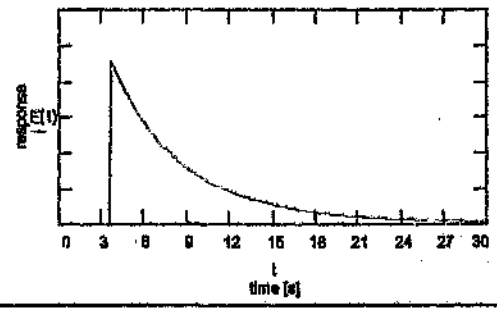
middle, right	4	3.6	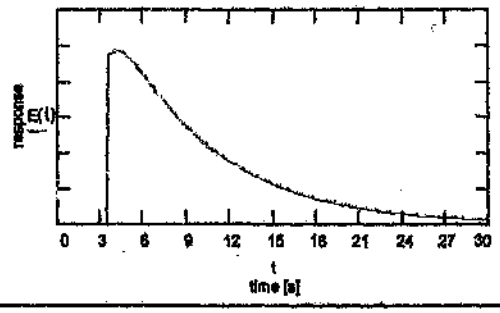
bottom, left	4	5.4	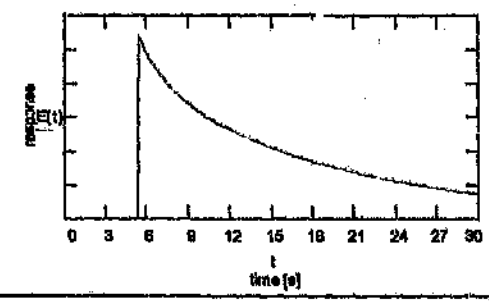
bottom, right	4	4.4	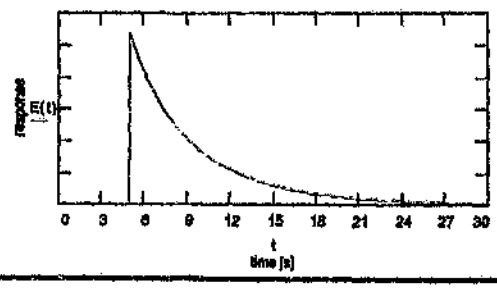

The detailed determinations of the furnace RTD's are provided in Appendix 1.3.

By summing the quotient of the vertical cell dimensions and upwards velocities predicted by AIOLOS at the furnace centre, an estimation of the minimum residence time (viz. the dead time) was made. These results are as presented in Table 6.

Table 6 : *Minimum Residence Times predicted by AIOLOS*

predicted minimum residence time	τ_d [s]
from top burner row	1.52
from centre burner row	2.42
from bottom burner row	4.01

It should be noted that the upwards velocities in the near burner regions would be less than at the furnace centre, which would explain why AIOLOS predicts considerably lower minimum residence times than were measured. An improved residence time prediction may be obtained if the vertical velocity components of a variety of furnace gas bundles were tracked. This would however require a dedicated sub-program within the post processor and was not attempted for the purpose of this investigation.

3.3 COAL PROPERTIES

As noted in section 2.3.1 of this report, both pf and raw coal from the mill feeder system were sampled. Proximate- and Ultimate analyses, as well as Calorific Value Determinations for the raw coal for various days of testing, are presented in Table 7.

Table 7 : *Properties of Raw Coal*

Property	31/01/96	01/02/96	05/02/96	07/02/96	08/02/96	17/02/96	25/02/96
[% by mass, air dried]							
Inherent Moisture	3.5	3.5		3.5	3.4	3.6	3.7
Ash	24.3	25.6	23.8	24.8	26.4	23.4	24.1
Volatile Matter	22.5	22.3	22.2	22.7	22.3	23.7	22.2
Fixed Carbon (by difference)	49.7	48.6	50.4	49.0	47.9	49.3	50.0
[% by mass, air dried]							
C	58.82	57.41	58.68	58.56	56.79	58.94	58.69
H	2.90	2.80	2.83	2.87	2.80	2.95	2.85
N	1.40	1.35	1.40	1.37	1.32	1.40	1.39
S	0.69	1.09	0.71	0.76	0.89	0.76	0.88
Carbonates	0.57	0.61	0.66	0.37	1.04	1.10	0.61
Oxygen (by difference)	7.82	7.64	8.33	7.77	7.36	7.85	7.98
Gross CV, [MJ/kg, air dried]	23.05	22.47	23.05	22.76	22.24	23.20	22.97

The basic chemical analyses of the pf samples taken as well as particle size analysis on each mill are shown in Table 8. Due to problems encountered by power station staff with the pf sampling equipment, pf samples could not be obtained after 9 February 1996.

Table 8 : *Properties of Pulverised Coal*

Property	31/01/96	01/02/96	05/02/96	07/02/96	08/02/96
[% by mass, air dried]					
Inherent Moisture	2.9	2.6	2.9	2.8	2.7
Ash	25.1	24.0	25.1	23.5	23.1
Volatile Matter	24.2	24.3	22.8	25.2	14.9
Fixed Carbon (by difference)	47.8	49.1	49.2	48.7	49.3
[% by mass, air dried]					
C	57.92	59.09	59.17	59.76	60.34
H	3.13	3.01	3.30	3.89	3.50
N	1.36	1.38	1.51	1.57	1.54
S	0.88	0.80	0.96	0.83	0.80
Carbonates	0.59	0.63	0.71	0.82	0.85
Oxygen (by difference)	8.12	8.49	6.35	7.03	7.17
Gross CV, [MJ/kg, air dried]	22.65	23.19	22.72	23.63	22.99
Particle Size Distribution	%	%	%	%	%
Mill A, <38 µm	64	25	63	64	43
38-75 µm	20	27	22	17	32
>75 µm	16	48	15	19	25
Mill B, <38 µm	47	74	31	78	-
38-75 µm	28	17	37	14	-
>75 µm	25	9	32	8	-
Mill C, <38 µm	-	-	-	-	44
38-75 µm	-	-	-	-	31
>75 µm	-	-	-	-	25
Mill D, <38 µm	49	65	39	78	72
38-75 µm	23	23	27	17	15
>75 µm	28	12	34	5	13
Mill E, <38 µm	32	-	40	44	42
38-75 µm	30	-	29	27	25
>75 µm	38	-	31	29	33
Mill F, <38 µm	46	54	74	73	49
38-75 µm	25	23	16	17	24
>75 µm	29	23	10	10	27

Detailed particle size analyses of the above pulverised coal samples have been attached in Appendix 2.3.

The R.C. Composite sample was subjected to a more extensive set of analyses, the results of which are presented in Table 9. Note that a kinetic summary for char combustion is included and will be referred to in section 3.5 of this report. Appendix 2.1 contains the detailed derivation of the kinetic parameters listed in Table 9.

Table 9 : *Coal Properties Summary for R.C. Composite*

Total Moisture : (as received)	9.8			
Proximate :	air dried	as received	dry	daf
Moisture	3.5	**9.8**		
Ash	25.0	**23.4**	25.9	
Volatiles	22.8	21.4	23.6	**31.9**
Fixed Carbon	48.7	45.4	50.5	**68.1**
Ultimate :				
Carbon	58.76	**55.06**	60.89	82.18
Hydrogen	3.02	**2.83**	3.13	4.22
Nitrogen	1.39	**1.30**	1.44	1.94
Sulphur	0.76	**0.71**	0.79	1.06
Carbonates	0.76	0.71	0.79	1.06
Oxygen	6.81	6.16	7.06	9.52
Oxygen + Carbonates		**6.87**		
Calorific Value	22.69	21.26	23.51	**31.73**
DTF DEVOLATILISATION				
Volatile Matter	28.025			
Q Factor[2]	**1.229**			
DTF FULL TEST				
Size Fraction	<38 µm	38-75 µm	< 75 µm	Unit
Pre-exponential Factor	4269	70549	3212	kg/m^2.s.atm
	4213	**69626**	**3170**	kg/m^2.s.bar
Activation Energy	144.5	181.6	132.98	kJ/mol
Activation Energy /R	**17380**	**21843**	**15995**	K

[2] When a coal is devolatilised at higher temperatures (and heating rates) than would be typical for a Proximate analysis, the coal produces a higher yield of volatile matter. The Q Factor accounts for this difference and is the ratio of the volatiles produced under simulated furnace conditions and the volatiles produced in laboratory standard Proximate analysis.

Further furnace simulations were performed with coal sampled from the feeder belt of the run of mine Washing Plant at the colliery that provides Hendrina Power Station with coal. These simulations were performed to assess the effect of coal with differing char combustion kinetics on furnace conditions. This coal is referred to as 'Washing Plant Feed'. Its properties summary is presented in Table 10, while Appendix 2.2 contains the derivations of the kinetic parameters.

Table 10 : *Coal Properties Summary for Washing Plant Feed*

Total Moisture : (as received)	8.7			
Proximate :	air dried	as received	dry	daf
Moisture	2	**8.70**		
Ash	29.6	**27.62**	30.20	
Volatiles	24.4	22.77	24.90	**35.67**
Fixed Carbon	44	40.92	44.90	**64.33**
Ultimate :				
Carbon	56.24	**52.47**	57.39	82.22
Hydrogen	3.34	**3.12**	3.41	4.88
Nitrogen	1.4	**1.31**	1.43	2.05
Sulphur	0.84	**0.78**	0.86	1.23
Carbonates	0.53	**0.49**	0.54	0.77
Oxygen	6.05	**5.51**	6.17	8.85
Oxygen + Carbonates		**6.01**		
Calorific Value	22	20.53	22.45	**32.16**
DTF DEVOLATILISATION				
Volatile Matter	29.92			
Q Factor	**1.226**			
DTF FULL TEST				
Size Fraction	<38 µm	38-75 µm	< 75 µm	Unit
Pre-exponential Factor	208	1077	286	$kg/m^2.s.atm$
	205	**1063**	**282**	$kg/m^2.s.bar$
Activation Energy	101.66	124.9	99.45	kJ/mol
Activation Energy /R	**12228**	**15023**	**11962**	K

3.4 ASSESSMENT OF THE AIOLOS DEVOLATILISATION MODEL

The results of the DTF tests performed to characterise the devolatilisation behaviour of the Hendrina R.C. Composite sample and the analysis to determine the kinetic parameters of the single step, temperature dependant reaction model used in AIOLOS are attached in Appendix 2.1.

Figure 29 shows the graphs of extent of devolatilisation vs. residence time for both size fractions tested, while Table 11 lists the kinetic parameters of the devolatilisation of the R.C. Composite coal.

Table 11 : *Kinetic Parameters of the Devolatilisation Process*

Size Fraction	< 38 µm	38 - 75 µm	AIOLOS Default
Pre-exponential Factor [1/s]	61.1	4.63	1.5E5
Activation Energy [kJ/mol]	49.7	11.6	74

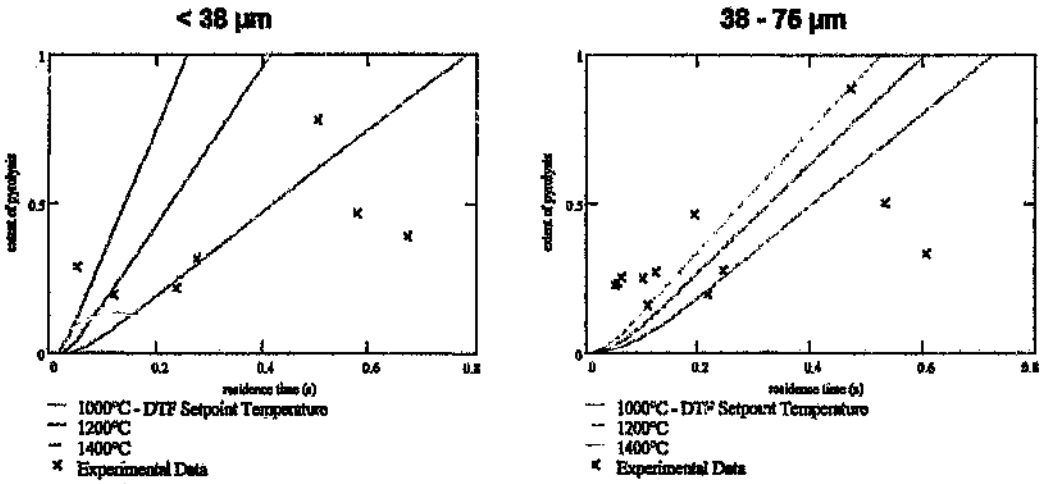

Figure 29 : *Coal Devolatilisation in DTF*

It was found that when the DTF devolatilisation kinetics were specified in the combustion model, the char combustion process was not activated. The AIOLOS default values were subsequently used.

In order to validate the DTF results, devolatilisation tests should be carried out on more Eskom coals. In the event of the presented results being confirmed, the devolatilisation model used in AIOLOS would have to be revisited and modified as in its current form the model clearly does not describe the devolatilsation process satisfactorily.

3.5 ASSESSMENT OF AIOLOS CHAR COMBUSTION MODEL

The char combustion model used in AIOLOS is based on the same model used in the determination of DTF kinetic parameters, and as such should be suitable for Eskom use. A model of the DTF utilising the char combustion model found in AIOLOS produces reasonable predictions of the experimental data. The kinetic parameters of

the R.C. Composite sample and the Washing Plant Feed have been summarised in Tables 9 and 10 respectively. Figures 30 and 31 show the predicted burnout profiles and DTF data of R.C. Composite sample used to determine the kinetic parameters, while Figures 32 and 33 do so for the Washing Plant Feed. The burnout profiles should ideally pass through the DTF data points given a certain DTF setpoint temperature.

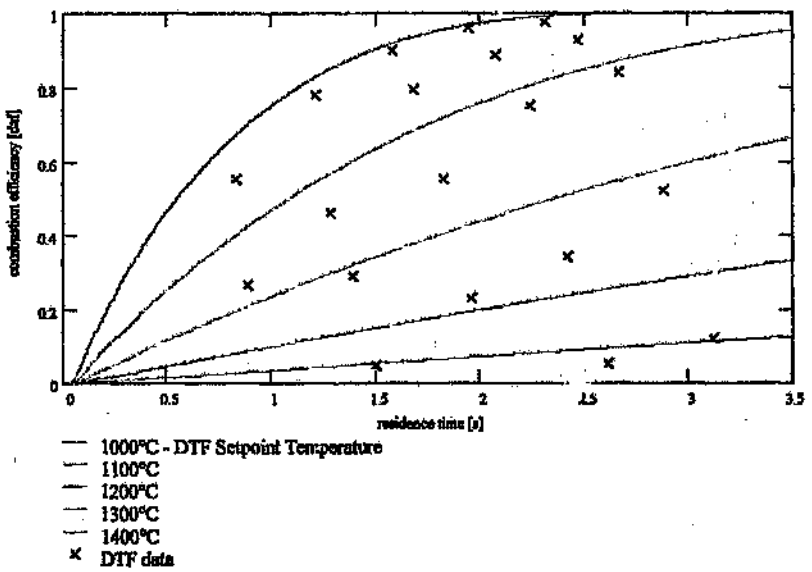

Figure 30 : ***Combustion Extent vs. time - R.C.Composite < 38 µm***

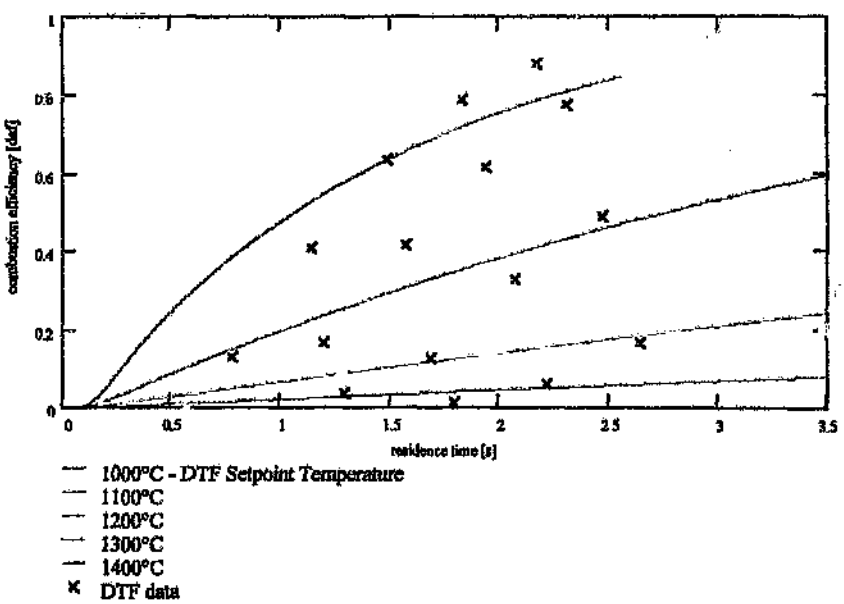

Figure 31 : ***Combustion Extent vs. time - R.C.Composite 38-75 µm***

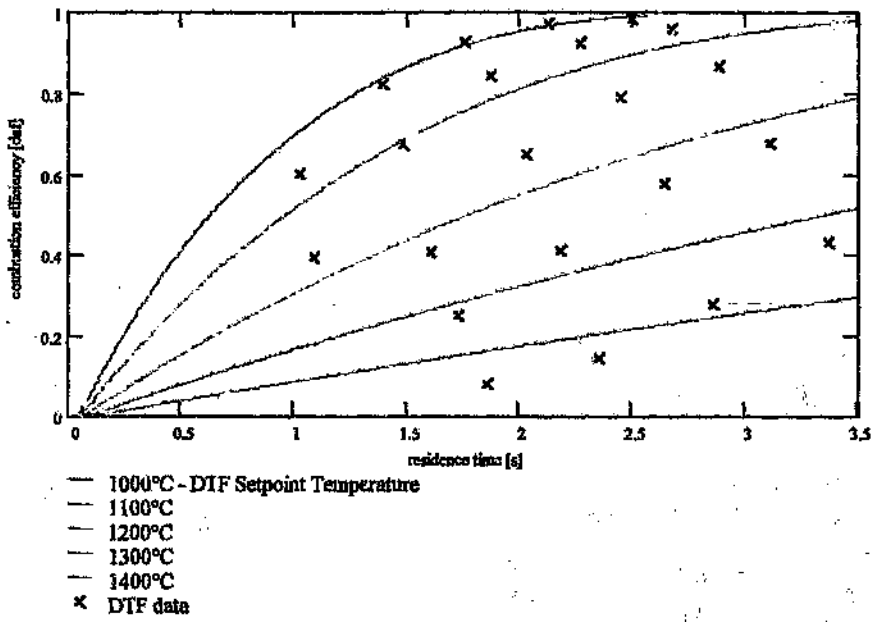

Figure 32: ***Combustion Extent vs. time - Washing Plant Feed.< 38 µm***

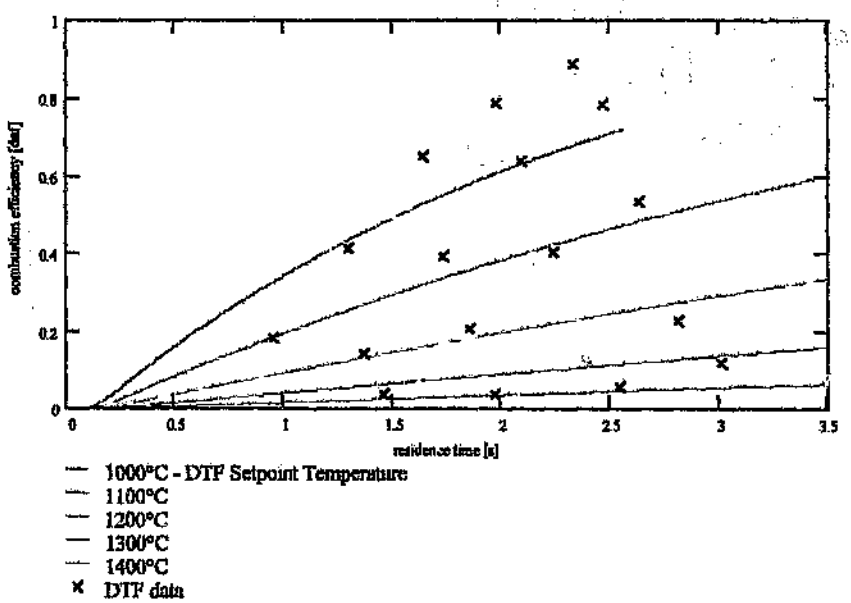

Figure 33 : ***Combustion Extent vs. time - Washing Plant Feed. 38-75 µm***

3.6 COMPARISON OF PREDICTED AND MEASURED FURNACE DATA

Contour plots of furnace conditions are shown for various furnace levels as indicated on the isometric diagrams of the furnace. The contour plots also show the position and results of measurements. For the purpose of comparing experimental and measured data, graphs of experimental vs. measured data are shown as well.

3.6.1 Furnace Exit Conditions :

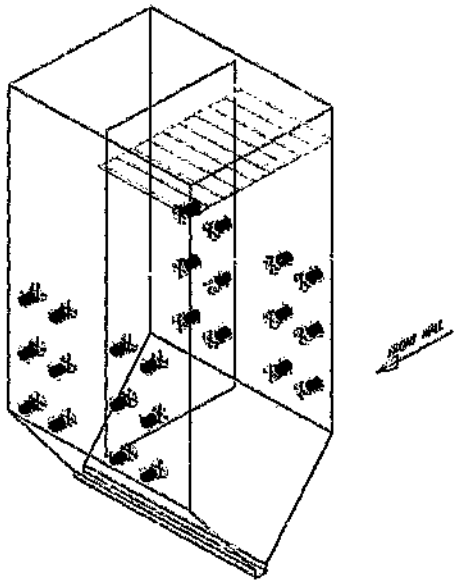

Figure 34 : ***Isometric View of Furnace showing the horizontal furnace plane at which data is presented***

3.6.1.1 Gas Temperatures :

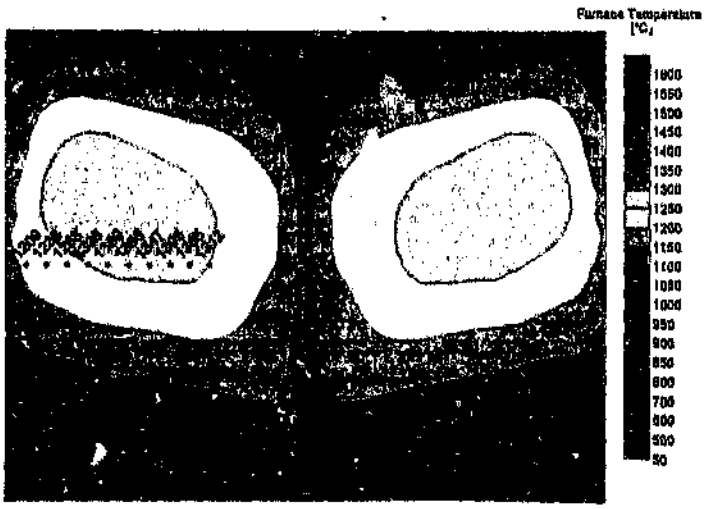

Figure 35 : ***Contour Plot of Furnace Exit Gas Temperature [°C]***

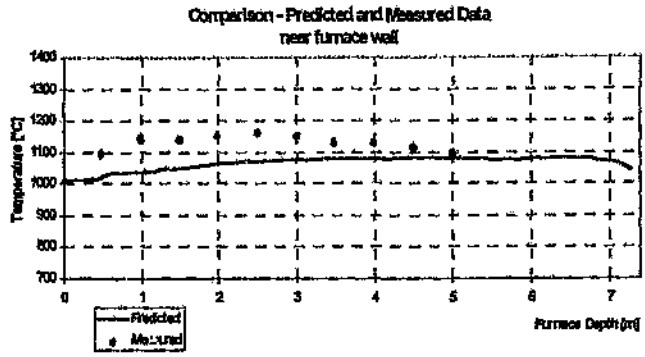

Figure 36 : *Furnace Exit Temperatures [°C]*

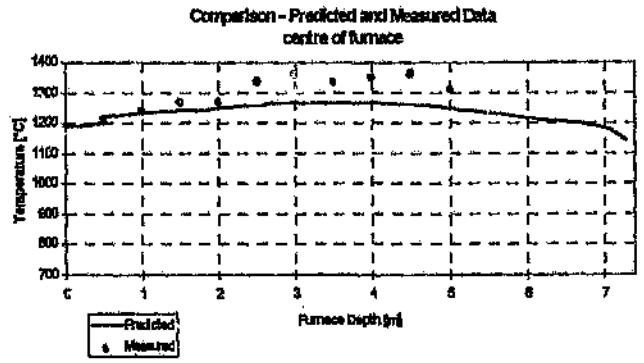

Figure 37 : *Furnace Exit Temperatures [°C]*

The furnace exit temperatures are an important indicator of furnace performance because high furnace exit temperatures suggest furnace under-performance which leads to high temperatures in the convective region of the boiler which, in turn, results in accelerated ageing of convective heat exchangers, fouling and possible control problems. High furnace exit temperatures may result from :

- delayed combustion in the furnace (typically from unreactive coal feedstocks or feedstocks that are not suited to that particular furnace design because the furnace residence times may be too short)
- over-firing (in which case some of the evaporator is used as a superheater)
- impaired radiative and convective heat transfer in the furnace region (caused primarily by insulating or reflective deposits on the furnace walls)

The predicted results tend to be lower than the measured temperatures. It should however be kept in mind that the fluctuactions in temperature at one point in the furnace exceeded the variance between predicted and measured data. The uncertainty in furnace temperature measurement together with the uncertainty of

some of the boundary conditions, particularly the ash deposit emissivity and the coal properties, may make predicting absolute furnace gas temperatures difficult. The effect of changes in coal combustion properties on combustion conditions has been explored, the results of which are presented 3.7 of this report.

3.6.1.2 Gas Flow Velocities

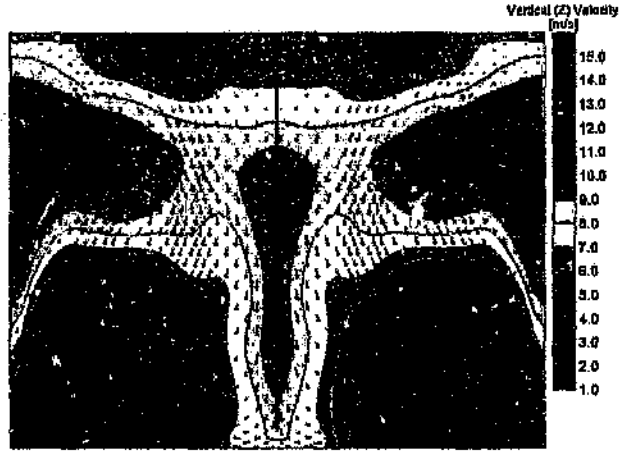

Figure 38 : ***Contour Plot of vertical velocities and Vector Plot of horizontal gas velocities. Peak horizontal velocity (represented by longest arrow) : 4.78 m/s***

The velocity distributions at the furnace exit should ideally be uniform - i.e. little or no variation in vertical velocity as this is the ideal condition for a convective pass heat exchange- viz. no skew flow. The furnace exit velocities in Figure 38 show quite clearly the effect of having only one row of the top burner rows in operation and how this results in skewing the flow at furnace exit.

3.6.1.3 O_2 Concentrations

By the furnace exit, combustion of the pulverised coal should be complete. This means that the furnace exit oxygen concentration should be consistent with the oxygen concentration measured at the economiser outlet (except for tramp O_2). More importantly however, mixing of the combustion product should be good at furnace exit so that a fairly uniform O_2 distribution should be observed.

The predicted and measured O_2 concentrations show a very good agreement, suggesting that the model describes the combustion process with respect to O_2 consumption satisfactorily.

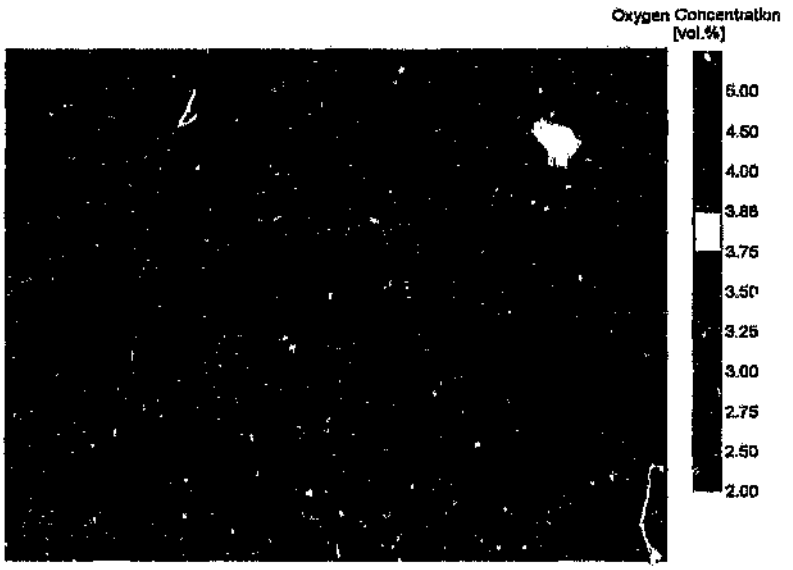

Figure 39 : ***Contour Plot of Furnace Exit Oxygen Concentrations***

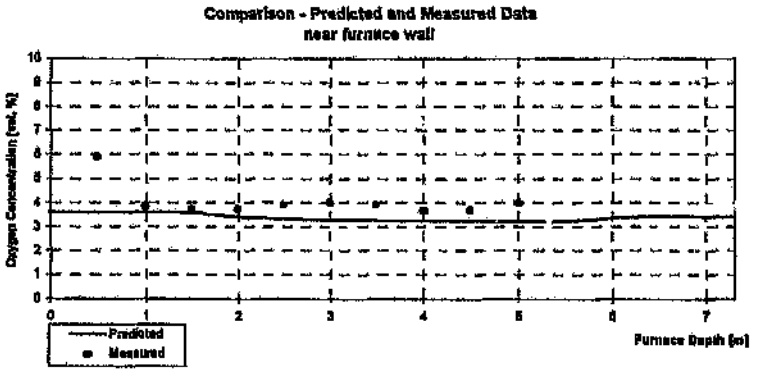

Figure 40 : ***Furnace Exit Oxygen Concentrations***

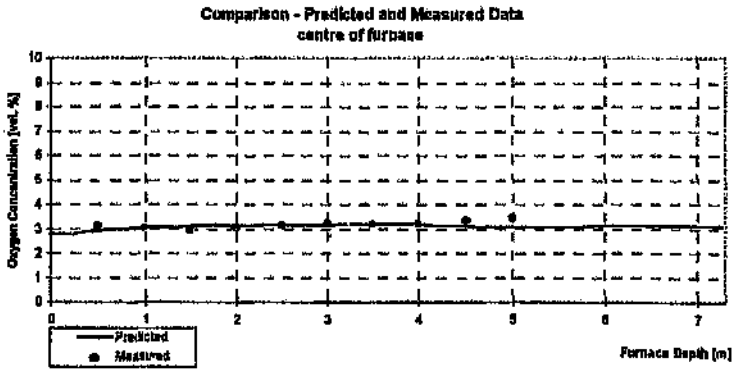

Figure 41 : ***Furnace Exit Oxygen Concentrations***

One anomaly (@ O_2 = 5.86%) is however evident in Figure 40, but is most likely attributable to an experimental error.

3.6.1.4 CO Concentrations

The CO concentrations predicted by the model were significantly higher than the measured values at furnace exit. Both the experimental technique used for the experimental measurement as well as the model should be revisited to determine the reason for these deviations.

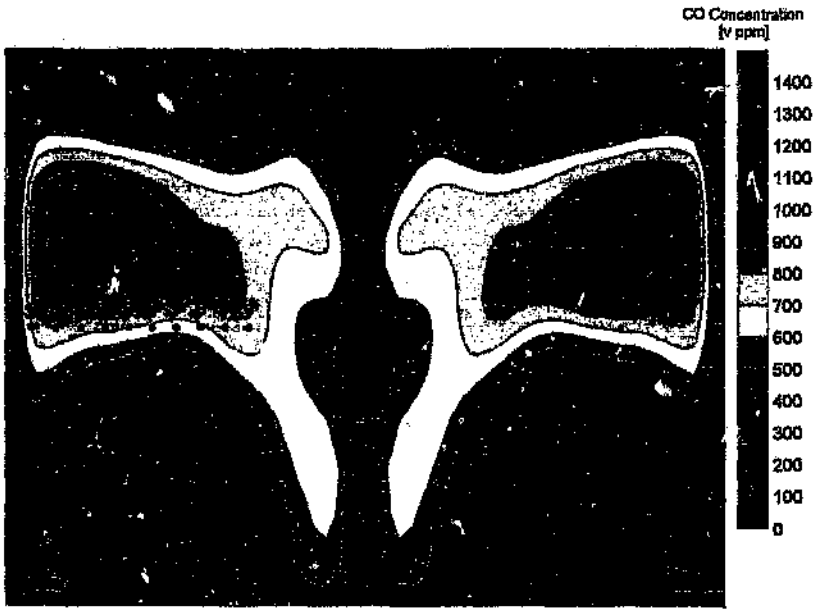

Figure 42 : *Contour Plot of CO Concentrations [vol. ppm]*

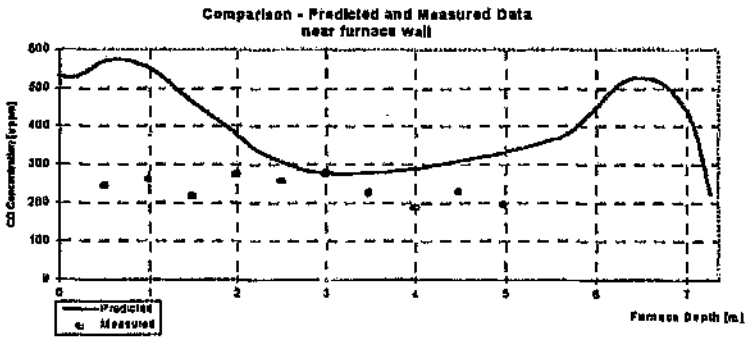

Figure 43 : *CO Concentrations*

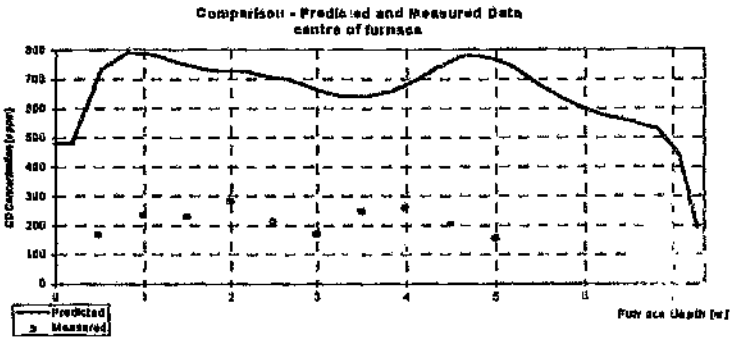

Figure 44 : ***CO Concentrations***

3.6.1.5 NOx Concentrations

The NOx predictions and measurements correspond very well suggesting that the NOx model in the combustion code functions for over stoichiometric combustion. Further validation of the NOx code will be required for sub-stoichiometric conditions, which would be needed to evaluate possible low-NOx strategies. Further validation work is planned when the Australian Combustion Technology Centre's (ACTC) NOx test furnace is modelled with a variety of primary stoichiometries fueled by Eskom feedstocks.

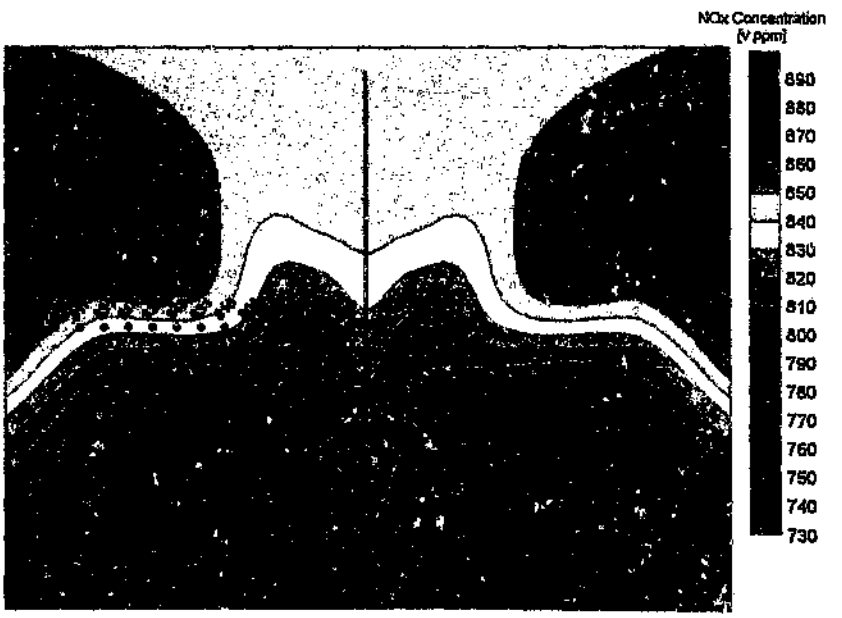

Figure 45 : ***Contour Plot of NOx Concentrations [vol. ppm]***

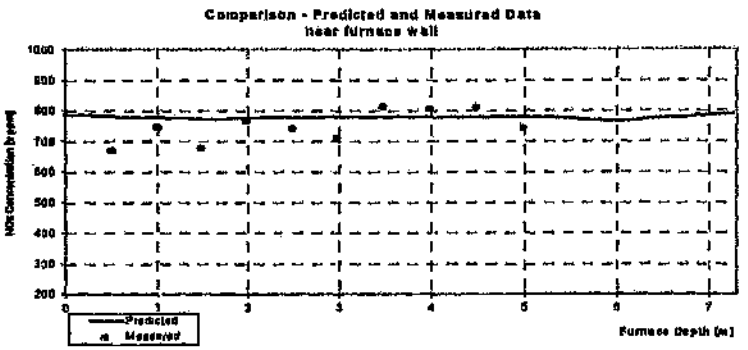

Figure 46 : *NOx Concentrations*

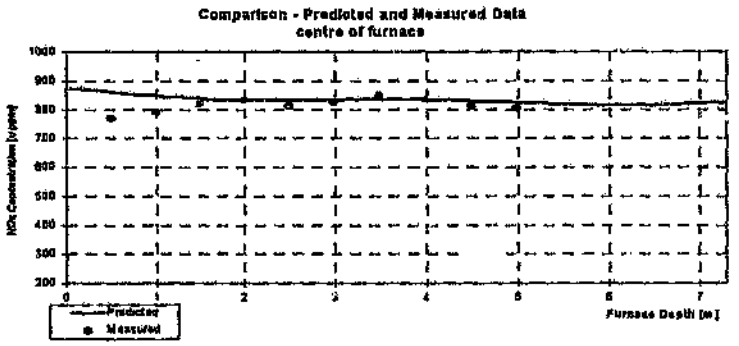

Figure 47 : *NOx Concentrations*

3.4.2 Top Burner Row

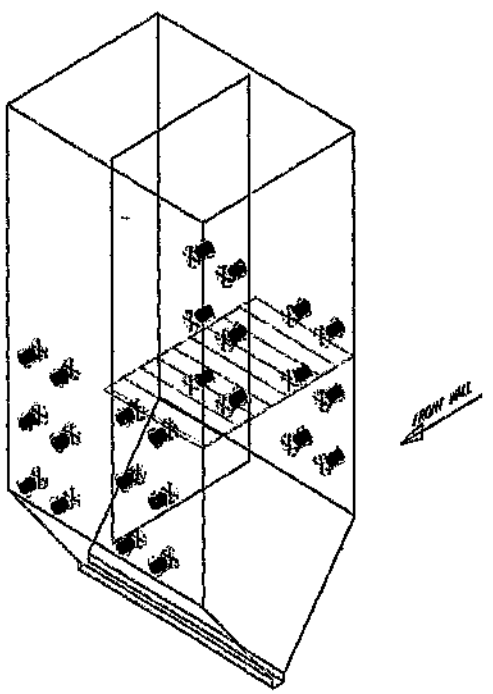

Figure 48: ***3D view furnace : hatched horizontal plane indicates level at which data is presented and measurements were made***

3.6.2.1 Gas Temperatures

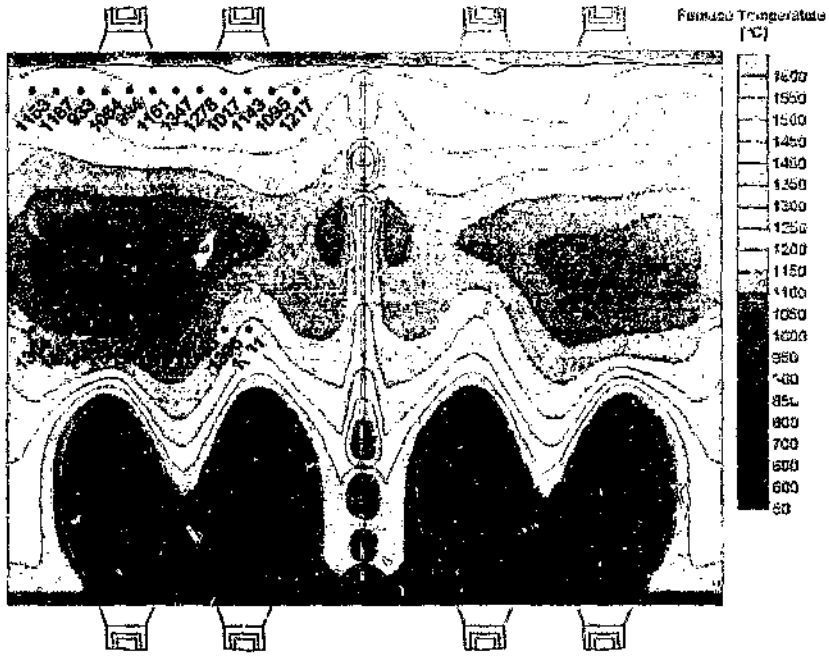

Figure 49 : ***Contour Plot of Furnace Temperatures on the top burner level***

There is a good agreement between predicted and measured gas temperatures on the top burner level. The results do however suggest that an even hotter region exits than the measurements showed with temperatures exceeding 1500°C.

A concern is noted about the considerable penetration of the relatively cold inlet streams through the top burner row. This would lead to poor predictions of other combustion properties in the near burner regions.

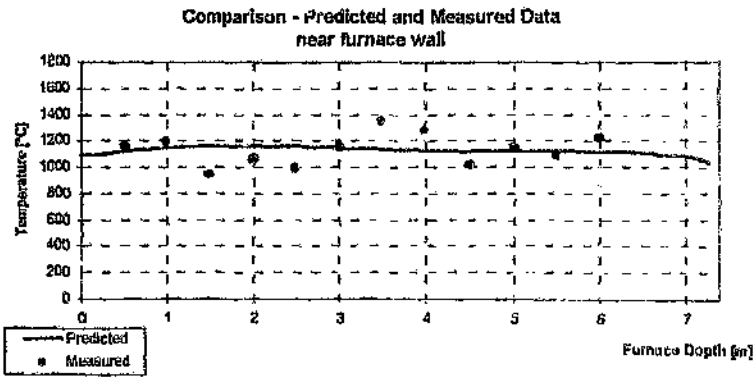

Figure 50 : ***Furnace Temperatures [°C]***

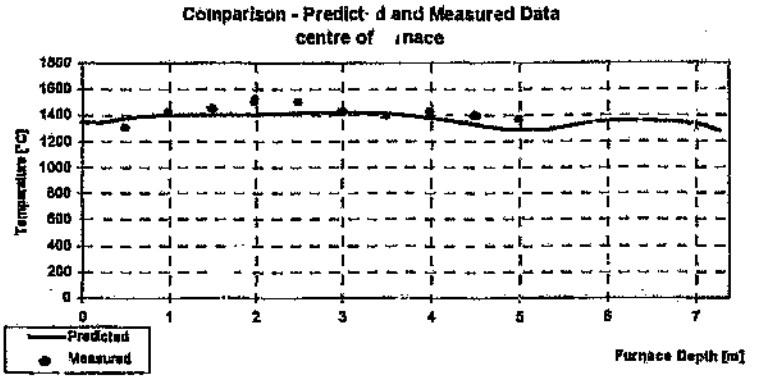

Figure 51 : ***Furnace Temperatures [°C]***

3.6.2.2 Gas Flow Velocities

The contour plot of the vertical velocity component (refer to Figure 52) shows the downwards flow between the burner pairs clearly. The horizontal flow pattern shows the well defined recirculation zones on either side of the operational burner pairs. An internal recirculation zone is not apparent from the results due to the near burner zone not being discretised sufficiently finely. The combustion model's local grid refinement capability may improve the results so that investigations into burner stability and design may be performed. It must however be noted that the burner itself may be modelled with the combustion code in question. Note also the less defined recirculation zones on either side of the out of commission burner pairs. This recirculation zone is caused by the strong recirculation of the operational burners 4m below.

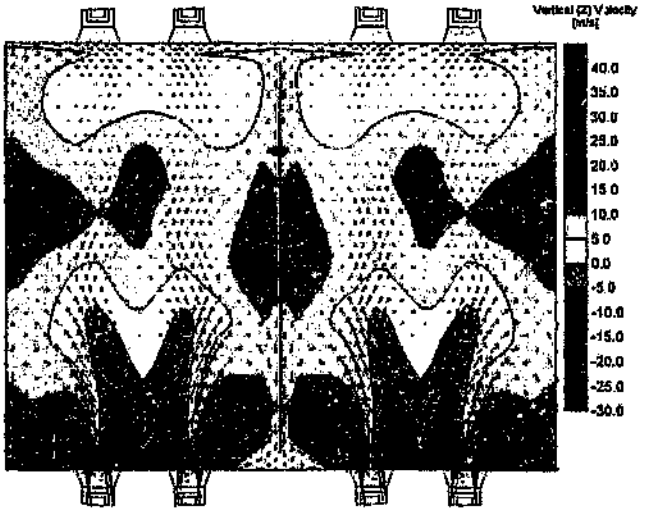

Figure 52 : ***Contour Plot of vertical velocities and Vector Plot of horizontal gas velocities. Peak horizontal velocity (represented by longest arrow) : 57.8m/s***

3.6.3 Middle Burner Row

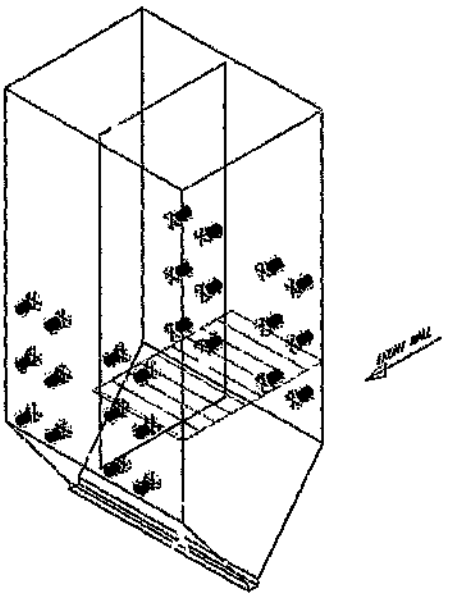

Figure 53: ***3D view of furnace (hatched horizontal plane indicates level at which data is presented and measurements were made)***

3.6.3.1 Gas Temperatures

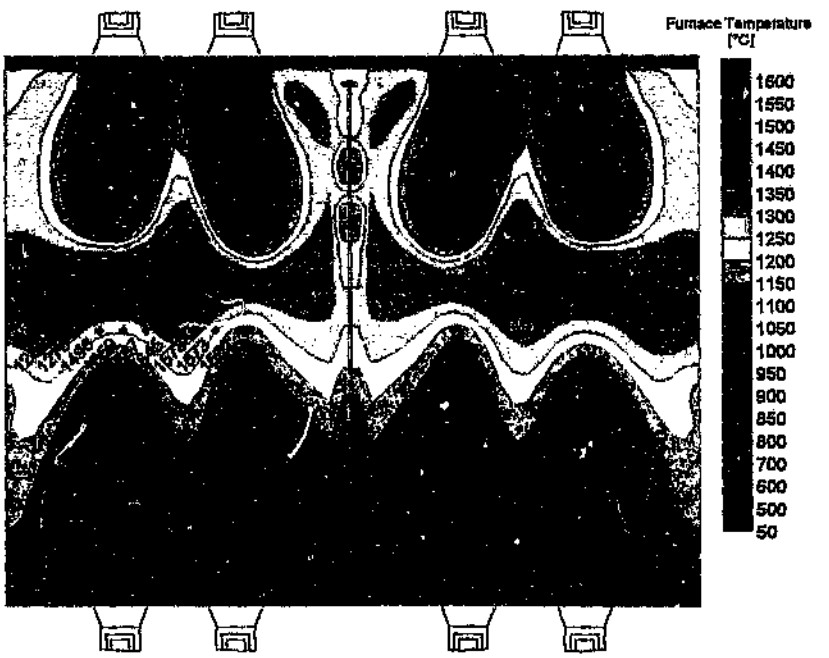

Figure 54 : ***Contour Plot of Furnace Temperatures on middle burner row***

The concern noted in 3.2.1 (see Figure 52) about the relatively deep penetration into the furnace of inlet streams through the burners has in this case (refer Figure 54) a bearing on the predicted furnace centre temperature results which are lower than the measured ones. The contour plot (refer Figure 54) does however show a significantly hotter region away from the centre of the furnace, which could be caused by the mode of operation in which one of the top burner rows was out of commission.
The fact that a considerable deviation in measured and predicted results exists suggest that the burner boundary conditions may have been specified incorrectly.

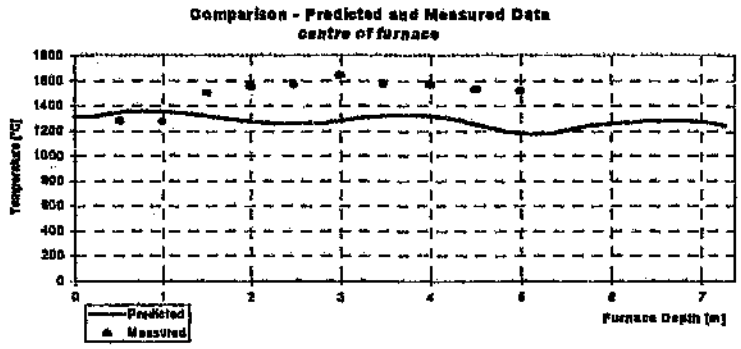

Figure 55 : ***Furnace Temperature [°C]***

3.6.3.2 Gas Flow Velocities

Here again the contour plot of the vertical velocity component (refer to Figure 56) shows a well defined downwards flow between the burner pairs and the upward flow on either side thereof. Note also the recirculation zones on either side of the burner pairs and the flow directed towards the walls. Given high particle temperatures, there is a possibility of slag formation on the furnace walls. At the time of testing significant slag deposits were not however observed.

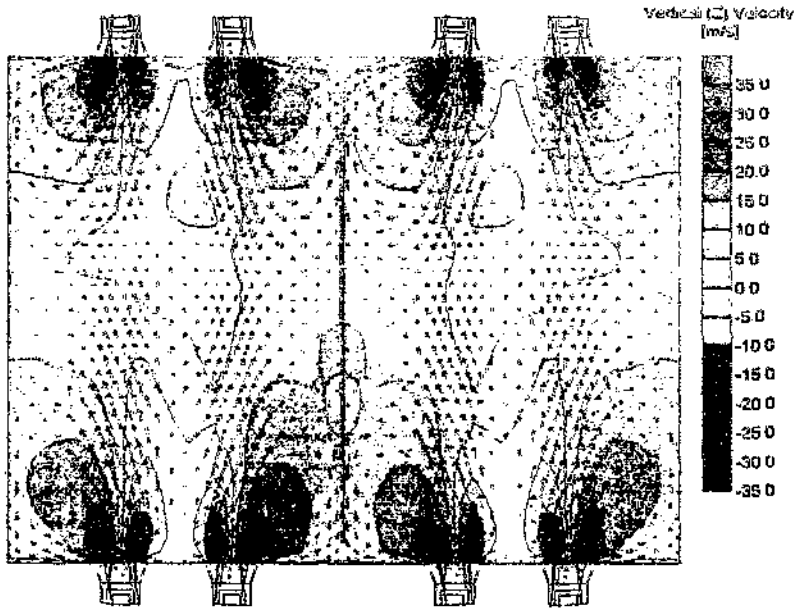

Figure 56 : ***Contour Plot of vertical velocities and Vector Plot of horizontal gas velocities. Peak horizontal velocity (represented by longest arrow) : 57.8m/s***

3.6.4 Bottom Burner Row

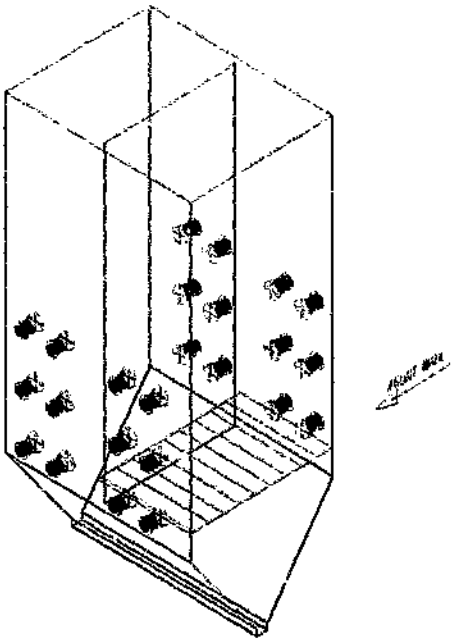

Figure 57 : *3D view of furnace : hatched horizontal plane indicates level at which data is presented and measurements were made*

3.6.4.1 Gas Temperatures :

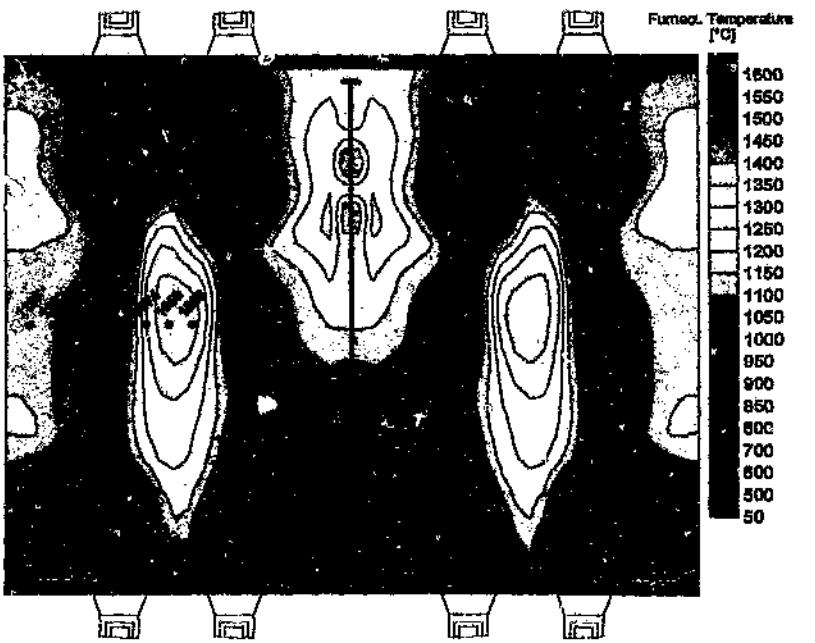

Figure 58 : *Contour Plot of Furnace Gas Temperatures - bottom burner row*

Note the skewness of the flame temperature contours (refer to Figure 58) on only one side of the furnace and further the difference in gas temperatures along the division wall of the furnace. This is due to the flow patterns having been established as a result of having one of the top burner rows out of operation (refer to Figures 52, 56 and 61).

Figures 59 and 60 show a good agreement between measured and predicted furnace temperatures. As mentioned before, the measurement of furnace gas temperatures near the burners was difficult in view of the fact that the conditions are not uniform and stable. Particularly the flame regions are highly turbulent and to obtain constant temperature readings is not possible.

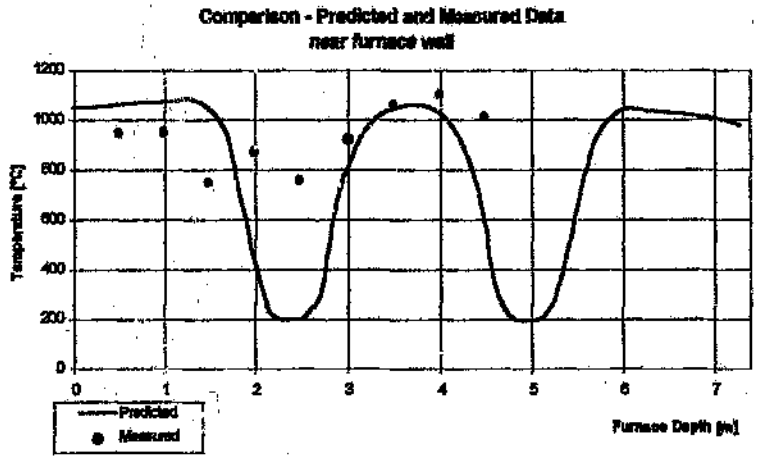

Figure 59 : ***Furnace Gas Temperatures [°C]***

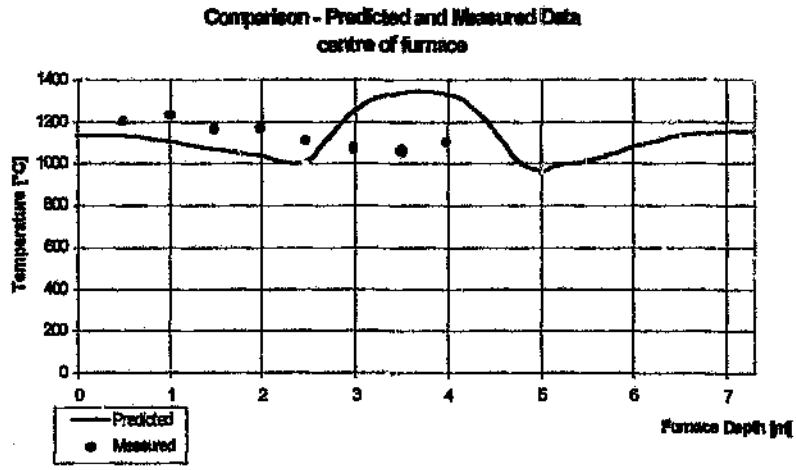

Figure 60 : ***Furnace Gas Temperatures [°C]***

3.6.4.2 Gas Flow Velocities

Similar gas flow patterns to the middle burner level are predicted for this burner level with the exception of the large area of downwards flow between the burner pairs on the rear furnace wall (refer to Figure 61). These results suggest that the burner pairs on the rear wall penetrate the furnace through it's centre while the front wall burners

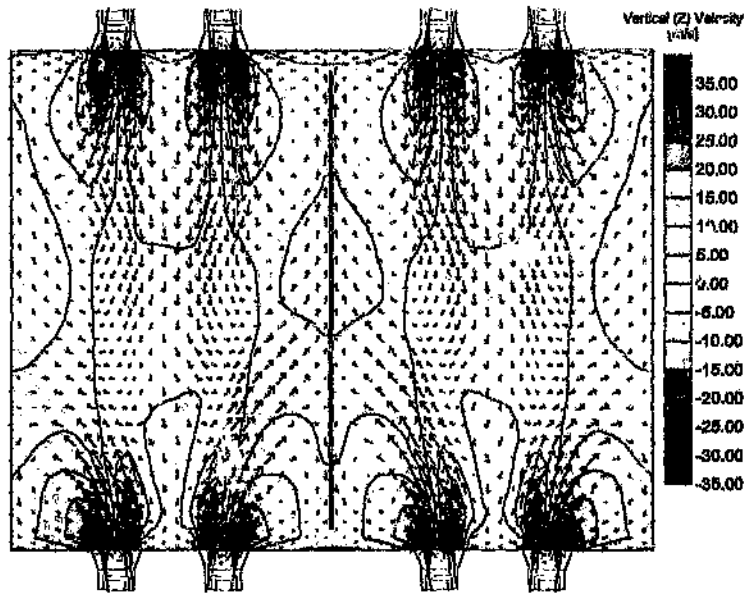

Figure 61 : ***Contour Plot of vertical velocities and Vector Plot of horizontal gas velocities. Peak horizontal velocity (represented by longest arrow) : 57.6m/s***

have their swirling flow deflected to either side of the stream emanating from the rear wall burners toward the furnace walls. This may be caused by the fact that the top row on the rear wall was not in operation which would allow the establishment of the observed flow pattern.

3.6.5 Furnace Heat Fluxes

The heat fluxes through the furnace water wall were measured using heat flux probes situated on the left wall of the furnace. These were found to be generally low compared to heat fluxes measured at Matimba using identical devices. Further, the furnace temperatures at Hendrina were significantly higher than furnace temperatures measured at Matimba. Low heat fluxes and high furnace temperatures suggests that Hendrina's furnace heat transfer is impaired. Since approximately 90% of the heat transfer in the furnace occurs by radiation, a possible explanation for this may be that the ash deposits either reflect the incident radiation back into the furnace or the deposit layer acts as an excellent insulator resulting in a much higher furnace surface wall temperature and a resultant reduction in furnace heat transfer. In specifying the boundary conditions for the furnace simulation it was therefore decided to assume an emissivity of 0.5 for the entire furnace instead of an emissivity of 0.65 to 0.7 which is normally assumed for a clean, operational furnace. Experimental techniques for the determination of wall emissivities should be explored.

Figure 62 shows an incident heat flux contour plot of the left wall of the furnace, as predicted by the combustion model, while the heat flux measurement data (actual heat flux through the furnace wall), as logged on 13 February 1996, of selected heat flux meters are shown as heat flux vs. time graphs. The arrow between the heat flux vs. time plot and the contour plot of the incident heat flux indicates the position of the probe on the furnace wall. The saw tooth type behaviour of the measured heat fluxes (refer to graph 1 and 3) indicates that when a reflective and/or insulating build up on the probe tips either falls off or is removed, a sudden heat flux increase is observed. The heat flux vs. time pattern exhibited in graphs 4 and 6 has been observed previously at Matimba for heat flux probes situated near wall blowers, as was also the case at Hendrina's Unit 9 furnace. The time of wall blowing corresponds with the sudden increase in heat flux. Note, however, the different lengths of time that the heat flux remains high after wall blowing. This is most likely a result of the different nature of the deposits at different points in the boiler, due mainly to variations in deposition temperature and impact velocity of combusting particles with the furnace wall surface.

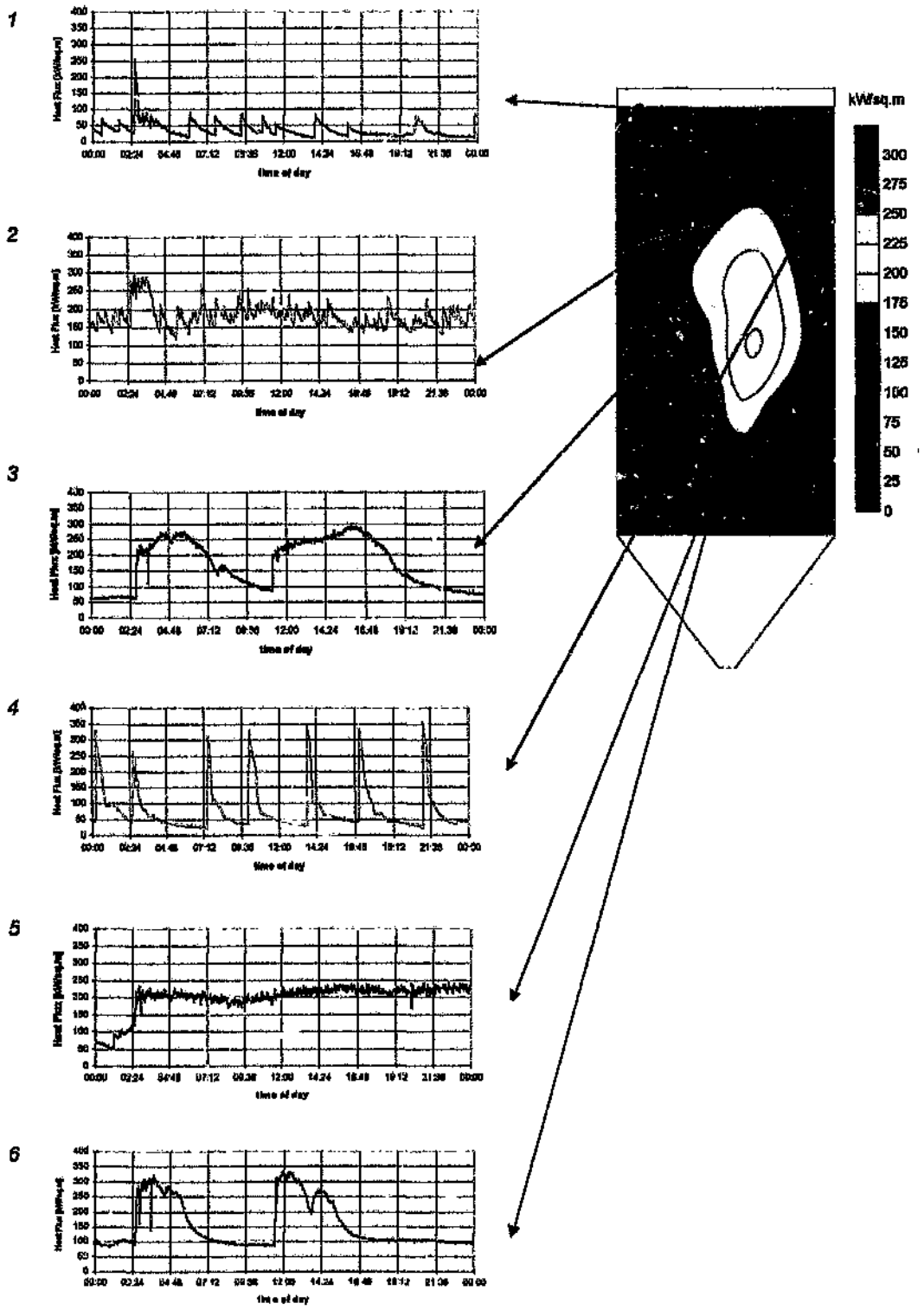

Figure 62: ***Predicted incident heat fluxes vs. measured heat fluxes through left furnace wall***

Figure 63 shows the incident heat flux distribution to all the furnace walls as predicted by the combustion model. Note the low heat flux intensities on the front wall burner belt, which has all three burner rows in operation. This is attributable to the pf absorbing much of the radiation directed towards the front wall.

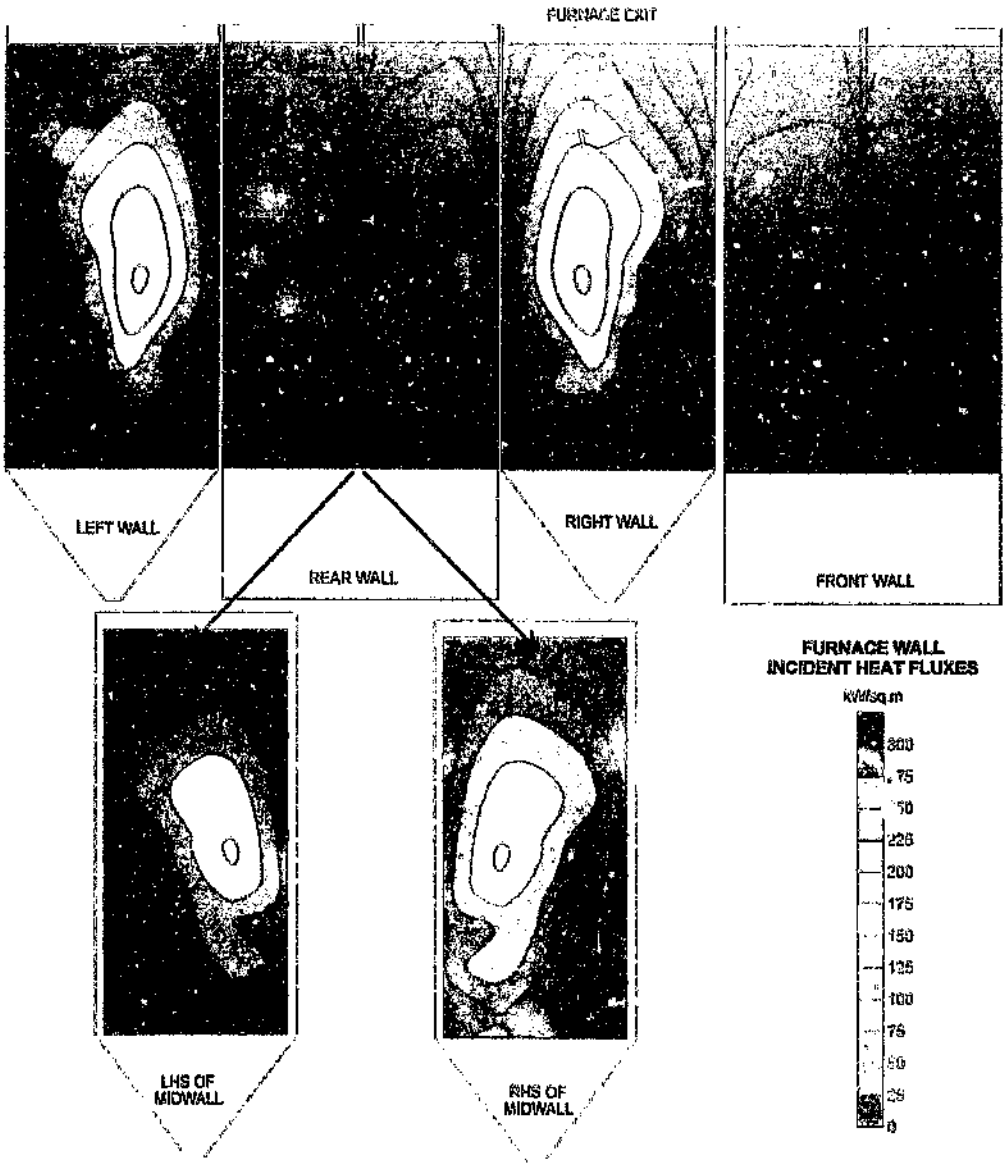

Figure 63: ***Incident heat flux to the furnace walls***

3.7 COMPARISON OF MODEL PREDICTIONS FOR DIFFERENT COAL FEEDSTOCKS

Combustion simulations were performed using the results of DTF characterisation of the Hendrina R.C. Composite and the Washing Plant Feed coals, to examine the sensitivity of the model to changes in a coal's combustion behaviour. Figure 64 shows the particle size class averaged burnout profiles of the coals in question.

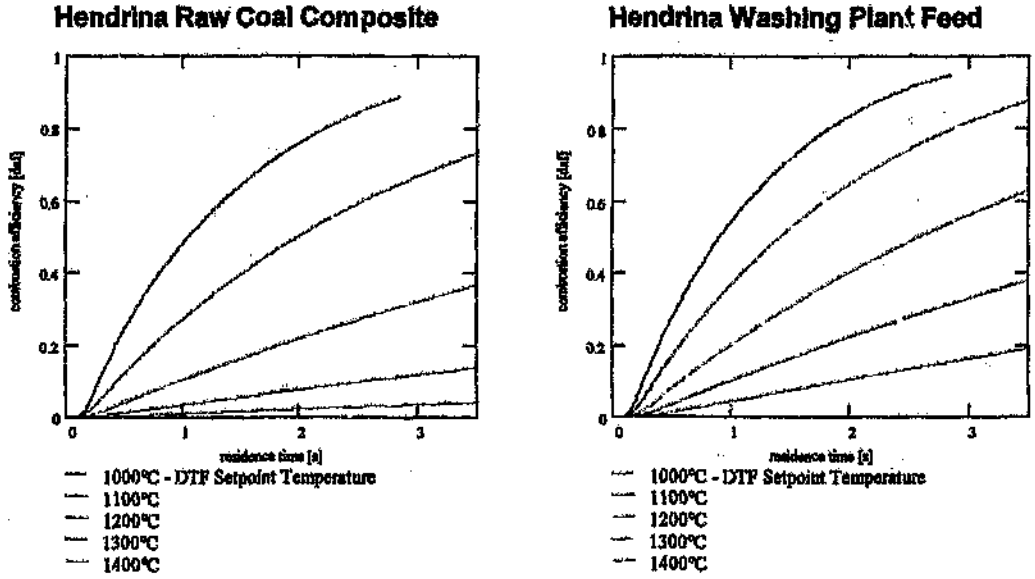

Figure 64 :
Burnout Profiles of Hendrina Feedstocks

The following simulation results show the effect of the different coals on furnace conditions.

3.7.1 Temperature Maps through the Furnace

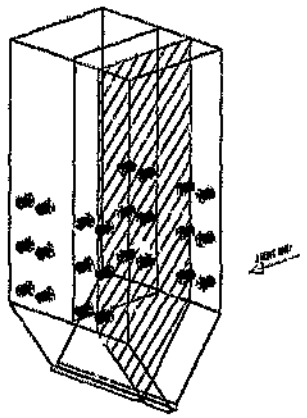

Figure 65 : ***Isometric View of Furnace showing the vertical furnace plane at which data is presented***

In order to compare the effect of a change in coal reactivity realistically, the input rate of coal for both simulations was adjusted so that the furnace exit oxygen concentrations were similar at around 3 - 3.5 % by volume (refer to Figure 67). Given identical primary and secondary air inlet flowrates, the input rate of more reactive coal (W.P. Feed) was less than the input rate of the less reactive coal (R.C. Composite), despite the W.P. Feed having a higher ash content. This is attributed to the W.P. Feed achieving a greater burnout by furnace exit.

Hendrina Raw Coal Composite **Hendrina Washing Plant Feed**

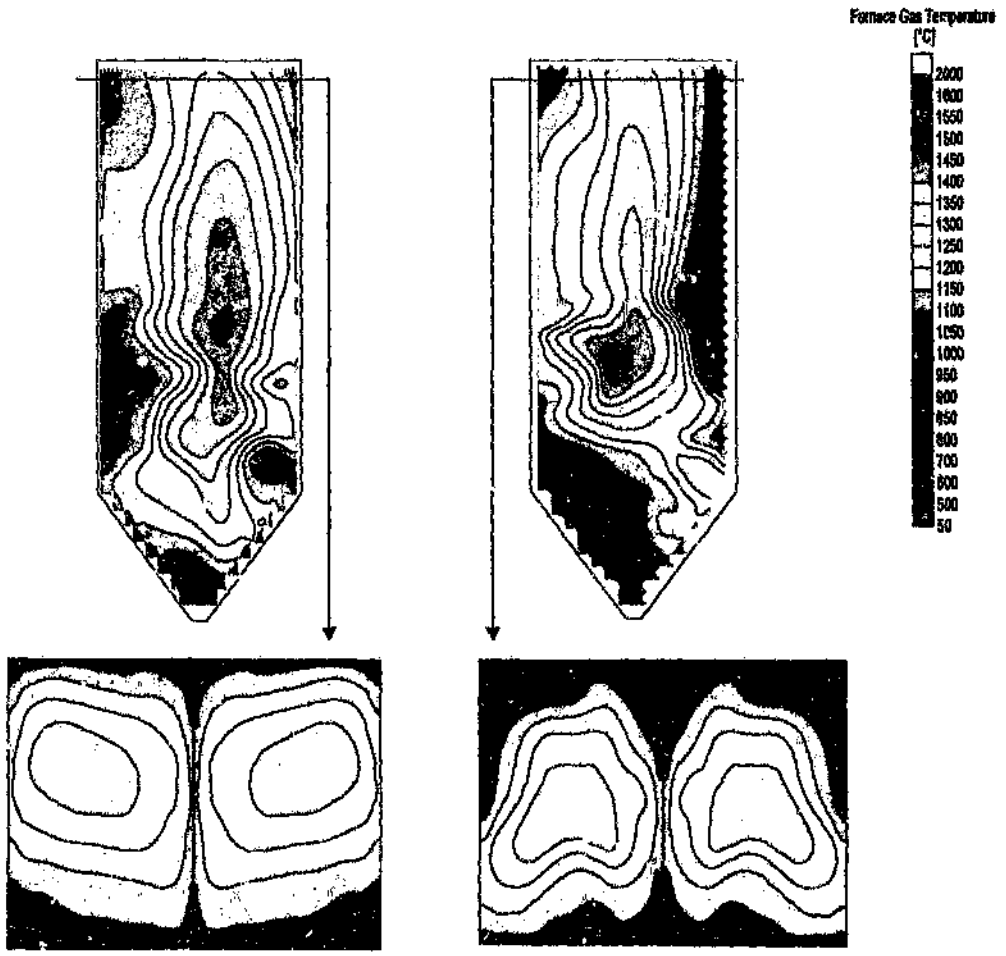

Figure 66 : ***Furnace Gas Temperature Maps***

Note also how the region where the temperature is greater than 1400°C concentrates much lower in the furnace for the W.P. Feed than for the R.C. Composite (refer to vertical temperature contour plots in Figure 66). The furnace exit temperatures are however comparable (refer to furnace exit temperature contours in Figure 66). It

should be noted however, that the more reactive coal achieved a higher furnace efficiency in view of the reduced carbon in ash, i.e. coal consumption.

3.7.2 O_2 Concentrations at Furnace Exit

Hendrina Raw Coal Composite **Hendrina Washing Plant Feed**

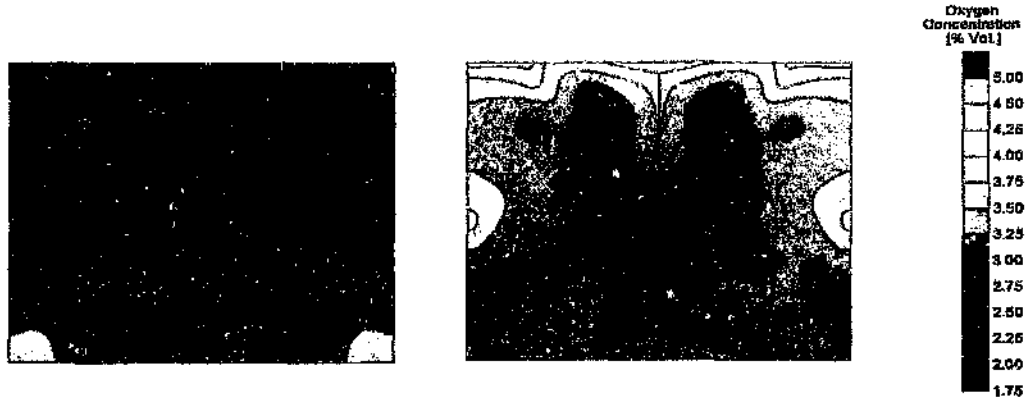

Figure 67 : *Furnace Exit O_2 Maps*

3.7.3 Heat Fluxes

Figure 68 shows heat flux contour plots onto the left wall for both feedstocks. Note how the more reactive feedstock shows high heatfluxes lower down in the furnace.

Hendrina Raw Coal Composite **Hendrina Washing Plant Feed**

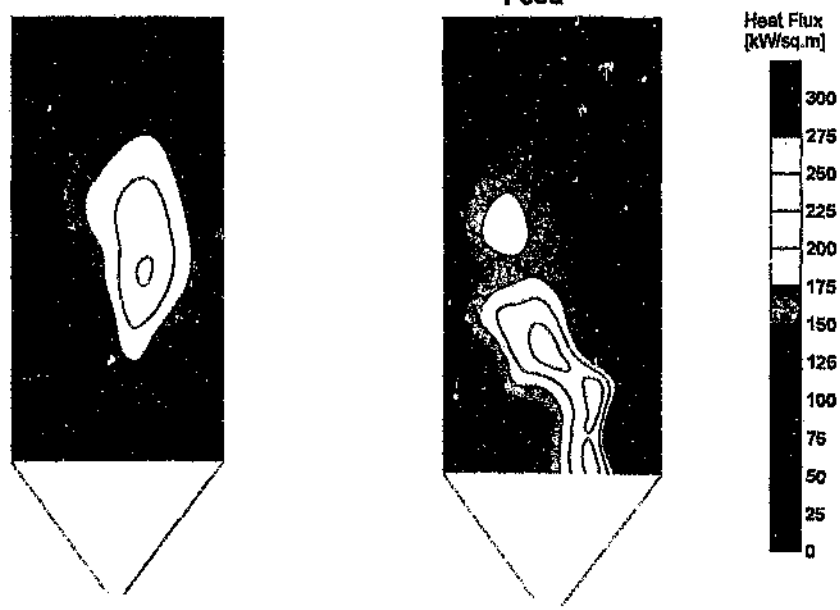

Figure 68 : *Furnace Heat Fluxes* ***(onto left wall)***

3.7.4 NOx Production

Most of the NOx originates from the oxidation of the nitrogen containing volatile species in the near burner zone as a direct result of the oxidising combustion conditions in this region. These conditions are typical for unstaged swirl burners. A significant difference in NOx levels at furnace exit was therefore not expected for the two coals. The simulation results (refer to NOx concentration contour plots in Figure 69) show this. Note, however, that the patterns of the contours differ. This is attributable to the differences in the flowfield, which depend strongly on the temperature distribution and, consequently, the density of combustion products in the furnace.

Hendrina Raw Coal Composite **Hendrina Washing Plant Feed**

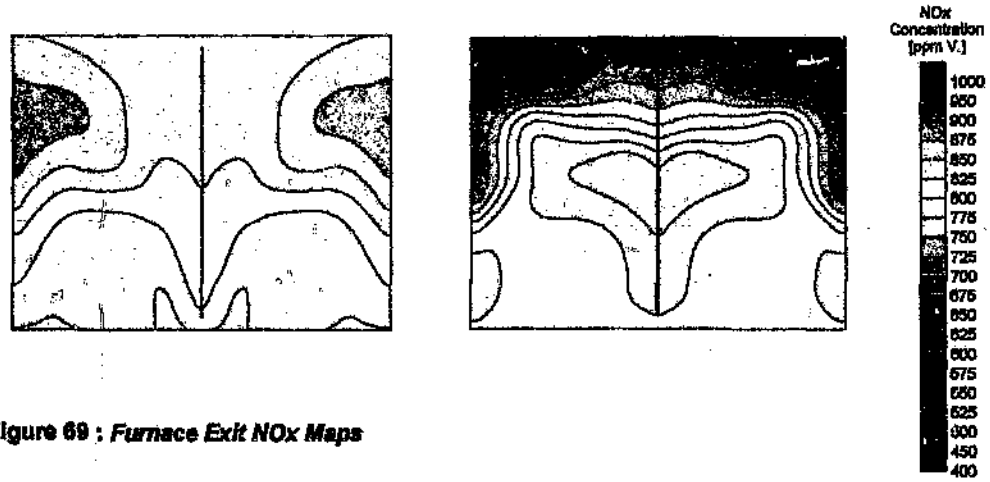

Figure 69 : ***Furnace Exit NOx Maps***

4. CONCLUSIONS

4.1 THE COMBUSTION MODEL VALIDATION

The combustion model predictions compare satisfactorily with furnace measurements. The use of the model is however at a developmental stage and therefore requires a critical review of the results. The model predictions depend to a great extent on accurate plant operation data which in many cases is not available. The use of reasonable estimates of this data is therefore required, and depending on the application of the model, should be borne in mind when reviewing combustion modelling results.

4.2 COMBUSTION MODELLING FOR COAL FEEDSTOCK ASSESSMENTS

The model showed that even a moderate difference in reactivity had a significant influence on the simulation results. The model appears therefore to be sufficiently sensitive to reactivity data for coal feedstock assessments.

4.3 THE COAL DEVOLATILISATION MODEL

The analysis of coal devolatilisation data obtained from DTF experiments suggested very low devolatilisation rates compared to what the University of Stuttgart assumes when this information is not available. When using the DTF experiment results in the combustion model, the model did not produce converged results. The University of Stuttgart default values were subsequently used as these produced acceptable results. The testing procedure designed to determine the pyrolysis kinetics does not produce results that can be used in setting the parameters of the pyrolysis sub-model used in the combustion code.

4.3 THE CHAR-COMBUSTION SUB-MODEL

The analysis of the DTF data for the coals in question suggests that char combustion model according to Field et al[11] (1967) was adequate. Refinements to the char combustion model may, however, improve the models capability to predict the effects of different coal feedstocks on furnace performance.

4.4 THE NOx PRODUCTION MODEL

The model allows for the specification of the nitrogen partitioning within the coal (viz. fraction of coal nitrogen reporting to the volatile matter and char respectively) and for the simulations presented herein, the model produces plausible results.

4.5 RESULTS OF THE FURNACE INVESTIGATION

Given the experimental furnace data, as well as the kinetic and other characterisation of the feedstock used at the time of testing, it became apparent that Hendrina's Unit 9 furnace does not have too short a residence from the top burner row (approx. 2.2s) for the coal that was burnt during the testing period. High furnace exit temperatures, low furnace heat fluxes as well as very high furnace temperatures (up to 1645°C) were however observed, which suggests that heat transfer to the furnace walls was impaired. The cause of this could either be a higher than usual emissivity of ash deposits on the furnace wall, or the insulating nature of the ash, or a combination of the aforementioned. The heat flux measurements did show that wall blowing did increase the heat flux to the furnace walls considerably, suggesting that the furnace performance may be improved by ensuring that the furnace walls remain clean. The extent to which this can be achieved by additional or modified wall blowing hardware, or changes to wall blower operation, should be investigated.

4.6 NEW FURNACE TEST METHODOLOGIES

The indirect method of furnace gas temperature measurement proved to be considerably more robust and dependable than the traditional direct temperature measurement using ceramic radiation shields.

Further, the furnace residence time distribution measurement technique has now been demonstrated for wall fired plant as well. In conjunction with the combustion characterisation of the Hendrina feedstock, it could be concluded that coal reactivity was not the primary contributor to the high furnace exit temperatures observed.

5. RECOMMENDATIONS

5.1 RECOMMENDATIONS PERTAINING TO THE COMBUSTION MODEL

The AIOLOS furnace model should be validated for the Matimba Unit 6 furnace as well. The experimental data available from Matimba for feedstocks of varying reactivity would provide an ideal validation data set.

The NOx validation testwork and modelling results should be reviewed in order to assess the combustion model's potential application in evaluating NOx reduction hardware.

Refinements to the code's char combustion sub-model should be explored. These refinements should include specifying the combustion kinetics for all size fractions tested in the DTF, as well as introducing a description of the effect of combustion extent on the combustion kinetics of the coal.

The coal devolatilisation model should be reviewed and a suitable test methodology to experimentally determine a coal's devolatilisation rates should be researched.

As the effect of furnace wall emissivity has a significant effect on simulation predictions, the possibility of measuring this property should be explored.

5.2 RECOMMENDATION PERTAINING TO THE FURNACE TESTWORK AT HENDRINA

Improved furnace wall cleaning at Hendrina Power Station may help reduce furnace exit temperatures. It is recommended that this be explored. It should, however, be noted that burner hardware condition, primary and secondary air temperatures as well as coal properties (including grindsize and reactivity), may contribute to high furnace exit temperatures and reduced furnace performance.

5.3. RECOMMENDATION PERTAINING TO THE FURNACE TESTING METHODOLOGIES

The indirect furnace gas temperature measurement technique should be explored further to improve its accuracy and reliability.

6. REFERENCES

[1]Adrian, F., Review of Research Activities on Pulverised Coal Firing Systems, *VGB Kraftwerkstechnik*, 68, No.12, pp1107, December 1988

[2]Land, T., Barber, R., The Design of Suction Pyrometers, Transactions of the Society of Instrument Technology, Vol 6, No.3, September 1954

[3]Idiatulin,Z.G., Petishvili, O.M, Measuring Gas Temperature in Furnace of Steam Generators with Combustion of Solid Fuel, Teploenergetika, 1977,24 (9) 32-34

[4]Blenkinsop, M.G, Eichhorn, N.W., Theron, J., DTF Correlations Project - Stage II - Matimba Unit 6, TRI Report TRR/P94/045, 1994

[5]Levenspiel, O., Chemical Reaction Engineering, John Wiley and Sons, 1972

[6]Field, M.A., Rate of Combustion of Size-Graded Fractions of Char from a Low-Rank Coal between 1200°K and 2000°K, Combustion and Flame 13, pp237, 1969

[7]Badzioch, S., Hawksley, P.G.W., Kinetics of Thermal Decomposition of Pulverised Coal Particles, Int. Eng. Chem. Des. Develop. 1970, Vol 9, pp 521, 1970

[8]Field, M.A., Measurements of the Effect of Rank on Combustion Rates of Pulverised Coals, Combustion and Flame, 14, pp237, 1970

[9]Laine, N.R., Vestola, F.J. and Walker, P.J., The Importance of Active Surface Area in the Carbon-Oxygen Reaction, Journal of Physical Chemistry, Vol 67, pp 2030, 1994

[10]Smoot, L.D., Pratt, D.T., Pulverised Coal and Combustion and Gasification, New York, Plenum Press, 1979

[11]Field, M.A., Gill, D.W., Morgan, B.B. and Hawksley, P.G.W., Combustion of Pulverised Coal, pp189-192 and 329-345, BCURA, Leatherhead, 1967

[12]Schnell, U., Berechnung der Stickoxidemissionen von Kohlestaubfeuerungen, Dissertation Universität Stuttgart, VDI-Fortschritt-Berichte Reihe 6, Nr. 250, Düsseldorf, 1991

[13]Epple, B., Modellbildung und Simulation von Strömungs-, Reactions- und NOx-Bildungsvorgängen in technischen Feuerungen, Dissertation Universität Stuttgart, VDI-Fortschritt-Berichte Reihe 6, Nr. 295, Düsseldorf, 1993

[14]Epple, B. Schnell, U., Domain Decomposition Method for the Simulation of Fluid Flow in Coal Combustion Furnaces, International Congress on Numerical Methods in Engineering and Applied Sciences, Conceopción, Chile, 16-20 November, 1992

[15]Epple, B., Schneider, R., Schnell, U., Hein, K.R.G., Computerised Analysis of Low-NOx Coal- Fired Utility Boilers, Second International Conference on Combustion Technologies for a Clean Environment, Lisbon, Portugal, 19-22 July 1993

[16]Schnell, U., Schneider, Magel, H.C., Risio, B., Lepper, J.,R., Hein, K.R.G., Numerical Simulation of Advanced Coal-Fired Combustion Systems with in-furnace NOx Control Technologies, 3rd International Conference on Combustion Technologies for a Clean Environment, Lisbon, Portugal, 19-22 July

[17]Epple, B., Dreidimensionale, turbulente Strömungs- und Mischungsgradberechnung mit dem PISO-Algorithmus, Forschung und Ingenieurwesen, 57, 105 (1991)

[18]Schnell, U., New Developments in Modelling Near Field Swirl Burner Flows, 6th International Conference on Numerical Methods in Laminar and Turbulent Flow, (C. Taylor, P. Gresho, R.L. Sani, J. Heüser, Eds.), Vol. 6, part 1, pp307, Swansea, 1989.

[19]Magnussen, B.F., On the structure of Turbulence and a Generalised Eddy Dissipation Concept for Chemical Reaction in Turbulent Flow, 19th AIAA Sc. Meeting, St. Louis, USA, 1981

[20]Magnussen, B.F., Hjertager, B.H., On the Mathematical Modelling of Turbulent Combustion with Special Emphasis on Soot Formation and Combustion, 16th Symp. (Int.) on Combustion, 1976, The Combustion Institute, Pittsburgh, pp719

[21]Denn, M.M., Process Modelling, Longman Scientific & Technical, (UK) 1987

[22]Schilling, H-D., Bonn, B., Krauß, U., Peters, W., Kohlevergasung - Bestehende Verfahren und neue Entwicklungen, Bergbau, Rohstoffe und Energia, Glückauf Verlag, Essen, 1981

[23]Viskanta , R., Radiative Heat Transfer, Advances in Chemical Engineering, 22A, 51., 1984

[24]Hottel, H.C., Sarofim, A.F., Radiation Transfer, McGraw Hill, New York, 1967

[25]Sidall, R.G., Selcuk, N., Evaluation of a New Six-Flux Model for Radiative Transfer in Rectangular Enclosures, Trans. IChmE, Vol. 57, 1979

[26]Sidall, R.G., Selcuk, N., Two-Flux Modelling of Two-Dimensional Radiative Transfer in Axisymetrical Furnaces, Journal of the Institute of Fuel, March 1976, pp10

[27]Filla, M., Maresa, G., A Flux Approach to Radiative Transfer in Cracking Furnaces, Riv. Combust. 7-8, 1975, pp 321

[28]De Marco, A.G., Lockwood, F.C., A New Flux Model for the Calculation of Radiation in Furnaces, La rivisita dei combustibili I Giornate Italiane delle Fiamme, 1975, pp 184

[29]Lockwood, F.C, Shah, N.G., An improved Model of Radiation Heat Transfer in Combustion Chambers, ASME-AIChE Heat Transfer Conference, St. Louis, USA, August 1976

[30]Shah, N.G., New Method of Computation of Radiation Heat Transfer in Combustion Chambers, PhD Thesis, University of London, 1970

[31]Steward, F.R., Cannon, P., The Calculation of Radiative Heat Flux in a Cylindrical Furnace Using the Monto-Carlo Method, Int. Journal of Heat and Mass Transfer 14, 1971, pp 245

[32]Guilbert, P.W., Comparison Monet-Carlo and Discrete-Transfer Methods for Modelling Thermal Radiation, 9th Members Conference of the Internaltional Flame Research Foundation at Nordwijkerhout, The Netherlands, May 1989

[33]Fiveland, W.A., Three-Dimensional Solutions of Radiative Heat Transfer Solutions by Discrete-Ordinates Method, 24th National Heat Transfer Conference and Exhibition, Pittsburgh, Pennsylvania, August 1987

[34]Fiveland, W.A., Discrete Ordinates Solutions of the Radiative Transport Equation for Rectangular Enclosures, Journal of Heat Transfer, November 1984, Vol. 106, pp 699

[35]Richter, W., Mathematische Modelle technischer Flammen, Dissertation, Universität Stuttgart, 1978

[36]Richter, W., Bauersfeld, G., Radiation Models for Use in Complete Mathematical Furnace Models, IFRF, 3rd Members Conference, 1974

[37]Eichhorn, N.W., Odenthal, H.-P., Mathematische Modellierung einer mit südafrikanischer Kohle gefeuerten Brennkammer, 17. Deutscher Flammentag, September 1995

[38]Zeldovich, J., The Oxidation of Nitrogen in Combustion and Explosions, Acta, Physiochimica, URSS 21 (1946), No. 4, pp 577

[39]De Soete, G., Overall Reaction Rates of NO and N_2 formation from Fuel Nitrogen, 15th International Symposium on Combustion, Combustion Institute, 1974, pp1093

[40]Hendrina Unit 6-10 C-Schedules, 1972

[41]Saito, M., Sadakata, M., Sakai, T., Combustion Science and Technology, Vol 51, 1987, pp109

[42] Massey, B.S., Mechanics of Fluids 3rd Edition, Van Nostrand Reinhold Company, 1976, pp155

INDEX OF APPENDICES

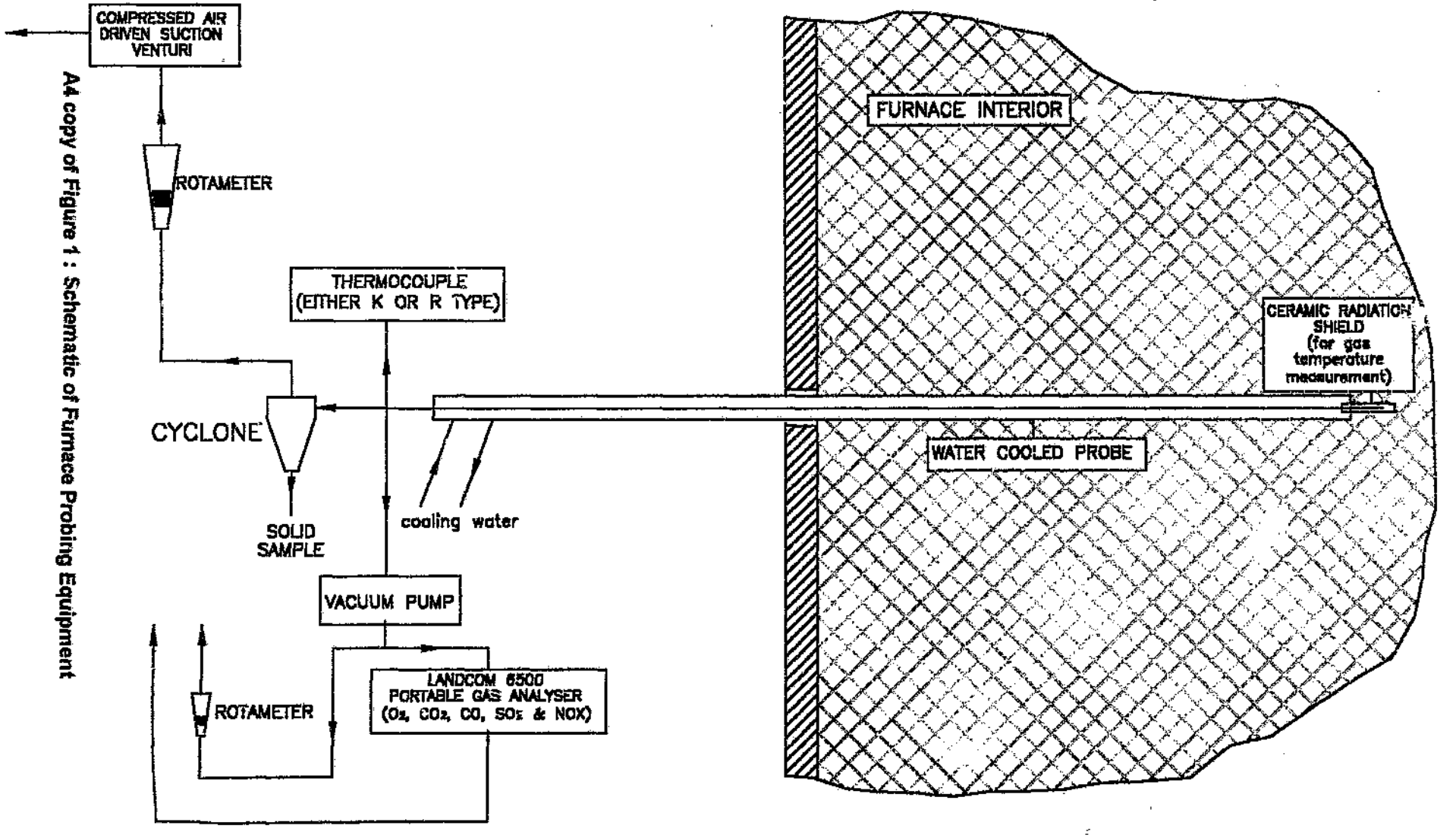

A4 copy of Figure 1 : Schematic of Furnace Probing Equipment

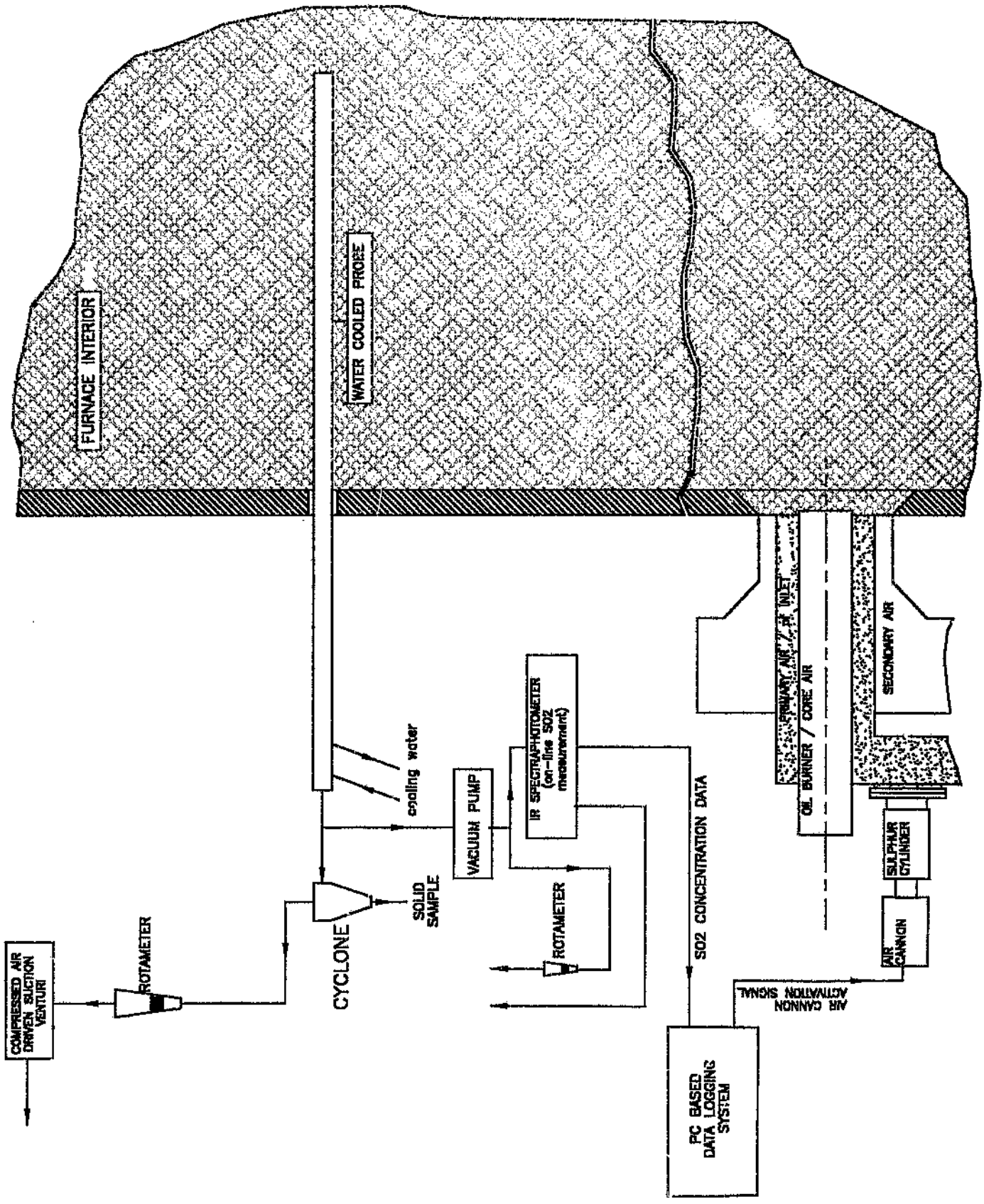

A4 copy of Figure 4 : Schematic of RTD Measurement Equipment

APPENDIX 1

Appendix 1.1.1

Design Sketch of the 6m water cooled suction pyrometer

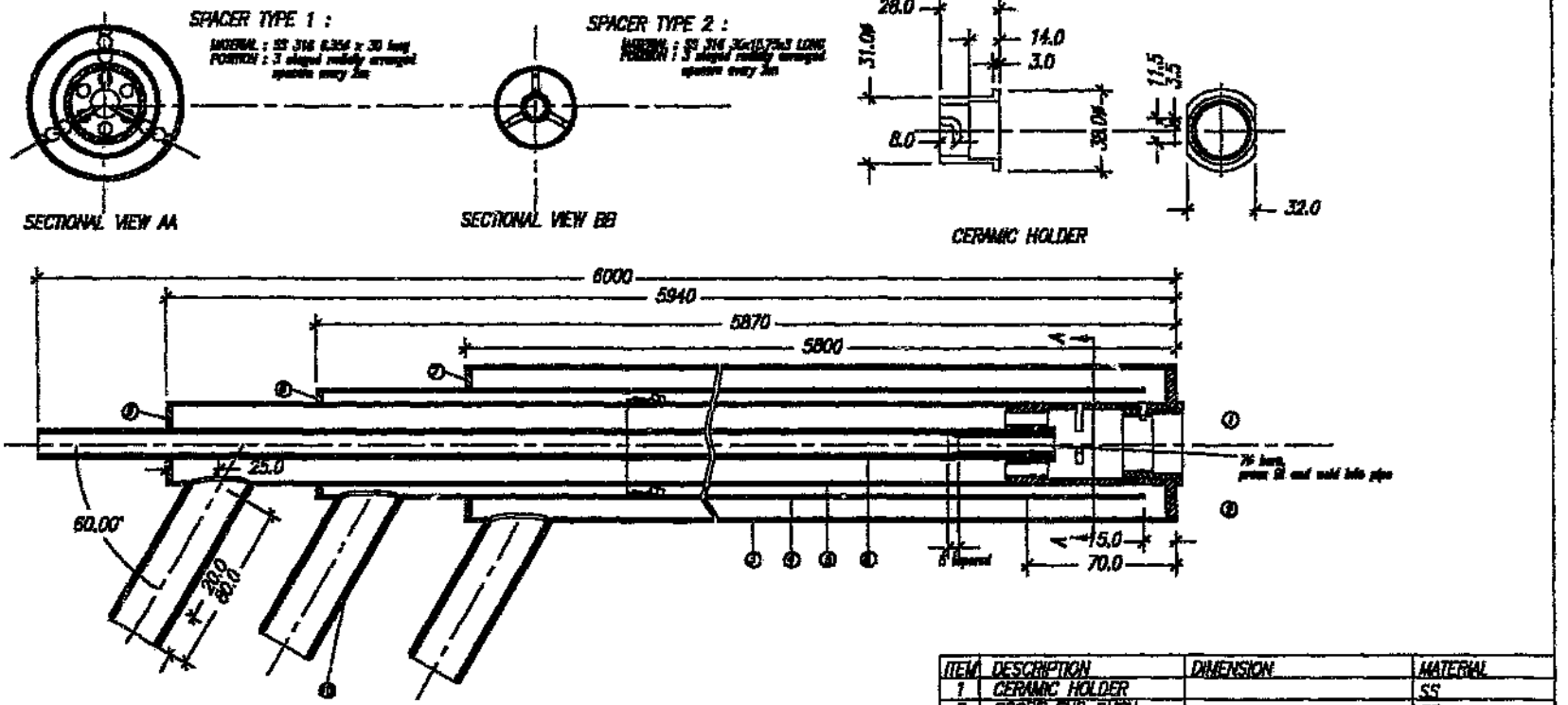

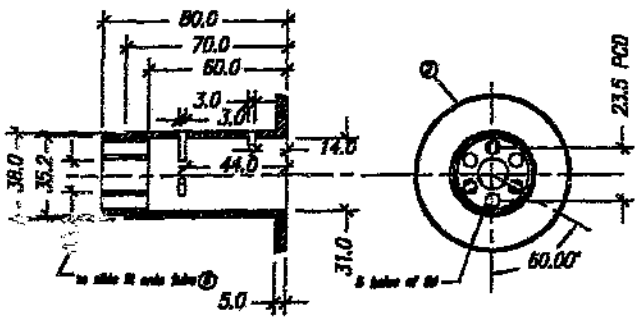

PROBE END BUSH

ITEM	DESCRIPTION	DIMENSION	MATERIAL
1	CERAMIC HOLDER		SS
2	PROBE END BUSH		SS
3	TUBE	73 OD x 69.2 ID	316 SS
4	TUBE	51 OD x 47.8 ID	316 SS
5	TUBE	38.3 OD x 35.2 ID	316 SS
6	TUBE	13.7 OD x 9.4 ID	304 SS
7	ANNULUS RING	to suit tubes	SS
8	ANNULUS RING	to suit tubes	SS
9	ANNULUS RING	to suit tubes	SS
10	GAS & WATER CONDUIT	standard with 3/4" thread	MS (galvanised)
11	SPACER TYPE 1	as specified	316 SS
12	SPACER TYPE 2	as specified	316 SS

date	24/06/94	title : BOILER GAS SAMPLING AND TEMPERATURE PROBE – 6m	ESKOM TRI ENERGY TECHNOLOGIES tel:(011)629 7436 fax:(011)629 7229
drawn	NME		
approved	copy		
revisions	n/a		
scale	to fit A4	drawing no : copy of OTS 1/78	

Appendix 1.1.2.1

Design Sketch of 12m water cooled suction pyrometer

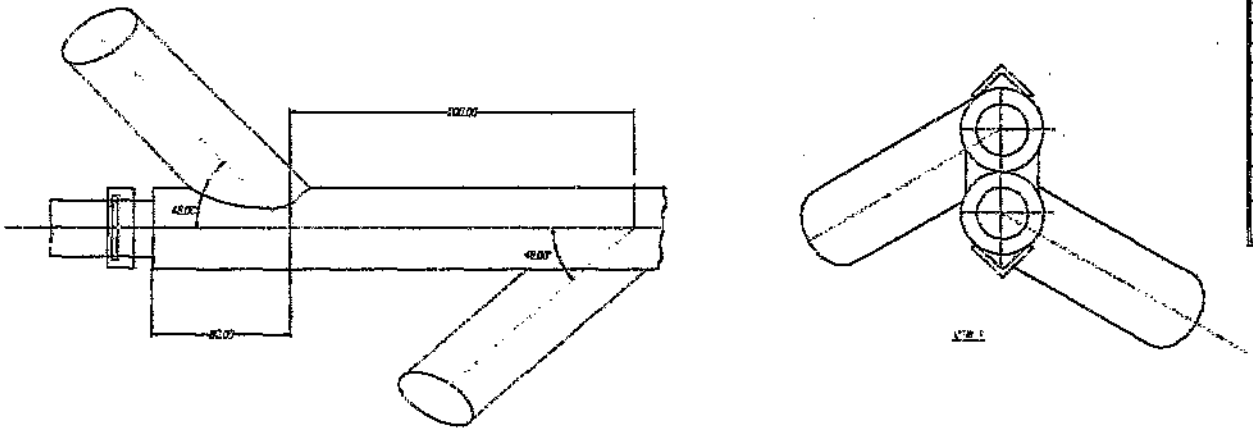

ITEM	DESCRIPTION	DIMENSION	MATERIAL	No. REQD
1	probe end bush	as per 12MP01	SS 316 L	2
2	seamless or welded pipe	33.4 OD, 1.65 WT x 6m	SS 316 L	4
3	seamless or welded pipe	48.26 OD, 2.77 WT x 6m	SS 316 L	4
4	angle	25 x 25 x 3 x 4m	SS 316 L	2
5	end cap fastener	as per 12MP05	SS 316 L	2
6	annulus ring	42.76 OD, 33.4 ID x 5	SS 316 L	2
7	annulus ring	37.06 OD, 33.4 ID x 3	SS 316 L	2
8	cooling water inlet/outlet	2" x 150 with 2" BSP male thread on one side	SS 316 L	2
9	spacer between inner and outer pipes	6 x 4 bar x 50	SS 316 L	30
10	cooling water conduit between lower and upper pipes	42.16 OD, 2.77 WT x 60	SS 316 L	1

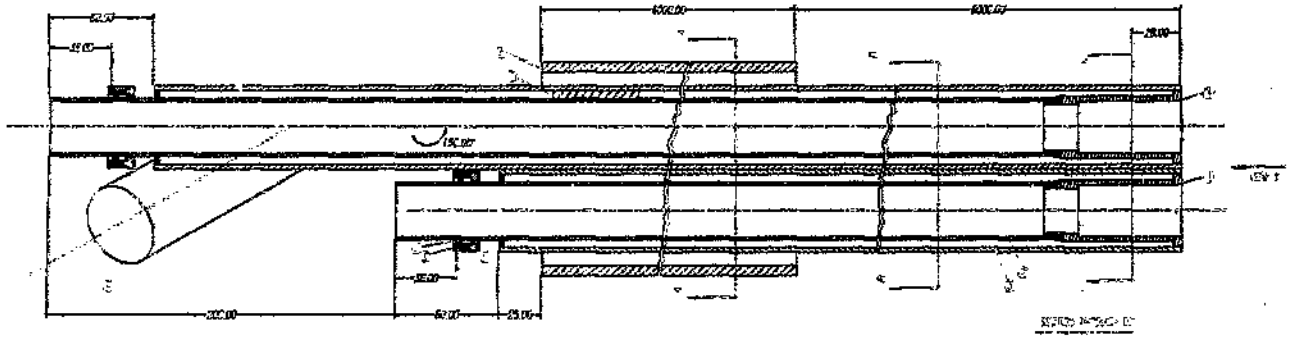

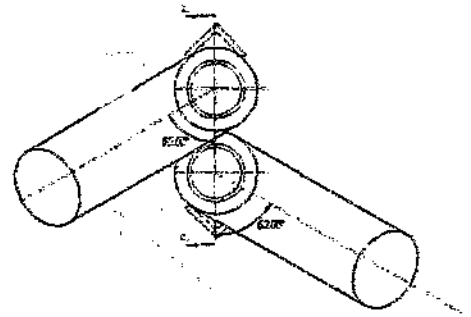

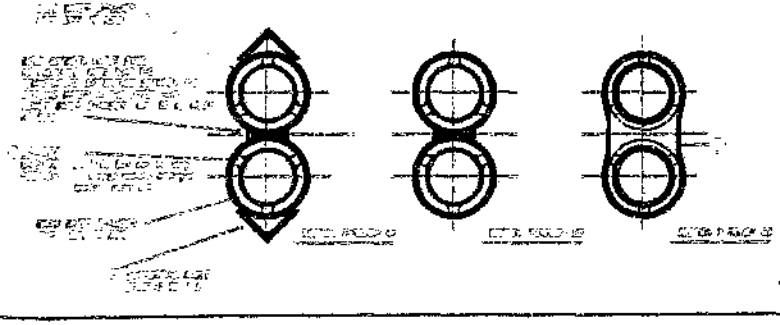

TOLERANCES	as per DIN 7168 m			
	0.5-6 ±0.1	>6-30 ±0.2	>30-120 ±0.3	>120 ±0.5

CAD FILENAME	12MPROBE.DWG	PROJECT: 7751E244R	
DRAWING No.	12MP00	DTF CORRELATIONS IC	
SCALE	1:3 ON A3	TITLE: WATER COOLED PROBE HOLDER	
CHECKED			
APPROVED			

This drawing is the property of ESKOM T-R-I. It is subject to copyright and may not be made available to third parties without prior written permission.

ISSUE	DATE	ALTERATIONS	NAME
3			
2			
1	10/08/95	ORIGINAL	MME

ESKOM
T-R-I

Appendix 1.1.2.2

Design Details for the 12m water cooled probe

Desig. of a water cooled suction probe :

1/08/95
SvS & NWE

1. Mechanical Analysis of probe sections :

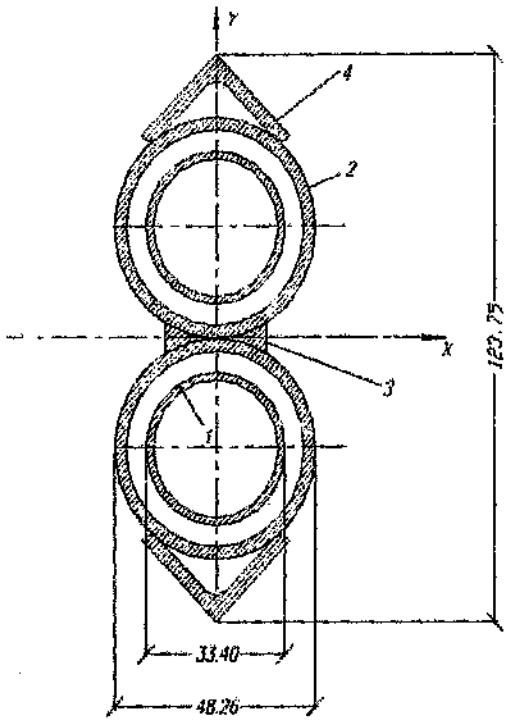

Area:	1457.433 sq mm
Perimeter:	1229.249 mm
Bounding box:	X: -24.13 -- 24.13 mm
	Y: 118.9821 -- 242.7354 mm
Centroid:	X: 0 mm
	Y: 180.8587 mm
Moments of inertia:	X: 4.933699e+007 sq mm sq mm
	Y: 277049.7 sq mm sq mm
Product of inertia:	XY: -5.295405e-009 sq mm sq mm
Radii of gyration:	X: 183.989 mm
	Y: 13.78747 mm
Principal moments(sq mm sq mm) and X-Y directions about centroid:	
	I: 277049.7 about [0 1]
	J: 1664532 about [1 0]

Item	Description
1	33.4 ø x 1.6 Wt 316L SS pipe
2	48.26 ø x 2.77 Wt 316L SS pipe
3	weld
4	25 x 25 x 3 Wt 316 SS angle

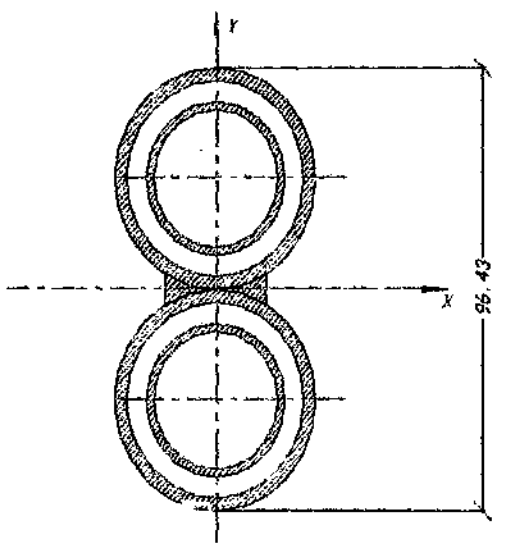

Area:	1173.609 sq mm
Perimeter:	1035.687 mm
Bounding box:	X: -24.13 -- 24.13 mm
	Y: -19.54357 -- 76.9761 mm
Centroid:	X: 0 mm
	Y: 28.71623 mm
Moments of inertia:	X: 1867645 sq mm sq mm
	Y: 251816.3 sq mm sq mm
Product of inertia:	XY: -0.00004467853 sq mm sq mm
Radii of gyration:	X: 39.89196 mm
	Y: 14.64806 mm
Principal moments(sq mm sq mm) and X-Y directions about centroid:	
	I: 251816.3 about [6.894358e-011 -1]
	J: 899861.1 about [1 2.605621e-006]

Moment of Inertia for section of probe without support bar about the X axis : $I_{us.x} = 899861.1 \cdot mm^4$

Moment of Inertia for section of probe with support bar about the X axis : $I_{s.x} = 1664532 \cdot mm^4$

Moment of Inertia of probe on its side (weakest) : $I_{us.y} = 251816.3 \cdot mm^4$

Cross sectional Area of stainless steel without support bar : $A_{us} = 1173.609 \cdot mm^2$

Cross sectional Area of stainless steel with support bar : $A_s = 1457.433 \cdot mm^2$

Cross sectional area where water flows :

OD of outer tube : $d_0 := 48.26 \cdot mm$

Wall thickness of outer tube $wt_0 = 2.77 \cdot mm$

OD of inner tube : $d_1 := 33.4 \cdot mm$

$$A_w := \left[\pi \cdot \left(\frac{d_0}{2} - wt_0\right)^2 - \pi \cdot \left(\frac{d_1}{2}\right)^2\right] + \left[\pi \cdot \left(\frac{d_0}{2} - wt_0\right)^2 - \pi \cdot \left(\frac{d_1}{2}\right)^2\right] \quad A_w = 1114.38 \cdot mm^2$$

Material Properties of AISA 316L SS : density : $\rho_{ss} := 8000 \cdot \frac{kg}{m^3}$

Elastic modulus : $E_{ss} := 19 \cdot 10^9 \cdot Pa$

Mass Property of water : density : $\rho_w := 1000 \cdot \frac{kg}{m^3}$

Determining the maximum length of unsupported probe :

Divided gravity force : $q := \left(A_{us} \cdot \rho_{ss} + A_w \cdot \rho_w\right) \cdot g$

Bending Moment :

$$BM\left(L_{tube}\right) := \int_{0 \cdot m}^{L_{tube}} q \cdot x \, dx$$

Calculation of the maximal bending stress occuring at a distance d0 of the neutral axis at the insertion point

$$\sigma_{max}\left(L_{tube}\right) := \frac{BM\left(L_{tube}\right) \cdot d_0}{I_{us.x}}$$

Calculation of the maximum deflection occuring at the end of the probe

$$\delta_{max}\left(L_{tube}\right) := \frac{\frac{1}{8} \cdot q \cdot \left(L_{tube}\right)^4}{E_{ss} \cdot I_{us.x}}$$

Safety factor n, most likely to be in the order of 2-2.5 $n = 2$

Maximum permissible tensile stress of stainless steel

$$\sigma_{maxpermissible} := \frac{205}{n} \cdot 10^6 \cdot Pa$$

$\sigma_{maxpermissible} = 102500000 \cdot Pa$ $L_{in} := 0 \cdot m, 0.2 \cdot m .. 10 \cdot m$

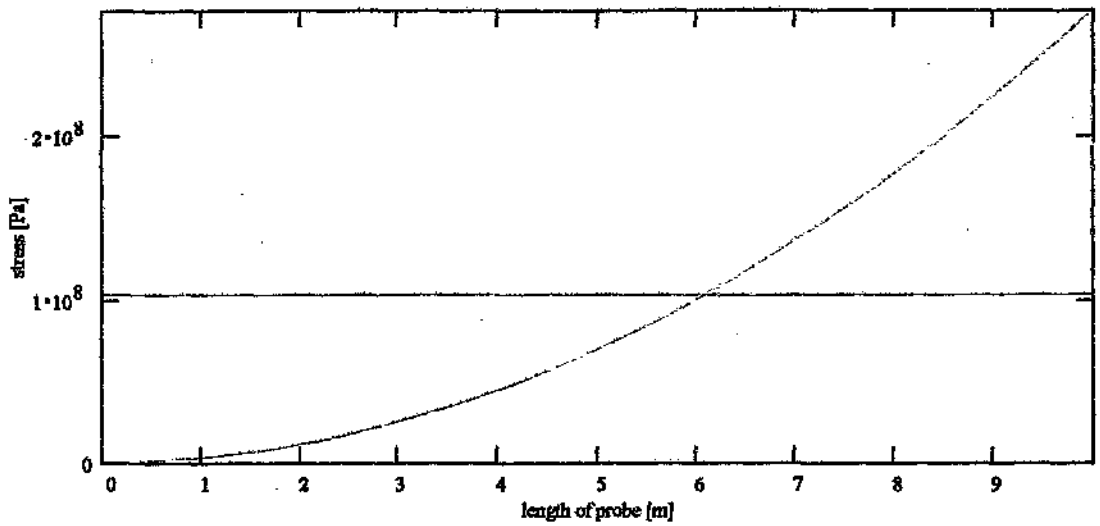

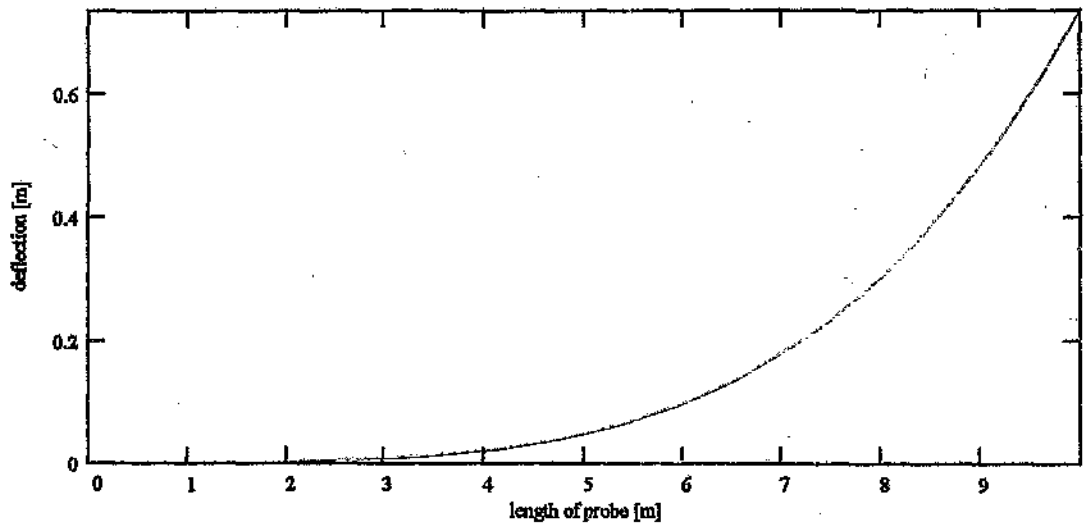

Determining the maximum length of unsupported probe :

$l_{max} := 8 \cdot m$ given $\sigma_{max}(l_{max}) = \sigma_{maxpermissible}$

$l_{max.1} := \text{find}(l_{max})$ $l_{max.1} = 6.09 \cdot m$

Calculating the mass of probe and water of the unsupported probe :

$\text{Mass}(L_{probe}) := (A_{us} \cdot \rho_{ss} + A_{w} \cdot \rho_{w}) \cdot L_{probe}$

$\text{Mass}(l_{max.1}) = 63.98 \cdot kg$ effecting a point load at the end of the supported probe

Concentrated load at end of supported probe :

$\text{Load}_{us} := \text{Mass}(l_{max.1}) \cdot g$

divided gravity force :

$$q_s := \left(A_s \cdot \rho_{ss} + A_w \cdot \rho_w\right) \cdot g$$

Bending Moment :

$$BM_s\left(L_{tube}\right) := \int_{0 \cdot m}^{L_{tube}} q \cdot x \, dx + Load_{us} \cdot L_{tube}$$

Finding the maximum length of probe for which

Calculation of the maximal bending stress occuring at a distance d0 of the neutral axis at the insertion point

$$\sigma_{max}\left(L_{tube}\right) := \frac{BM_s\left(L_{tube}\right) \cdot d_0}{I_{s.x}}$$

Calculation of the maximum deflection occuring at the end of the probe

$$\delta_{max}\left(L_{tube}\right) := \frac{\frac{1}{8} \cdot q_s \cdot \left(L_{tube}\right)^4 + \frac{1}{2} \cdot Load_{us} \cdot L_{tube}^3}{E_{ss} \cdot I_{s.x}}$$

Safety factor n, most likely to be in the order of 2-2.5

$n := 2$

Maximum permissible tensile stress of stainless steel

$$\sigma_{maxpermissible} := \frac{205}{n} \cdot 10^6 \cdot Pa$$

$\sigma_{maxpermissible} = 102500000 \cdot Pa$ $\qquad L_{in} := 0 \cdot m, 0.2 \cdot m .. 8 \cdot m$

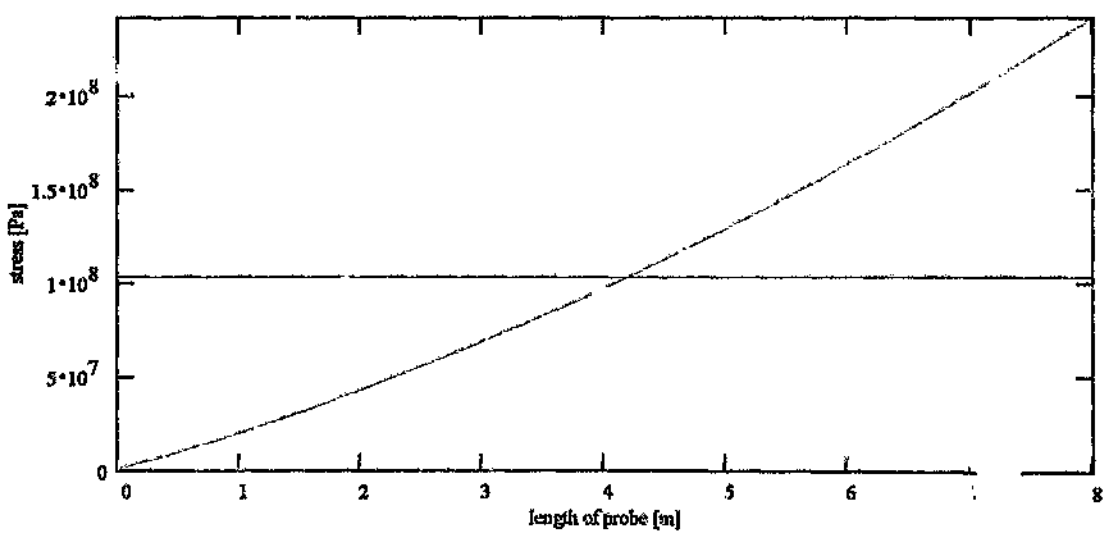

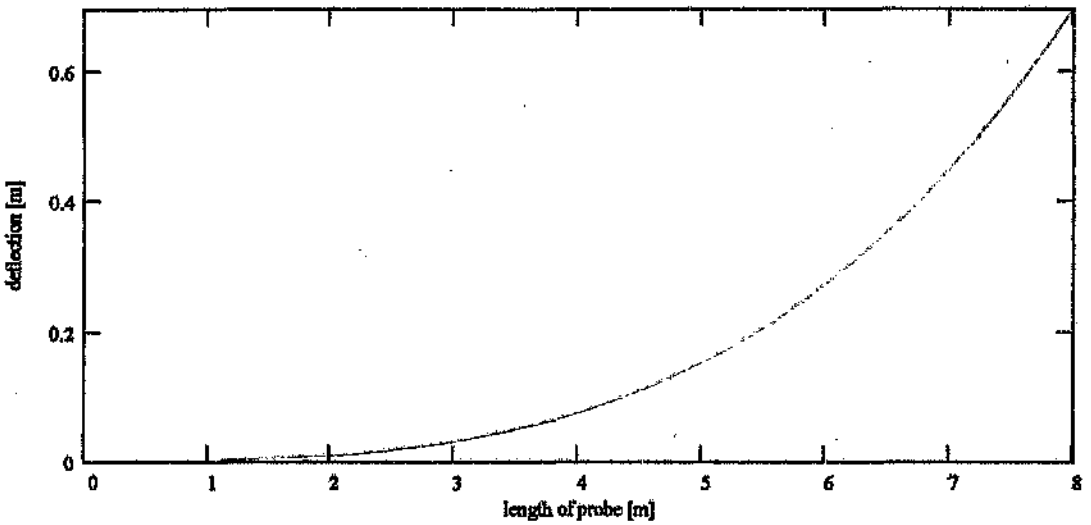

Determining the maximum length of unsupported probe :

$l_{max} := 3 \cdot m$ given $\sigma_{max}(l_{max}) = \sigma_{maxpermissible}$

$l_{max.2} := \text{find}(l_{max})$ $l_{max.2} = 4.19 \cdot m$

Maximum Probe Length past cantilever point : $l_{max} := l_{max.1} + l_{max.2}$

$l_{max} = 10.28 \cdot m$

Total mass of probe without water : $mass_{total} := l_{max.1} \cdot A_{us} \cdot \rho_{ss} + (l_{max} - l_{max.1}) \cdot A_s \cdot \rho_{ss}$

$mass_{total} = 106.07 \cdot kg$

Transporting the probe on its side : $Load := mass_{total} \cdot g$

Estimated Bending Moment at centre $BM_c := \frac{Load \cdot l_{max}}{8}$

Estimating the maximum bending stress on the probe on its side : $\frac{BM_c \cdot \frac{d_0}{2}}{I_{us.y}} = 128.13 \cdot 10^6 \cdot Pa$

Calculated safety factor $\frac{n \cdot \sigma_{maxpermissible}}{\frac{BM_c \cdot \frac{d_0}{2}}{I_{us.y}}} = 1.6$

Heat Tranrfer Calculation :

Insertion Depth $i := 0..100$ $L_{tube_i} := \frac{i+1}{10}\cdot m$

maximum expected heat flux in furnace : $q_{max} := 500\cdot\frac{kW}{m^2}$

total area subjected to this heat flux : $A_{q_i} := \pi\cdot d_0\cdot 2\cdot L_{tube_i}$

maximum rate of energy removal from probe holder :

$Q_{max_i} := q_{max}\cdot A_{q_i}$

maximum increase in cooling water temperature :

$\Delta T_{cw} := (50)\cdot K$

average specific heat of water : $Cp_{cw} := 4.186\cdot 10^3\cdot\frac{joule}{K\cdot kg}$

energy balance around probe, where f = flowrate of water in kg/s :

$$f_i := \frac{Q_{max_i}}{\Delta T_{cw}\cdot Cp_{cw}}$$

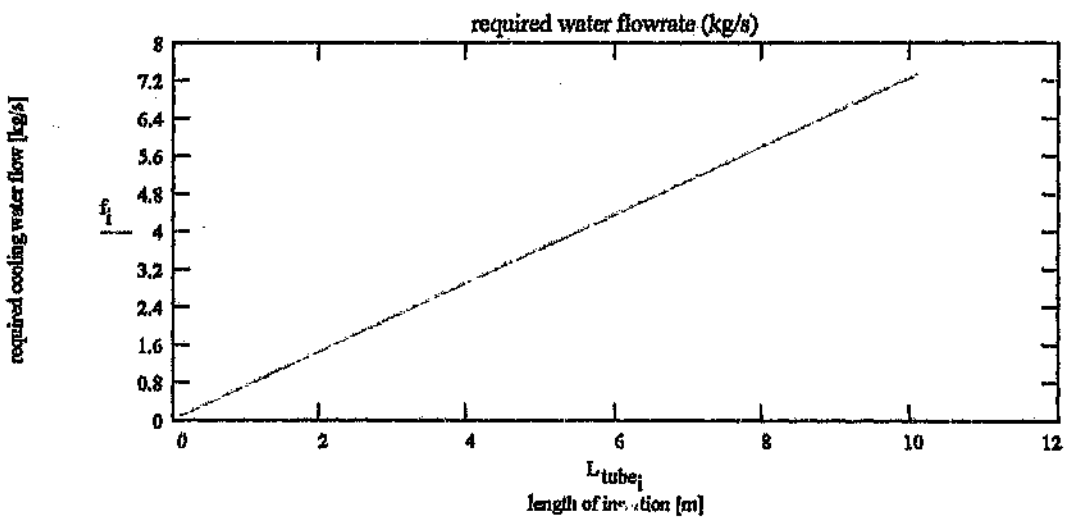

Estimation of pressure drop through probe :

hydraulic mean diameter of annulus :

$$d_m := \frac{4 \cdot \left[\pi \cdot \left[\left(\frac{d_0 - wt_0 \cdot 2}{2} \right)^2 - \left(\frac{d_1}{2} \right)^2 \right] \right]}{\pi \cdot (d_0 - wt_0 \cdot 2) + \pi \cdot d_1}$$

Friction loss due to 180° bend at probe end : $bends := 120$ diameters

Average Viscosity of water between 280 and 360°K : $\mu_{cw} := 0.65 \cdot 10^{-3} \cdot poise$

Area available for Flow : $A_{cw} := \frac{A_w}{2}$

Velocity of water through pipe : $v_{cw_i} := \frac{f_i}{A_{cw} \cdot \rho_w}$

Reynolds Number : $Re_i := \frac{d_m \cdot v_{cw_i} \cdot \rho_w}{\mu_{cw}}$

Friction factor (according to Blasius for smooth pipe): $f_{0_i} := 0.0395 \cdot (Re_i)^{-0.25}$

Equivalent length of pipe through probe : $L_{eq} := 2 \cdot 12 \cdot m + bends \cdot d_m$

$L_{eq} = 25.12 \cdot m$

The energy loss due to friction in the pipe is thus : $F_i := f_{0_i} \cdot 4 \cdot \frac{L_{eq}}{d_m} \cdot (v_{cw_i})^2$

This translates into a pressure drop of : $\Delta P_i := F_i \cdot \rho_w$ Pa

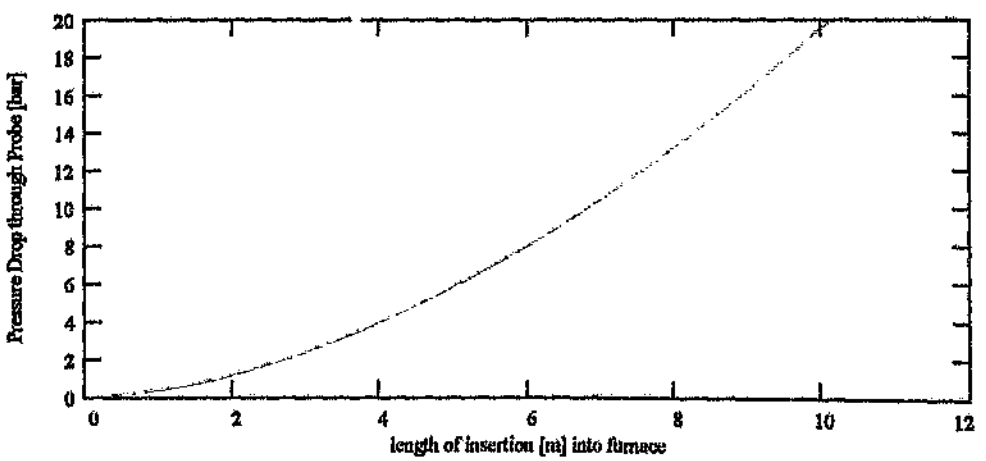

Estimating the pumping requirements :

Meximum continuous water pressure of supply at required flowrate : $P_{in} := 10 \cdot 101325 \cdot Pa$

Minimum Pressure at outlet : $P_{out} := 2 \cdot 101325 \cdot Pa$

Efficiency of pump : $efficiency := 60 \cdot \%$

Power of pump : $Power_i := \dfrac{f_i \cdot \dfrac{\Delta P_i - P_{in} + P_{out}}{\rho_w}}{efficiency}$

negative power requirements obviate the need for a pump : $Power_i := if(Power_i < 0 \cdot kW, 0 \cdot kW, Power_i)$

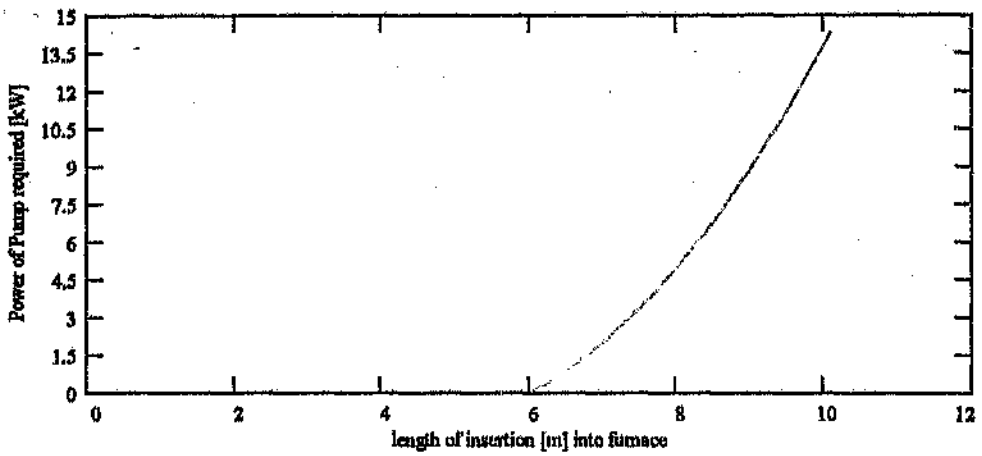

Appendix 1.1.3

Design Sketch for the Hendrina Burner Door

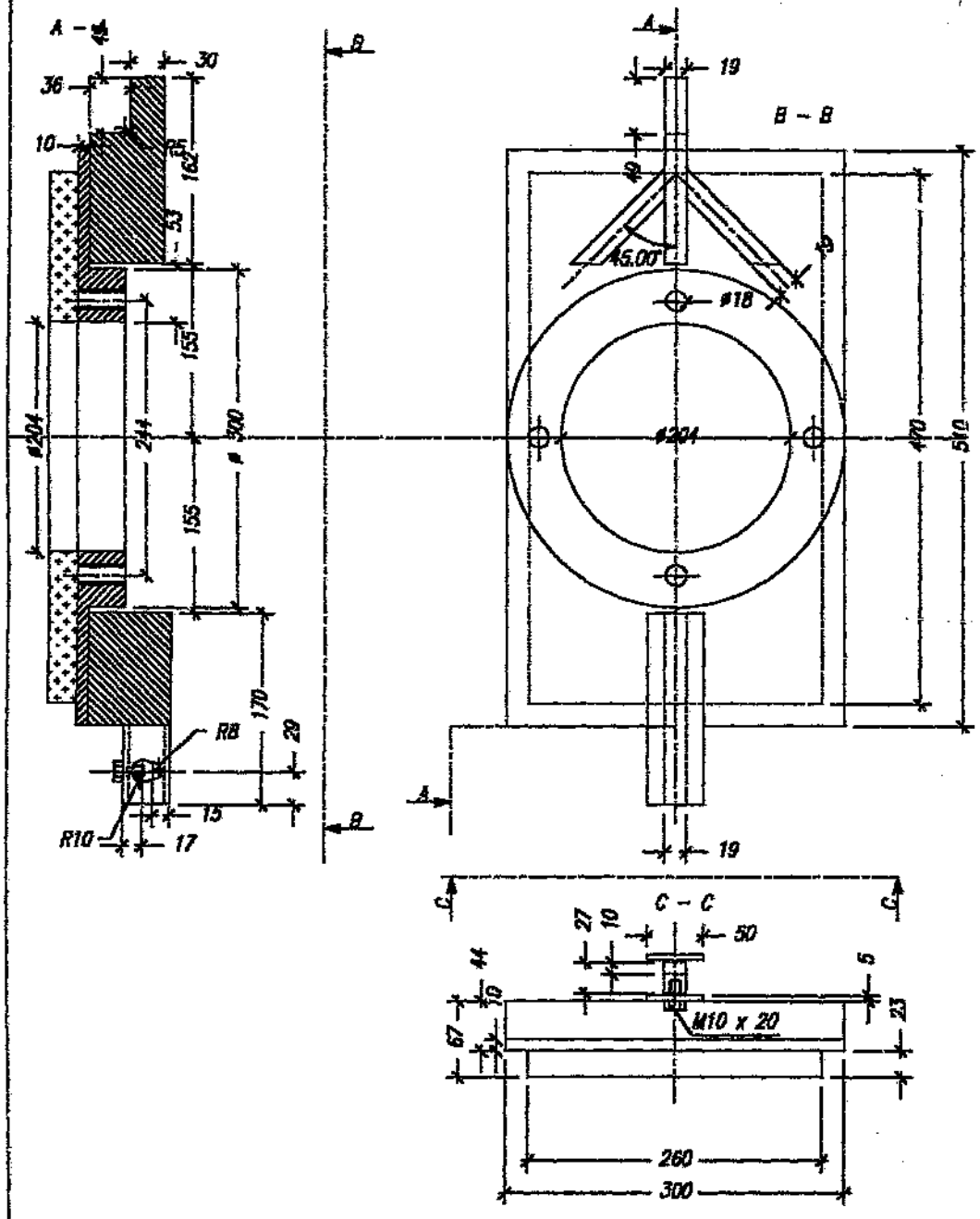

CAD FILENAME	BURNDOOR	PROJECT: 7751E244R	
DRAWING No.		PLANT SIMULATION	
SCALE	scaled to fit A4	TITLE: HENDRINA BURNER DOOR FOR SULPHUR INJECTION DEVICE	
CHECKED			
APPROVED			

This drawing is the property of ESKOM T-R-I. It is subject to copyright and may not be made available to third parties without prior written permission.

ISSUE	DATE	ALTERATIONS	INIT
3			
2			
1	14/06/95	ORIGINAL	

ESKOM
T-R-I

Appendix 1.1.4

Design Sketch for the tracer injection device
comprising the air cannon and sulphur discharge canister assembly

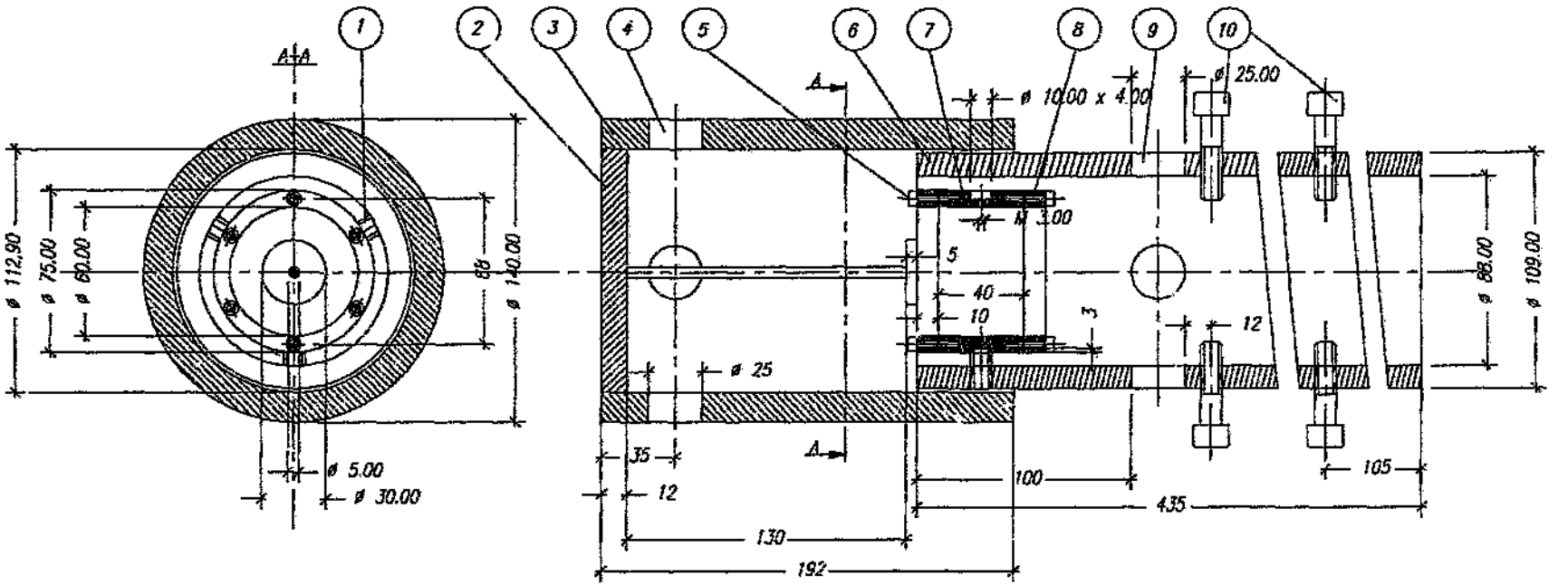

ITEM NO.	NO. REQD.	DESCRIPTION	DIMENSION	MATERIAL
1	3 off	GRUB SCREW WITH ALAN CAP	M10 X 20	
2	1 off	CYLINDER COVER		PERSPEX
3	4 off	AIR INLET HOLE		
4	1 off	OUTER CYLINDER	140 od, 12,7 t	HDPE
5	12 off	ALAN CAP BOLT	M4 X 20	
6	1 off	PROBE HOLDER CYLINDER	109 od, 5 t	HDPE
7	1 off	SO2 CONTAINER CYLINDER	75 x 60	HDPE
8	2 off	SO2 CONTAINER FLANGE		HDPE
9	4 off	AIR INLET HOLE		
10	8 off	ALAN CAP BOLT	M10 X 60	

CAD FILENAME	SO2INJEC.DWG	PROJECT: 7751E2441			
DRAWING No.	01	DTF Correlations			
SCALE	1:3 on A4	TITLE: SO2 injection probe for RTD measurement in water cooled suction pyrometers			
CHECKED					
APPROVED					
This drawing is the property of ESKOM T-R-I. It is subject to copyright and may not be made available to third parties without prior written permission.		3			
		2			
		1	22/04/95	ORIGINAL	SvS/nwe
		ISSUE	DATE	ALTERATIONS	NAME

ESKOM
T-R-I

Appendix 1.1.5

SO_2 injection device for the determination of the probe RTD

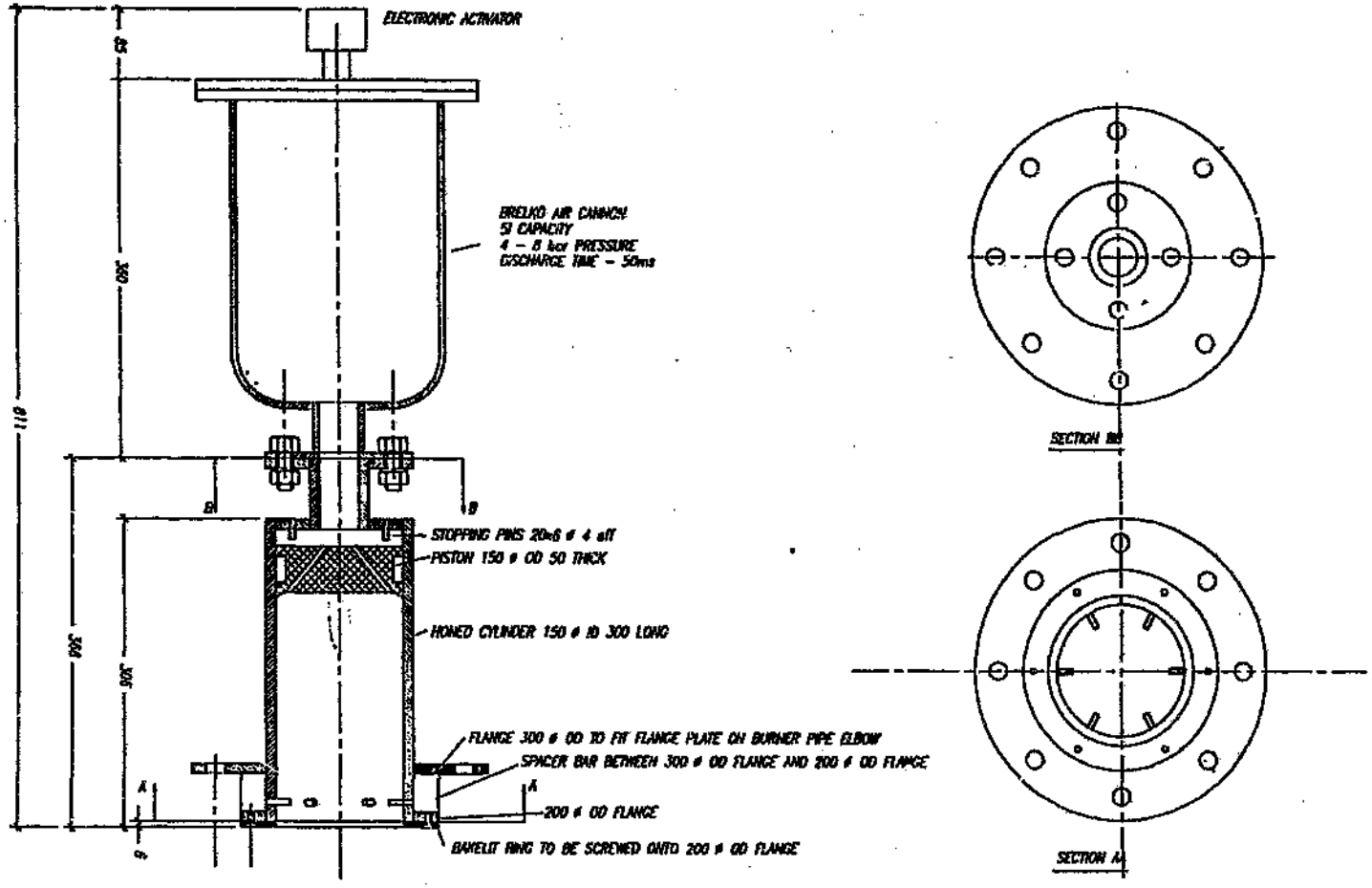

date	24/06/94	title : PULVERISED TRACER INJECTION DEVICE AS USED FOR MAFIKWA DIF CORRELATIONS INVESTIGATION	ESKOM TRI ENERGY TECHNOLOGIES tel:(011)629 7438 fax:(011)629 7229
drawn	NWF.		
approved			
revisions			
scale	to fit A4	SCALED KEY SITE REFERENCE SKETCH	

Appendix 1.1.6

Design Sketch for the heat flux probe

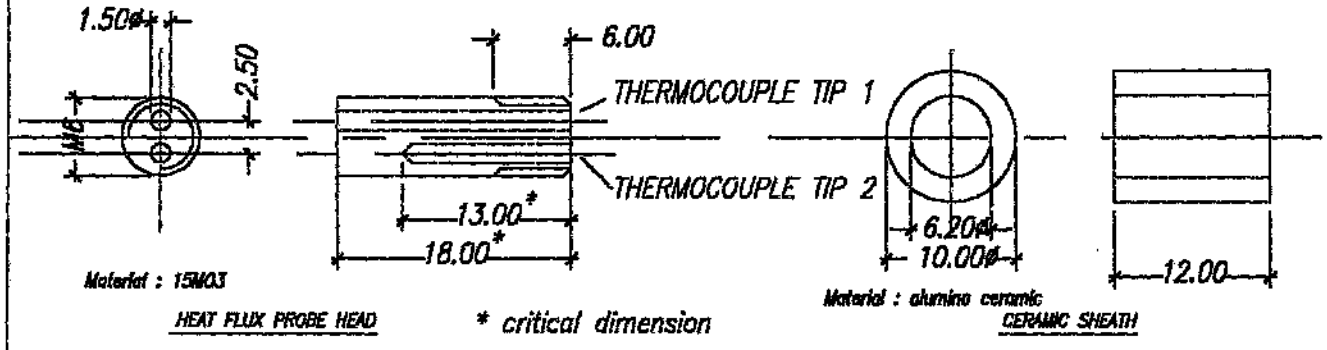

HEAT FLUX PROBE HEAD

* critical dimension

CERAMIC SHEATH

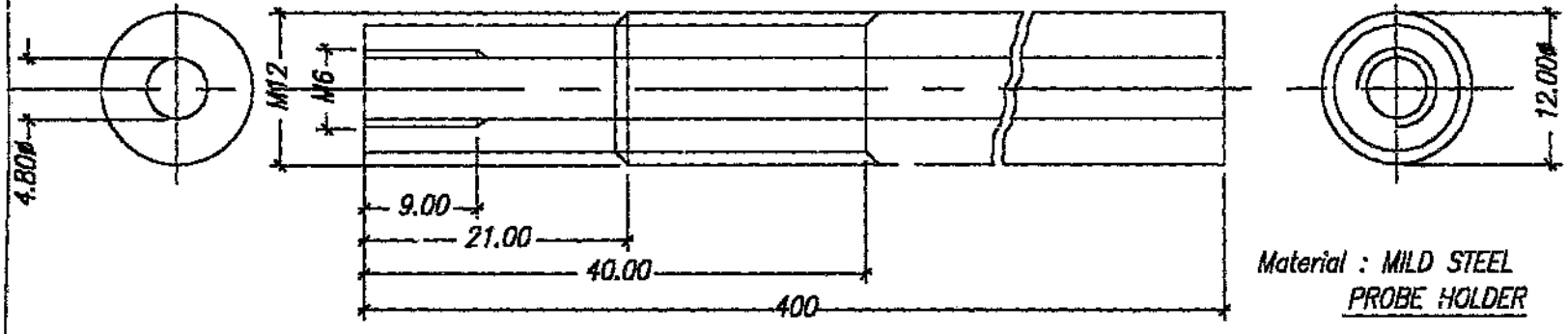

Material : MILD STEEL

PROBE HOLDER

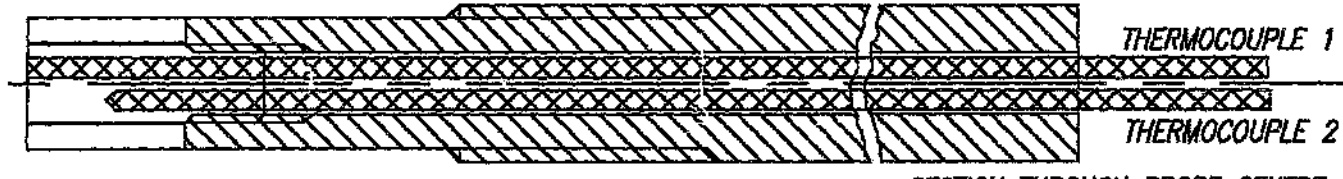

SECTION THROUGH PROBE CENTRE OF ASSEMBLED PROBE

MATERIAL	as indicated
No. REQD	refer enquiry
TOLERANCES	as per DIN 7168 m: 0.5–6 ±0.1 | >6–30 ±0.2 | >30–120 ±0.3 | >120 ±0.5

date	30/08/95
drawn	NWE
approved	copy
revisions	02
scale	2:1

title : FURNACE HEAT FLUX PROBE

ESKOM TRI
ENERGY TECHNOLOGIES
tel:(011)629 5438
fax:(011)629 5229

Appendix 1.2

Furnace Testing Procedures

1. Equipment Requirement

1. water cooled suction pyrometers
2. pyrometer trestles
3. cooling water hoses with fire hydrant fittings (source → pyrometer → drain)
4. suction line hoses (3.5 " Teflon lined)
5. cyclone filter for solids sampling (fits onto rear part of pyrometer)
6. air ejector (compressed air driven suction venturi)
7. compressed air hoses and fittings
8. silicon hose and fittings for gas sampling
9. petrol filter for gas sample line
10. membrane dryer for gas sample
11. suction pump (to draw gas sample through portable gas analyser)
12. rotameter to monitor gas flowrate though gas analyser
13. thermocouples with suitable compensating leads and displays (or datalogger)
14. ceramic shields for thermocouples (if using direct temperature measurement technique)

2. Equipment Setup

2.1 Cooling Water System

The cooling water inlet should be connected to the outer cooling jacket of the suction pyrometer and should be adjusted so that the cooling water outlet temperature is at around 60°C. Condensation in the sampled gas stream should be avoided.

2.2 Temperature Measurement - direct method using R-type thermocouple

Insert probe (with the ceramic radiation shields and thermocouple in place - refer Figure 1) into furnace with the suction turned to minimum. Once probe is at the desired furnace depth, adjust the cooling water flowrate so that the outlet water temperature is as specified in 2 1. Gradually increase the suction while observing the temperature reading. Once an increase in temperature reading is no longer apparent with an increase in suction, note the temperature reading. If the temperature reading begins to decrease, check the suction flowrate. The decrease in temperature may be attributable to the ceramic radiation shields having become blocked with molten ash deposits and as a result, the suction flowrate would be low. Remove probe and replace fouled components.

2.3 Gas Analysis and Solids Sampling

Insert probe (with cyclone and gas sample line in place - refer to Figure 1) into furnace to desired depth, adjust cooling water flowrate (this is critical in this instance) with the suction at minimum. Gradually increase suction until a steady trickle of combustion residue falls through the sampling cyclone into the glass collector bottle. The gas sample is drawn off the main sample stream before the cyclone using the sampling point on the probe. Silicon tubing takes the gas sample through a petrol filter (to remove any combustion residue solids) to a suction pump. The outlet of the suction pump passes through a T piece to split the flow into a gas sample for the portable gas analyser and bypass flow, which is monitored through a rotameter. Note that this flowrate may never be negative. Note further, that the gas sample to be analysed must first be passed through a dryer.

Appendix 1.3

Residence Time Distribution manipulations

Appendix 1.3.1 Top Right Burner to Furnace Exit - 2m into boiler

RTD Manipulations :
(Deconvolution of probe response from overall measured response)

Experimental Data

Substance injected	sulfur
Boiler Level at injection	24 m (mill B, right burner)
Probe	2 m in the boiler
Boiler Level at Probe	35.64 m

Read Data from File : RTD := READPRN(decob)

time vector $t := RTD^{\langle 0 \rangle}$

Probe Response $P := RTD^{\langle 2 \rangle}$

Overall Response $C_{out} := RTD^{\langle 1 \rangle}$

# of rows in vector $n := rows(RTD) - 1$ $n = 679$

vector pointer $i := 0 .. n$

Plot of experimental overall and probe response to dirac tracer injection

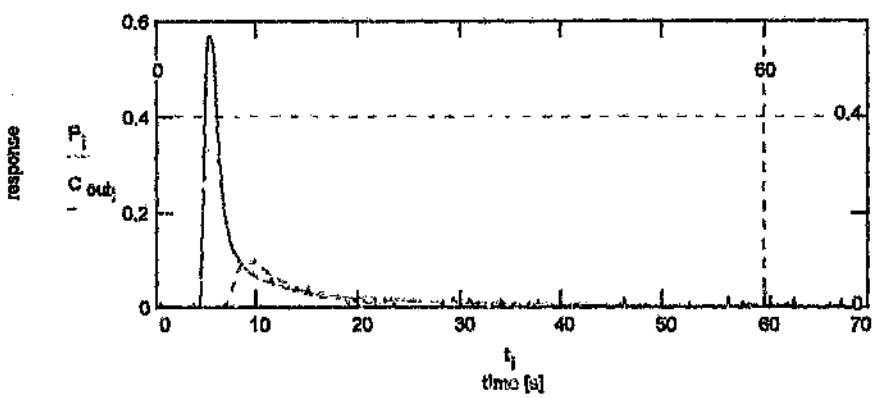

Time Domain Response Definitions

The function below depicts a general form of the time domain responses. This function is fitted to the measured response data by fitting of the function parameters.

$$C(t, \tau_1, \tau_2, \tau_d, const) := const \cdot \left(\frac{1}{\tau_1 - \tau_2}\right) \cdot \left[\left[\exp\left[(t - \tau_d)\cdot\tau_1\right] - \exp\left[(t - \tau_d)\cdot\tau_2\right]\right] \cdot \Phi(t - \tau_d)\right]$$

Probe Response : (visual best function fit to data)

$\tau_{p1} := 0.77$ $\tau_{p2} := 2.69$ $\tau_{pd} := 4.64$ parameters for RTD

$P_{an}(t) := C(t, \tau_{p1}, \tau_{p2}, \tau_{pd}, const_p)$ $const_p := 2.52$

$E(\tau_1, \tau_2, \tau_d) := \sum_{j=1}^{n} (P_j - P_{an}(t_j))^2$ define squared error

$E(\tau_{p1}, \tau_{p2}, \tau_{pd}) = 0.2$

Graph comparing measured and curve fitted RTD

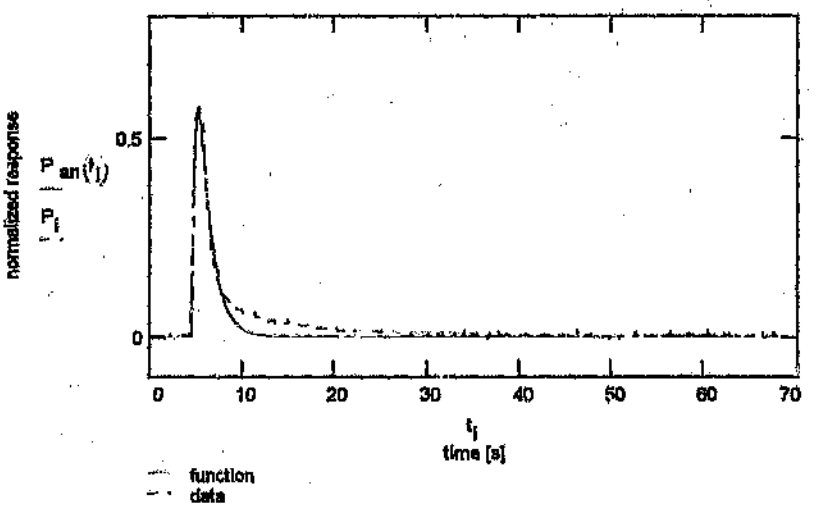

Overall Response : (best function fit to data)

$\tau_{o1} := 0.36$ $\tau_{o2} := 0.5$ $\tau_{od} := 7.4$ $const_o := 0.103$ parameters for RTD

$C_{outan}(t) := C(t, \tau_{o1}, \tau_{o2}, \tau_{od}, const_o)$

$E(\tau_1, \tau_2, \tau_d) := \sum_{j=1}^{n} (C_{outj} - C_{outan}(t_j))^2$ $E(\tau_{o1}, \tau_{o2}, \tau_{od}) = 0.007$ define squared error

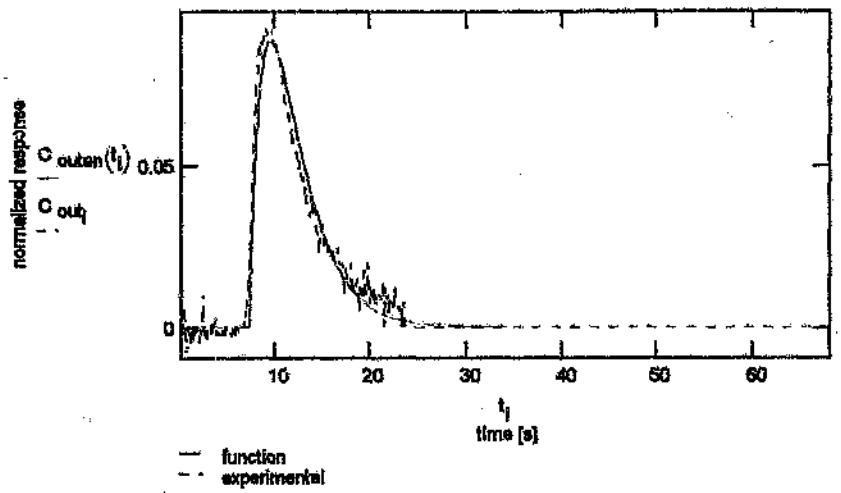

Analytical time domain responses expressed in the Laplace domain (2nd order system with dead time)

Probe Response :

$$P_{an}(t) := const_p \cdot \left(\frac{1}{\tau_{p1} - \tau_{p2}}\right) \cdot \left[\exp\left[(t - \tau_{pd}) \cdot \tau_{p1}\right] - \exp\left[(t - \tau_{pd}) \cdot \tau_{p2}\right]\right] \cdot \Phi(t - \tau_{pd})$$

Overall Response :

$$C_{outexp}(t) := const_o \cdot \left(\frac{1}{\tau_{o1} - \tau_{o2}}\right) \cdot \left[\exp\left[(t - \tau_{od}) \cdot \tau_{o1}\right] - \exp\left[(t - \tau_{od}) \cdot \tau_{o2}\right]\right] \cdot \Phi(t - \tau_{od})$$

Laplace Transforms can be taken of the above expressions, after which the required deconvolution can occur in the Laplace domain. By taking the inverse Laplace transform of the expression obtained by the deconvolution and normalizing the result, the RTD of the boiler can be determined.

Laplace inverting the deconvoluted expression from the Laplace domain :

$$A := \frac{(\tau_{o1} - \tau_{p1}) \cdot (\tau_{o1} - \tau_{p2})}{\tau_{o1} - \tau_{o2}} \qquad B := \frac{(\tau_{o2} - \tau_{p1}) \cdot (\tau_{o2} - \tau_{p2})}{\tau_{o2} - \tau_{o1}}$$

$A = 6.824 \quad B = -4.224 \quad \tau_{Ed} := \tau_{od} - \tau_{pd}$

$$E(t) := \frac{const_o}{const_p} \cdot \Phi(t - \tau_{Ed}) \cdot \left[A \cdot \exp\left[(t - \tau_{Ed}) \cdot \tau_{o1}\right] - B \cdot \exp\left[(t - \tau_{Ed}) \cdot \tau_{o2}\right]\right]$$

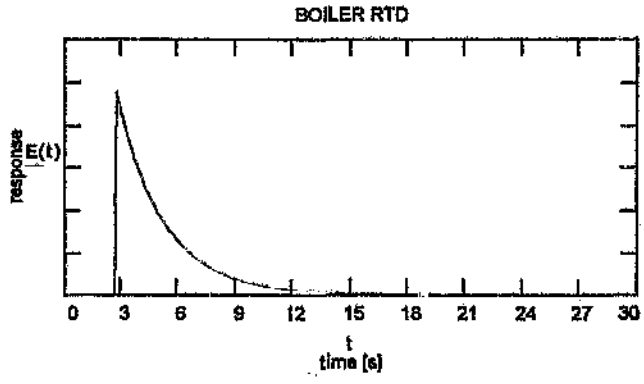

Dead Time : $\tau_{Ed} = 2.76$ s

Appendix 1.3.2 Top Left Burner to Furnace Exit - 2m into boiler

RTD Manipulations :
(Deconvolution of probe response from overall measured response)

Experimental Data

Substance injected	sulfur
Boiler Level at injection	24 m (mill B, left burner)
Probe	2m in the boiler
Boiler Level at Probe	31.64 m

Read Data from File : RTD := READPRN(decoa)

time vector $t := RTD^{<0>}$

Probe Response $P := RTD^{<2>}$

Overall Response $C_{out} := RTD^{<1>}$

# of rows in vector $n := rows(RTD) - 1$ $n = 679$

vector pointer $i := 0..n$

Plot of experimental overall and probe response to dirac tracer injection

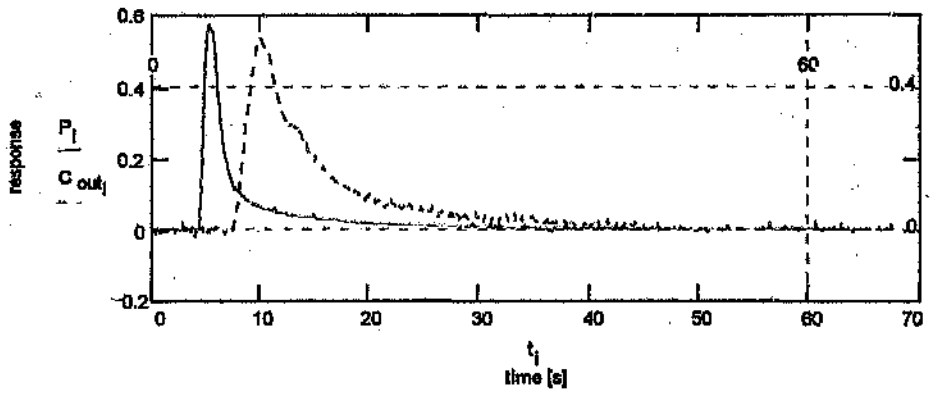

Time Domain Response Definitions

The function below depicts a general form of the time domain responses. This function is fitted to the measured response data by fitting of the function parameters.

$$C(t, \tau_1, \tau_2, \tau_d, const) := const \cdot \left(\frac{1}{\tau_1 - \tau_2}\right) \cdot \left[\exp\left[(t - \tau_d) \cdot \tau_1\right] - \exp\left[(t - \tau_d) \cdot \tau_2\right]\right] \cdot \Phi(t - \tau_d)$$

Probe Response : (best function fit to data)

$\tau_{p1} := 0.77$ $\tau_{p2} := 2.69$ $\tau_{pd} := 4.64$ $const_p := 2.52$ parameters for RTD

$P_{an}(t) := C(t, \tau_{p1}, \tau_{p2}, \tau_{pd}, const_p)$

$E(\tau_1, \tau_2, \tau_d) := \sum_{j=1}^{n} (P_j - P_{an}(t_j))^2$ define squared error $E(\tau_{p1}, \tau_{p2}, \tau_{pd}) = 0.2$

Graph comparing measured and curve fitted RTD

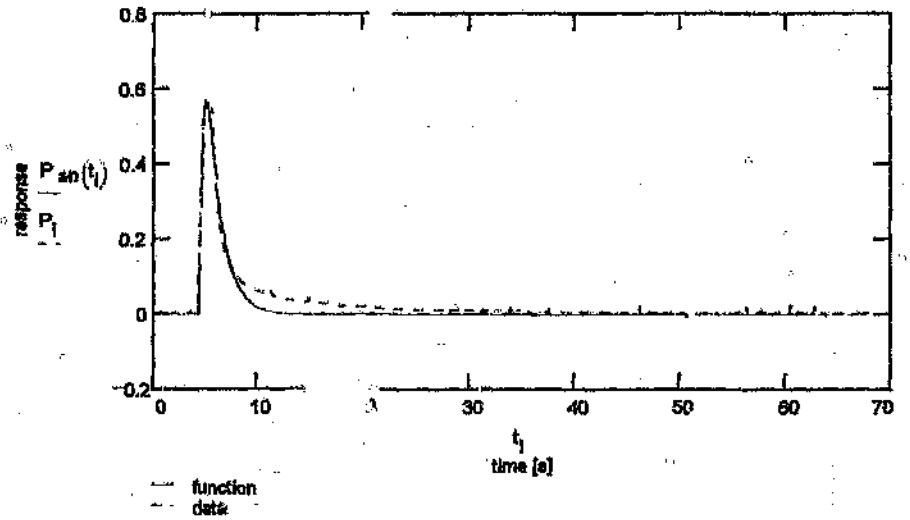

Overall Response : (best function fit to data)

$\tau_{o1} := 0.20$ $\tau_{o2} := 1.0$ $\tau_{od} := 7.8$ $const_o := 0.75$ parameters for RTD

$C_{outan}(t) := C(t, \tau_{o1}, \tau_{o2}, \tau_{od}, const_o)$

$E(\tau_1, \tau_2, \tau_d) := \sum_{j=1}^{n} (C_{out_j} - C_{outan}(t_j))^2$ define squared error

$E(\tau_{o1}, \tau_{o2}, \tau_{od}) = 0.343$

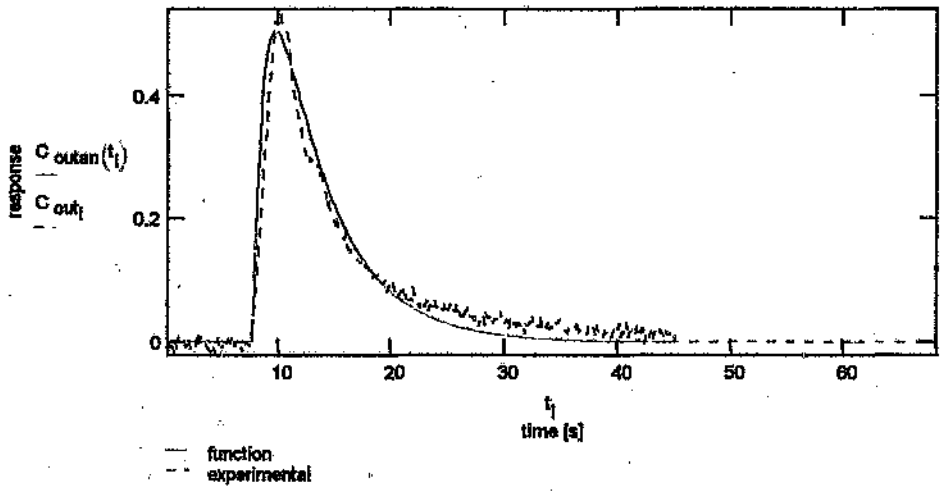

Analytical time domain responses expressed in the Laplace domain (2nd order system with dead time)

Probe Response : $P_{an}(t) := const_p \cdot \left(\frac{1}{\tau_{p1} - \tau_{p2}}\right) \cdot \left[\exp\left[(t - \tau_{pd}) \cdot \tau_{p1}\right] - \exp\left[(t - \tau_{pd}) \cdot \tau_{p2}\right]\right] \cdot \Phi(t - \tau_{pd})$

Overall Response $C_{outan}(t) := const_o \cdot \left(\frac{1}{\tau_{o1} - \tau_{o2}}\right) \cdot \left[\exp\left[(t - \tau_{od}) \cdot \tau_{o1}\right] - \exp\left[(t - \tau_{od}) \cdot \tau_{o2}\right]\right] \cdot \Phi(t - \tau_{od})$

Laplace Transforms can be taken of the above expressions, after which the required deconvolution can occur in the Laplace domain. By taking the inverse Laplace transform of the expression obtained by the deconvolution and normalizing the result, the RTD of the boiler can be determined.

Laplace inverting the deconvoluted expression from the Laplace domain :

$A := \frac{(\tau_{o1} - \tau_{p1}) \cdot (\tau_{o1} - \tau_{p2})}{\tau_{o1} - \tau_{o2}}$ $\qquad$ $B := \frac{(\tau_{o2} - \tau_{p1}) \cdot (\tau_{o2} - \tau_{p2})}{\tau_{o2} - \tau_{o1}}$

$A = 1.774$ $\qquad$ $B = 0.486$ $\qquad$ $\tau_{Ed} := \tau_{od} - \tau_{pd}$

$E(t) := \frac{const_o}{const_p} \cdot \Phi(t - \tau_{Ed}) \cdot \left[A \cdot \exp\left[(t - \tau_{Ed}) \cdot \tau_{o1}\right] - B \cdot \exp\left[(t - \tau_{Ed}) \cdot \tau_{o2}\right]\right]$

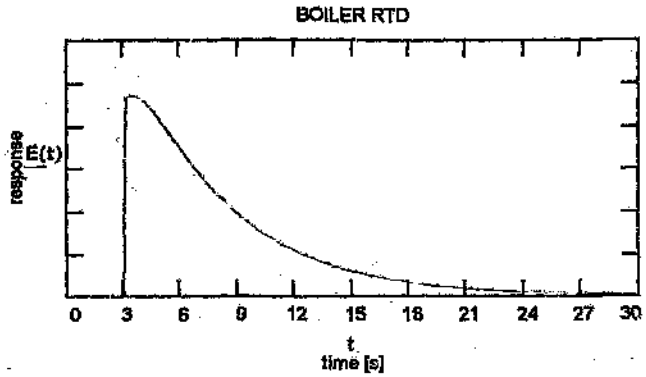

Dead Time : $t_{Ed} = 3.16$ s

Appendix 1.3.3 Top Right Burner to Furnace Exit - 3m into boiler

RTD Manipulations :
(Deconvolution of probe response from overall measured response)
Experimental Data

Substance injected	sulfur
Boiler Level at injection	24 m (mill B,right burner)
Probe	3m in the furnace
Boiler Level at Probe	35.64 m

Read Data from File : RTD := READPRN(decol)

time vector $t := RTD^{<0>}$

Probe Response $P := RTD^{<2>}$

Overall Response $C_{out} := RTD^{<1>}$

# of rows in vector $n := rows(RTD) - 1$ $n = 679$

vector pointer $i := 0..n$

Plot of experimental overall and probe response to dirac tracer injection

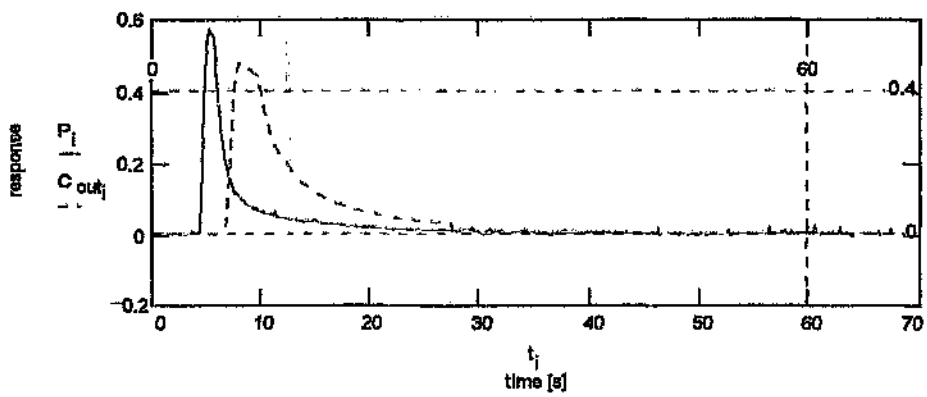

Time Domain Response Definitions

The function below depicts a general form of the time domain responses. This function is fitted to the measured response data by fitting of the function parameters.

$$C(t, \tau_1, \tau_2, \tau_d, const) := const \cdot \left(\frac{1}{\tau_1 - \tau_2}\right) \cdot \left[\exp\left[(t - \tau_d) \cdot \tau_1\right] - \exp\left[(t - \tau_d) \cdot \tau_2\right]\right] \cdot \Phi(t - \tau_d)$$

Probe Response : (visual best function fit to data)

$\tau_{p1} := 0.77$ $\tau_{p2} := 2.69$ $\tau_{pd} := 4.64$ $const_p := 2.52$ parameters for RTD

$P_{an}(t) := C(t, \tau_{p1}, \tau_{p2}, \tau_{pd}, const_p)$

$E(\tau_1, \tau_2, \tau_d) := \sum_{j=1}^{n} (P_j - P_{an}(t_j))^2$ define squared error $E(\tau_{p1}, \tau_{p2}, \tau_{pd}) = 0.2$

Graph comparing measured and curve fitted RTD

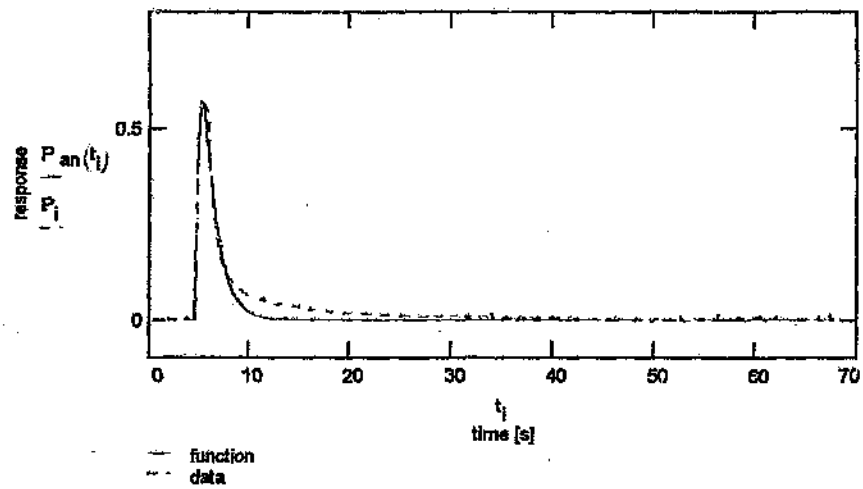

1

Overall Response : (best function fit to data)

$\tau_{o1} := 0.21$ $\tau_{o2} := 2.1$ $\tau_{od} := 7.0$ $const_o := 1.31$ parameters for RTD

$C_{outan}(t) := C(t, \tau_{o1}, \tau_{o2}, \tau_{od}, const_o)$

$E(\tau_1, \tau_2, \tau_d) := \sum_{j=1}^{n} (C_{out_j} - C_{outan}(t_j))^2$ define squared error

$E(\tau_{o1}, \tau_{o2}, \tau_{od}) = 0.113$

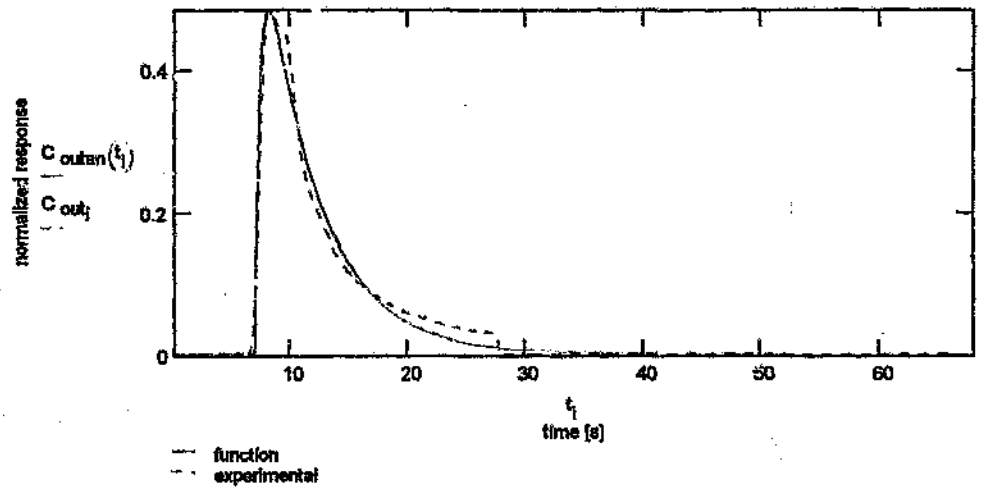

Analytical time domain responses expressed in the Laplace domain (2nd order system with dead time)

Probe Response : $P_{an}(t) := const_p \cdot \left(\frac{1}{\tau_{p1} - \tau_{p2}}\right) \cdot \left[\exp\left[(t - \tau_{pd}) \cdot \tau_{p1}\right] - \exp\left[(t - \tau_{pd}) \cdot \tau_{p2}\right]\right] \cdot \Phi(t - \tau_{pd})$

Overall Response $C_{outan}(t) := const_o \cdot \left(\frac{1}{\tau_{o1} - \tau_{o2}}\right) \cdot \left[\exp\left[(t - \tau_{od}) \cdot \tau_{o1}\right] - \exp\left[(t - \tau_{od}) \cdot \tau_{o2}\right]\right] \cdot \Phi(t - \tau_{od})$

Laplace Transforms can be taken of the above expressions, after which the required deconvolution can occur in the Laplace domain. By taking the inverse Laplace transform of the expression obtained by the deconvolution and normalizing the result, the RTD of the boiler can be determined.

Laplace inverting the deconvoluted expression from the Laplace domain :

$A := \frac{(\tau_{o1} - \tau_{p1}) \cdot (\tau_{o1} - \tau_{p2})}{\tau_{o1} - \tau_{o2}}$ $\quad$ $B := \frac{(\tau_{o2} - \tau_{p1}) \cdot (\tau_{o2} - \tau_{p2})}{\tau_{o2} - \tau_{o1}}$

$A = 0.735$ $\quad$ $B = 0.415$ $\quad$ $\tau_{Ed} := \tau_{od} - \tau_{pd}$ $\quad$ $\tau_{Ed} = 2.36$

$E(t) := \frac{const_o}{const_p} \cdot \Phi(t - \tau_{Ed}) \cdot \left[A \cdot \exp\left[(t - \tau_{Ed}) \cdot \tau_{o1}\right] - B \cdot \exp\left[(t - \tau_{Ed}) \cdot \tau_{o2}\right]\right]$

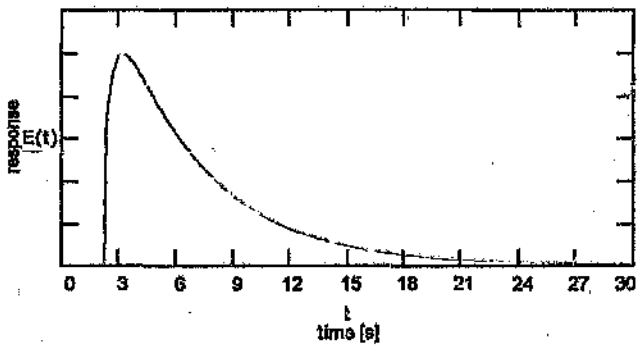
response
E(t)
0
3
6
9
12
15
18
21
24
27
30
t
time [s]

Appendix 1.3.4 Top Left Burner to Furnace Exit - 4m into boiler

RTD Manipulations : (Deconvolution of probe response from overall measured response)

Experimental Data

Substance injected	sulfur
Boiler Level at injection	24 m (mill B, left burner)
Probe	4m in the boiler
Boiler Level at Probe	35.64 m

Read Data from File : RTD := READPRN(decog)

time vector $t := RTD^{<0>}$

Probe Response $P := RTD^{<2>}$

Overall Response $C_{out} := RTD^{<1>}$

# of rows in vector $n := rows(RTD) - 1$ $n = 679$

vector pointer $i := 0..n$

Plot of experimental overall and probe response to dirac tracer injection

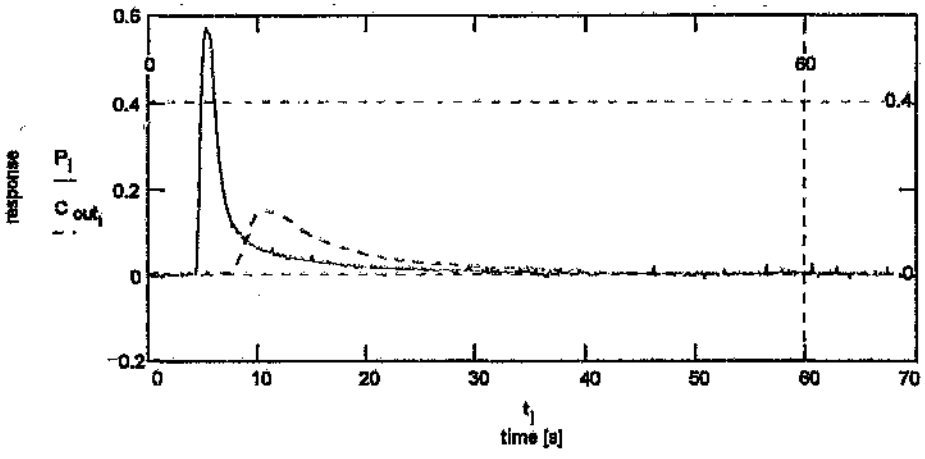

Time Domain Response Definitions

The function below depicts a general form of the time domain responses. This function is fitted to the measured response data by fitting of the function parameters.

$$C(t,\tau_1,\tau_2,\tau_d,const) := const\cdot\left(\frac{1}{\tau_1-\tau_2}\right)\cdot\left[\exp\left[(t-\tau_d)\cdot\tau_1\right]-\exp\left[(t-\tau_d)\cdot\tau_2\right]\right]\cdot\Phi(t-\tau_d)$$

Probe Response : (visual best function fit to data)

$\tau_{p1} := 0.77$ $\tau_{p2} := 2.69$ $\tau_{pd} := 4.64$ $const_p := 2.52$ parameters for RTD

$P_{an}(t) := C(t, \tau_{p1}, \tau_{p2}, \tau_{pd}, const_p)$

$E(\tau_1, \tau_2, \tau_d) := \sum_{j=1}^{n} (P_j - P_{an}(t_j))^2$ define squared error $E(\tau_{p1}, \tau_{p2}, \tau_{pd}) = 0.2$

Graph comparing measured and curve fitted RTD

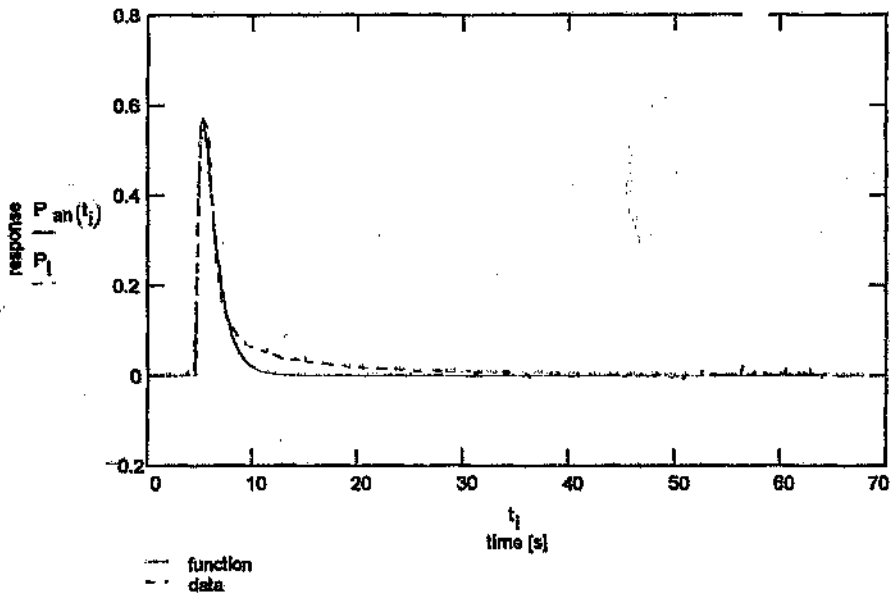

Overall Response : (best function fit to data)

$\tau_{o1} := 0.20$ $\tau_{o2} := 0.4$ $\tau_{od} := 8.01$ $const_o := 0.118$ parameters for RTD

$C_{outan}(t) := C(t, \tau_{o1}, \tau_{o2}, \tau_{od}, const_o)$

$E(\tau_1, \tau_2, \tau_d) := \sum_{j=1}^{n} (C_{out_j} - C_{outan}(t_j))^2$ define squared error

$E(\tau_{o1}, \tau_{o2}, \tau_{od}) = 0.032$

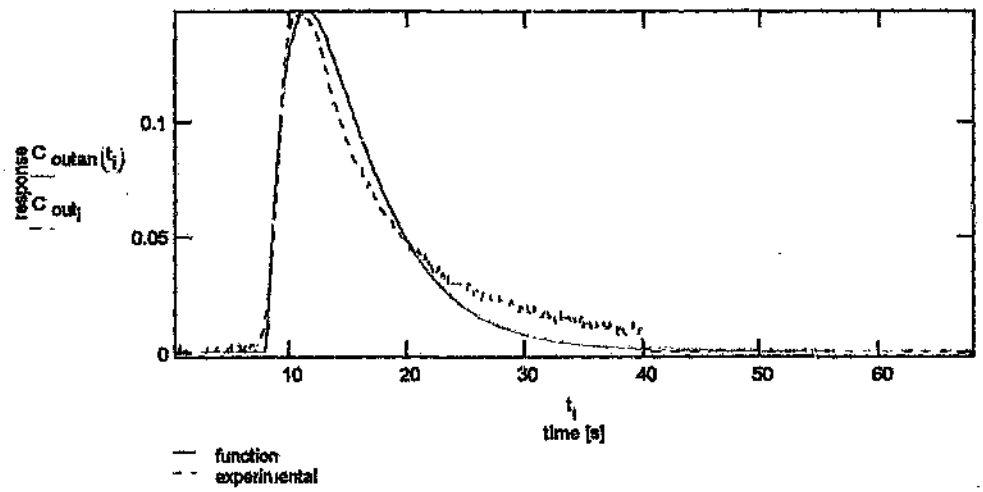

Analytical time domain responses expressed in the Laplace domain (2nd order system with dead time)

Probe Response : $P_{an}(t) := const_p \cdot \left(\frac{1}{\tau_{p1} - \tau_{p2}}\right) \cdot \left[\exp\left[(t - \tau_{pd}) \cdot \tau_{p1}\right] - \exp\left[(t - \tau_{pd}) \cdot \tau_{p2}\right]\right] \cdot \Phi(t - \tau_{pd})$

Overall Response : $C_{outan}(t) := const_o \cdot \left(\frac{1}{\tau_{o1} - \tau_{o2}}\right) \cdot \left[\exp\left[(t - \tau_{od}) \cdot \tau_{o1}\right] - \exp\left[(t - \tau_{od}) \cdot \tau_{o2}\right]\right] \cdot \Phi(t - \tau_{od})$

Laplace Transforms can be taken of the above expressions, after which the required deconvolution can occur in the Laplace domain. By taking the inverse Laplace transform of the expression obtained by the deconvolution and normalizing the result, the RTD of the boiler can be determined.

Laplace inverting the deconvoluted expression from the Laplace domain :

$A := \frac{(\tau_{o1} - \tau_{p1}) \cdot (\tau_{o1} - \tau_{p2})}{\tau_{o1} - \tau_{o2}}$ $\quad$ $B := \frac{(\tau_{o2} - \tau_{p1}) \cdot (\tau_{o2} - \tau_{p2})}{\tau_{o2} - \tau_{o1}}$

$A = 7.096$ $\quad$ $B = -4.237$ $\quad$ $\tau_{Ed} := \tau_{od} - \tau_{pd}$ $\quad$ $\tau_{Ed} = 3.37$

$E(t) := \frac{const_o}{const_p} \cdot \Phi(t - \tau_{Ed}) \cdot \left[A \cdot \exp\left[(t - \tau_{Ed}) \cdot \tau_{o1}\right] - B \cdot \exp\left[(t - \tau_{Ed}) \cdot \tau_{o2}\right]\right]$

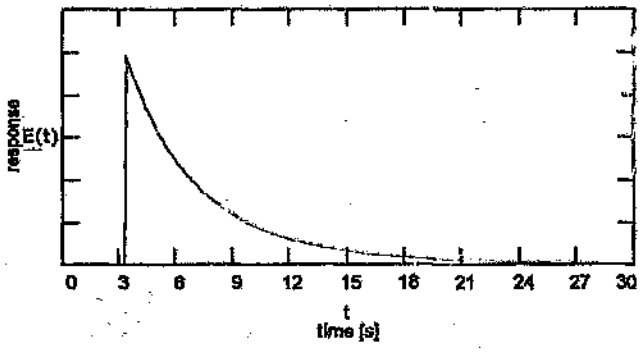
response
E(t)
0
3
6
9
12
15
18
21
24
27
30
t
time [s]

Appendix 1.3.5 Top Right Burner to Furnace Exit - 4m into boiler

RTD Manipulations :
(Deconvolution of probe response from overall measured response)

Experimental Data

Substance injected	sulfur
Boiler Level at injection	24m (mill B, right burner)
Probe	4 m in the boiler
Boiler Level at Probe	35.64 m

Read Data from File : RTD := READPRN(decoh)

time vector $t := RTD^{<0>}$

Probe Response $P := RTD^{<2>}$

Overall Response $C_{out} := RTD^{<1>}$

# of rows in vector $n := rows(RTD) - 1$ $n = 679$

vector pointer $i := 0..n$

Plot of experimental overall and probe response to dirac tracer injection

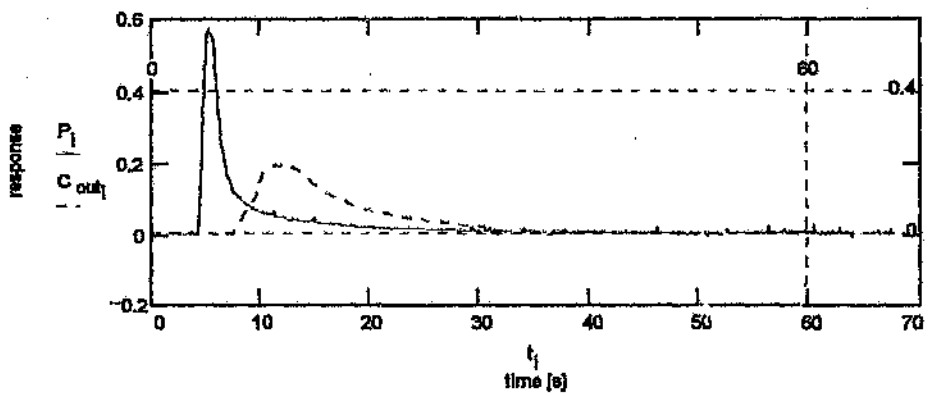

Time Domain Response Definitions

The function below depicts a general form of the time domain responses. This function is fitted to the measured response data by fitting of the function parameters.

$$C(t, \tau_1, \tau_2, \tau_d, const) := const \cdot \left(\frac{1}{\tau_1 - \tau_2}\right) \cdot \left[\exp\left[(t - \tau_d) \cdot \tau_1\right] - \exp\left[(t - \tau_d) \cdot \tau_2\right]\right] \cdot \Phi(t - \tau_d)$$

Probe Response : (visual best function fit to data)

$\tau_{p1} := 0.77$ $\tau_{p2} := 2.69$ $\tau_{pd} := 4.64$ $const_p := 2.52$ parameters for RTD

$P_{an}(t) := C(t, \tau_{p1}, \tau_{p2}, \tau_{pd}, const_p)$

$E(\tau_1, \tau_2, \tau_d) := \sum_{j=1}^{n} (P_j - P_{an}(t_j))^2$ define squared error $E(\tau_{p1}, \tau_{p2}, \tau_{pd}) = 0.2$

Graph comparing measured and curve fitted RTD

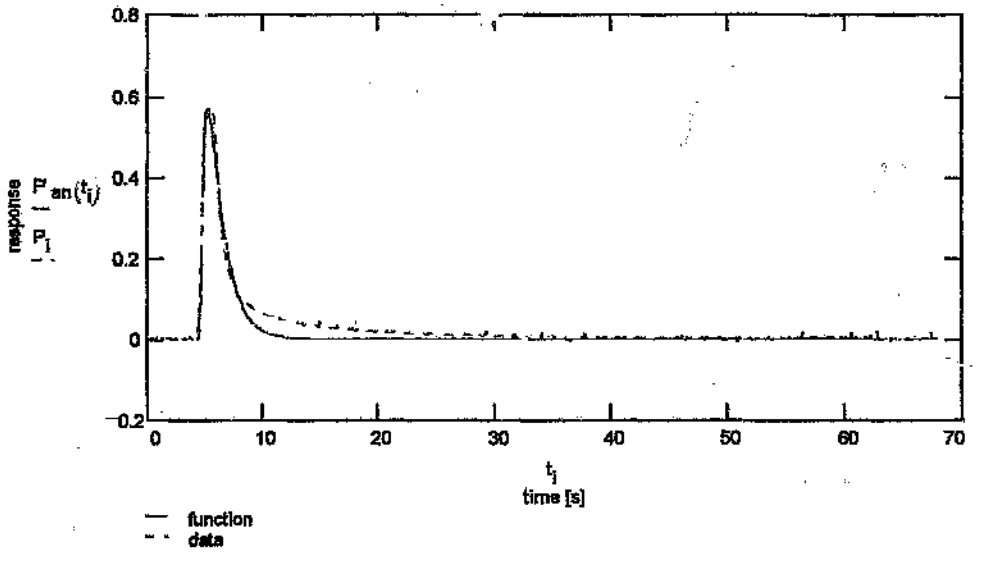

Overall Response : (best function fit to data)

$\tau_{o1} := 0.12$ $\tau_{o2} := 0.7$ $\tau_{od} := 8.1$ $const_o := 0.19$ parameters for RTD

$C_{outan}(t) := C(t, \tau_{o1}, \tau_{o2}, \tau_{od}, const_o)$

$E(\tau_1, \tau_2, \tau_d) := \sum_{j=1}^{n} (C_{out_j} - C_{outan}(t_j))^2$ define squared error

$E(\tau_{o1}, \tau_{o2}, \tau_{od}) = 0.089$

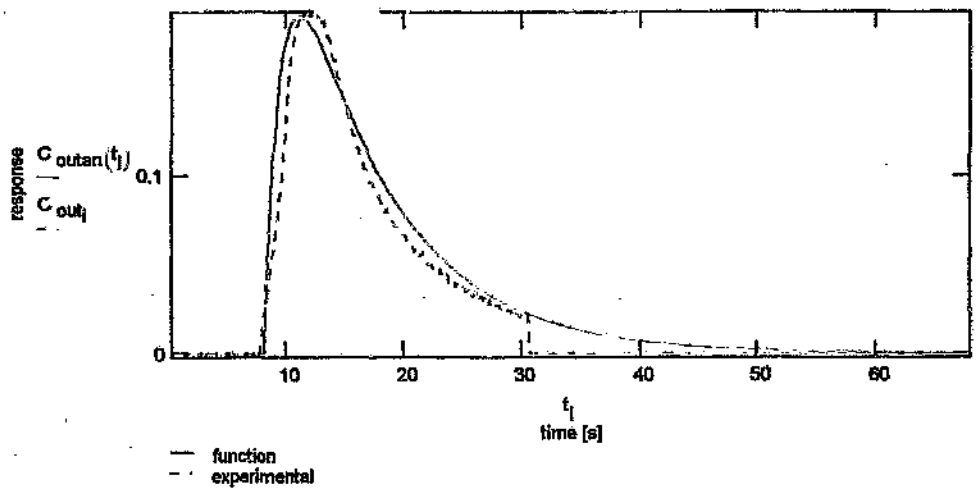

Analytical time domain responses expressed in the Laplace domain (2nd order system with dead time)

Probe Response : $P_{an}(t) := const_p \cdot \left(\frac{1}{\tau_{p1} - \tau_{p2}}\right) \cdot \left[\exp\left[(t - \tau_{pd}) \cdot \tau_{p1}\right] - \exp\left[(t - \tau_{pd}) \cdot \tau_{p2}\right]\right] \cdot \Phi(t - \tau_{pd})$

Overall Response $C_{outan}(t) := const_o \cdot \left(\frac{1}{\tau_{o1} - \tau_{o2}}\right) \cdot \left[\exp\left[(t - \tau_{od}) \cdot \tau_{o1}\right] - \exp\left[(t - \tau_{od}) \cdot \tau_{o2}\right]\right] \cdot \Phi(t - \tau_{od})$

Laplace Transforms can be taken of the above expressions, after which the required deconvolution can occur in the Laplace domain. By taking the inverse Laplace transform of the expression obtained by the deconvolution and normalizing the result, the RTD of the boiler can be determined.

Laplace inverting the deconvoluted expression from the Laplace domain :

$$A := \frac{(\tau_{o1} - \tau_{p1}) \cdot (\tau_{o1} - \tau_{p2})}{\tau_{o1} - \tau_{o2}} \qquad B := \frac{(\tau_{o2} - \tau_{p1}) \cdot (\tau_{o2} - \tau_{p2})}{\tau_{o2} - \tau_{o1}}$$

$A = 2.88$ $B = -0.24$ τ_{Ed} τ_{od} τ_{pd}

$$E(t) := \frac{const_o}{const_p} \cdot \Phi(t - \tau_{Ed}) \cdot \left[A \cdot \exp\left[(t - \tau_{Ed}) \cdot \tau_{o1}\right] - B \cdot \exp\left[(t - \tau_{Ed}) \cdot \tau_{o2}\right]\right]$$

$\tau_{Ed} = 3.46$

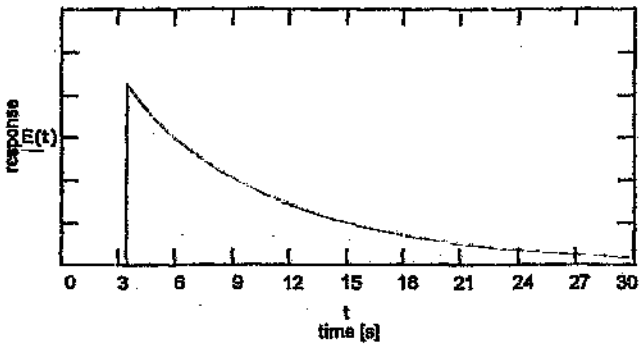

$\tau_{Ed} = 3.46$ s

Appendix 1.3.6 Middle Left Burner to Furnace Exit - 4m into boiler

RTD Manipulations :
(Deconvolution of probe response from overall measured response)

Experimental Data

Substance injected	sulfur
Boiler Level at injection	20 m (mill C, left burner)
Probe	4 m in the furnace
Boiler Level at Probe	35.64 m

Read Data from File : RTD := READPRN(decok)

time vector $t := RTD^{<0>}$

Probe Response $P := RTD^{<2>}$

Overall Response $C_{out} := RTD^{<1>}$

# of rows in vector $n := rows(RTD) - 1$ $n = 679$

vector pointer $i := 0..n$

Plot of experimental overall and probe response to dirac tracer injection

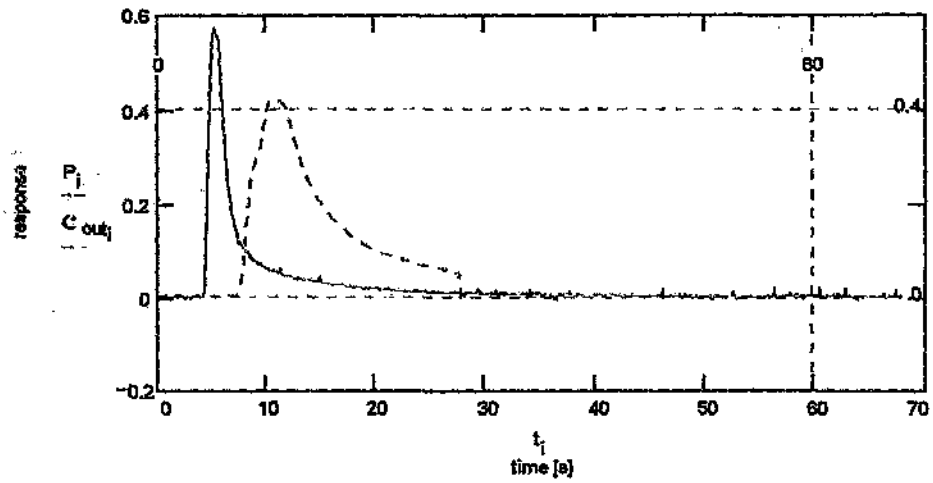

Time Domain Response Definitions

The function below depicts a general form of the time domain responses. This function is fitted to the measured response data by fitting of the function parameters.

$$C(t, \tau_1, \tau_2, \tau_d, const) := const \cdot \left(\frac{1}{\tau_1 - \tau_2}\right) \cdot \left[\exp\left[(t - \tau_d)\cdot\tau_1\right] - \exp\left[(t - \tau_d)\cdot\tau_2\right]\right] \cdot \Phi(t - \tau_d)$$

Probe Response : (visual best function fit to data)

$\tau_{p1} := 0.77$ $\tau_{p2} := 2.69$ $\tau_{pd} := 4.64$ $const_p := 2.52$ parameters for RTD

$P_{an}(t) := C(t, \tau_{p1}, \tau_{p2}, \tau_{pd}, const_p)$

$E(\tau_1, \tau_2, \tau_d) := \sum_{j=1}^{n} (P_j - P_{an}(t_j))^2$ define squared error $E(\tau_{p1}, \tau_{p2}, \tau_{pd}) = 0.2$

Graph comparing measured and curve fitted RTD

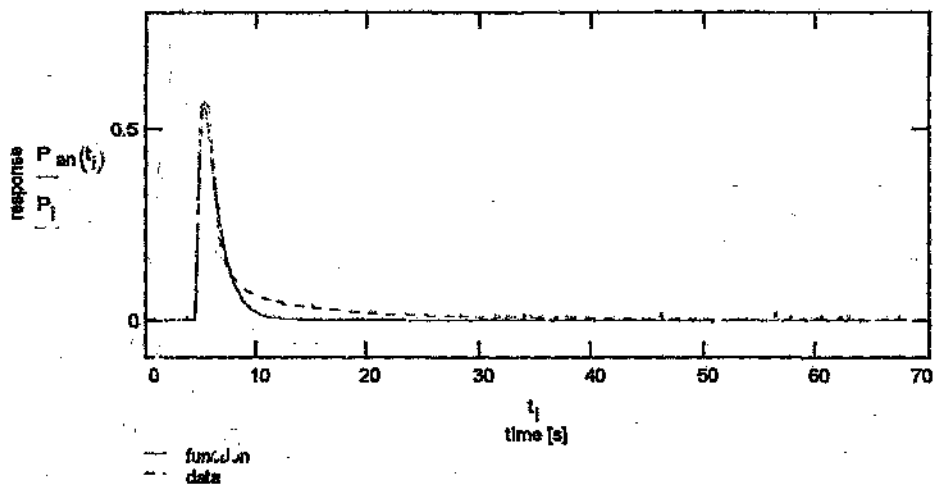

Overall Response : (best function fit to data)

$\tau_{o1} := 0.15$ $\tau_{o2} := 1.0$ $\tau_{od} := 8.2$ $const_o := .59$ parameters for RTD

$C_{outan}(t) := C(t, \tau_{o1}, \tau_{o2}, \tau_{od}, const_o)$

$E(\tau_1, \tau_2, \tau_d) := \sum_{j=1}^{n} (C_{out_j} - C_{outan}(t_j))^2$ define squared error

$E(\tau_{o1}, \tau_{o2}, \tau_{od}) = 0.212$

Probe Response : (visual best function fit to data)

$\tau_{p1} := 0.77$ $\tau_{p2} := 2.69$ $\tau_{pd} := 4.64$ $const_p := 2.52$ parameters for RTD

$P_{an}(t) := C(t, \tau_{p1}, \tau_{p2}, \tau_{pd}, const_p)$

$E(\tau_1, \tau_2, \tau_d) := \sum_{j=1}^{n} (P_j - P_{an}(t_j))^2$ define squared error $E(\tau_{p1}, \tau_{p2}, \tau_{pd}) =$

Graph comparing measured and curve fitted RTD

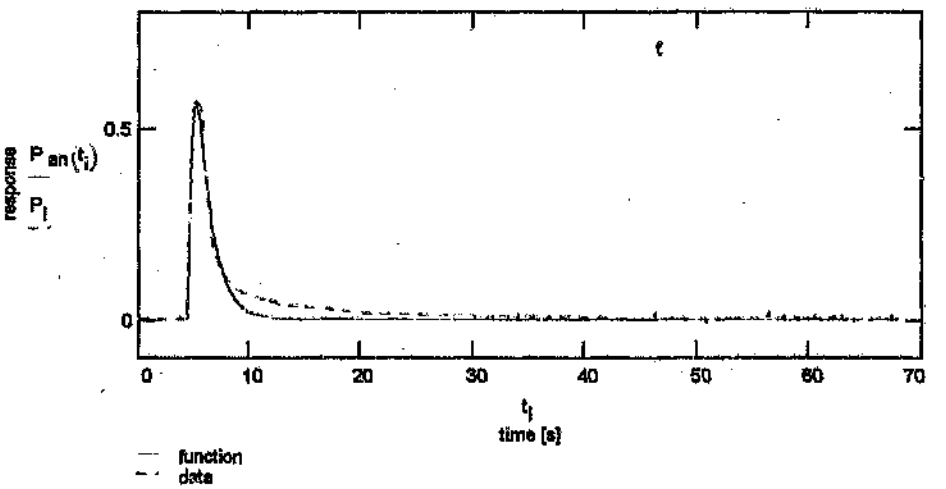

Overall Response : (best function fit to data)

$\tau_{o1} := 0.15$ $\tau_{o2} := 1.0$ $\tau_{od} := 8.2$ $const_o := .59$ parameters for RTD

$C_{outan}(t) := C(t, \tau_{o1}, \tau_{o2}, \tau_{od}, const_o)$

$E(\tau_1, \tau_2, \tau_d) := \sum_{j=1}^{n} (C_{out_j} - C_{outan}(t_j))^2$ define squared error

$E(\tau_{o1}, \tau_{o2}, \tau_{od}) = 0.212$

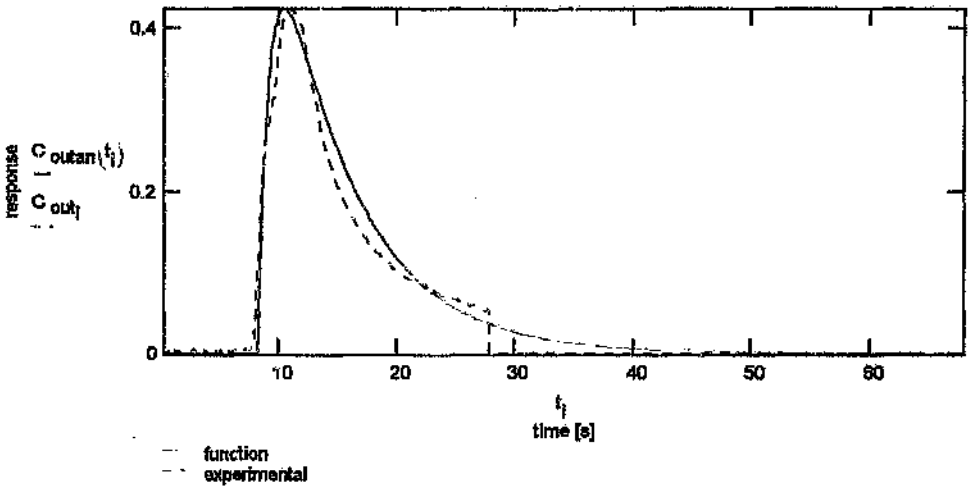

Analytical time domain responses expressed in the Laplace domain (2nd order system with dead time)

Probe Response : $P_{an}(t) := const_p \cdot \left(\frac{1}{\tau_{p1} - \tau_{p2}}\right) \cdot \left[\exp\left[(t - \tau_{pd}) \cdot \tau_{p1}\right] - \exp\left[(t - \tau_{pd}) \cdot \tau_{p2}\right]\right] \cdot \Phi(t - \tau_{pd})$

Overall Response : $C_{outan}(t) := const_o \cdot \left(\frac{1}{\tau_{o1} - \tau_{o2}}\right) \cdot \left[\exp\left[(t - \tau_{od}) \cdot \tau_{o1}\right] - \exp\left[(t - \tau_{od}) \cdot \tau_{o2}\right]\right] \cdot \Phi(t - \tau_{od})$

Laplace Transforms can be taken of the above expressions, after which the required deconvolution can occur in the Laplace domain. By taking the inverse Laplace transform of the expression obtained by the deconvolution and normalizing the result, the RTD of the boiler can be determined.

Laplace inverting the deconvoluted expression from the Laplace domain :

$A := \frac{(\tau_{o1} - \tau_{p1}) \cdot (\tau_{o1} - \tau_{p2})}{\tau_{o1} - \tau_{o2}}$ $\quad$ $B := \frac{(\tau_{o2} - \tau_{p1}) \cdot (\tau_{o2} - \tau_{p2})}{\tau_{o2} - \tau_{o1}}$

$A = 1.853$ $\quad$ $B = 0.457$ $\quad$ $\tau_{Ed} := \tau_{od} - \tau_{pd}$ $\quad$ $\tau_{Ed} = 3.56$

$E(t) := \frac{const_o}{const_p} \cdot \Phi(t - \tau_{Ed}) \cdot \left[A \cdot \exp\left[(t - \tau_{Ed}) \cdot \tau_{o1}\right] - B \cdot \exp\left[(t - \tau_{Ed}) \cdot \tau_{o2}\right]\right]$

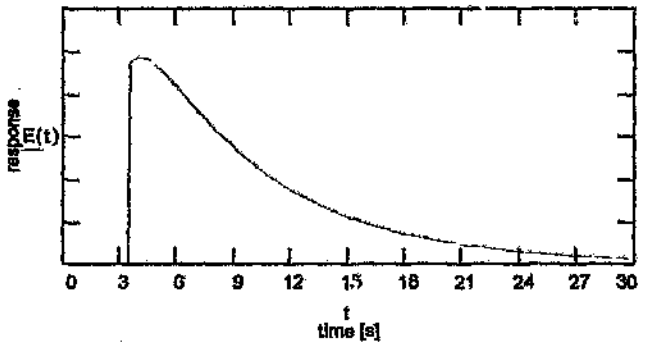
response
E(t)
0
3
6
9
12
15
18
21
24
27
30
t
time [s]

Appendix 1.3.7 Middle Right Burner to Furnace Exit - 4m into boiler

RTD Manipulations : (Deconvolution of probe response from overall measured response)

Experimental Data

Substance injected	sulfur
Boiler Level at injection	20 m (mill C, right burner)
Probe	4 m in the furnace
Boiler Level at Probe	35.64 m

Read Data from File : RTD := READPRN(decol)

time vector $t := RTD^{<0>}$

Probe Response $P := RTD^{<2>}$

Overall Response $C_{out} := RTD^{<1>}$

# of rows in vector $n := rows(RTD) - 1$ $n = 679$

vector pointer $I := 0..n$

Plot of experimental overall and probe response to dirac tracer injection

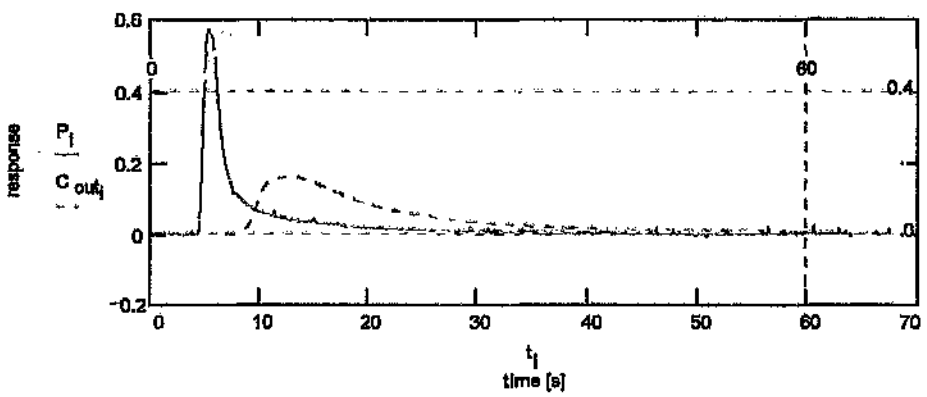

Time Domain Response Definitions

The function below depicts a general form of the time domain responses. This function is fitted to the measured response data by fitting of the function parameters.

$$C(t,\tau_1,\tau_2,\tau_d,const) := const\cdot\left(\frac{1}{\tau_1-\tau_2}\right)\cdot\left[\exp\left[(t-\tau_d)\cdot\tau_1\right]-\exp\left[(t-\tau_d)\cdot\tau_2\right]\right]\cdot\Phi(t-\tau_d)$$

Probe Response : (visual best function fit to data)

$\tau_{p1} := 0.77$ $\tau_{p2} := 2.69$ $\tau_{pd} := 4.64$ $const_p := 2.52$ purameters for RTD

$P_{an}(t) := C(t, \tau_{p1}, \tau_{p2}, \tau_{pd}, const_p)$

$E(\tau_1, \tau_2, \tau_d) := \sum_{j=1}^{n} (P_j - P_{an}(t_j))^2$ define squared error $E(\tau_{p1}, \tau_{p2}, \tau_{pd}) = 0.2$

Graph comparing measured and curve fitted RTD

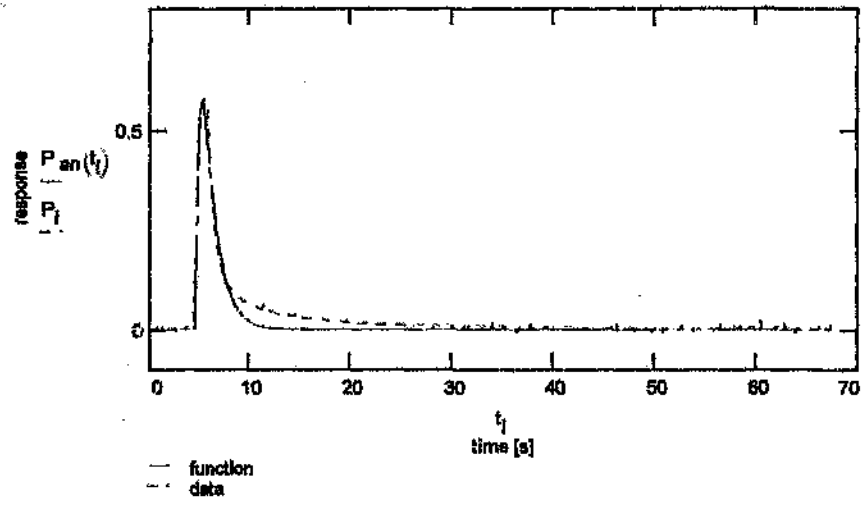

Overall Response : (best function fit to data)

$\tau_{o1} := 0.15$ $\tau_{o2} := 0.3$ $\tau_{od} := 8.32$ $const_o := 0.095$ parameters for RTD

$C_{outan}(t) := C(t, \tau_{o1}, \tau_{o2}, \tau_{od}, const_o)$

$E(\tau_1, \tau_2, \tau_d) := \sum_{j=1}^{n} (C_{out_j} - C_{outan}(t_j))^2$ define squared error

$E(\tau_{o1}, \tau_{o2}, \tau_{od}) = 0.042$

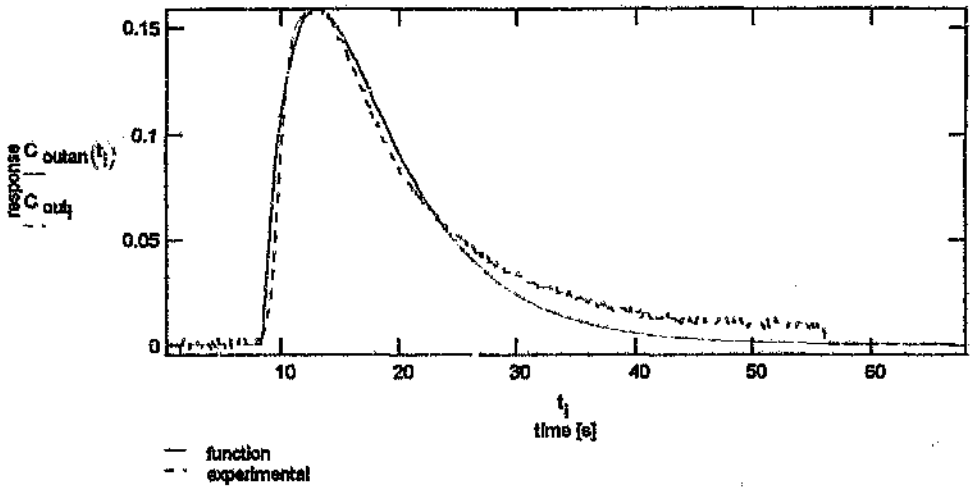

Analytical time domain responses expressed in the Laplace domain (2nd order system with dead time)

Probe Response : $P_{an}(t) := const_p \cdot \left(\frac{1}{\tau_{p1} - \tau_{p2}}\right) \cdot \left[\exp\left[(t - \tau_{pd}) \cdot \tau_{p1}\right] - \exp\left[(t - \tau_{pd}) \cdot \tau_{p2}\right]\right] \cdot \Phi(t - \tau_{pd})$

Overall Response : $C_{outan}(t) := const_o \cdot \left(\frac{1}{\tau_{o1} - \tau_{o2}}\right) \cdot \left[\exp\left[(t - \tau_{od}) \cdot \tau_{o1}\right] - \exp\left[(t - \tau_{od}) \cdot \tau_{o2}\right]\right] \cdot \Phi(t - \tau_{od})$

Laplace Transforms can be taken of the above expressions, after which the required deconvolution can occur in the Laplace domain. By taking the inverse Laplace transform of the expression obtained by the deconvolution and normalizing the result, the RTD of the boiler can be determined.

Laplace inverting the deconvoluted expression from the Laplace domain :

$A := \frac{(\tau_{o1} - \tau_{p1}) \cdot (\tau_{o1} - \tau_{p2})}{\tau_{o1} - \tau_{o2}}$ $\quad$ $B := \frac{(\tau_{o2} - \tau_{p1}) \cdot (\tau_{o2} - \tau_{p2})}{\tau_{o2} - \tau_{o1}}$

$A = 10.499$ $\quad$ $B = -7.469$ $\quad$ $\tau_{Ed} := \tau_{od} - \tau_{pd}$ $\quad$ $\tau_{Ed} = 3.68$

$E(t) := \frac{const_o}{const_p} \cdot \Phi(t - \tau_{Ed}) \cdot \left[A \cdot \exp\left[(t - \tau_{Ed}) \cdot \tau_{o1}\right] - B \cdot \exp\left[(t - \tau_{Ed}) \cdot \tau_{o2}\right]\right]$

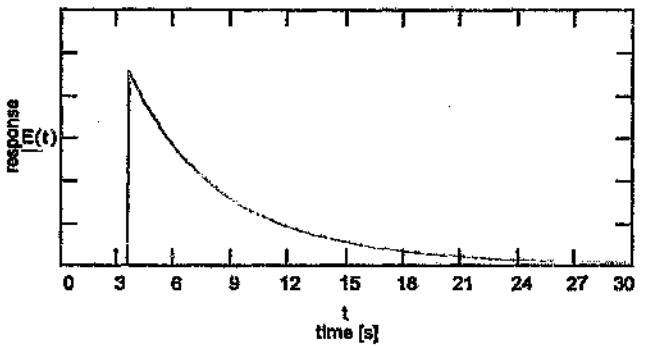
response
E(t)
0
3
6
9
12
15
18
21
24
27
30
t
time [s]

Appendix 1.3.8 Bottom Left Burner to Furnace Exit – 4m into boiler

RTD Manipulations :
(Deconvolution of probe response from overall measured response)

Experimental Data

Substance injected	sulfur
Boiler Level at injection	16 m (mill D, left burner)
Probe	4 m in the furnace
Boiler Level at Probe	35.64 m

Read Data from File : RTD := READPRN(decol)

time vector $t := RTD^{<0>}$

Probe Response $P := RTD^{<2>}$

Overall Response $C_{out} := RTD^{<1>}$

# of rows in vector $n := rows(RTD) - 1$ $n = 679$

vector pointer $i := 0..n$

Plot of experimental overall and probe response to dirac tracer injection

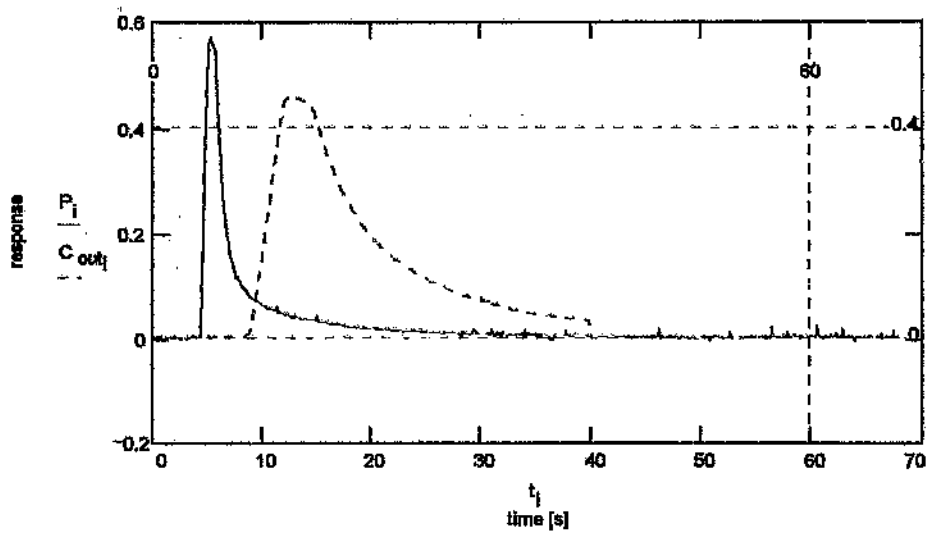

Time Domain Response Definitions

The function below depicts a general form of the time domain responses. This function is fitted to the measured response data by fitting of the function parameters.

$$C(t, \tau_1, \tau_2, \tau_d, const) := const \cdot \left(\frac{1}{\tau_1 - \tau_2}\right) \cdot \left[\exp\left[(t - \tau_d) \cdot \tau_1\right] - \exp\left[(t - \tau_d) \cdot \tau_2\right]\right] \cdot \Phi(t - \tau_d)$$

Probe Response : (visual best function fit to data)

$\tau_{p1} := 0.77$ $\tau_{p2} := 2.69$ $\tau_{pd} := 4.64$ $const_p := 2.52$ parameters for RTD

$P_{an}(t) := C(t, \tau_{p1}, \tau_{p2}, \tau_{pd}, const_p)$

$E(\tau_1, \tau_2, \tau_d) := \sum_{j=1}^{n} (P_j - P_{an}(t_j))^2$ define squared error $E(\tau_{p1}, \tau_{p2}, \tau_{pd}) = 0.2$

Graph comparing measured and curve fitted RTD

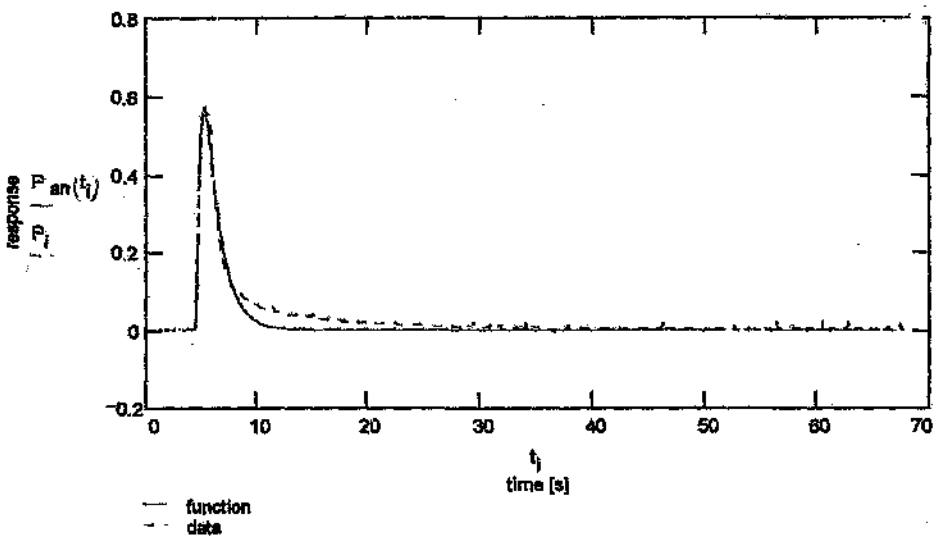

Overall Response : (best function fit to data)

$\tau_{o1} := 0.18$ $\tau_{o2} := 0.4$ $\tau_{od} := 9.6$ $const_o := 0.35$ parameters for RTD

$C_{outan}(t) := C(t, \tau_{o1}, \tau_{o2}, \tau_{od}, const_o)$

$E(\tau_1, \tau_2, \tau_d) := \sum_{j=1}^{n} (C_{out_j} - C_{outan}(t_j))^2$ define squared error

$E(\tau_{o1}, \tau_{o2}, \tau_{od}) = 0.224$

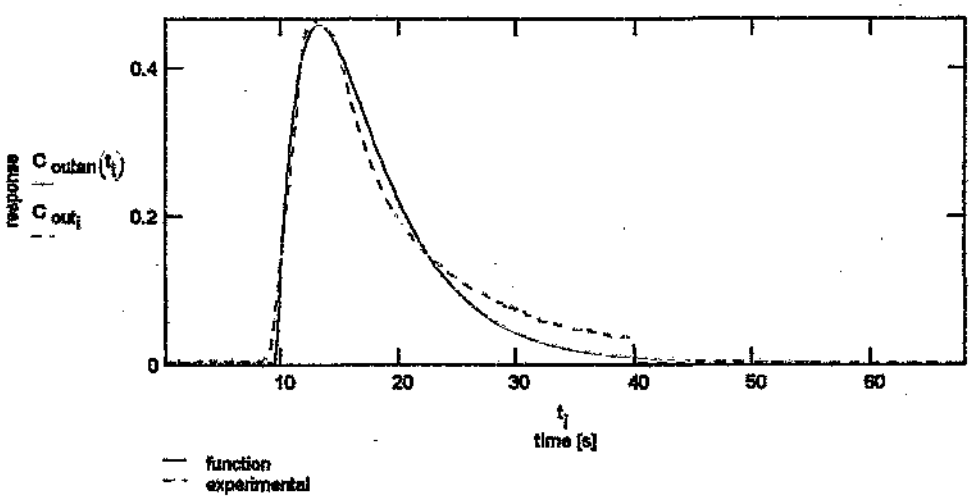

Analytical time domain responses expressed in the Laplace domain (2nd order system with dead time)

Probe Response : $P_{an}(t) := const_p \cdot \left(\frac{1}{\tau_{p1} - \tau_{p2}}\right) \cdot \left[\exp\left[(t - \tau_{pd}) \cdot \tau_{p1}\right] - \exp\left[(t - \tau_{pd}) \cdot \tau_{p2}\right]\right] \cdot \Phi(t - \tau_{pd})$

Overall Response $C_{outan}(t) := const_o \cdot \left(\frac{1}{\tau_{o1} - \tau_{o2}}\right) \cdot \left[\exp\left[(t - \tau_{od}) \cdot \tau_{o1}\right] - \exp\left[(t - \tau_{od}) \cdot \tau_{o2}\right]\right] \cdot \Phi(t - \tau_{od})$

Laplace Transforms can be taken of the above expressions, after which the required deconvolution can occur in the Laplace domain. By taking the inverse Laplace transform of the expression obtained by the deconvolution and normalizing the result, the RTD of the boiler can be determined.

Laplace inverting the deconvoluted expression from the Laplace domain :

$A := \frac{(\tau_{o1} - \tau_{p1}) \cdot (\tau_{o1} - \tau_{p2})}{\tau_{o1} - \tau_{o2}}$ $B := \frac{(\tau_{o2} - \tau_{p1}) \cdot (\tau_{o2} - \tau_{p2})}{\tau_{o2} - \tau_{o1}}$

$A = 6.731$ $B = -3.651$ $\tau_{Ed} := \tau_{od} - \tau_{pd}$ $\tau_{Ed} = 4.96$

$E(t) := \frac{const_o}{const_p} \cdot \Phi(t - \tau_{Ed}) \cdot \left[A \cdot \exp\left[(t - \tau_{Ed}) \cdot \tau_{o1}\right] - B \cdot \exp\left[(t - \tau_{Ed}) \cdot \tau_{o2}\right]\right]$

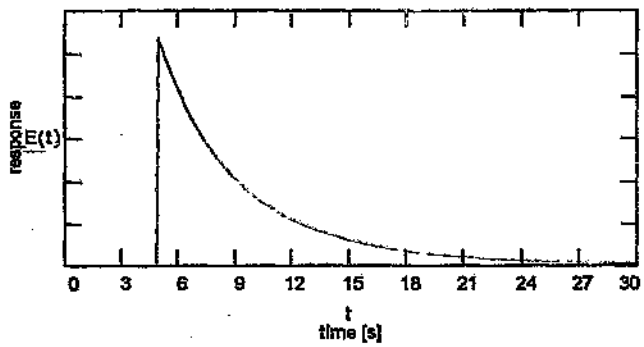
response
E(t)
0
3
6
9
12
15
18
21
24
27
30
t
time [s]

Appendix 1.3.9 Bottom Right Burner to Furnace Exit – 4m into boiler

RTD Manipulations :
(Deconvolution of probe response from overall measured response)
Experimental Data

Substance injected	sulfur
Boiler Level at injection	16 m (mill D, right burner)
Probe	4 m in the furnace
Boiler Level at Probe	35.64 m

Read Data from File : RTD := READPRN(deco)

time vector $t := RTD^{<0>}$

Probe Response $P := RTD^{<2>}$

Overall Response $C_{out} := RTD^{<1>}$

# of rows in vector $n := rows(RTD) - 1$ $n = 679$

vector pointer $i := 0..n$

Plot of experimental overall and probe response to dirac tracer injection

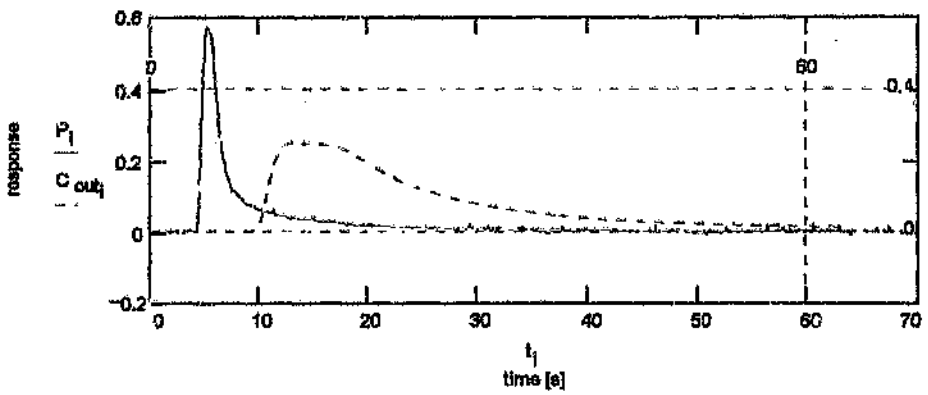

Time Domain Response Definitions

The function below depicts a general form of the time domain responses. This function is fitted to the measured response data by fitting of the function parameters.

$$C(t, \tau_1, \tau_2, \tau_d, const) := const \cdot \left(\frac{1}{\tau_1 - \tau_2}\right) \cdot \left[\exp\left[(t - \tau_d) \cdot \tau_1\right] - \exp\left[(t - \tau_d) \cdot \tau_2\right]\right] \cdot \Phi(t - \tau_d)$$

Probe Response : (visual best function fit to data)

$\tau_{p1} := 0.77$ $\tau_{p2} := 2.69$ $\tau_{pd} := 4.64$ $const_p := 2.52$ parameters for RTD

$P_{an}(t) := C(t, \tau_{p1}, \tau_{p2}, \tau_{pd}, const_p)$

$E(\tau_1, \tau_2, \tau_d) := \sum_{j=1}^{n} (P_j - P_{an}(t_j))^2$ define squared error $E(\tau_{p1}, \tau_{p2}, \tau_{pd}) = 0.2$

Graph comparing measured and curve fitted RTD

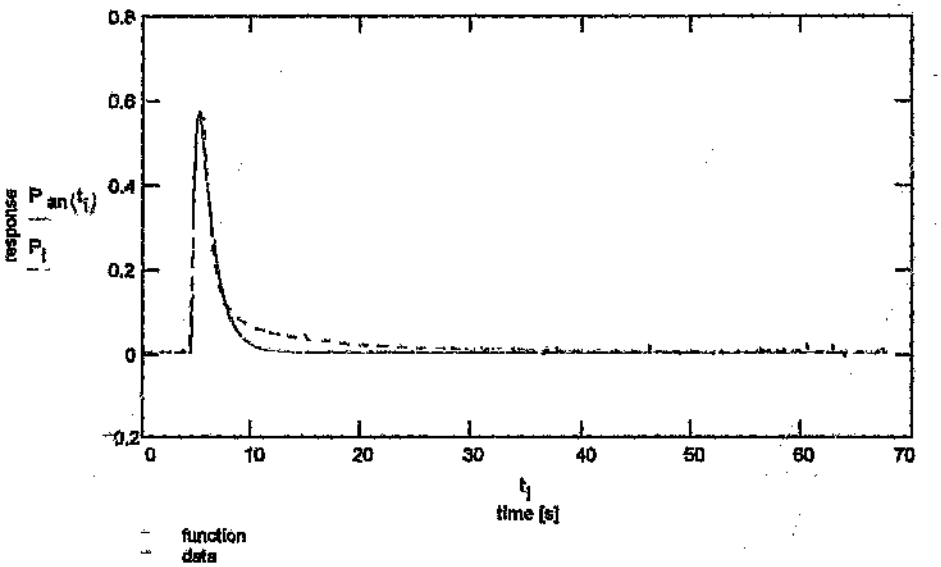

Overall Response : (best function fit to data)

$\tau_{o1} := 0.07$ $\tau_{o2} := 0.5$ $\tau_{od} := 10.0$ $const_o := 0.17$ parameters for RTD

$C_{outan}(t) := C(t, \tau_{o1}, \tau_{o2}, \tau_{od}, const_o)$

$E(\tau_1, \tau_2, \tau_d) := \sum_{j=1}^{n} (C_{out_j} - C_{outan}(t_j))^2$ $E(\tau_{o1}, \tau_{o2}, \tau_{od}) = 0.073$ define squared error

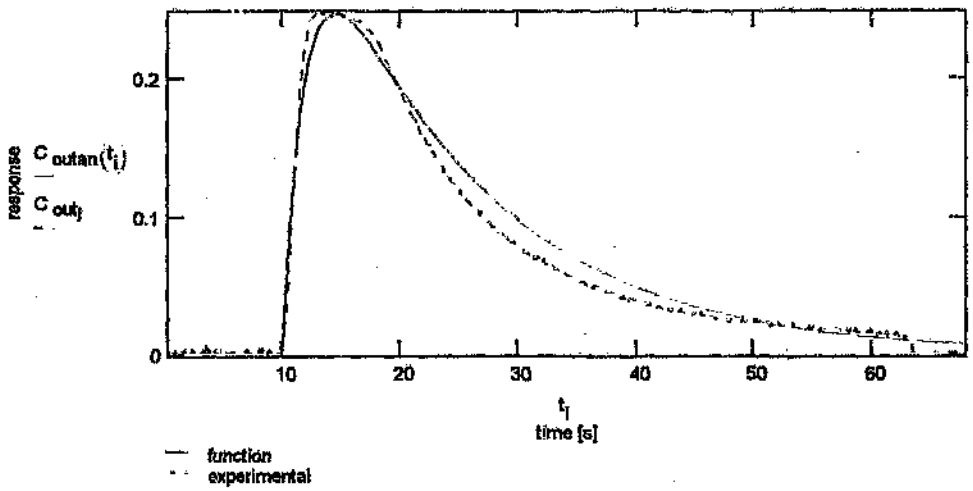

Analytical time domain responses expressed in the Laplace domain (2nd order system with dead time)

Probe Response : $P_{an}(t) := const_p \cdot \left(\frac{1}{\tau_{p1} - \tau_{p2}}\right) \cdot \left[\exp\left[(t - \tau_{pd}) \cdot \tau_{p1}\right] - \exp\left[(t - \tau_{pd}) \cdot \tau_{p2}\right]\right] \cdot \Phi(t - \tau_{pd})$

Overall Response $C_{outan}(t) := const_o \cdot \left(\frac{1}{\tau_{o1} - \tau_{o2}}\right) \cdot \left[\exp\left[(t - \tau_{od}) \cdot \tau_{o1}\right] - \exp\left[(t - \tau_{od}) \cdot \tau_{o2}\right]\right] \cdot \Phi(t - \tau_{od})$

Laplace Transforms can be taken of the above expressions, after which the required deconvolution can occur in the Laplace domain. By taking the inverse Laplace transform of the expression obtained by the deconvolution and normalizing the result, the RTD of the boiler can be determined.

Laplace inverting the deconvoluted expression from the Laplace domain :

$A := \frac{(\tau_{o1} - \tau_{p1}) \cdot (\tau_{o1} - \tau_{p2})}{\tau_{o1} - \tau_{o2}}$ $\quad B := \frac{(\tau_{o2} - \tau_{p1}) \cdot (\tau_{o2} - \tau_{p2})}{\tau_{o2} - \tau_{o1}}$

$A = 4.265$ $\quad B = -1.375$ $\quad \tau_{Ed} := \tau_{od} - \tau_{pd}$ $\quad \tau_{Ed} = 5.36$

$$E(t) := \frac{const_o}{const_p} \cdot \Phi(t - \tau_{Ed}) \cdot \left[A \cdot \exp\left[(t - \tau_{Ed}) \cdot \tau_{o1}\right] - B \cdot \exp\left[(t - \tau_{Ed}) \cdot \tau_{o2}\right]\right]$$

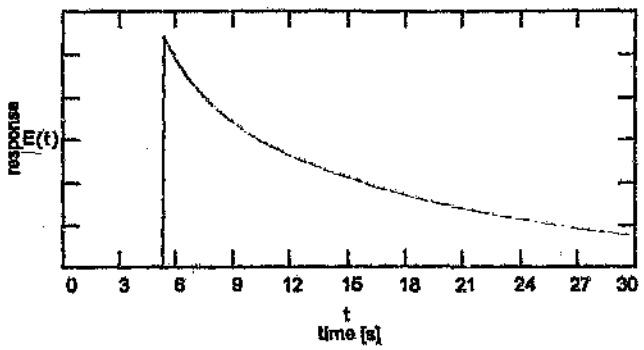
response
E(t)
0
3
6
9
12
15
18
21
24
27
30
t
time [s]

APPENDIX 2

Appendix 2.1.1

Hendrina R.C. Composite: Basic Analysis Datasheet

COAL : Hendrina - RC Composite

Preparation of Coal Analysis Data for specification in AIOLOS

Analysis by TRI Coal Labs all entries in mass% except where otherwise noted

Total Moisture : (as received)	9.8			
Proximate :	air dried	as received	dry	daf
Moisture	3.5	**9.8000**		
	25	**23.4250**	25.9067	
	22.8	21.3636	23.6269	**31.8881**
Fixed Carbon	48.7	45.4114	50.4663	**68.1119**
Ultimate :				
Carbon	58.76	**0.5506**	60.8912	82.1818
Hydrogen	3.02	**0.0283**	3.1295	4.2238
Nitrogen	1.39	**0.0130**	1.4404	1.9441
Sulphur	0.76	**0.0071**	0.7876	1.0629
Carbonates	0.76	0.0071	0.7876	1.0629
Oxygen	6.81	0.0638	7.0570	9.5245
Oxygen + Carbonates		**0.0687**		
Calorific Value	22.69	21.26053	23.513	**31.73426573**
DTF DEVOL.				
Volatile Matter	28.025			
Q Factor	**1.229**			
DTF FULL TEST				
Size Fraction	<38 µm	38-75 µm	< 75 µm	Unit
Pre-exponential Factor	4269	70549	3212	$kg/m^2.s.atm$
	4213	**69626**	**3170**	$kg/m^2.s.bar$
Activation Energy	144.5	181.6	132.98	kJ/mol
Activation Energy /R	**17380**	**21843**	**15995**	K

Coal Name:	HENDRINA RC COMP.
Origin:	Optimum Colliery
Coal Preparation:	as per Hendrina P/S feed

Table :

PROXIMATE ANALYSIS			METHOD
Inherent Moisture:	3.5	(m% of coal - air dried)	ESKOM 103
Ash :	25		ESKOM 101
Volatile Matter :	22.8		ESKOM 102
Fixed Carbon (by difference) :	48.7		ESKOM 128
ULTIMATE ANALYSIS			
Carbon:	58.76	(m% of coal - air dried)	ESKOM 118
Hydrogen:	3.02		ESKOM 118
Nitrogen:	1.39		ESKOM 118
Total Sulphur:	0.76		ESKOM 104
Carbonates (as CO2):	0.76		ESKOM 100
Oxygen (by difference):	6.81		ESKOM 132
Gross Calorific Value:	22.69	(MJ/kg)	ESKOM 105
HARDGROVE INDEX:	51		ESKOM 117
ABRASIVENESS:	477	(mg Fe/4kg coal)	ESKOM 123
ASH FUSION TEMPERATURES			ESKOM 125
Initial Deformation Temperature:	1493	(°C)	
Softening Temperature:	1525		
Hemispherical Temperature:	1544		
Flow Temperature:	1552		

'-1' indicates that the result of that analysis is not available
RAW COAL PREPARATION BY SABS 0135 PART 2 - 1977

Appendix 2.1.2

Hendrina R.C. Composite: Detemination of the Pyrolysis Kinetics

Determination DTF derived single step, zero order, Arrhenius pyrolysis kinetics for use with AIOLOS combustion code

---

Universal Gas Constant $R := 8.314 \quad \frac{J}{mol \cdot K}$

Coal Parameters

Volatile Matter (DTF) $Vols_{DTF} := 29.92 \cdot \%$

Density of coal : $\rho_{coal} := 1642 \quad \frac{kg}{m^3}$

Ash content of dry coal : $Ash_{dry} := 29.6 \cdot \%$

Particle Diameter : $dp_o := 22 \cdot 10^{-6} \quad m$

Particle Mass : $m_p := \frac{\pi \cdot dp_o^{\,3}}{6} \cdot \rho_{coal}$

Initial dry ash free volatile content : $V_{daf.0} := \frac{Vols_{DTF}}{1 - Ash_{dry}} \qquad V_{daf.0} = 42.5 \cdot \%$

Heat Exchange Parameters and constants

Stefan Boltzmann constant : $\sigma := 5.67 \cdot 10^{-8} \quad \frac{W}{m^2 \cdot K^4}$

average emissivity between particle and wall : $\varepsilon := 0.9$

Nusselt Number for boundary layer convective heat exchange : $Nu := 2$

Convective heat exchange coefficient : $\lambda(T_p, T_g) := 2.43 \cdot 10^{-5} \left[\frac{\left(\frac{T_p + T_g}{2} \right)}{273} \right]^{0.82} \quad \frac{W}{m \cdot K}$

Heat capacity of coal : $Cp_{coal} := 1250 \quad \frac{J}{kg \cdot K}$

Particle Surface Area : $A_{part} := \pi \cdot dp_o^{\,2}$

Estimating Overall Rate :

$$k_{p_k} := \frac{1 - \left(\frac{V_{daf}(DTF_{k,2})}{V_{daf.0}} \right)}{DTF_{k,1}}$$

Hendrina R.C. Composite : <38 µm

Calculating Particle Temperature:

Iterative solution of Energy Balance between particle, hot gas and reactor wall :

$$0 = \varepsilon \cdot \sigma \cdot \left(T_w^4 - T_p^4\right) \cdot A_{part} + \frac{Nu \cdot \lambda\left(T_p, T_g\right)}{dp_o} \cdot \left[\left(\frac{T_g + T_p}{2}\right) - T_g\right] \cdot A_{part}$$

$$T_{particle}\left(T_w, T_g\right) := \text{find}\left(T_p\right)$$

$$DTF_{k,4} := T_{particle}\left(DTF_{k,0} + 273, DTF_{k,3} + 273\right) - 273$$

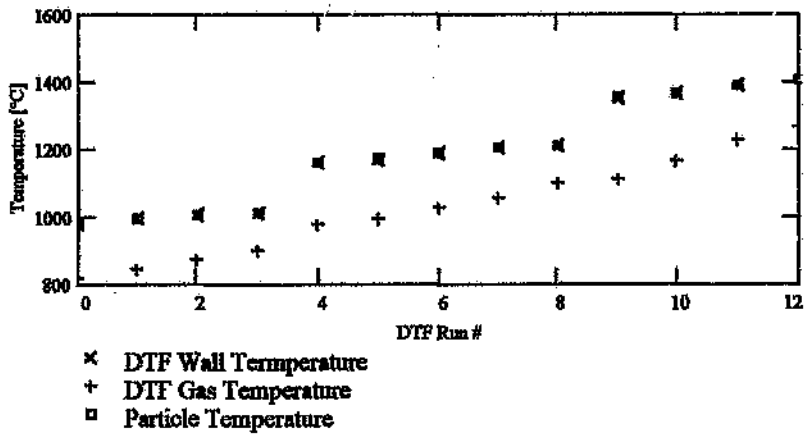

Determining the Pyrolysis Kinetics from the experimental data :

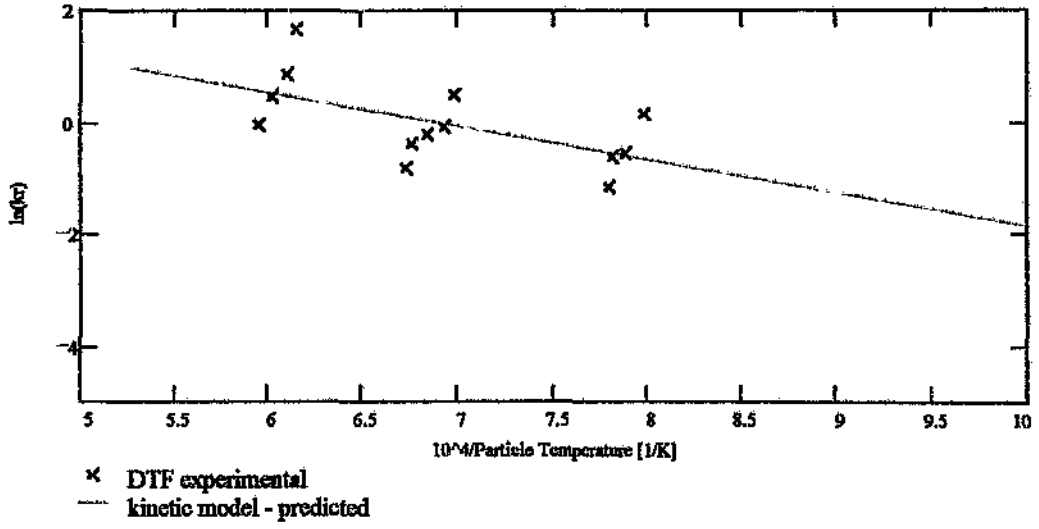

Coal pyrolysis kinetics Description :

Pre-exponential factor : $\exp(Preexp) = 61.095 \quad \frac{1}{s}$

Activation Energy : $-EonR \cdot \frac{R}{10^3} = 49.684 \quad \frac{kJ}{mol}$

$-EonR = 5975.987 \quad K$

Function describing the pyrolysis reaction rate : $k_1(Tp) := k_{0.1} \cdot \exp\left(\frac{EonR}{Tp}\right)$

Equation describing all modes of heat transfer (shrinking core assumption)

radiation $dT_{rad}(T_p, T_w) := \frac{\varepsilon\sigma \cdot A_{part}\left(T_w^4 - T_p^4\right)}{Cp_{coal} m_p}$

convection $dT_{conv}(T_p, T_g) := \frac{Nu \cdot A_{part} \lambda(T_p, T_g) \cdot \left[\left(\frac{T_g + T_p}{2}\right) - T_p\right]}{Cp_{coal} m_p}$

Estimation of the initial particle heating rate at DTF setpoint temperature of 1400°C:

$T_{init} := 25 + 273 \quad K \qquad dT_{rad}(T_{init}, 1416) + dT_{conv}(T_{init}, 1335) = 2.721 \cdot 10^4 \frac{K}{s}$

Solution of differential equations

Initial Conditions :

Volatiles (%) $x_0 := 1$

Particle Temperature $x_1 := 300$

Simultaneous Differential Equations :

$$\frac{d}{dt}V = -k_1(x_1)$$

$$\frac{d}{dt}Tp = dT_{rad}(x_0, x_1) + dT_{conv}(x_0, x_1)$$

Note on Solution Methodology :

The simultaneous equations are solved by a 4th order Runge Kutta solution algorithm for each DTF setpoint temperature. An average furnace wall and furnace gas temperature have been specified for each DTF setpoint temperature

DTF Pyrolysis Evaluation Results :

Coal pyrolysis kinetics Description :

Pre-exponential factor : $\exp(Preexp) = 61.095 \quad \frac{1}{s}$

Activation Energy : $EonR \cdot \frac{R}{10^3} = 49.684 \quad \frac{kJ}{mol} \qquad EonR = 5975.987 \quad K$

Function describing the pyrolysis reaction rate : $k_1(Tp) := k_{o,1} \cdot \exp\left(\frac{EonR}{Tp}\right)$

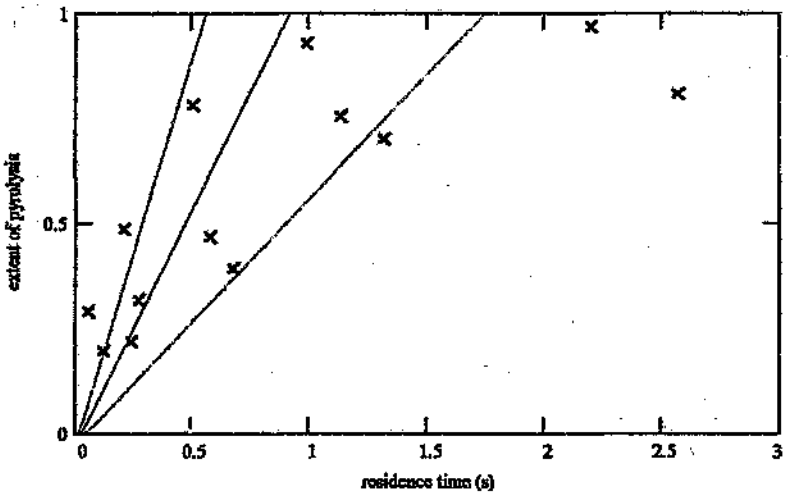

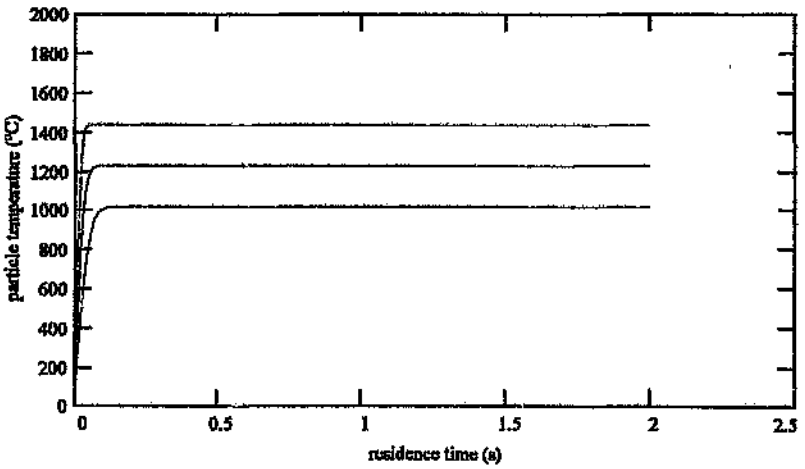

Hendrina R.C. Composite : <38 µm

Determination DTF derived single step, zero order, Arrhenius pyrolysis kinetics for use with AIOLOS combustion code

---

Universal Gas Constant $R := 8.314 \quad \frac{J}{mol \cdot K}$

Coal Parameters

Volatile Matter (DTF) $Vols_{DTF} := 29.92 \cdot \%$

Density of coal : $\rho_{coal} := 1642 \quad \frac{kg}{m^3}$

Ash content of dry coal : $Ash_{dry} := 29.6 \cdot \%$

Particle Diameter : $dp_o := 59.95 \cdot 10^{-6} \quad m$

Particle Mass : $m_p := \frac{\pi \cdot dp_o^{\,3}}{6} \cdot \rho_{coal}$

Initial dry ash free volatile content : $V_{daf.0} := \frac{Vols_{DTF}}{1 - Ash_{dry}} \qquad V_{daf.0} = 42.5 \cdot \%$

Heat Exchange Parameters and constants

Stefan Boltzmann constant : $\sigma := 5.67 \cdot 10^{-8} \quad \frac{W}{m^2 \cdot K^4}$

average emissivity between particle ar ' wall : $\varepsilon := 0.9$

Nusselt Number for boundary layer convective heat exchange : $Nu := 2$

Convective heat exchange coefficient : $\lambda(T_p, T_g) := 2.43 \cdot 10^{-5} \cdot \left[\frac{\left(\frac{T_p + T_g}{2} \right)}{273} \right]^{0.82} \quad \frac{W}{m \cdot K}$

Heat capacity of coal : $Cp_{coal} := 1250 \quad \frac{J}{kg \cdot K}$

Particle Surface Area : $A_{part} := \pi \cdot dp_o^{\,2}$

Estimating Overall Rate : $k_{p_k} := \frac{1 - \left(\frac{V_{daf}(DTF_{k,2})}{V_{daf.0}} \right)}{DTF_{k,1}}$

Hendrina R.C. Composite : 38-75 μm

Calculating Particle Temperature:

Iterative solution of Energy Balance between particle, hot gas and reactor wall :

$$0 = \varepsilon \cdot \sigma \cdot \left(T_w^4 - T_p^4\right) \cdot A_{part} + \frac{Nu \cdot \lambda\left(T_p, T_g\right)}{dp_o} \cdot \left[\left(\frac{T_g + T_p}{2}\right) - T_g\right] \cdot A_{part}$$

$$T_{particle}\left(T_w, T_g\right) := \text{find}\left(T_p\right)$$

$$DTF_{k,4} := T_{particle}\left(DTF_{k,0} + 273, DTF_{k,3} + 273\right) - 273$$

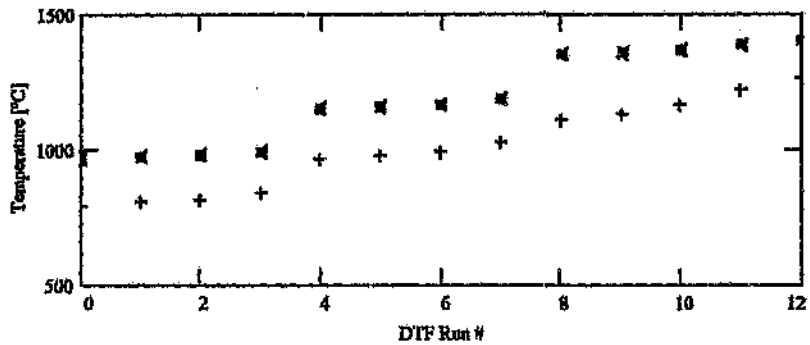

Determining the Pyrolysis Kinetics from the experimental data :

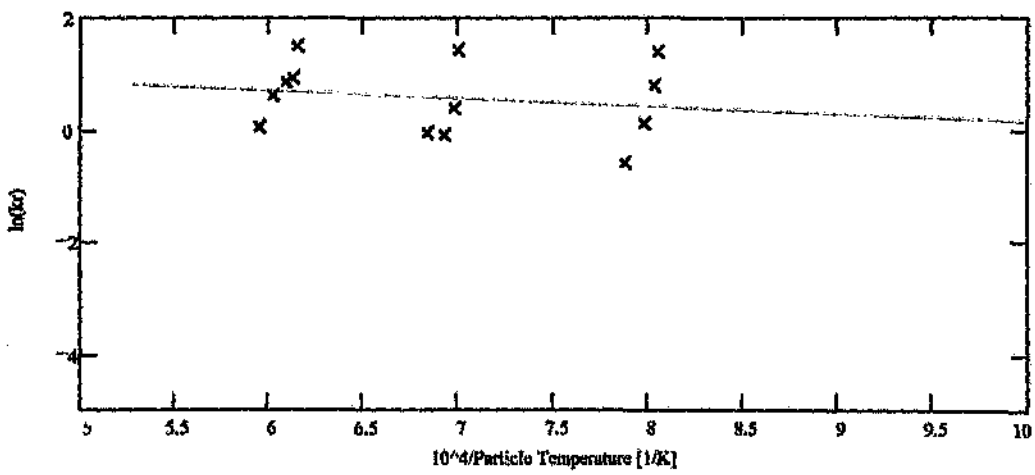

Coal pyrolysis kinetics Description :

Pre-exponential factor : $\exp(Preexp) = 4.632 \quad \frac{1}{s}$

Activation Energy : $-EonR \cdot \frac{R}{10^3} = 11.586 \quad \frac{kJ}{mol}$

$-EonR = 1393.503 \quad K$

Function describing the pyrolysis reaction rate : $k_1(Tp) := k_{0.1} \cdot \exp\left(\frac{EonR}{Tp}\right)$

Equation describing all modes of heat transfer (shrinking core assumption)

radiation $dT_{rad}(T_p, T_w) := \frac{\varepsilon \sigma \cdot A_{part} \cdot \left(T_w^4 - T_p^4\right)}{Cp_{coal} \cdot m_p}$

convection $dT_{conv}(T_p, T_g) := \frac{Nu \cdot A_{part} \lambda(T_p, T_g) \cdot \left[\left(\frac{T_g + T_p}{2}\right) - T_p\right]}{Cp_{coal} \cdot m_p}$

Estimation of the initial particle heating rate at DTF setpoint temperature of 1400°C:

$T_{init} := 25 + 273 \quad K \qquad dT_{rad}(T_{init}, 1416) + dT_{conv}(T_{init}, 1335) = 9.984 \cdot 10^3 \ \frac{K}{s}$

Solution of differential equations

Initial Conditions :

Volatiles (%) $\quad x_0 := 1$

Particle Temperature $\quad x_1 := 300$

Simultaneous Differential Equations :

$$\frac{d}{dt}V = -k_1(x_1)$$

$$\frac{d}{dt}Tp = dT_{rad}(x_0, x_1) + dT_{conv}(x_0, x_1)$$

Note on Solution Methodology :

The simultaneous equations are solved by a 4th order Runge Kutta solution algorithm for each DTF setpoint temperature. An average furnace wall and furnace gas temperature have been specified for each DTF setpoint temperature

DTF Pyrolysis Evaluation Results :

Coal pyrolysis kinetics Description :

Pre-exponential factor : $\exp(\text{Preexp}) = 4.632 \quad \frac{1}{s}$

Activation Energy : $-\text{EonR}\cdot\frac{R}{10^3} = 11.586 \quad \frac{kJ}{mol} \qquad -\text{EonR} = 1393.503 \quad K$

Function describing the pyrolysis reaction rate : $k_1(Tp) := k_{0.1}\cdot\exp\left(\frac{\text{EonR}}{Tp}\right)$

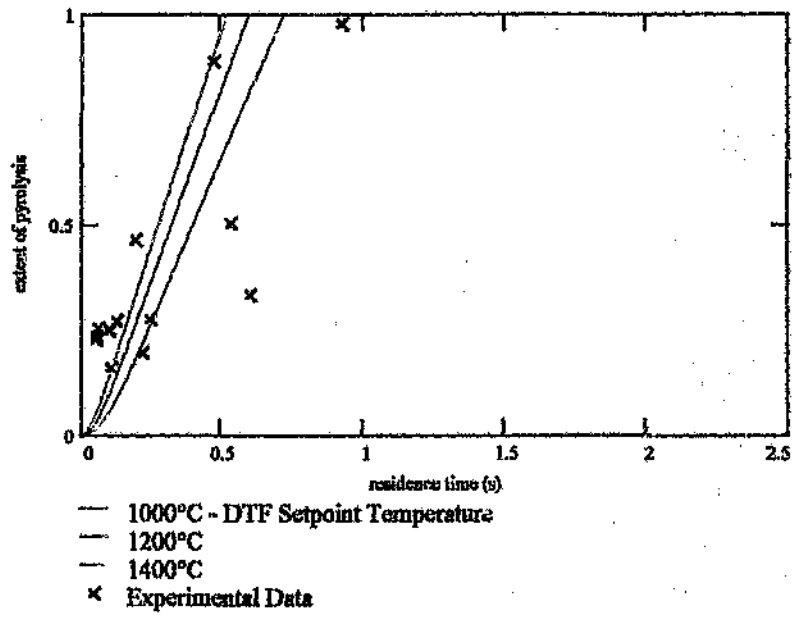

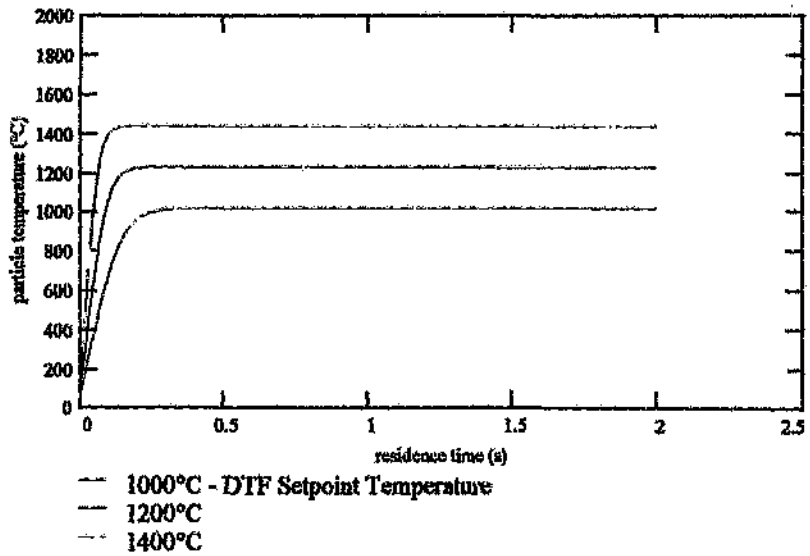

Hendrina R.C. Composite : 38-75 µm

Appendix 2.1.3

Hendrina R.C. Composite: Determination of the Char Combustion Kinetics

Determination of DTF combustion kinetics for use with AIOLOS combustion code

---

Universal Gas Constant $R := 8.314 \quad \frac{J}{mol \cdot K}$

DTF Operation and Char Description :

Ash in Coal $Ash_{coal} := DTF_{0.0} \cdot \%$

Ash in Char $Ash_{char} := DTF_{0.7} \cdot \%$

Volatile Matter (after DTF devolatilisation) $Vols_{DTF} := 1 - Ash_{coal} - \frac{Ash_{coal}}{Ash_{char}} \cdot (1 - Ash_{char})$

Density of coal : $\rho_{coal} := 1678 \quad \frac{kg}{m^3}$

Density of Char (initially) : (shrinking core assumption) $\rho_{char.0} := (1 - Vols_{DTF}) \cdot \rho_{coal} \quad \rho_{char.0} = 1.204 \cdot 10^3 \quad \frac{kg}{m^3}$

Initial Particle Diameter : $dp_{0.0} := DTF_{0.0} \quad m \quad dp_0 = 2.18 \cdot 10^{-5} \quad m$

Pressure in DTF : $P := 0.85 \cdot 10^5 \quad Pa$

Volume Oxygen Flowrate into DTF : $V_{O2} := \frac{0.6 \cdot 10^{-3}}{60} \quad \frac{m^3}{s} \quad M_{W.O2} := 32 \cdot 10^{-3} \quad \frac{kg}{mol}$

VolumeNitrogen Flowrate into DTF : $V_{N2} := \frac{19.66 \cdot 10^{-3}}{60} \quad \frac{m^3}{s} \quad M_{W.N2} := 28 \cdot 10^{-3} \quad \frac{kg}{mol}$

Mass Flowrate of Oxygen : $m_{O2} := \frac{V_{O2} \cdot P \cdot M_{W.O2}}{R \cdot 298} \quad \frac{kg}{s}$

Mass Flowrate of Nitrogen : $m_{N2} := \frac{V_{N2} \cdot P \cdot M_{W.N2}}{R \cdot 298} \quad \frac{kg}{s}$

Char Feedrate : $m_{char} := \frac{0.1066 \cdot 10^{-3}}{60} \quad \frac{kg}{s}$

Initial Char Concentration $C_{char.0} := \frac{m_{char}}{m_{char} + m_{O2} + m_{N2}} \quad \frac{kg}{kg_{mix}}$

Initial Fixed Carbon Concentration $C_{c.0} := C_{char.0} \cdot (1 - Ash_{char}) \quad C_{c.0} = 3.4659 \cdot 10^{-3} \quad \frac{kg}{kg_{mix}}$

Ash Concentration : $C_{ash} := C_{char.0} \cdot (Ash_{char}) \quad C_{ash} = 1.9587 \cdot 10^{-3} \quad \frac{kg}{kg_{mix}}$

Heat Exchange Parameters and constants

Stefan Boltzmann constant $\sigma := 5.67 \cdot 10^{-8} \quad \frac{W}{m^2 \cdot K^4}$

average emissivity between particle and wall $\varepsilon := 0.85$

reaction energy : C to CO : $\Delta h := 9.614 \cdot 10^6 \quad \frac{J}{kg}$

Nusselt Number for boundary layer convective heatexchange $Nu := 2$

convective heat exchange coefficient $\lambda(T_p, T_g) := 2.43 \cdot 10^{-11} \cdot \left[\frac{\left(\frac{T_p + T_g}{2} \right)}{273} \right]^{0.82} \quad \frac{W}{m \cdot K}$

heat capacity of char : $Cp_{char} := 1250 \quad \frac{J}{kg \cdot K}$

Particle Surface Area as a function of combustion extent :

swelling index $n_B := \frac{2}{3}$ 1 - swelling coals
2/3 - 'non swelling' coals

$$A_{part.c}(C_c) := \frac{6}{\rho_{char.o} \cdot dp_o} \cdot C_{c.0} \cdot \left(\frac{C_c}{C_{c.0}} \right)^{n_B} \quad \frac{m^2}{kg_{mix}}$$

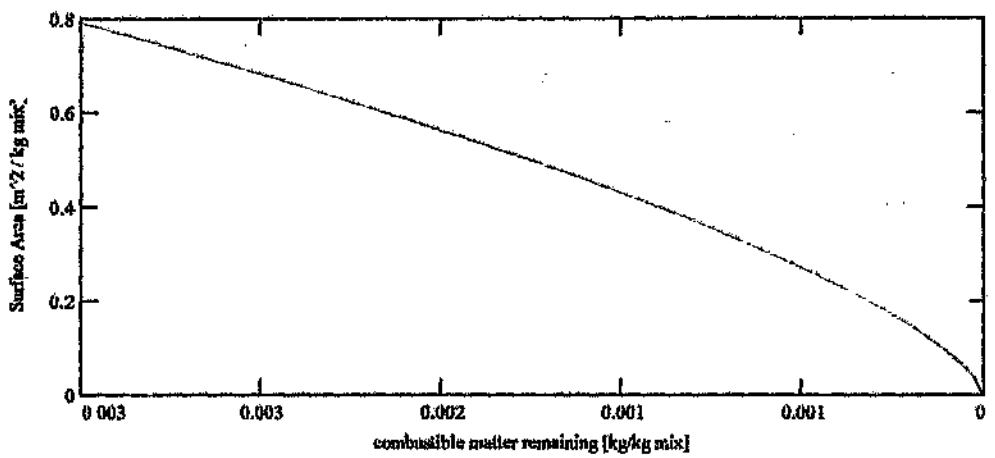

Partial Pressure of Oxygen in DTF : $P_{O2} := \frac{V_{O2}}{V_{O2} + V_{N2}} \quad P_{O2} = 0.03 \quad bar$

Function defining mass of combustible matter remaining as a function ash content in the sampled residue

$$C_c(ash_{residue}) := \left[\frac{Ash_{char}}{1 - Ash_{char}} \cdot \frac{1 - \left(\frac{ash_{residue}}{100} \right)}{\left(\frac{ash_{residue}}{100} \right)} \right] \cdot C_{c.0}$$

$ash_{residue}$ in % by mass

Hendrina R.C. Composite : < 38 µm

Calculating Overall Rate :

$$k_{o_k} = \frac{\int_{C_{o.0}}^{C_o(DTF_{k,4})} \frac{1}{A_{part.o}(C_o)}\, dC_o}{-P_{O2} \cdot DTF_{k,3}}$$

Calculating Particle Temperature:

Iterative solution of Energy Balance between particle, hot gas and reactor wall :

$$\Delta h \cdot \frac{C_o(Ash_{res}) - C_{o.0}}{t_r} = \left[\varepsilon \cdot \sigma \cdot \left(T_w^{\,4} - T_p^{\,4} \right) - \frac{Nu \cdot \lambda(T_p, T_g)}{dp_o} \cdot \left[\left(\frac{T_g + T_p}{2} \right) - T_g \right] \right] \cdot A_{part.o}(C_{o.0})$$

$$T_{particle}(Ash_{res}, t_r, T_w, T_g) := find(T_p)$$

$$DTF_{k,6} := T_{particle}(DTF_{k,4}, DTF_{k,3}, DTF_{k,2} + 273, DTF_{k,5} + 273) - 273$$

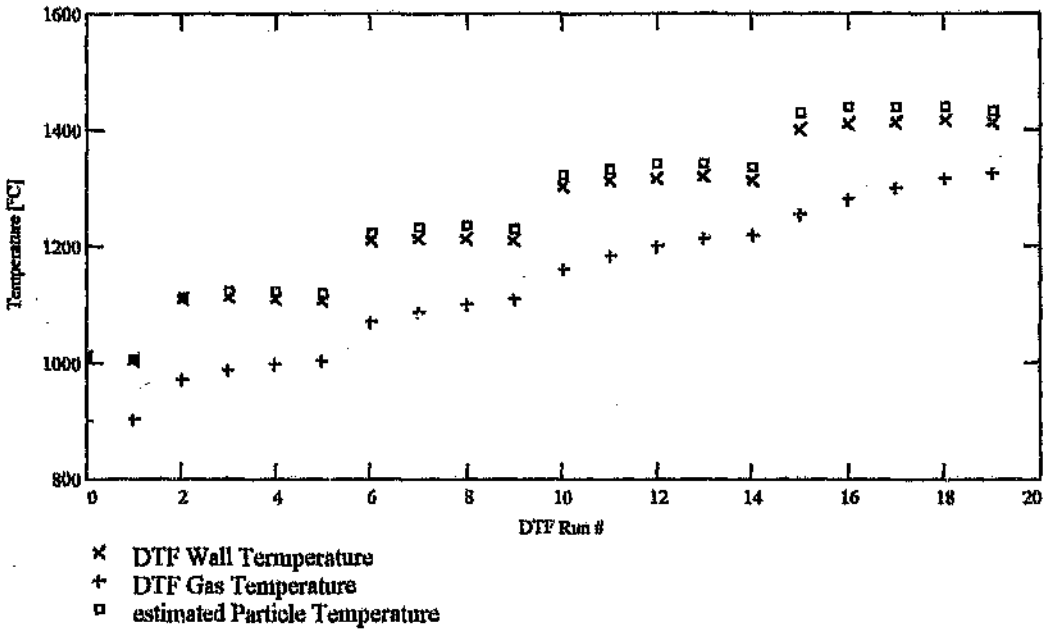

Oxygen Diffusion reaction rate as a function particle Temperature

O2 diffusion constant at 1600K : $D_{O2.1600K} := 3.39 \cdot 10^{-4} \ \frac{m^2}{s}$

mechanism factor : $\phi := 2$ $\phi = 2$ for CO, and 1 for CO2

$$k_{d.char}(Tp, Tg, dp) := \frac{24 \cdot \phi \cdot D_{O2.1600K} \cdot \left[\frac{(Tg + Tp) \cdot 0.5}{1600} \right]^{1.75}}{R \cdot 10^5 \cdot dp \cdot Tg} \ \frac{kg}{m^2 \cdot s \cdot bar}$$

Source : AIOLOS - combustion model

Hendrina R.C. Composite : < 38 µm

Determining the Chemical Reaction Rate from the experimental data :

$$kr_k := \left[\frac{1}{\left(\frac{1}{k_{o_k}}\right) - \frac{1}{k_{d.char}(DTF_{k,6} + 273, DTF_{k,5} + 273, DTF_{k,0})}} \right]$$

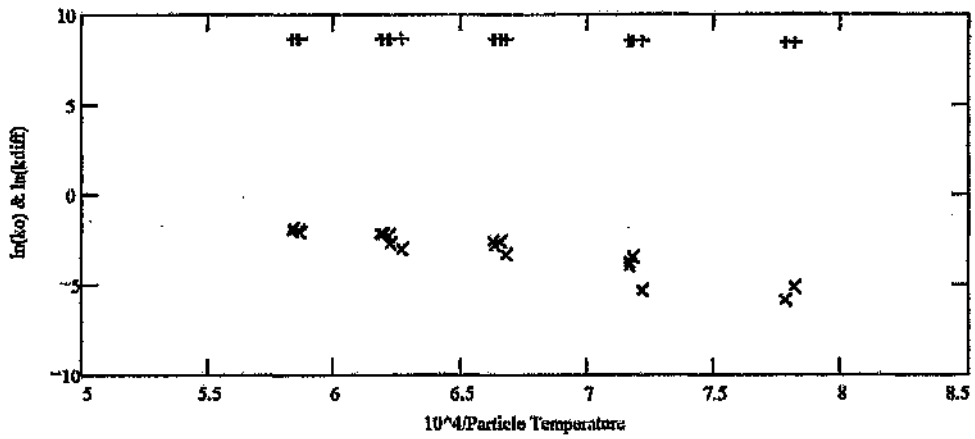

NB : if the +'s lie beneath the x's, the overall reaction rate could be diffusion controlled

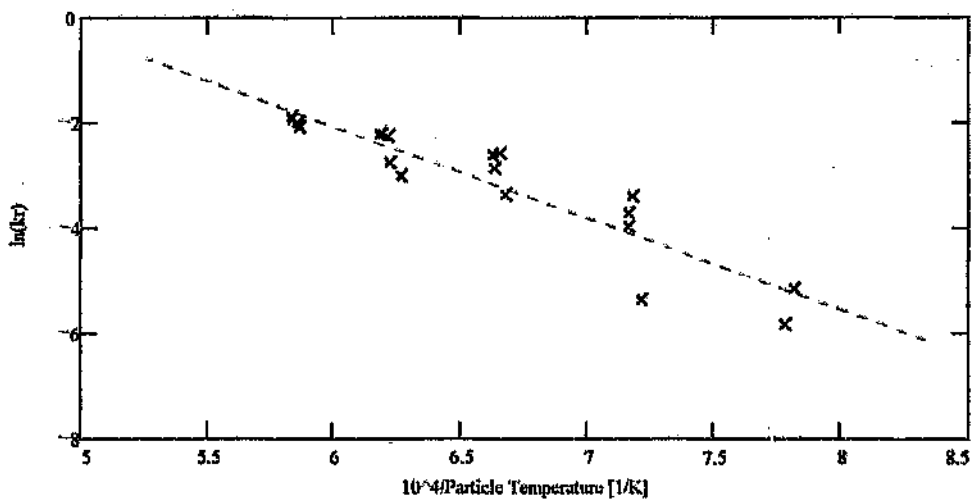

Char chemical combustion kinetics Description :

Pre-exponential factor : $\exp(Preexp) = 4269.228$ $\frac{kg}{m^2 \cdot s \cdot bar}$

Activation Energy : $EonR \cdot \frac{R}{10^3} = 144.495$ $\frac{kJ}{mol}$

$EonR = 17379.72$ K

Function describing chemical reaction rate : $k_{r.char}(Tp) := k_{rch.o} \cdot \exp\left(\frac{EonR}{Tp}\right)$

Hendrina R.C. Composite : < 38 µm

Defining the overall reaction rate function :

$$k_r(Tp, Tg, dp) := \frac{1}{\left(\frac{1}{k_{r.char}(Tp)} + \frac{1}{k_{d.char}(Tp, Tg, dp)}\right)}$$

Equation describing all modes of heat transfer (shrinking core assumption)

radiation

$$dT_{rad}(C_c, T_p, T_w) := \frac{\varepsilon \cdot \sigma \cdot \left(T_w^4 - T_p^4\right)}{(C_c + C_{ash}) \cdot Cp_{char}} \cdot A_{part.c}(C_{c.0})$$

convection

$$dT_{conv}(C_c, T_p, T_g) := \frac{\frac{Nu \cdot \lambda(T_p, T_g)}{dp_0} \cdot \left[\left(\frac{T_g + T_p}{2}\right) - T_g\right]}{(C_c + C_{ash}) \cdot Cp_{char}} \cdot A_{part.c}(C_{c.0})$$

reaction

$$dT_{gen}(C_c, T_p, T_g) := \frac{-\Delta h}{(C_c + C_{ash}) \cdot Cp_{char}} \cdot \left(-k_r(T_p, T_g, dp_0) \cdot P_{O2} \cdot A_{part.c}(C_c)\right)$$

estimation of initial particle heating rate at DTF setpoint Temperature of 1400°C :

$T_{init} := 2 \cdot + 273 \quad K \quad dT_{rad}(C_{c.0}, T_{init}, 1416 + 273) + dT_{conv}(C_{c.0}, T_{init}, 1335 + 273) = 4.579 \cdot 10^4 \quad \frac{K}{s}$

Solution of differential equations

Initial Conditions : combustion extent — $x_0 := C_{c.0}$

particle temperature — $x_1 := 300 \quad K$

Simultaneous Differential Equations :

combustion extent — $\frac{d}{dt} C_c = -k_r(x_1, T_g, dp_0) \cdot P_{O2} \cdot A_{part.c}(x_0)$

particle temperature — $\frac{d}{dt} Tp = dT_{rad}(x_0, x_1, T_w) + dT_{conv}(x_0, x_1, T_g) + dT_{gen}(x_0, x_1, T_g)$

Note on the Solution Methodology

The simultaneous equations are solved by a 4th order Runge Kutta solution algorithm for each DTF setpoint Temperature. An average furnace wall and furnace gas temperature have been specified for each DTF setpoint temperature.

DTF Kinetic Evaluation Results -

Char chemical combustion kinetics Description :

Pre-exponential factor : $\exp(\text{Preexp}) = 4269.228 \quad \frac{kg}{m^2 \cdot s \cdot bar}$

Activation Energy : $\text{EouR} \cdot \frac{R}{10^3} = 144.49 \quad \frac{kJ}{mol} \quad \text{EonR} = 17379.72 \quad K$

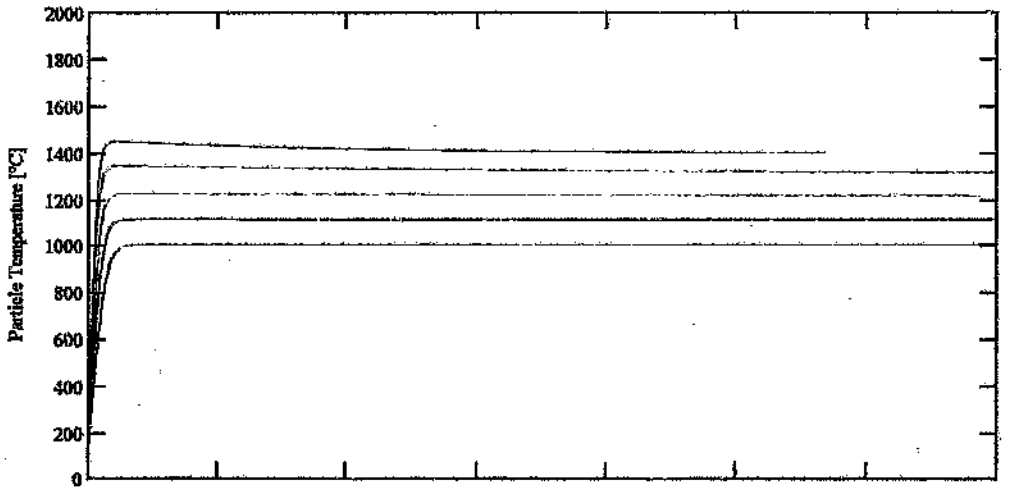

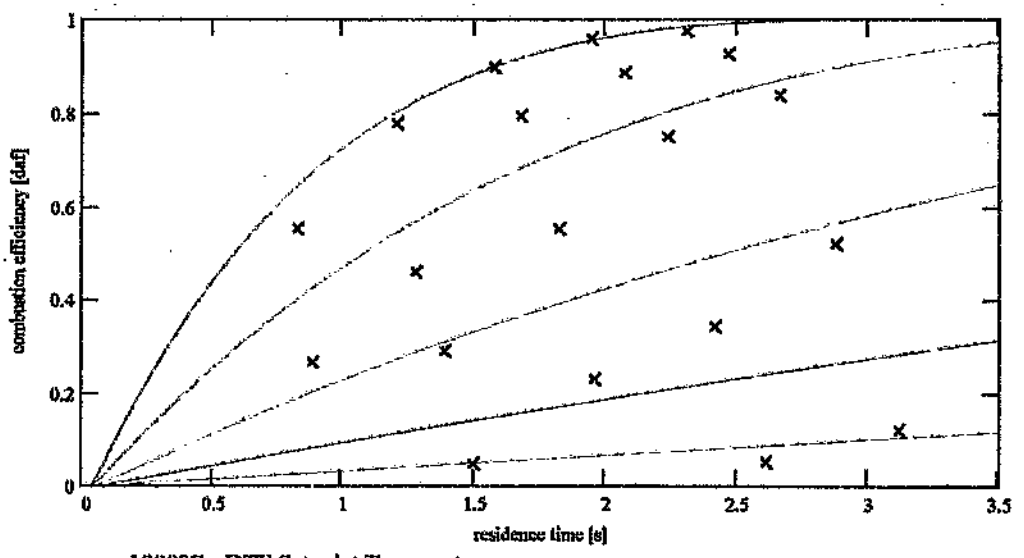

1000°C - DTF Setpoint Temperature
1100°C
1200°C
1300°C
1400°C
× DTF data

Determination of DTF combustion kinetics for use with AIOLOS combustion code

---

Universal Gas Constant $R := 8.314 \quad \frac{J}{mol \cdot K}$

DTF Operation and Char Description :

Ash in Coal $Ash_{coal} := DTF_{0.8} \cdot \%$

Ash in Char $Ash_{char} := DTF_{0.7} \cdot \%$

Volatile Matter (after DTF devolatilisation) $Vols_{DTF} := 1 - Ash_{coal} - \frac{Ash_{coal}}{Ash_{char}} \cdot (1 - Ash_{char})$

Density of coal : $\rho_{coal} := 1678 \quad \frac{kg}{m^3}$

Density of Char (initially) : (shrinking core assumption) $\rho_{char.o} := (1 - Vols_{DTF}) \cdot \rho_{coal} \quad \rho_{char.o} = 1.189 \cdot 10^3 \quad \frac{kg}{m^3}$

Initial Particle Diameter : $dp_o := DTF_{0.0} \quad m \quad dp_o = 6 \cdot 10^{-5} \quad m$

Pressure in DTF : $P := 0.85 \cdot 10^5 \quad Pa$

Volume Oxygen Flowrate into DTF : $V_{O2} := \frac{0.6 \cdot 10^{-3}}{60} \quad \frac{m^3}{s} \quad M_{W.O2} := 32 \cdot 10^{-3} \quad \frac{kg}{mol}$

VolumeNitrogen Flowrate into DTF : $V_{N2} := \frac{19.66 \cdot 10^{-3}}{60} \quad \frac{m^3}{s} \quad M_{W.N2} := 28 \cdot 10^{-3} \quad \frac{kg}{mol}$

Mass Flowrate of Oxygen : $m_{O2} := \frac{V_{O2} \cdot P \cdot M_{W.O2}}{R \cdot 298} \quad \frac{kg}{s}$

Mass Flowrate of Nitrogen : $m_{N2} := \frac{V_{N2} \cdot P \cdot M_{W.N2}}{R \cdot 298} \quad \frac{kg}{s}$

Char Feedrate : $m_{char} := \frac{0.1066 \cdot 10^{-3}}{60} \quad \frac{kg}{s}$

Initial Char Concentration $C_{char.0} := \frac{m_{char}}{m_{char} + m_{O2} + m_{N2}} \quad \frac{kg}{kg_{mix}}$

Initial Fixed Carbon Concentration $C_{c.0} := C_{char.0} \cdot (1 - Ash_{char}) \quad C_{c.0} = 3.4407 \cdot 10^{-3} \quad \frac{kg}{kg_{mix}}$

Ash Concentration : $C_{ash} := C_{char.0} \cdot (Ash_{char}) \quad C_{ash} = 1.984 \cdot 10^{-3} \quad \frac{kg}{kg_{mix}}$

Heat Exchange Parameters and constants

Stefan Boltzmann constant $\sigma := 5.67 \cdot 10^{-8} \quad \frac{W}{m^2 \cdot K^4}$

average emissivity between particle and wall $\varepsilon := 0.85$

reaction energy : C to CO : $\Delta h := 9.614 \cdot 10^6 \quad \frac{J}{kg}$

Nusselt Number for boundary layer convective heatexchange $Nu := 2$

convective heat exchange coefficient $\lambda(T_p, T_g) := 2.43 \cdot 10^{-11} \cdot \left[\frac{\left(\frac{T_p + T_g}{2}\right)}{273}\right]^{0.82} \quad \frac{W}{m \cdot K}$

heat capacity of char : $Cp_{char} := 1250 \quad \frac{J}{kg \cdot K}$

Particle Surface Area as a function of combustion extent :

swelling index $n_B := \frac{2}{3}$ 1 - swelling coals; 2/3 - 'non swelling' coals

$$A_{part.c}(C_c) := \frac{6}{\rho_{char.o} \cdot dp_o} \cdot C_{c.0} \cdot \left(\frac{C_c}{C_{c.0}}\right)^{n_B} \quad \frac{m^2}{kg_{mix}}$$

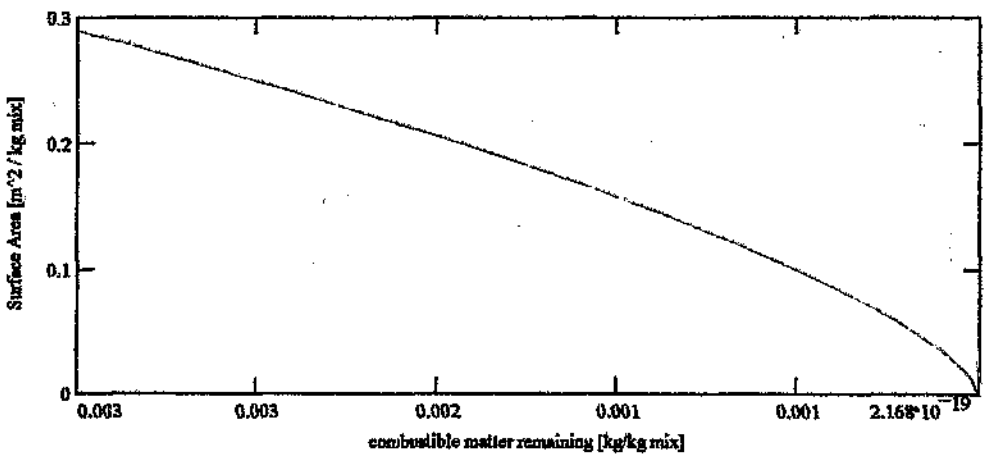

Partial Pressure of Oxygen in DTF : $P_{O2} := \frac{V_{O2}}{V_{O2} + V_{N2}} \quad P_{O2} = 0.03$ bar

Function defining mass of combustible matter remaining as a function ash content in the sampled residue

$$C_c(ash_{residue}) := \left[\frac{Ash_{char}}{1 - Ash_{char}} \cdot \frac{1 - \left(\frac{ash_{residue}}{100}\right)}{\left(\frac{ash_{residue}}{100}\right)}\right] \cdot C_{c.0}$$

$ash_{residue}$ in % by mass

Calculating Overall Rate :

$$k_{o_k} = \frac{\int_{C_{c.0}}^{C_c(DTF_{k,4})} \frac{1}{A_{part.c}(C_c)}\, dC_c}{\cdot P_{O2} \cdot DTF_{k,3}}$$

Calculating Particle Temperature:

Iterative solution of Energy Balance between particle, hot gas and reactor wall :

$$\Delta h \cdot \frac{C_c(Ash_{res}) - C_{c.0}}{t_r} = \left[\varepsilon \cdot \sigma \cdot \left(T_w^{\,4} - T_p^{\,4} \right) - \frac{Nu \cdot \lambda(T_p, T_g)}{dp_0} \cdot \left[\left(\frac{T_g + T_p}{2} \right) - T_g \right] \right] \cdot A_{part.c}(C_{c.0})$$

$$T_{particle}(Ash_{res}, t_r, T_w, T_g) := \text{find}(T_p)$$

$$DTF_{k,6} := T_{particle}(DTF_{k,4}, DTF_{k,3}, DTF_{k,2} + 273, DTF_{k,5} + 273) - 273$$

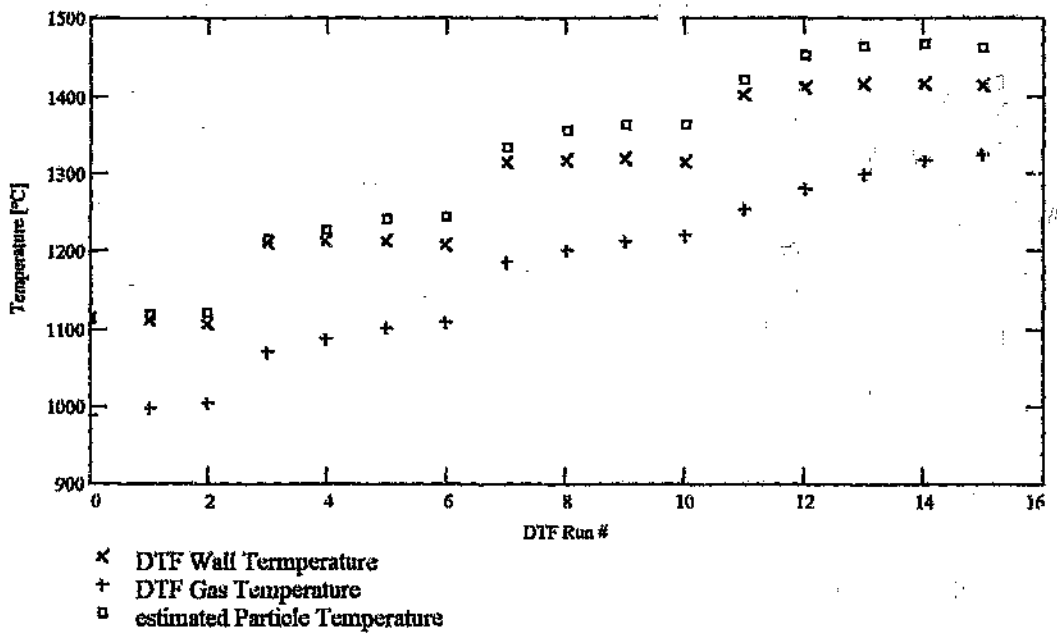

Oxygen Diffusion reaction rate as a function particle Temperature

C2 diffusion constant at 1600K : $D_{O2.1600K} := 3.39 \cdot 10^{-4} \ \frac{m^2}{s}$

mechanism factor : $\phi := 2$ $\phi = 2$ for CO, and 1 for CO2

$$k_{d.char}(Tp, Tg, dp) := \frac{24 \cdot \phi \cdot D_{O2.1600K} \cdot \left[\frac{(Tg + Tp) \cdot 0.5}{1600} \right]^{1.75}}{R \cdot 10^{5} \cdot dp \cdot Tg} \ \frac{kg}{m^2 \cdot s \cdot bar}$$

Source : AIOLOS - combustion model

Hendrina R.C. Composite : 38-75 µm

Determining the Chemical Reaction Rate from the experimental data :

$$kr_k := \left[\frac{1}{\left(\frac{1}{k_{o_k}}\right) - \frac{1}{k_{d.char}\left(DTF_{k,6} + 273, DTF_{k,5} + 273, DTF_{k,0}\right)}} \right]$$

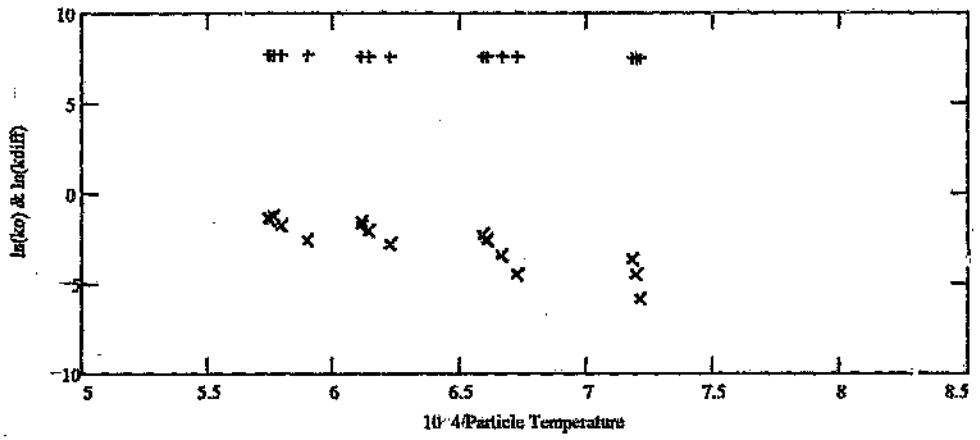

NB : if the +'s lie beneath the x's, the overall reaction rate could be diffusion controlled

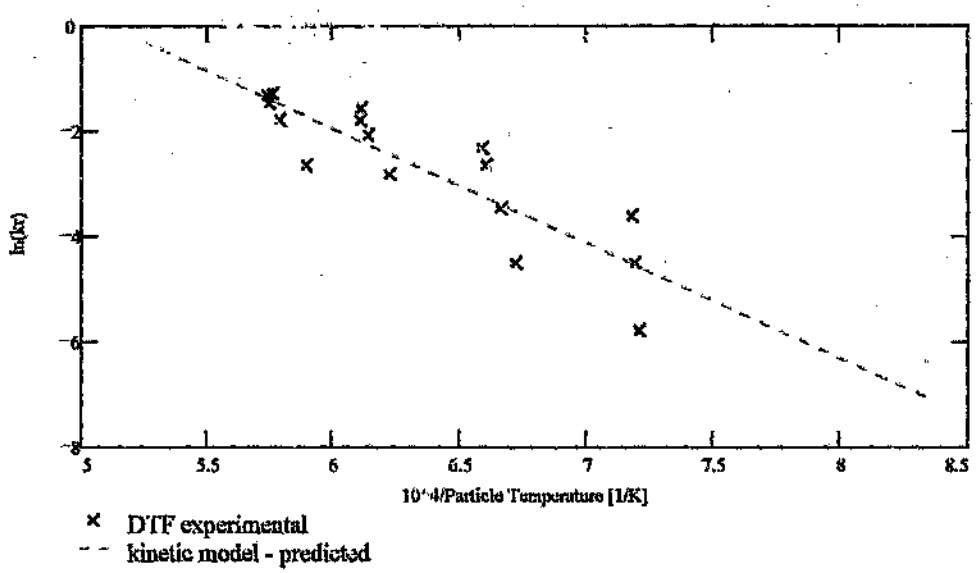

Char chemical combustion kinetics Description :

Pre-exponential factor : $\exp(Preexp) = 70549.225 \quad \frac{kg}{m^2 \cdot s \cdot bar}$

Activation Energy : $EonR \cdot \frac{R}{10^3} = 181.596 \quad \frac{kJ}{mol}$

$EonR = 21842.138 \quad K$

Function describing chemical reaction rate : $k_{r.char}(Tp) := k_{rch.o} \cdot \exp\left(\frac{-EonR}{Tp}\right)$

Hendrina R.C. Composite : 38-75 µm

Defining the overall reaction rate function :

$$k_r(Tp, Tg, dp) := \frac{1}{\left(\frac{1}{k_{r.char}(Tp)} + \frac{1}{k_{d.char}(Tp, Tg, dp)}\right)}$$

Equation describing all modes of heat transfer (shrinking core assumption)

radiation

$$dT_{rad}(C_c, T_p, T_w) := \frac{\varepsilon \cdot \sigma \cdot \left(T_w^4 - T_p^4\right)}{(C_c + C_{ash}) \cdot Cp_{char}} \cdot A_{part.c}(C_{c.0})$$

convection

$$dT_{conv}(C_c, T_p, T_g) := \frac{\frac{Nu \cdot \lambda(T_p, T_g)}{dp_0} \cdot \left| \left(\frac{T_g + T_p}{2}\right) - T_g \right|}{(C_c + C_{ash}) \cdot Cp_{char}} \cdot A_{part.c}(C_{c.0})$$

reaction

$$dT_{gen}(C_c, T_p, T_g) := \frac{-\Delta h}{(C_c + C_{ash}) \cdot Cp_{char}} \cdot \left(-k_r(T_p, T_g, dp_0) \cdot P_{O2} \cdot A_{part.c}(C_c)\right)$$

estimation of initial particle heating rate at DTF setpoint Temperature of 1400°C :

$$T_{init} := 25 + 273 \quad K \quad dT_{rad}(C_{c.0}, T_{init}, 1416 + 273) + dT_{conv}(C_{c.0}, T_{init}, 1335 + 273) = 1.673 \cdot 10^4 \quad \frac{K}{s}$$

Solution of differential equations

Initial Conditions : combustion extent — $x_0 := C_{c.0}$

particle temperature — $x_1 := 300$ K

Simultaneous Differential Equations :

combustion extent — $\frac{d}{dt} C_c = -k_r(x_1, T_g, dp_0) \cdot P_{O2} \cdot A_{part.c}(x_0)$

particle temperature — $\frac{d}{dt} Tp = dT_{rad}(x_0, x_1, T_w) + dT_{conv}(x_0, x_1, T_g) + dT_{gen}(x_0, x_1, T_g)$

Note on the Solution Methodology

The simultaneous equations are solved by a 4th order Runge Kutta solution algorithm for each DTF setpoint Temperature. An average furnace wall and furnace gas temperature have been specified for each DTF setpoint temperature.

DTF Kinetic Evaluation Results -

Char chemical combustion kinetics Description :

Pre-exponential factor : $\exp(\text{Preexp}) = 70549.225 \quad \frac{kg}{m^2 \cdot s \cdot bar}$

Activation Energy : $\text{EonR} \cdot \frac{R}{10^3} = 181.60 \quad \frac{kJ}{mol} \qquad \text{EonR} = 21842.138 \quad K$

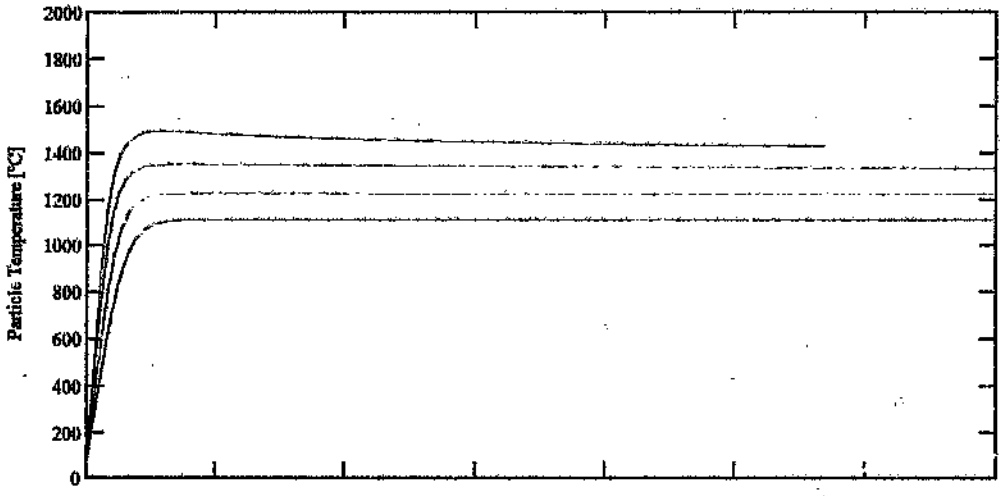

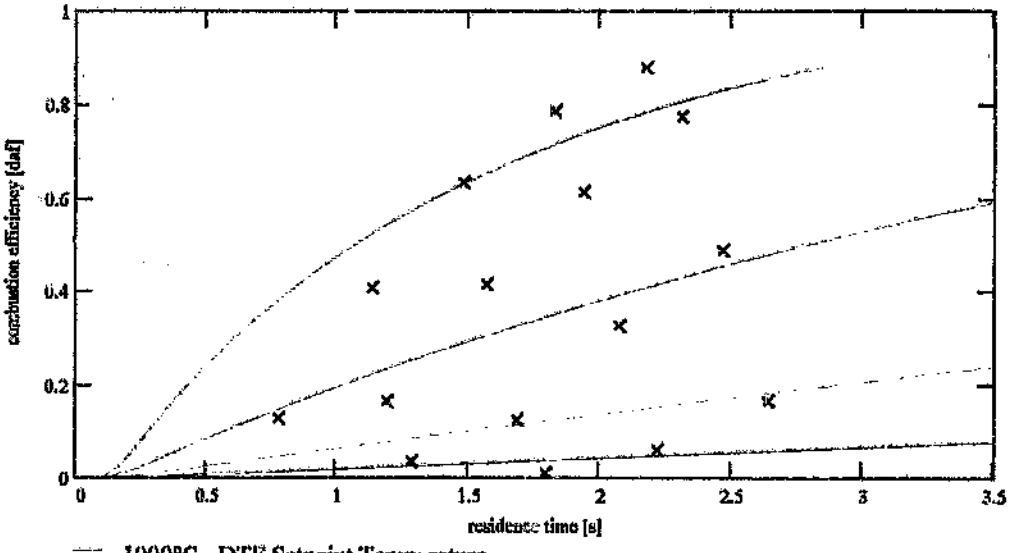

1000°C - DTF Setpoint Temperature
1100°C
1200°C
1300°C
1400°C
DTF data

Determination of DTF combustion kinetics for use with AIOLOS combustion code

---

Universal Gas Constant $R := 8.314 \quad \frac{J}{mol \cdot K}$

DTF Operation and Char Description :

Ash in Coal $Ash_{coal} := DTF_{0,8} \cdot \%$

Ash in Char $Ash_{char} := DTF_{0,7} \cdot \%$

Volatile Matter (after DTF devolatilisation) $Vols_{DTF} := 1 - Ash_{coal} - \frac{Ash_{coal}}{Ash_{char}} \cdot \left(1 - Ash_{char}\right)$

Density of coal : $\rho_{coal} := 1678 \quad \frac{kg}{m^3}$

Density of Char (initially) : (shrinking core assumption) $\rho_{char.o} := \left(1 - Vols_{DTF}\right) \cdot \rho_{coal} \quad \rho_{char.o} = 1.189 \cdot 10^3 \quad \frac{kg}{m^3}$

Initial Particle Diameter : $dp_o := DTF_{0,0} \quad m \qquad dp_o = 6 \cdot 10^{-5} \quad m$

Pressure in DTF : $P := 0.85 \cdot 10^5 \quad Pa$

Volume Oxygen Flowrate into DTF : $V_{O2} := \frac{0.6 \cdot 10^{-3}}{60} \quad \frac{m^3}{s} \qquad M_{W.O2} := 32 \cdot 10^{-3} \quad \frac{kg}{mol}$

VolumeNitrogen Flowrate into DTF : $V_{N2} := \frac{19.66 \cdot 10^{-3}}{60} \quad \frac{m^3}{s} \qquad M_{W.N2} := 28 \cdot 10^{-3} \quad \frac{kg}{mol}$

Mass Flowrate of Oxygen : $m_{O2} := \frac{V_{O2} \cdot P \cdot M_{W.O2}}{R \cdot 298} \quad \frac{kg}{s}$

Mass Flowrate of Nitrogen : $m_{N2} := \frac{V_{N2} \cdot P \cdot M_{W.N2}}{R \cdot 298} \quad \frac{kg}{s}$

Char Feedrate : $m_{char} := \frac{0.1066 \cdot 10^{-3}}{60} \quad \frac{kg}{s}$

Initial Char Concentration $C_{char.0} := \frac{m_{char}}{m_{char} + m_{O2} + m_{N2}} \quad \frac{kg}{kg_{mix}}$

Initial Fixed Carbon Concentration $C_{c.0} := C_{char.0} \cdot \left(1 - DTF_{0,7} \cdot \%\right) \quad C_{c.0} = 3.4407 \cdot 10^{-3} \quad \frac{kg}{kg_{mix}}$

$C_{c.1} := C_{char.0} \cdot \left(1 - DTF_{13,7} \cdot \%\right) \quad C_{c.1} = 3.4407 \cdot 10^{-3} \quad \frac{kg}{kg_{mix}}$

Ash Concentration : $C_{ash} := C_{char.0} \cdot \left(Ash_{char}\right) \quad C_{ash} = 1.984 \cdot 10^{-3} \quad \frac{kg}{kg_{mix}}$

Hendrina RC Composite : <75 µm

Heat Exchange Parameters and constants

Stefan Boltzmann constant $\sigma := 5.67 \cdot 10^{-8}$ $\frac{W}{m^2 \cdot K^4}$

average emissivity between particle and wall $\varepsilon := 0.85$

reaction energy : C to CO : $\Delta h := 9.614 \cdot 10^6$ $\frac{J}{kg}$

Nusselt Number for boundary layer convective heatexchange $Nu := 2$

convective heat exchange coefficient $\lambda(T_p, T_g) := 2.43 \cdot 10^{-5} \cdot \left[\frac{\left(\frac{T_p + T_g}{2} \right)}{273} \right]^{0.82}$ $\frac{W}{m \cdot K}$

heat capacity of char : $Cp_{char} := 1250$ $\frac{J}{kg \cdot K}$

Particle Surface Area as a function of combustion extent :

swelling index $n_B := \frac{2}{3}$ 1 - swelling coals
2/3 - 'non swelling' coals

$$A_{part.o}(C_o) := \frac{6}{\rho_{char.o} \cdot dp_o} \cdot C_{c.0} \cdot \left(\frac{C_o}{C_{c.0}} \right)^{n_B} \qquad \frac{m^2}{kg_{mix}}$$

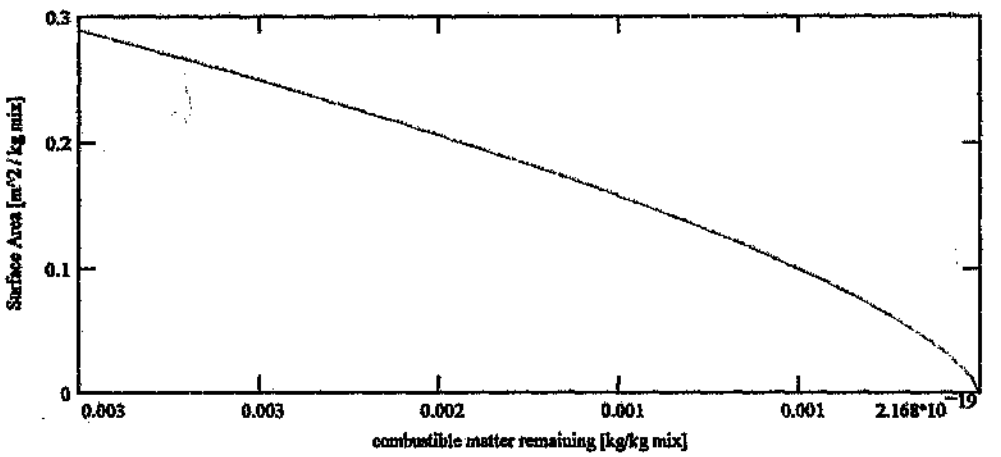

Partial Pressure of Oxygen in DTF : $P_{O2} := \frac{V_{O2}}{V_{O2} + V_{N2}}$ $P_{O2} = 0.03$ bar

Function defining mass of combustible matter remaining as a function ash content in the sampled residue

$$C_c(ash_{residue}) := \left[\frac{Ash_{char} \cdot \left(1 - \left(\frac{ash_{residue}}{100} \right) \right)}{1 - Ash_{char} \cdot \left(\frac{ash_{residue}}{100} \right)} \right] \cdot C_{c.0}$$

$ash_{residue}$ in % by mass

Hendrina RC Composite : <75 µm

Calculating Overall Rate :

$$k_{o_k} := \frac{\int_{C_o(DTF_{k,7})}^{C_o(DTF_{k,4})} \frac{1}{A_{part.o}(C_o)}\, dC_o}{-P_{O2}\cdot DTF_{k,3}}$$

Calculating Particle Temperature:

Iterative solution of Energy Balance between particle, hot gas and reactor wall :

$$\Delta h \cdot \frac{C_o(Ash_{res}) - C_{o.0}}{t_r} = \left[s\cdot\sigma\cdot\left(T_w^{\,4} - T_p^{\,4}\right) - \frac{Nu\cdot\lambda(T_p,T_g)}{dp}\cdot\left[\left(\frac{T_g+T_p}{2}\right) - T_g\right]\right]\cdot A_{part.o}(C_{o.0})$$

$$T_{particle}(Ash_{res}, t_r, T_w, T_g, dp) := find(T_p)$$

$$DTF_{k,6} := T_{particle}(DTF_{k,4}, DTF_{k,3}, DTF_{k,2}+273, DTF_{k,5}+273, DTF_{k,0}) - 273$$

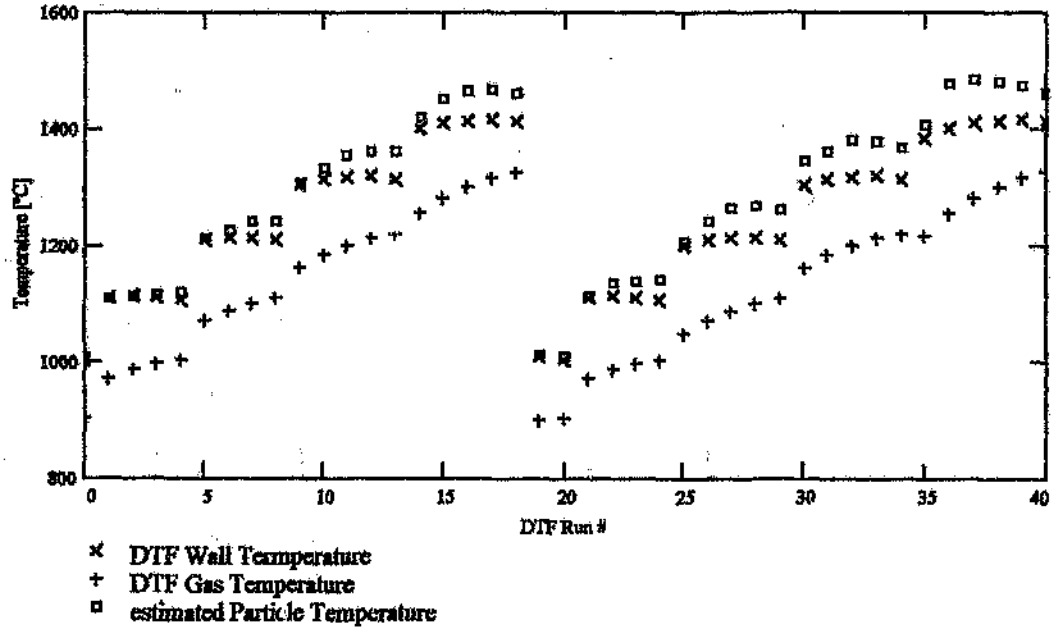

Oxygen Diffusion reaction rate as a function particle Temperature

O2 diffusion constant at 1600K : $D_{O2.1600K} := 3.39\cdot10^{-4}\ \frac{m^2}{s}$

mechanism factor : $\phi := 2$ ϕ = 2 for CO, and 1 for CO2

$$k_{d.char}(Tp, Tg, dp) := \frac{24\cdot\phi\cdot D_{O2.1600K}\cdot\left[\frac{(Tg+Tp)\cdot0.5}{1600}\right]^{1.75}}{R\cdot10^{-5}\cdot dp\cdot Tg} \quad \frac{kg}{m^2\cdot s\cdot bar}$$

Source : AIOLOS - combustion model

Hendrina RC Composite : <75 µm

Determining the Chemical Reaction Rate from the experimental data :

$$kr_k := \left[\frac{1}{\left(\frac{1}{k_{o_k}}\right) - \frac{1}{k_{d.char}\left(DTF_{k,6} + 273, DTF_{k,5} + 273, DTF_{k,0}\right)}} \right]$$

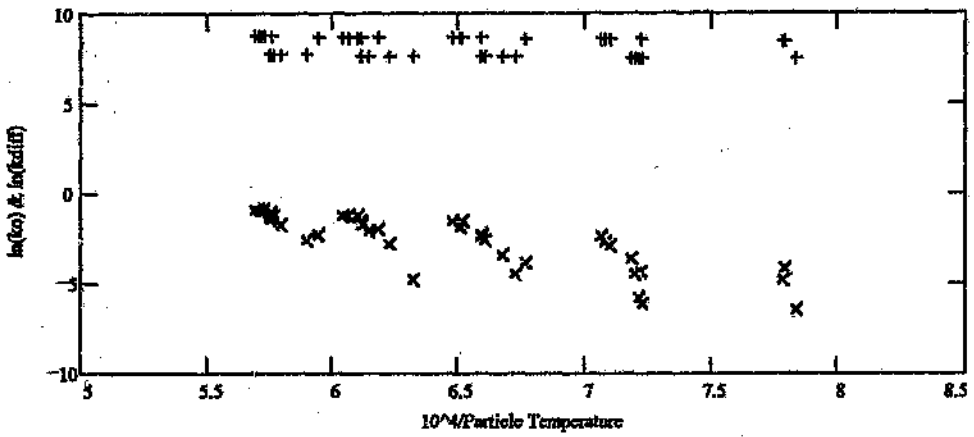

NB : if the +'s lie beneath the x's, the overall reaction rate could be diffusion controlled

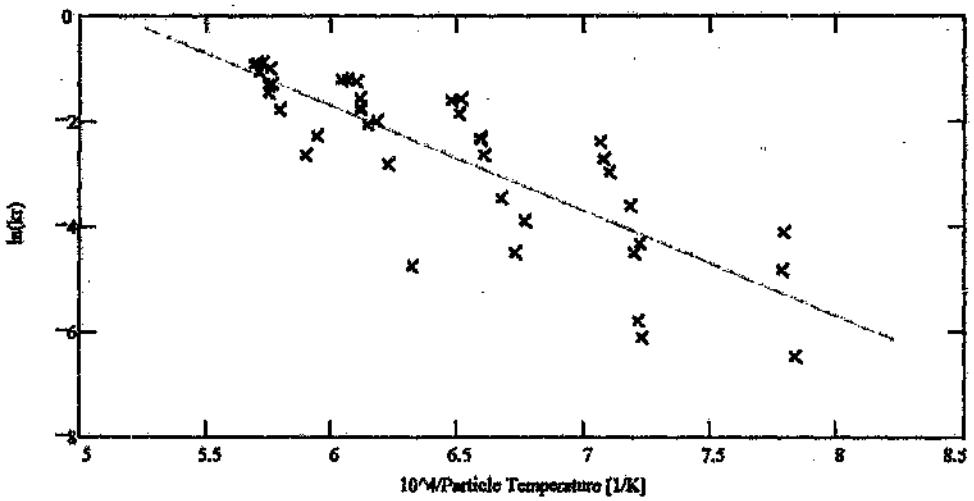

Char chemical combustion kinetics Description :

Pre-exponential factor : $\exp(Preexp) = 28418.03 \quad \frac{kg}{m^2 \cdot s \cdot bar}$

Activation Energy : $-EonR \cdot \frac{R}{10^3} = 165.716 \quad \frac{kJ}{mol}$

$-EonR = 19932.114 \quad K$

Function describing chemical reaction rate : $k_{r.char}(Tp) := k_{rch.o} \cdot \exp\left(\frac{EonR}{Tp}\right)$

Hendrina RC Composite : <75 µm

DTF Kinetic Evaluation Results -

Char chemical combustion kinetics Description :

Pre-exponential factor : $\exp(\text{Preexp}) = 282.185 \quad \frac{kg}{m^2 \cdot s \cdot bar}$

Activation Energy : $-\text{EonR} \cdot \frac{R}{10^3} = 99.45 \quad \frac{kJ}{mol} \quad -\text{EonR} = 11961.304 \quad K$

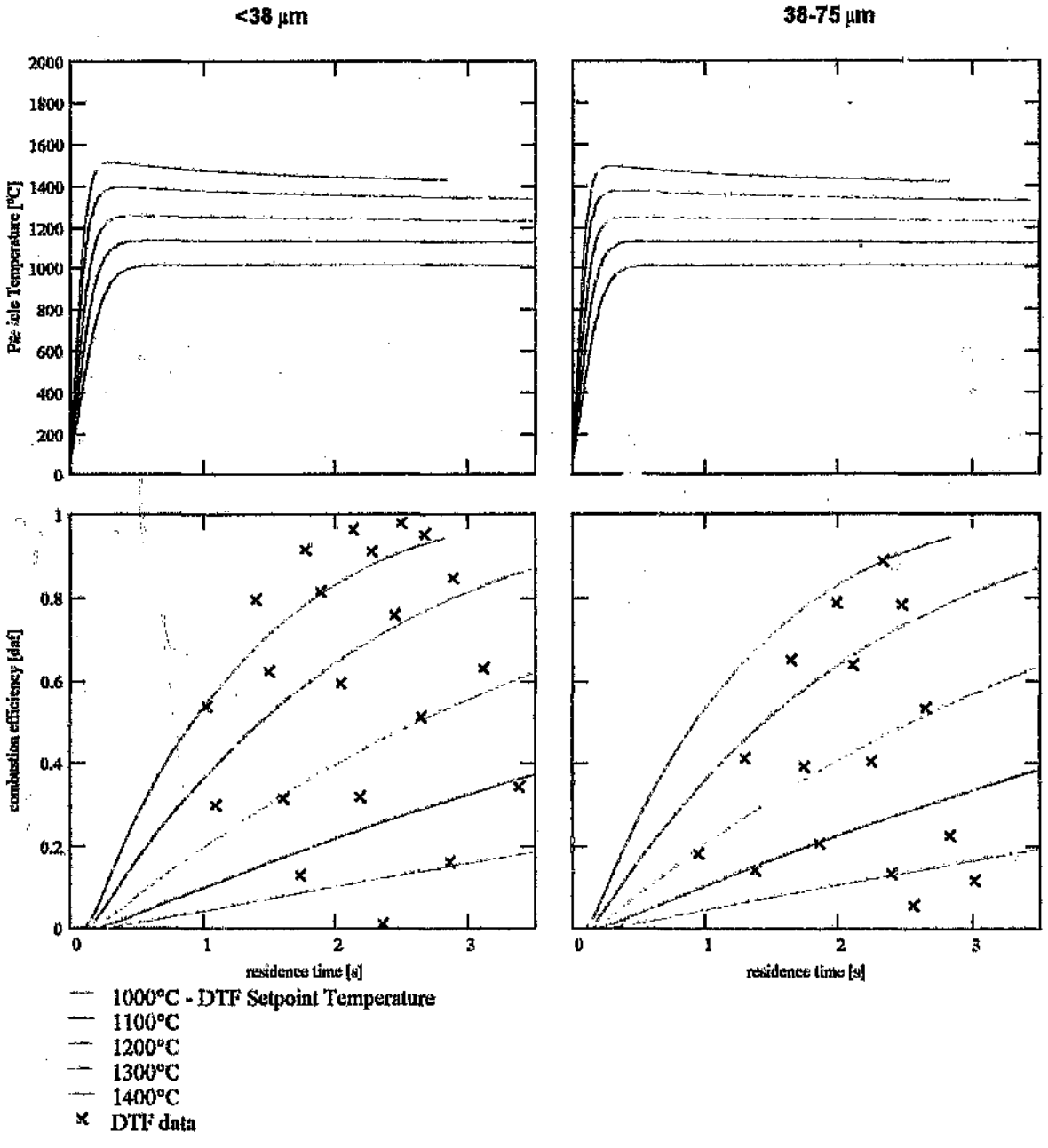

Defining the overall reaction rate function :

$$k_r(Tp, Tg, dp) := \frac{1}{\left(\frac{1}{k_{r.char}(Tp)} + \frac{1}{k_{d.char}(Tp, Tg, dp)}\right)}$$

Equation describing all modes of heat transfer (shrinking core assumption)

radiation

$$dT_{rad}(C_c, T_p, T_w, dp) := \frac{\varepsilon\sigma\cdot\left(T_w^4 - T_p^4\right)}{\left(C_c + C_{ash}\right)\cdot Cp_{char}}\cdot if\left(dp > 38\cdot 10^{-6}, A_{part.c}(C_{c.1}), A_{part.c}(C_{c.0})\right)$$

convection

$$dT_{conv}(C_c, T_p, T_g, dp) := \frac{\frac{Nu\cdot\lambda(T_p, T_g)}{dp}\cdot\left[\left(\frac{T_g + T_p}{2}\right) - T_g\right]}{\left(C_c + C_{ash}\right)\cdot Cp_{char}}\cdot A_{part.c}(C_{c.0})$$

reaction

$$dT_{gen}(C_c, T_p, T_g, dp) := \frac{-\Delta h}{\left(C_c + C_{ash}\right)\cdot Cp_{char}}\cdot\left(-k_r(T_p, T_g, dp)\cdot P_{O2}\cdot A_{part.c}(C_c)\right)$$

estimation of initial particle heating rate at DTF setpoint Temperature of 1400°C :

$$dT_{rad}(C_{c.0}, 298, DTF_{s_5,2} + 273, DTF_{s_5,0}) + dT_{conv}(C_{c.0}, 298, DTF_{s_5,5} + 273, DTF_{s_5,0}) = 1.660\cdot 10^4\,\frac{K}{s}$$

Solution of differential equations

Initial Conditions : combustion extent — $x_0 := C_c(DTF_{0,7})$

particle temperature — $x_1 := 300\ K$

Simultaneous Differential Equations :

combustion extent — $\frac{d}{dt}C_c = -k_r(x_1, T_g, dp_{initial})\cdot P_{O2}\cdot A_{part.c}(x_0)$

particle temperature — $\frac{d}{dt}Tp = dT_{rad}(x_0, x_1, T_w) + dT_{conv}(x_0, x_1, T_g) + dT_{gen}(x_0, x_1, T_g)$

Note on the Solution Methodology

The simultaneous equations are solved by a 4th order Runge Kutta solution algorithm for each DTF setpoint Temperature. An average furnace wall and furnace gas temperature have been specified for each DTF set,oint temperature.

DTF Kinetic Evaluation Results -

Char chemical combustion kinetics Description :

Pre-exponential factor : $\exp(\text{Preexp}) = 28418.03$ $\frac{kg}{m^2 \cdot s \cdot bar}$

Activation Energy : $-\text{EonR} \cdot \frac{R}{10^3} = 165.72$ $\frac{kJ}{mol}$ $-\text{EonR} = 19932.114$ K

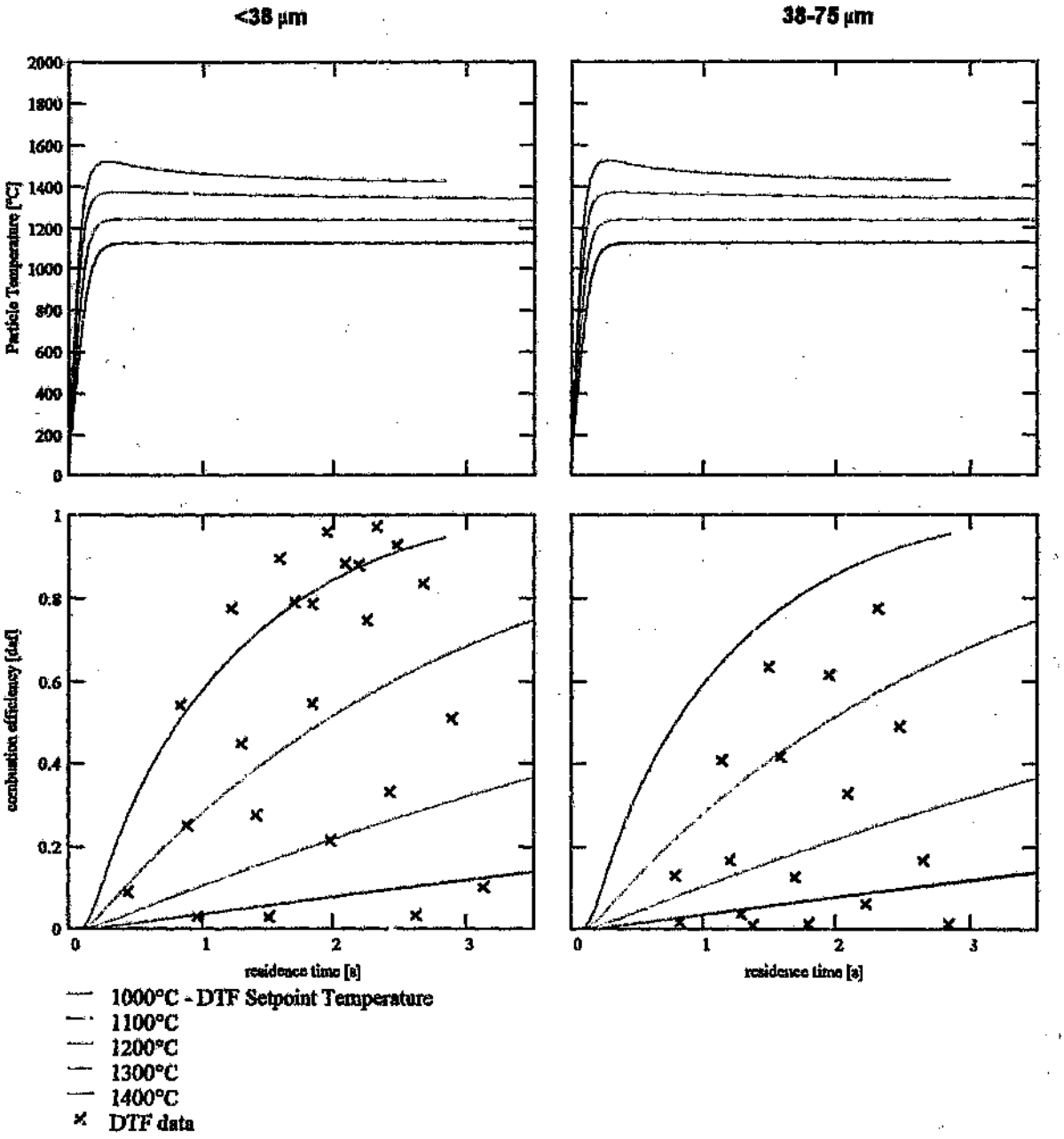

Appendix 2.2.1

Hendrina Washing Plant Feed: Basic Analysis Datasheet

COAL : Hendrina - Washing Plant Feed

Preparation of Coal Analysis Data for specification in AIOLOS

Analysis by TRI Coal Labs all entries in mass% except where otherwise noted

Total Moisture : (as received)	8.7			
Proximate :	air dried	as received	dry	daf
Moisture	2	**8.70**		
	29.6	**27.62**	30.20	
	24.4	22.77	24.90	**35.67**
Fixed Carbon	44	40.92	44.90	**64.33**
Ultimate :				
Carbon	56.24	**0.52**	57.39	82.22
Hydrogen	3.34	**0.03**	3.41	4.88
Nitrogen	1.4	**0.01**	1.43	2.05
Sulphur	0.84	**0.01**	0.86	1.23
Carbonates	0.53	0.00	0.54	0.77
Oxygen	6.05	0.06	6.17	8.85
Oxygen + Carbonates		**0.06**		
Calorific Value	22	20.53	22.45	**32.16**
DTF DEVOL				
Volatile Matter	29.92			
Q Factor	**1.226**			
DTF FULL TEST				
Size Fraction	<38 µm	38-75 µm	< 75 µm	Unit
Pre-exponential Factor	208	1077	286	$kg/m^2.s.atm$
	205	**1063**	**282**	$kg/m^2.s.bar$
Activation Energy	101.66	124.9	99.45	kJ/mol
Activation Energy /R	**12228**	**15023**	**11962**	K

Coal Name: HENDRINA

Origin: Hendrina P/S

Coal Preparation:

Table :

PROXIMATE ANALYSIS			METHOD
Inherent Moisture:	2	(m% of coal - air dried)	ESKOM 103
Ash :	29.6		ESKOM 101
Volatile Matter :	24.4		ESKOM 102
Fixed Carbon (by difference) :	44		ESKOM 128
ULTIMATE ANALYSIS			
Carbon:	56.24	(m% of coal - air dried)	ESKOM 118
Hydrogen:	3.34		ESKOM 118
Nitrogen:	1.4		ESKOM 118
Total Sulphur:	0.84		ESKOM 104
Carbonates (as CO2):	0.53		ESKOM 100
Oxygen (by difference):	6.05		ESKOM 132
Gross Calorific Value:	22	(MJ/kg)	ESKOM 105
HARDGROVE INDEX:	-1		ESKOM 117
ABRASIVENESS:	-1	(mg Fe/4kg coal)	ESKOM 123
ASH FUSION TEMPERATURES			ESKOM 125
Initial Deformation Temperature:	-1	(°C)	
Softening Temperature:	-1		
Hemispherical Temperature:	-1		
Flow Temperature:	-1		

'-1' Indicates that the result of that analysis is not available
RAW COAL PREPARATION BY SABS 0135 PART 2 - 1977

Appendix 2.2.2

Hencrina Washing Plant Feed: Determination of the Char Combustion Kinetics

Determination of DTF combustion kinetics for use with AIOLOS combustion code

---

Universal Gas Constant $R := 8.314 \quad \frac{J}{mol \cdot K}$

DTF Operation and Char Description :

Ash in Coal $Ash_{coal} := DTF_{0.8} \cdot \%$

Ash in Char $Ash_{char} := DTF_{0.7} \cdot \%$

Volatile Matter (after DTF devolatilisation) $Vols_{DTF} := 1 - Ash_{coal} \cdot \frac{Ash_{coal}}{Ash_{char}} \cdot (1 - Ash_{char})$

Density of coal : $\rho_{coal} := 1678 \quad \frac{kg}{m^3}$

Density of Char (initially) : (shrinking core assumption) $\rho_{char.o} := (1 - Vols_{DTF}) \cdot \rho_{coal} \quad \rho_{char.o} = 1.179 \cdot 10^3 \quad \frac{kg}{m^3}$

Initial Particle Diameter : $dp_o := DTF_{0.0} \quad m \quad dp_o = 2.41 \cdot 10^{-5} \quad m$

Pressure in DTF : $P := 0.85 \cdot 10^5 \quad Pa$

Volume Oxygen Flowrate into DTF : $V_{O2} := \frac{0.6 \cdot 10^{-3}}{60} \quad \frac{m^3}{s} \quad M_{W.O2} := 32 \cdot 10^{-3} \quad \frac{kg}{mol}$

VolumeNitrogen Flowrate into DTF : $V_{N2} := \frac{19.66 \cdot 10^{-3}}{60} \quad \frac{m^3}{s} \quad M_{W.N2} := 28 \cdot 10^{-3} \quad \frac{kg}{mol}$

Mass Flowrate of Oxygen : $m_{O2} := \frac{V_{O2} \cdot P \cdot M_{W.O2}}{R \cdot 298} \quad \frac{kg}{s}$

Mass Flowrate of Nitrogen : $m_{N2} := \frac{V_{N2} \cdot P \cdot M_{W.N2}}{R \cdot 298} \quad \frac{kg}{s}$

Char Feedrate : $m_{char} := \frac{0.1066 \cdot 10^{-3}}{60} \quad \frac{kg}{s}$

Initial Char Concentration $C_{char.0} := \frac{m_{char}}{m_{char} + m_{O2} + m_{N2}} \quad \frac{kg}{kg_{mix}}$

Initial Fixed Carbon Concentration $C_{c.0} := C_{char.0} \cdot (1 - Ash_{char}) \quad C_{c.0} = 3.0928 \cdot 10^{-3} \quad \frac{kg}{kg_{mix}}$

Ash Concentration : $C_{ash} := C_{char.0} \cdot (Ash_{char}) \quad C_{ash} = 2.3318 \cdot 10^{-3} \quad \frac{kg}{kg_{mix}}$

Hendrina Washing Plant Feed : < 38 µm

Heat Exchange Parameters and constants

Stefan Boltzmann constant $\sigma := 5.67 \cdot 10^{-8} \quad \frac{W}{m^2 \cdot K^4}$

average emissivity between particle and wall $\varepsilon := 0.85$

reaction energy : C to CO : $\Delta h := 9.614 \cdot 10^{6} \quad \frac{J}{kg}$

Nusselt Number for boundary layer convective heatexchange $Nu := 2$

convective heat exchange coefficient $\lambda(T_p, T_g) := 2.43 \cdot 10^{-11} \cdot \left[\frac{\left(\frac{T_p + T_g}{2} \right)}{273} \right]^{0.82} \quad \frac{W}{m \cdot K}$

heat capacity of char : $Cp_{char} := 1250 \quad \frac{J}{kg \cdot K}$

Particle Surface Area as a function of combustion extent :

swelling index $n_B := \frac{2}{3}$ 1 - swelling coals
2/3 - 'non swelling' coals

$$A_{part.o}(C_o) := \frac{6}{\rho_{char.o} \cdot dp_o} \cdot C_{o.0} \cdot \left(\frac{C_o}{C_{o.0}} \right)^{n_B} \quad \frac{m^2}{kg_{mix}}$$

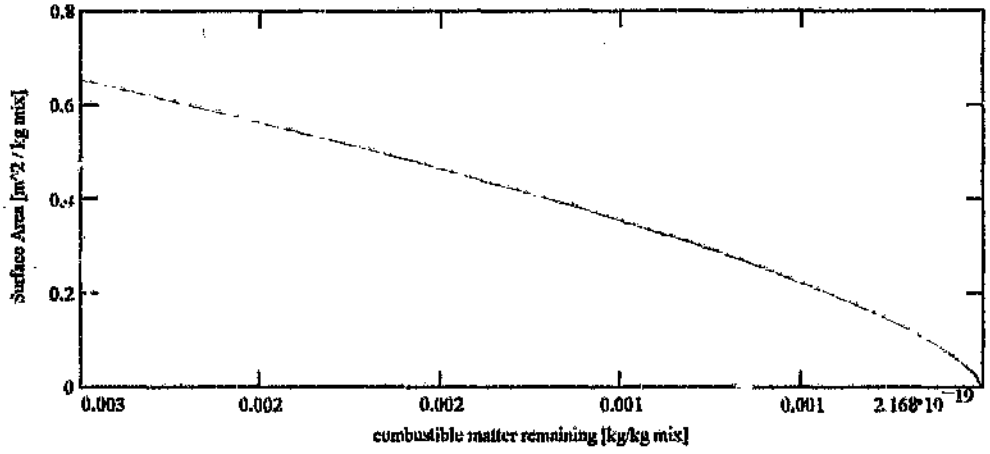

Partial Pressure of Oxygen in DTF : $P_{O2} := \frac{V_{O2}}{V_{O2} + V_{N2}} \quad P_{O2} = 0.03$ bar

Function defining mass of combustible matter remaining as a function ash content in the sampled residue

$$C_o(ash_{residue}) := \left[\frac{Ash_{char} \cdot \left(1 - \left(\frac{ash_{residue}}{100} \right) \right)}{1 - Ash_{char} \cdot \left(\frac{ash_{residue}}{100} \right)} \right] \cdot C_{o.0}$$

$ash_{residue}$ in % by mass

Hendrina Washing Plant Feed : < 38 µm

Calculating Overall Rate .

$$k_{o_k} = \frac{\int_{C_{c.0}}^{C_c(DTF_{k,4})} \frac{1}{A_{part}\cdot(C_c)}\, dC_c}{\cdot P_{O2}\cdot DTF_{k,3}}$$

Calculating Particle Temperature:

Iterative solution of Energy Balance between particle, hot gas and reactor wall :

$$\frac{\Delta h\cdot\left(C_c(Ash_{res}) - C_{c.0}\right)}{t_r} = \left[s\cdot\sigma\cdot\left[(T_w)^4 - (T_p)^4\right] + \frac{Nu\cdot\lambda(T_p, T_g)}{dp_o}\cdot\left[\left(\frac{T_g + T_p}{2}\right) - (T_g)\right]\right]\cdot A_{part.c}(C_{c.0})$$

$$T_{particle}(Ash_{res}, t_r, T_w, T_g) := \text{find}(T_p)$$

$$DTF_{k,6} := T_{particle}(DTF_{k,4}, DTF_{k,3}, DTF_{k,2} + 273, DTF_{k,5} + 273) - 273$$

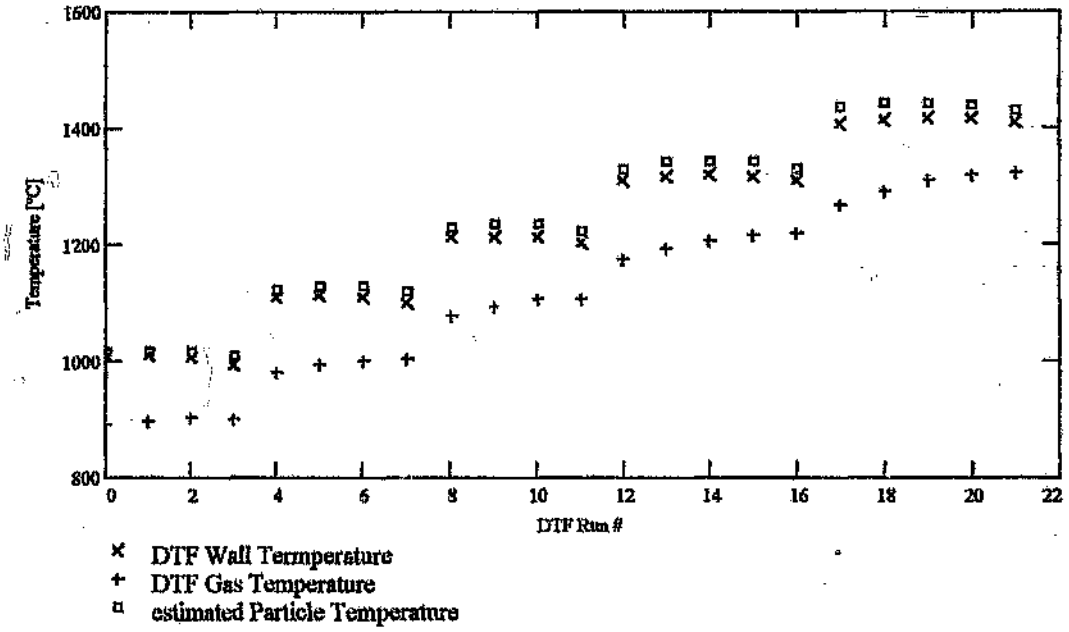

Oxygen Diffusion reaction rate as a function particle Temperature

O2 diffusion constant at 1600K : $D_{O2.1600K} := 3.39\cdot10^{-4}\ \frac{m^2}{s}$

mechanism factor : $\phi := 2$ $\phi = 2$ for CO, and 1 for CO2

$$k_{d.char}(Tp, Tg, dp) := \frac{24\cdot\phi\cdot D_{O2.1600K}\cdot\left[\frac{(Tg + Tp)\cdot0.5}{1600}\right]^{1.75}}{R\cdot10^5\cdot dp\cdot Tg}\ \frac{kg}{m^2\cdot s\cdot bar}$$

Source : AIOLOS - combustion model

Hendrina Washing Plant Feed : < 38 µm

Determining the Chemical Reaction Rate from the experimental data :

$$kr_k = \left[\frac{1}{\left(\frac{1}{k_{o_k}} \right) - \frac{1}{k_{d.char}(DTF_{k,6} + 273, DTF_{k,5} + 273, DTF_{k,0})}} \right]$$

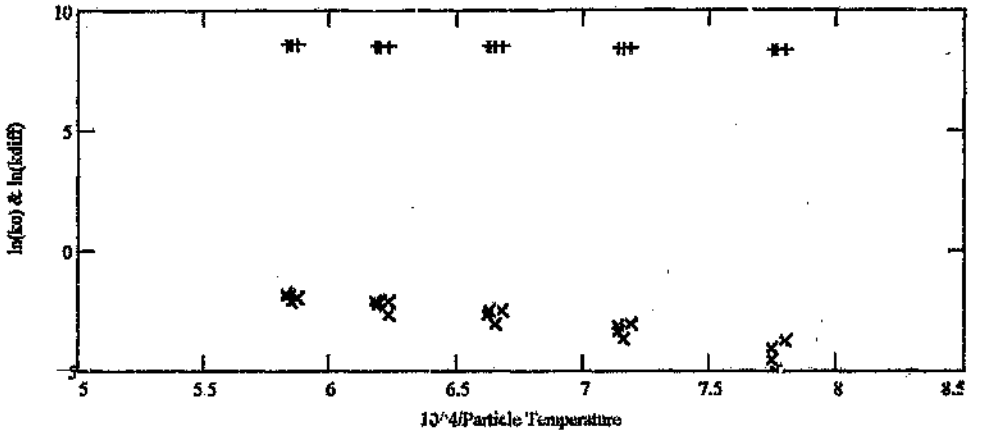

NB : if the +'s lie beneath the x's, the overall reaction rate could be diffusion controlled

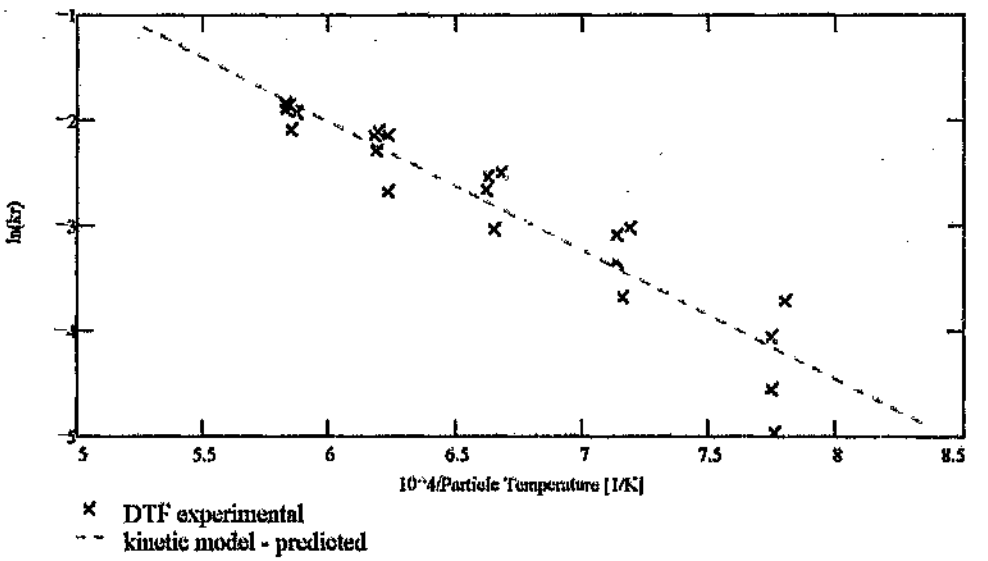

Char chemical combustion kinetics Description :

Pre-exponential factor : $\exp(Preexp) = 204.918$ $\frac{kg}{m^2 \cdot s \cdot bar}$

Activation Energy : $EonR \cdot \frac{R}{10^3} = 101.659$ $\frac{kJ}{mol}$

$EonR = 12227.406$ K

Function describing chemical reaction rate : $k_{r.char}(Tp) := k_{reh.o} \cdot \exp\left(\frac{EonR}{Tp}\right)$

Hendrina Washing Plant Fe d : < 38 µm

Defining the overall reaction rate function :

$$k_r(Tp, Tg, dp) := \frac{1}{\left(\frac{1}{k_{r.char}(Tp)} + \frac{1}{k_{d.char}(Tp, Tg, dp)}\right)}$$

Equation describing all modes of heat transfer (shrinking core assumption)

radiation

$$dT_{rad}(C_c, T_p, T_w) := \frac{\varepsilon\sigma\cdot\left(T_w^4 - T_p^4\right)}{(C_c + C_{ash})\cdot Cp_{char}}\cdot A_{part.c}(C_{c.0})$$

convection

$$dT_{conv}(C_c, T_p, T_g) := \frac{\frac{Nu\cdot\lambda(T_p, T_g)}{dp_0}\cdot\left[\left(\frac{T_g + T_p}{2}\right) - T_p\right]}{(C_c + C_{ash})\cdot Cp_{char}}\cdot A_{part.c}(C_{c.0})$$

reaction

$$dT_{gen}(C_c, T_p, T_g) := \frac{-\Delta h}{(C_c + C_{ash})\cdot Cp_{char}}\cdot(-k_r(T_p, T_g, dp_0)\cdot P_{O2}\cdot A_{part.c}(C_c))$$

estimation of initial particle heating rate at DTF setpoint Temperature of 1400°C :

$$T_{init} := 25 + 273 \quad K \quad dT_{rad}(C_{c.0}, T_{init}, 1416 + 273) + dT_{conv}(C_{c.0}, T_{init}, 1335 + 273) = 3.774\cdot 10^4 \quad \frac{K}{s}$$

Solution of differential equations

Initial Conditions : combustion extent — $x_0 := C_{c.0}$

particle temperature — $x_1 := 300$ K

Simultaneous Differential Equations :

combustion extent — $\frac{d}{dt}C_c = -k_r(x_1, T_g, dp_0)\cdot P_{O2}\cdot A_{part.c}(x_0)$

particle temperature — $\frac{d}{dt}Tp = dT_{rad}(x_0, x_1, T_w) + dT_{conv}(x_0, x_1, T_g) + dT_{gen}(x_0, x_1, T_g)$

Note on the Solution Methodology

The simultaneous equations are solved by a 4th order Runge Kutta solution algorithm for each DTF setpoint Temperature. An average furnace wall and furnace gas temperature have been specified for each DTF setpoint temperature.

Hendrina Washing Plant Feed : < 38 µm

DTF Kinetic Evaluation Results -

Char chemical combustion kinetics Description :

Pre-exponential factor : $\exp(\text{Preexp}) = 204.918 \quad \frac{kg}{m^2 \cdot s \cdot bar}$

Activation Energy : $-\text{EonR} \cdot \frac{R}{10^3} = 101.66 \quad \frac{kJ}{mol} \qquad -\text{EonR} = 12227.406 \quad K$

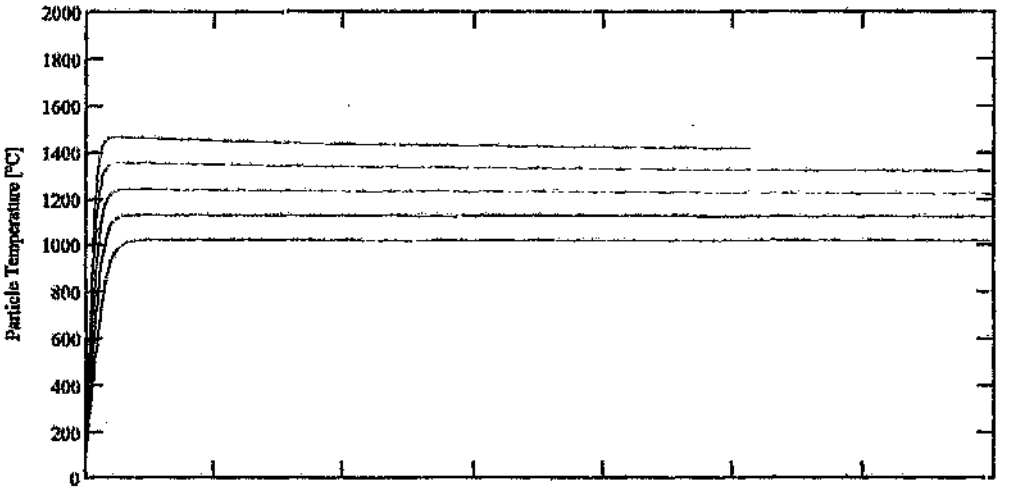

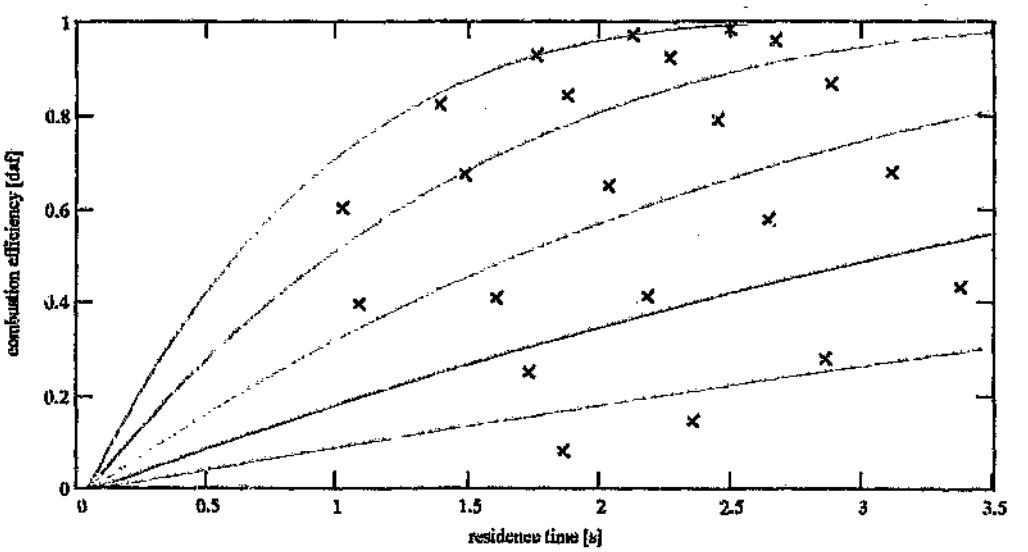

1000°C - DTF Setpoint Temperature
1100°C
1200°C
1300°C
1400°C
DTF data

Hendrina Washing Plant Feed : < 38 µm

Determination of DTF combustion kinetics for use with AIOLOS combustion code

---

Universal Gas Constant $R := 8.314 \quad \frac{J}{mol \cdot K}$

DTF Operation and Char Description :

Ash in Coal $Ash_{coal} := DTF_{0.8} \cdot \%$

Ash in Char $Ash_{char} := DTF_{0.7} \cdot \%$

Volatile Matter (after DTF devolatilisation) $Vols_{DTF} := 1 - Ash_{coal} - \frac{Ash_{coal}}{Ash_{char}} \cdot (1 - Ash_{char})$

Density of coal : $\rho_{coal} := 1678 \quad \frac{kg}{m^3}$

Density of Char (initially) : (shrinking core assumption) $\rho_{char.o} := (1 - Vols_{DTF}) \cdot \rho_{coal} \quad \rho_{char.o} = 1.087 \cdot 10^3 \quad \frac{kg}{m^3}$

Initial Particle Diameter : $dp_o := DTF_{0.0} \quad m \quad dp_o = 6.48 \cdot 10^{-5} \quad m$

Pressure in DTF : $P := 0.85 \cdot 10^5 \quad Pa$

Volume Oxygen Flowrate into DTF : $V_{O2} := \frac{0.6 \cdot 10^{-3}}{60} \quad \frac{m^3}{s} \quad M_{W.O2} := 32 \cdot 10^{-3} \quad \frac{kg}{mol}$

VolumeNitrogen Flowrate into DTF : $V_{N2} := \frac{19.66 \cdot 10^{-3}}{60} \quad \frac{m^3}{s} \quad M_{W.N2} := 28 \cdot 10^{-3} \quad \frac{kg}{mol}$

Mass Flowrate of Oxygen : $m_{O2} := \frac{V_{O2} \cdot P \cdot M_{W.O2}}{R \cdot 298} \quad \frac{kg}{s}$

Mass Flowrate of Nitrogen : $m_{N2} := \frac{V_{N2} \cdot P \cdot M_{W.N2}}{R \cdot 298} \quad \frac{kg}{s}$

Char Feedrate : $m_{char} := \frac{0.1066 \cdot 10^{-3}}{60} \quad \frac{kg}{s}$

Initial Char Concentration $C_{char.0} := \frac{m_{char}}{m_{char} + m_{O2} + m_{N2}} \quad \frac{kg}{kg_{mix}}$

Initial Fixed Carbon Concentration $C_{c.0} := C_{char.0} \cdot (1 - Ash_{char}) \quad C_{c.0} = 2.8942 \cdot 10^{-3} \quad \frac{kg}{kg_{mix}}$

Ash Concentration : $C_{ash} := C_{char.0} \cdot (Ash_{char}) \quad C_{ash} = 2.5304 \cdot 10^{-3} \quad \frac{kg}{kg_{mix}}$

Hendrina Washing Plant Feed : 38-75 µm

Heat Exchange Parameters and constants

Stefan Boltzmann constant $\sigma := 5.67 \cdot 10^{-8}$ $\frac{W}{m^2 \cdot K^4}$

average emissivity between particle and wall $\varepsilon := 0.85$

reaction energy : C to CO : $\Delta h := 9.614 \cdot 10^6$ $\frac{J}{kg}$

Nusselt Number for boundary layer convective heatexchange $Nu := 2$

convective heat exchange coefficient $\lambda(T_p, T_g) := 2.43 \cdot 10^{-11} \cdot \left[\frac{\left(\frac{T_p + T_g}{2}\right)}{273}\right]^{0.82}$ $\frac{W}{m \cdot K}$

heat capacity of char : $Cp_{char} := 1250$ $\frac{J}{kg \cdot K}$

Particle Surface Area as a function of combustion extent :

swelling index $n_B := \frac{2}{3}$ 1 - swelling coals
2/3 - 'non swelling' coals

$$A_{part.c}(C_c) := \frac{6}{\rho_{char.o} \cdot dp_o} \cdot C_{c.0} \cdot \left(\frac{C_c}{C_{c.0}}\right)^{n_B} \qquad \frac{m^2}{kg_{mix}}$$

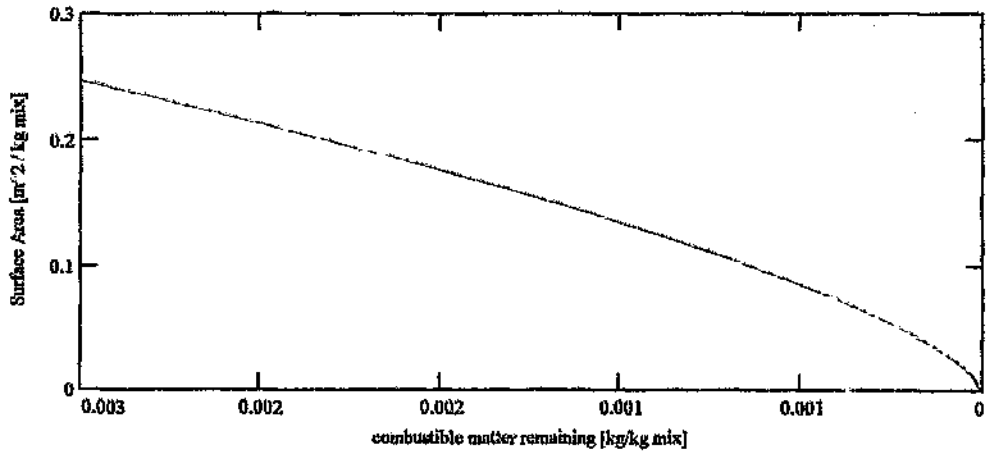

Partial Pressure of Oxygen in DTF : $P_{O2} := \frac{V_{O2}}{V_{O2} + V_{N2}}$ $P_{O2} = 0.03$ bar

Function defining mass of combustible matter remaining as a function ash content in the sampled residue

$$C_c(ash_{residue}) := \left[\frac{Ash_{char} \cdot \left(1 - \left(\frac{ash_{residue}}{100}\right)\right)}{1 - Ash_{char} \cdot \left(\frac{ash_{residue}}{100}\right)}\right] \cdot C_{c.0}$$

$ash_{residue}$ in % by mass

Calculating Overall Rate :

$$k_{o_k} = \frac{\int_{C_{c.0}}^{C_c(DTF_{k,4})} \frac{1}{A_{part.c}(C_c)}\, dC_c}{-P_{O2} \cdot DTF_{k,3}}$$

Calculating Particle Temperature:

Iterative solution of Energy Balance between particle, hot gas and reactor wall :

$$\frac{\Delta h \cdot (C_c(Ash_{res}) - C_{c.0})}{t_r} = \left[\varepsilon \cdot \sigma \cdot \left[(T_w)^4 - (T_p)^4 \right] + \frac{Nu \cdot \lambda(T_p, T_g)}{dp_o} \cdot \left[\left(\frac{T_g + T_p}{2} \right) - (T_g) \right] \right] \cdot A_{part.c}(C_{c.0})$$

$$T_{particle}(Ash_{res}, t_r, T_w, T_g) := find(T_p)$$

$$DTF_{k,6} := T_{particle}(DTF_{k,4}, DTF_{k,3}, DTF_{k,2} + 273, DTF_{k,5} + 273) - 273$$

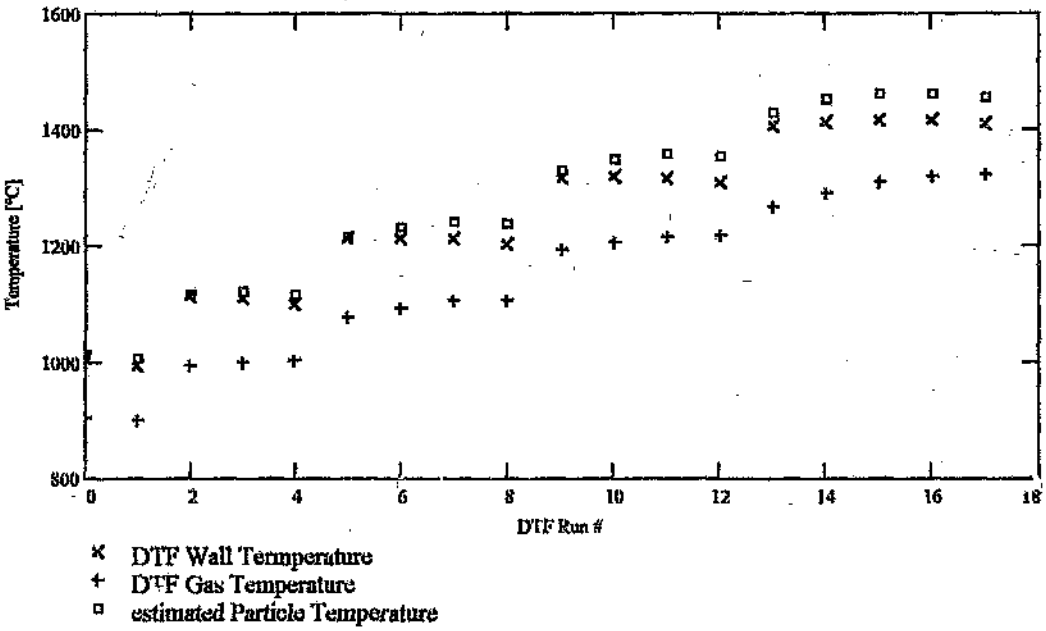

Oxygen Diffusion reaction rate as a function particle Temperature

O2 diffusion constant at 1600K : $D_{O2.1600K} := 3.39 \cdot 10^{-4} \ \frac{m^2}{s}$

mechanism factor : $\phi := 2$ $\phi = 2$ for CO, and 1 for CO2

$$k_{d.char}(Tp, Tg, dp) := \frac{24 \cdot \phi \cdot D_{O2.1600K} \left[\frac{(Tg + Tp) \cdot 0.5}{1600} \right]^{1.75}}{R \cdot 10^5 \cdot dp \cdot Tg} \ \frac{kg}{m^2 \cdot s \cdot bar}$$

Source : AIOLOS - combustion model

Hendrina Washing Plant Feed : 38 75 µm

Determining the Chemical Reaction Rate from the experimental data :

$$kr_k := \left[\frac{1}{\left(\frac{1}{ko_k}\right) - \frac{1}{k_{d.char}(DTF_{k,6}+273, DTF_{k,5}+273, DTF_{k,0})}} \right]$$

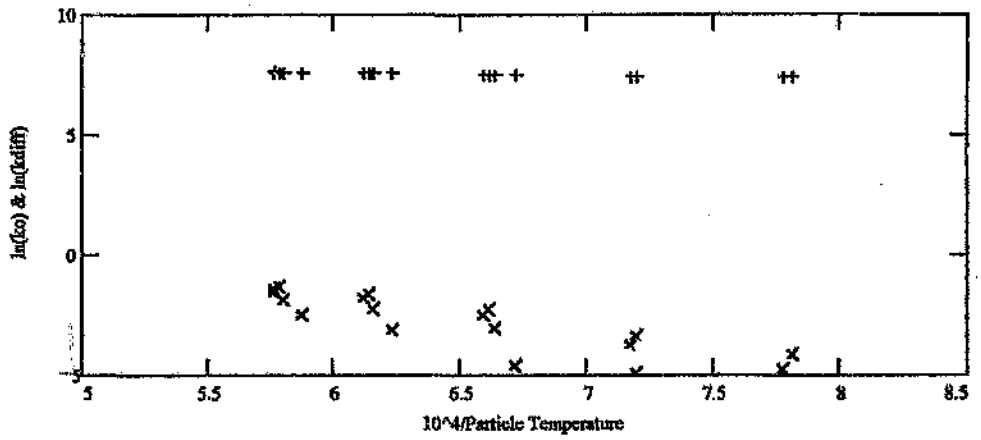

NB : if the +'s lie beneath the x's, the overall reaction rate could be diffusion controlled

---

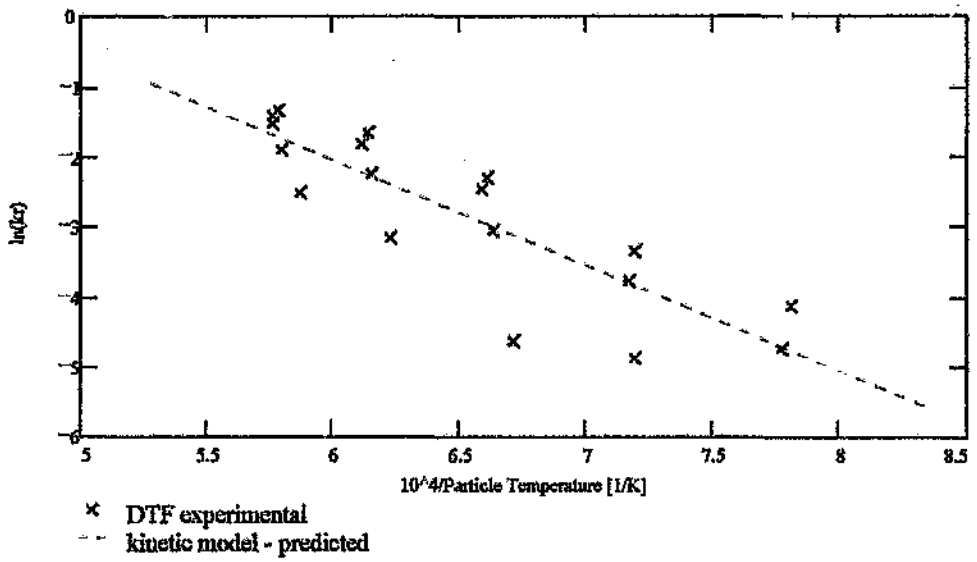

Char chemical combustion kinetics Description :

Pre-exponential factor : $\exp(Preexp) = 1063.044 \quad \frac{kg}{m^2 \cdot s \cdot bar}$

Activation Energy : $-EonR \cdot \frac{R}{10^3} = 124.897 \quad \frac{kJ}{mol}$

$-EonR = 15022.456 \quad K$

Function describing chemical reaction rate : $k_{r.char}(Tp) := k_{rch.o} \cdot \exp\left(\frac{EonR}{Tp}\right)$

Hendrina Washing Plant Feed : 38-75 µm

Defining the overall reaction rate function :

$$k_r(Tp, Tg, dp) := \frac{1}{\left(\frac{1}{k_{r.char}(Tp)} + \frac{1}{k_{d.char}(Tp, Tg, dp)}\right)}$$

Equation describing all modes of heat transfer (shrinking core assumption)

radiation

$$dT_{rad}(C_c, T_p, T_w) := \frac{\varepsilon \cdot \sigma \cdot (T_w^4 - T_p^4)}{(C_c + C_{ash}) \cdot Cp_{char}} \cdot A_{part.c}(C_{c.0})$$

convection

$$dT_{conv}(C_c, T_p, T_g) := \frac{\frac{Nu \cdot \lambda(T_p, T_g)}{dp_0} \cdot \left[\left(\frac{T_g + T_p}{2}\right) - T_p\right]}{(C_c + C_{ash}) \cdot Cp_{char}} \cdot A_{part.c}(C_{c.0})$$

reaction

$$dT_{gen}(C_c, T_p, T_g) := \frac{-\Delta h}{(C_c + C_{ash}) \cdot Cp_{char}} \cdot (-k_r(T_p, T_g, dp_0) \cdot P_{O2} \cdot A_{part.c}(C_c))$$

estimation of initial particle heating rate at DTF setpoint Temperature of 1400°C :

$$T_{init} := 25 + 273 \quad K \quad dT_{rad}(C_{c.0}, T_{init}, 1416 + 273) + dT_{conv}(C_{c.0}, T_{init}, 1335 + 273) = 1.425 \cdot 10^4 \quad \frac{K}{s}$$

Solution of differential equations

Initial Conditions : combustion extent — $x_0 := C_{c.0}$

particle temperature — $x_1 := 300$ K

Simultaneous Differential Equations :

combustion extent — $\frac{d}{dt} C_c = -k_r(x_1, T_g, dp_0) \cdot P_{O2} \cdot A_{part.c}(x_0)$

particle temperature — $\frac{d}{dt} Tp = dT_{rad}(x_0, x_1, T_w) + dT_{conv}(x_0, x_1, T_g) + dT_{gen}(x_0, x_1, T_g)$

Note on the Solution Methodology

The simultaneous equations are solved by a 4th order Runge Kutta solution algorithm for each DTF setpoint Temperature. An average furnace wall and furnace gas temperature have been specified for each DTF setpoint temperature.

DTF Kinetic Evaluation Results -

Char chemical combustion kinetics Description :

Pre-exponential factor : $\exp(\text{Preexp}) = 1063.044 \quad \frac{kg}{m^2 \cdot s \cdot bar}$

Activation Energy : $-\text{EonR} \cdot \frac{R}{10^3} = 124.90 \quad \frac{kJ}{mol} \quad -\text{EonR} = 15022.456 \quad K$

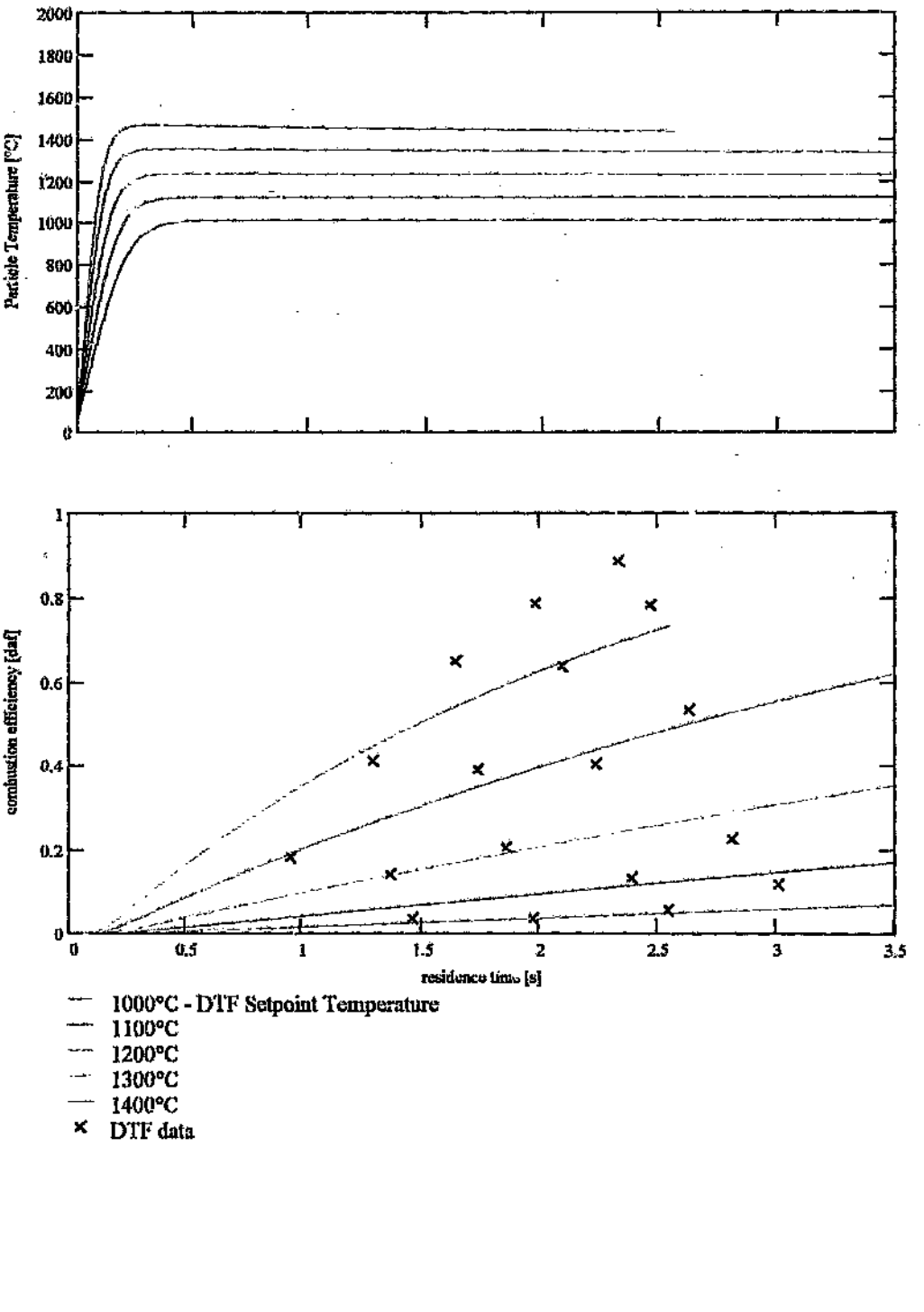

Determination of DTF combustion kinetics for use with AIOLOS combustion code

---

Universal Gas Constant $R := 8.314 \quad \frac{J}{mol \cdot K}$

DTF Operation and Char Description :

Ash in Coal $Ash_{coal} := DTF_{0,8} \cdot \%$

Ash in Char $Ash_{char} := DTF_{0,7} \cdot \%$

Volatile Matter (after DTF devolatilisation) $Vols_{DTF} := 1 - Ash_{coal} - \frac{Ash_{coal}}{Ash_{char}} \cdot (1 - Ash_{char})$

Density of coal : $\rho_{coal} := 1678 \quad \frac{kg}{m^3}$

Density of Char (initially) : (shrinking core assumption) $\rho_{char.o} := (1 - Vols_{DTF}) \cdot \rho_{coal} \quad \rho_{char.o} = 1.087 \cdot 10^3 \quad \frac{kg}{m^3}$

Initial Particle Diameter : $dp_o := DTF_{0,0} \quad m \quad dp_o = 6.48 \cdot 10^{-5} \quad m$

Pressure in DTF : $P := 0.85 \cdot 10^5 \quad Pa$

Volume Oxygen Flowrate into DTF : $V_{O2} := \frac{0.6 \cdot 10^{-3}}{60} \quad \frac{m^3}{s} \quad M_{W.O2} := 32 \cdot 10^{-3} \quad \frac{kg}{mol}$

VolumeNitrogen Flowrate into DTF : $V_{N2} := \frac{19.66 \cdot 10^{-3}}{60} \quad \frac{m^3}{s} \quad M_{W.N2} := 28 \cdot 10^{-3} \quad \frac{kg}{mol}$

Mass Flowrate of Oxygen : $m_{O2} := \frac{V_{O2} \cdot P \cdot M_{W.O2}}{R \cdot 298} \quad \frac{kg}{s}$

Mass Flowrate of Nitrogen : $m_{N2} := \frac{V_{N2} \cdot P \cdot M_{W.N2}}{R \cdot 298} \quad \frac{kg}{s}$

Char Feedrate : $m_{char} := \frac{0.1066 \cdot 10^{-3}}{60} \quad \frac{kg}{s}$

Initial Char Concentration $C_{char.0} := \frac{m_{char}}{m_{char} + m_{O2} + m_{N2}} \quad \frac{kg}{kg_{mix}}$

Initial Fixed Carbon Concentration $C_{c.0} := C_{char.0} \cdot (1 - DTF_{0,7} \cdot \%) \quad C_{c.0} = 2.8942 \cdot 10^{-3} \quad \frac{kg}{kg_{mix}}$

$C_{c.1} := C_{char.0} \cdot (1 - DTF_{13,7} \cdot \%) \quad C_{c.1} = 2.8942 \cdot 10^{-3} \quad \frac{kg}{kg_{mix}}$

Ash Concentration : $C_{ash} := C_{char.0} \cdot (Ash_{char}) \quad C_{ash} = 2.5304 \cdot 10^{-3} \quad \frac{kg}{kg_{mix}}$

Hendrina Washing Plant Feed : <75 µm

Heat Exchange Parameters and constants

Stefan Boltzmann constant $\sigma := 5.67 \cdot 10^{-8}$ $\frac{W}{m^2 \cdot K^4}$

average emissivity between particle and wall $\varepsilon := 0.85$

reaction energy : C to CO : $\Delta h := 9.614 \cdot 10^{6}$ $\frac{J}{kg}$

Nusselt Number for boundary layer convective heatexchange $Nu := 2$

convective heat exchange coefficient $\lambda(T_p, T_g) := 2.43 \cdot 10^{-11} \cdot \left[\frac{\left(\frac{T_p + T_g}{2}\right)}{273}\right]^{0.82}$ $\frac{W}{m \cdot K}$

heat capacity of char : $Cp_{char} = 1250$ $\frac{J}{kg \cdot K}$

Particle Surface Area as a function of combustion extent :

swelling index $n_B := \frac{2}{3}$ 1 - swelling coals
2/3 - 'non swelling' coals

$$A_{part.c}(C_c) := \frac{6}{\rho_{char.o} \cdot dp_o} \cdot C_{c.0} \cdot \left(\frac{C_c}{C_{c.0}}\right)^{n_B} \qquad \frac{m^2}{kg_{mix}}$$

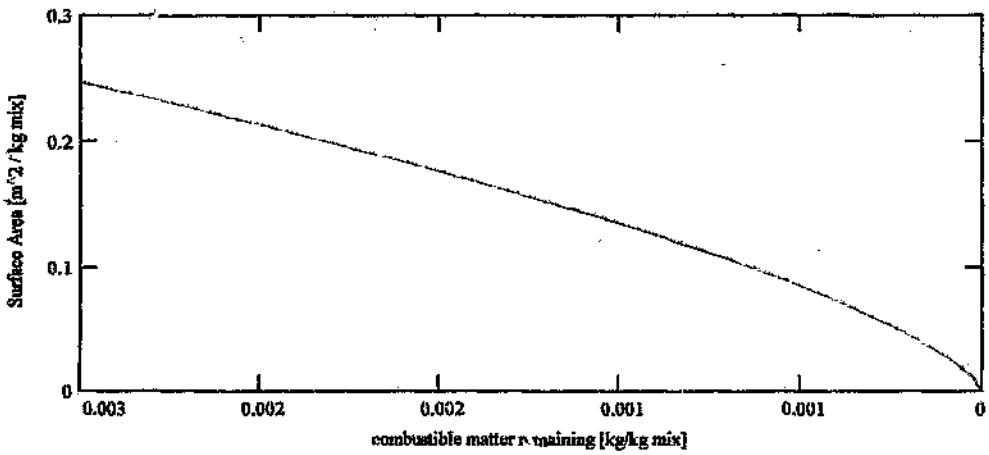

Partial Pressure of Oxygen in DTF : $P_{O2} := \frac{V_{O2}}{V_{O2} + V_{N2}}$ $P_{O2} = 0.03$ bar

Function defining mass of combustible matter remaining as a function ash content in the sampled residue

$$C_c(ash_{residue}) := \left[\frac{Ash_{char} \cdot \left(1 - \left(\frac{ash_{residue}}{100}\right)\right)}{1 - Ash_{char} \cdot \left(\frac{ash_{residue}}{100}\right)}\right] \cdot C_{c.0}$$

$ash_{residue}$ in % by mass

Calculating Overall Rate :

$$k_{o_k} = \frac{\int_{C_c(DTF_{k,7})}^{C_c(DTF_{k,4})} \frac{1}{A_{part.c}(C_c)}\, dC_c}{P_{O2} \cdot DTF_{k,3}}$$

Calculating Particle Temperature:

Iterative solution of Energy Balance between particle, hot gas and reactor wall :

$$\frac{\Delta h \cdot C_c(Ash_{res}) - C_{c.0}}{t_r} = \left[\varepsilon\sigma\cdot\left(T_w^{\,4} - T_p^{\,4}\right) - \frac{Nu\cdot\lambda(T_p, T_g)}{dp}\cdot\left[\left(\frac{T_g + T_p}{2}\right) - T_g\right]\right]\cdot A_{part.c}(C_{c.0})$$

$$T_{particle}(Ash_{res}, t_r, T_w, T_g, dp) := find(T_p)$$

$$DTF_{k,6} := T_{particle}(DTF_{k,4}, DTF_{k,3}, DTF_{k,2} + 273, DTF_{k,5} + 273, DTF_{k,0}) - 273$$

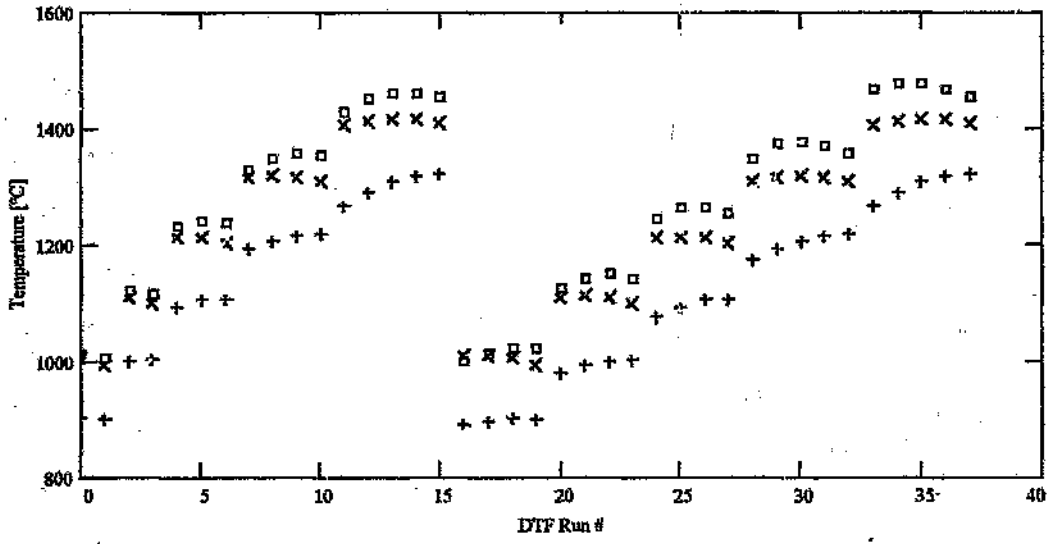

Oxygen Diffusion reaction rate as a function particle Temperature

O2 diffusion constant at 1600K : $D_{O2.1600K} := 3.39\cdot10^{-4}\ \frac{m^2}{s}$

mechanism factor : $\phi := 2$ ϕ = 2 for CO, and 1 for CO2

$$k_{d.char}(Tp, Tg, dp) := \frac{24\cdot\phi\cdot D_{O2.1600K}\cdot\left[\frac{(Tg + Tp)\cdot 0.5}{1600}\right]^{1.75}}{R\cdot10^{5}\cdot dp\cdot Tg} \quad \frac{kg}{m^2\cdot s\cdot bar}$$

Source : AIOLOS - combustion model

Hendrina Washing Plant Feed : <75 µm

Determining the Chemical Reaction Rate from the experimental data :

$$kr_k := \left[\frac{1}{\left(\frac{1}{k_{o_k}}\right) - \frac{1}{k_{d.char}(DTF_{k,6} + 273, DTF_{k,5} + 273, DTF_{k,0})}} \right]$$

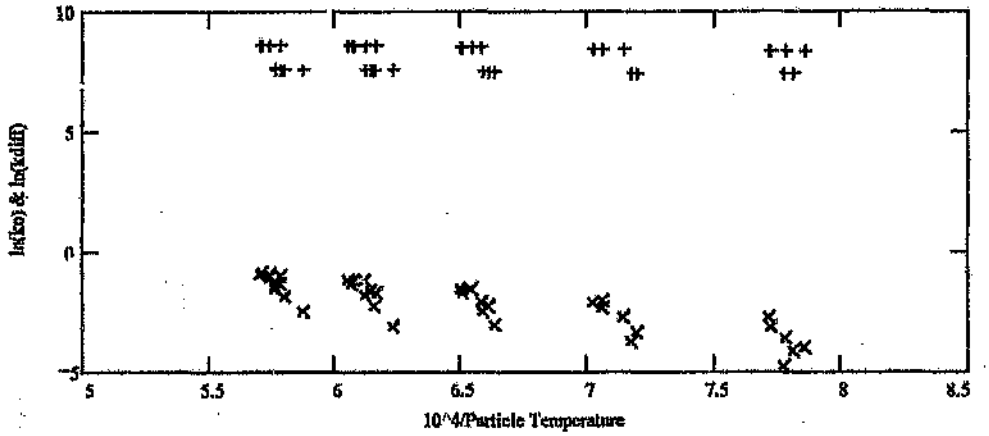

NB : if the +'s lie beneath the x's, the overall reaction rate could be diffusion controlled

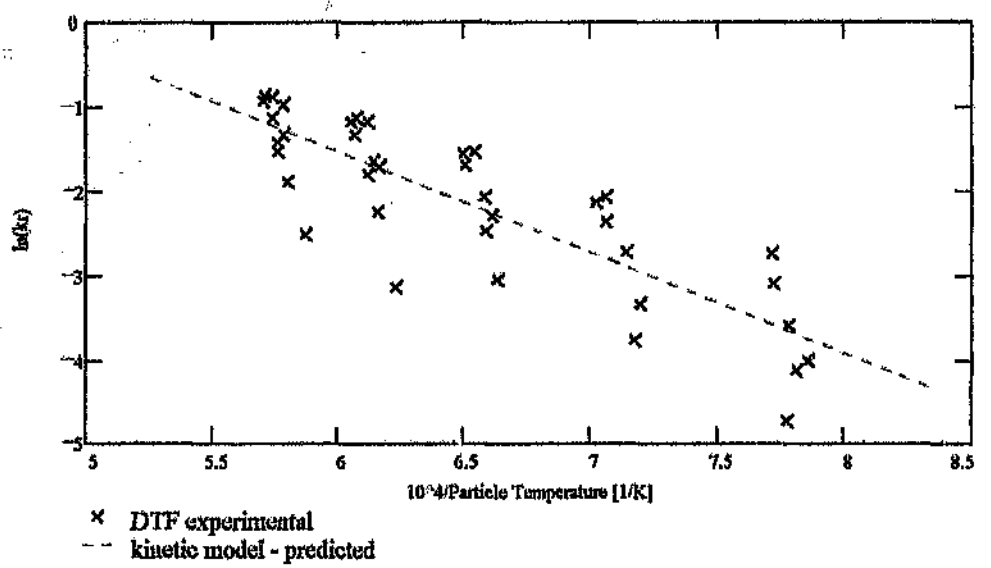

Char chemical combustion kinetics Description :

Pre-exponential factor : $\exp(Preexp) = 282.185$ $\frac{kg}{m^2 \cdot s \cdot bar}$

Activation Energy : $-EonR \cdot \frac{R}{10^3} = 99.446$ $\frac{kJ}{mol}$

$-EonR = 11961.304$ K

Function describing chemical reaction rate : $k_{r.char}(Tp) := k_{rch.o} \cdot \exp\left(\frac{EonR}{Tp}\right)$

Hendrina Washing Plant Feed : <75 µm

Defining the overall reaction rate function :

$$k_r(Tp, Tg, dp) := \frac{1}{\left(\frac{1}{k_{r.char}(Tp)} + \frac{1}{k_{d.char}(Tp, Tg, dp)}\right)}$$

Equation describing all modes of heat transfer (shrinking core assumption)

radiation

$$dT_{rad}(C_c, T_p, T_w, dp) := \frac{\varepsilon \cdot \sigma \cdot \left(T_w^4 - T_p^4\right)}{(C_c + C_{ash}) \cdot Cp_{char}} \cdot \text{if}\left(dp > 38 \cdot 10^{-6}, A_{part.c}(C_{c.1}), A_{part.c}(C_{c.0})\right)$$

convection

$$dT_{conv}(C_c, T_p, T_g, dp) := \frac{\frac{Nu \cdot k(T_p, T_g)}{dp} \cdot \left[\left(\frac{T_g + T_p}{2}\right) - T_g\right]}{(C_c + C_{ash}) \cdot Cp_{char}} \cdot A_{part.c}(C_{c.0})$$

reaction

$$dT_{gen}(C_c, T_p, T_g, dp) := \frac{-\Delta h}{(C_c + C_{ash}) \cdot Cp_{char}} \cdot \left(-k_r(T_p, T_g, dp) \cdot P_{O2} \cdot A_{part.c}(C_c)\right)$$

estimation of initial particle heating rate at DTF setpoint Temperature of 1400°C :

$$dT_{rad}\left(C_{c.0}, 298, DTF_{s_5,2} + 273, DTF_{s_5,0}\right) + dT_{conv}\left(C_{c.0}, 298, DTF_{s_5,5} + 273, DTF_{s_5,0}\right) = 1.401 \cdot 10^4 \frac{K}{s}$$

Solution of differential equations

Initial Conditions : combustion extent — $x_0 := C_c(DTF_{0,7})$

particle temperature — $x_1 := 300 \quad K$

Simultaneous Differential Equations :

combustion extent — $\frac{d}{dt} C_c = -k_r(x_1, T_g, dp_{initial}) \cdot P_{O2} \cdot A_{part.c}(x_0)$

particle temperature — $\frac{d}{dt} Tp = dT_{rad}(x_0, x_1, T_w) + dT_{conv}(x_0, x_1, T_g) + dT_{gen}(x_0, x_1, T_g)$

Note on the Solution Methodology

The simultaneous equations are solved by a 4th order Runge Kutta solution algorithm for each DTF setpoint Temperature. An average furnace wall and furnace gas temperature have been specified for each DTF setpoint temperature.

Appendix 2.3

Particle Size Distributions
for
HENDRINA UNIT 9

from
31 January 1996
to
7 February 1996

The particle size analysis results presented herein are indexed as follows :

Unit Number Mill PF Pipe
Sampling Date

eg.

9 B P1 - 4
31/01/96

refers to Herdrina Unit 9, Mill B, PF Pipes 1 to 4, sampled on 31 January 1996

PF SAMPLES :Run Number 6

9 B P1 - 4
31/01/96

Sample File Name: GENWATER, Record: 38 Source: Analysed
Measured on: Mon, Apr 01, 1996 7:45AM Last saved on: Mon, Apr 01, 1996 7:46AM

Presentation: 2$$D
Very Polydisperse model

Volume Result

Focus = 300 mm.

Residual = 0.172 %
d (0.5) = 40.62 µm
D [4, 3] = 54.18 µm
Sauter Mean (D[3,2]) = 15.92 µm
Specific Surface Area = 0.3768 sq. m. / gm

Concentration = 0.064 %
d (0.1) = 6.89 µm
Span = 2.68

Obscuration = 24.96 %
d (0.9) = 116.30 µm

Mode = 61.45 µm
Density = 1.00 gm. / c.c.

Size (Lo) µm	Result In %	Size (Hi) µm	Result Below %
0.50	0.50	1.32	0.50
1.32	0.41	1.60	0.91
1.60	0.42	1.95	1.33
1.95	0.59	2.38	1.92
2.38	0.82	2.90	2.74
2.90	1.09	3.53	3.84
3.53	1.42	4.30	5.26
4.30	1.76	5.24	7.02
5.24	2.10	6.39	9.12
6.39	2.41	7.78	11.53
7.78	2.74	9.48	14.27
9.48	3.10	11.55	17.37
11.55	3.53	14.08	20.90
14.08	4.03	17.15	24.93
17.15	4.59	20.90	29.52
20.90	5.20	25.46	34.72

Size (Lo) µm	Result In %	Size (Hi) µm	Result Below %
25.46	5.86	31.01	40.58
31.01	6.62	37.79	47.20
37.79	7.39	46.03	54.59
46.03	8.13	56.09	62.72
56.09	8.37	68.33	71.09
68.33	8.01	83.26	79.11
83.26	6.91	101.44	86.01
101.44	5.51	123.59	91.52
123.59	3.75	150.57	95.27
150.57	2.26	183.44	97.52
183.44	1.21	223.51	98.73
223.51	0.64	272.31	99.37
272.31	0.33	331.77	99.71
331.77	0.17	404.21	99.88
404.21	0.08	492.47	99.96
492.47	0.04	600.00	100.00

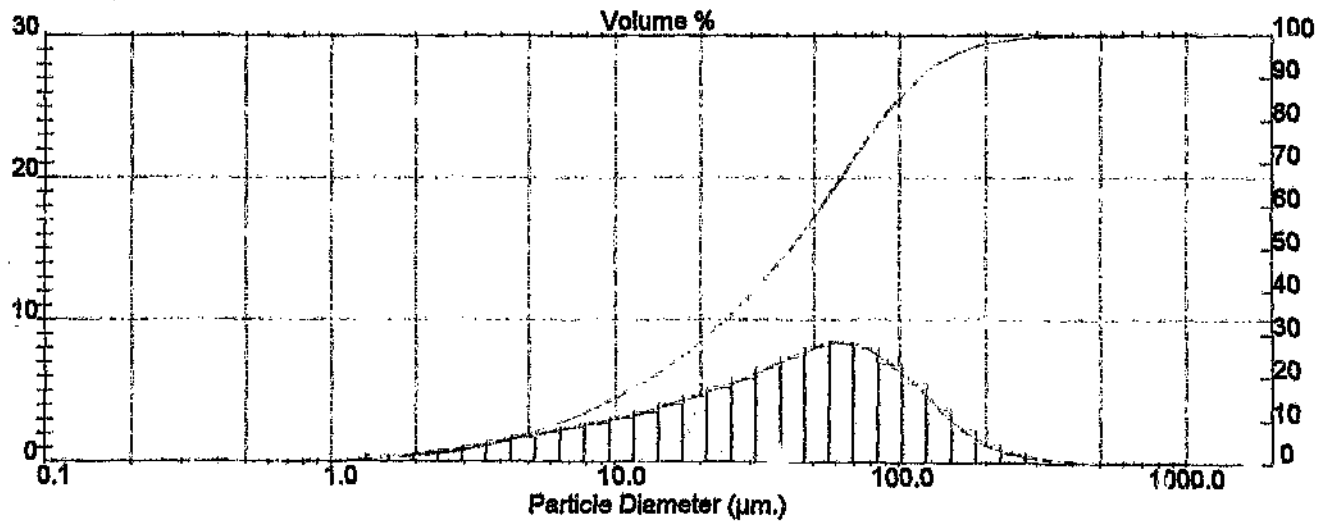

MALVERN MASTERSIZER X

Version 1.2b

Tue, Apr 02, 1996 10:07AM

PF SAMPLES :Run Number 7

9 D P1 - 4
31/01/96

Sample File Name: GENWATER, Record: 39
Measured on: Mon, Apr 01, 1996 9:04AM Last saved on: Mon, Apr 01, 1996 9:05AM

Source: Analysed

Presentation: 2$D
Very Polydisperse model

Volume Result

Focus = 300 mm.

Residual = 0.236 %
d (0.5) = 35.40 µm
D [4, 3] = 56.24 µm
Sauter Mean (D[3,2]) = 13.83 µm
Specific Surface Area = 0.4338 sq. m. / gm

Concentration = 0.052 %
d (0.1) = 5.76 µm
Span = 3.07

Obscuration = 23.74 %
d (0.9) = 126.92 µm

Mode = 70.26 µm
Density = 1.00 gm. / c.c.

Size (Lo) µm	Result In %	Size (Hi) µm	Result Below %
0.50	0.71	1.32	0.71
1.32	0.57	1.60	1.28
1.60	0.58	1.95	1.86
1.95	0.80	2.38	2.66
2.38	1.06	2.90	3.72
2.90	1.36	3.53	5.09
3.53	1.71	4.30	6.80
4.30	2.08	5.24	8.88
5.24	2.45	6.39	11.32
6.39	2.78	7.78	14.11
7.78	3.10	9.48	17.20
9.48	3.40	11.55	20.61
11.55	3.73	14.08	24.34
14.08	4.09	17.15	28.43
17.15	4.45	20.90	32.88
20.90	4.82	25.46	37.70

Size (Lo) µm	Result In %	Size (Hi) µm	Result Below %
25.46	5.23	31.01	42.93
31.01	5.78	37.79	48.71
37.79	6.34	46.03	55.05
46.03	7.02	56.09	62.07
56.09	7.36	68.33	69.43
68.33	7.37	83.26	76.80
83.26	6.72	101.44	83.53
101.44	5.80	123.59	89.32
123.59	4.30	150.57	93.62
150.57	2.86	183.44	96.48
183.44	1.67	223.51	98.15
223.51	0.94	272.31	99.09
272.31	0.50	331.77	99.59
331.77	0.25	404.21	99.84
404.21	0.11	492.47	99.95
492.47	0.05	600.00	100.00

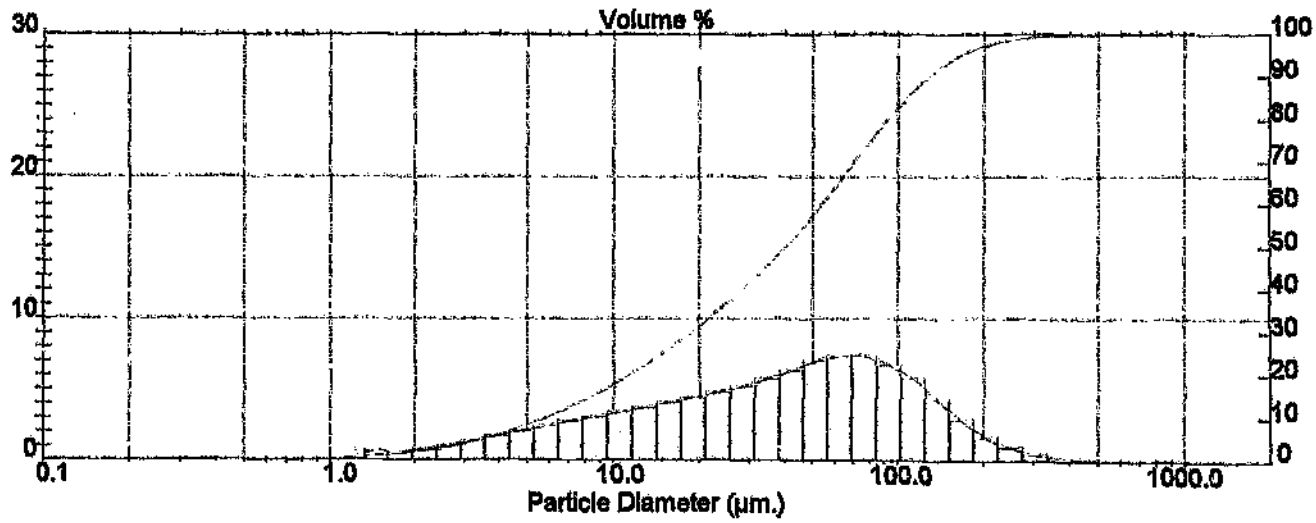

MASTERSIZER X

Version 1.2b

Tue, Apr 02, 1996 10:09AM

PF SAMPLES :Run Number 8

9 E P 1 - 4
31/01/96

Sample File Name: GENWATER, Record: 40 Source: Analysed
Measured on: Mon, Apr 01, 1996 9:08AM Last saved on: Mon, Apr 01, 1996 9:09AM

Preservation: 2$$D
Very Polydisperse model

Volume Result

Focus = 300 mm.

Residual = 0.297 %
d (0.5) = 61.47 µm
D [4, 3] = 74.04 µm
Sauter Mean (D[3,2]) = 21.64 µm
Specific Surface Area = 0.2772 sq. m. / gm

Concentration = 0.094 %
d (0.1) = 10.43 µm
Span = 2.24

Obscuration = 26.74 %
d (0.9) = 148.03 µm

Mode = 79.07 µm
Density = 1.00 gm. / c.c.

Size (Lo) µm	Result In %	Size (Hi) µm	Result Below %
0.50	0.41	1.32	0.41
1.32	0.32	1.60	0.73
1.60	0.32	1.95	1.05
1.95	0.43	2.38	1.48
2.38	0.56	2.90	2.04
2.90	0.71	3.53	2.75
3.53	0.88	4.30	3.63
4.30	1.06	5.24	4.69
5.24	1.26	6.39	5.95
6.39	1.47	7.78	7.41
7.78	1.68	9.48	9.10
9.48	1.94	11.55	11.04
11.55	2.24	14.08	13.28
14.08	2.61	17.15	15.89
17.15	3.04	20.90	18.93
20.90	3.58	25.46	22.51
25.46	4.23	31.01	26.75
31.01	5.16	37.79	31.91
37.79	6.27	46.03	38.17
46.03	7.77	56.09	45.94
56.09	9.09	68.33	55.02
68.33	10.05	83.26	65.07
83.26	9.85	101.44	74.92
101.44	8.90	123.59	83.83
123.59	6.64	150.57	90.47
150.57	4.32	183.44	94.79
183.44	2.44	223.51	97.23
223.51	1.36	272.31	98.59
272.31	0.73	331.77	99.32
331.77	0.39	404.21	99.72
404.21	0.19	492.47	99.91
492.47	0.09	600.00	100.00

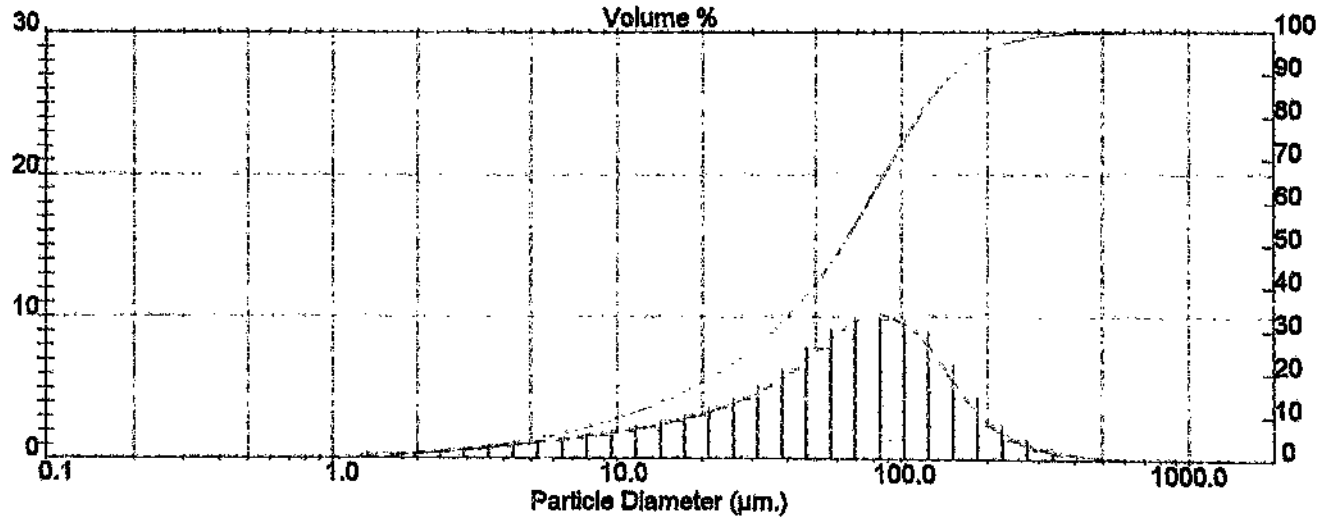

PF SAMPLES :Run Number 9

9 F P1 - 4
31/01/96

Sample File Name: GENWATER, Record: 41 Source: Analysed
Measured on: Mon, Apr 01, 1996 9:13AM Last saved on: Mon, Apr 01, 1996 9:15AM

Presentation: 2$$D
Very Polydisperse model

Volume Result

Focus = 300 mm.

Residual = 0.247 %
d (0.5) = 43.93 µm
D [4, 3] = 59.62 µm
Sauter Mean (D[3,2]) = 13.88 µm
Specific Surface Area = 0.4323 sq. m. / gm

Concentration = 0.057 %
d (0.1) = 5.79 µm
Span = 2.87

Obscuration = 25.67 %
d (0.9) = 131.73 µm

Mode = 75.64 µm
Density = 1.00 gm. / c.c.

Size (Lo) µm	Result In %	Size (Hi) µm	Result Below %
0.50	0.80	1.32	0.80
1.32	0.63	1.60	1.43
1.60	0.63	1.95	2.06
1.95	0.84	2.38	2.89
2.38	1.08	2.90	3.97
2.90	1.33	3.53	5.30
3.53	1.63	4.30	6.93
4.30	1.95	5.24	8.88
5.24	2.32	6.39	11.19
6.39	2.66	7.78	13.86
7.78	2.96	9.48	16.82
9.48	3.24	11.55	20.06
11.55	3.51	14.08	23.58
14.08	3.78	17.15	27.36
17.15	4.05	20.90	31.41
20.90	4.34	25.46	35.74

Size (Lo) µm	Result In %	Size (Hi) µm	Result Below %
25.46	4.68	31.01	40.42
31.01	5.20	37.79	45.63
37.79	5.87	46.03	51.49
46.03	6.81	56.09	58.30
56.09	7.57	68.33	65.87
68.33	8.02	83.26	73.90
83.26	7.61	101.44	81.51
101.44	6.69	123.59	88.20
123.59	4.90	150.57	93.10
150.57	3.16	183.44	96.26
183.44	1.78	223.51	98.03
223.51	0.99	272.31	99.02
272.31	0.52	331.77	99.55
331.77	0.27	404.21	99.82
404.21	0.13	492.47	99.94
492.47	0.06	600.00	100.00

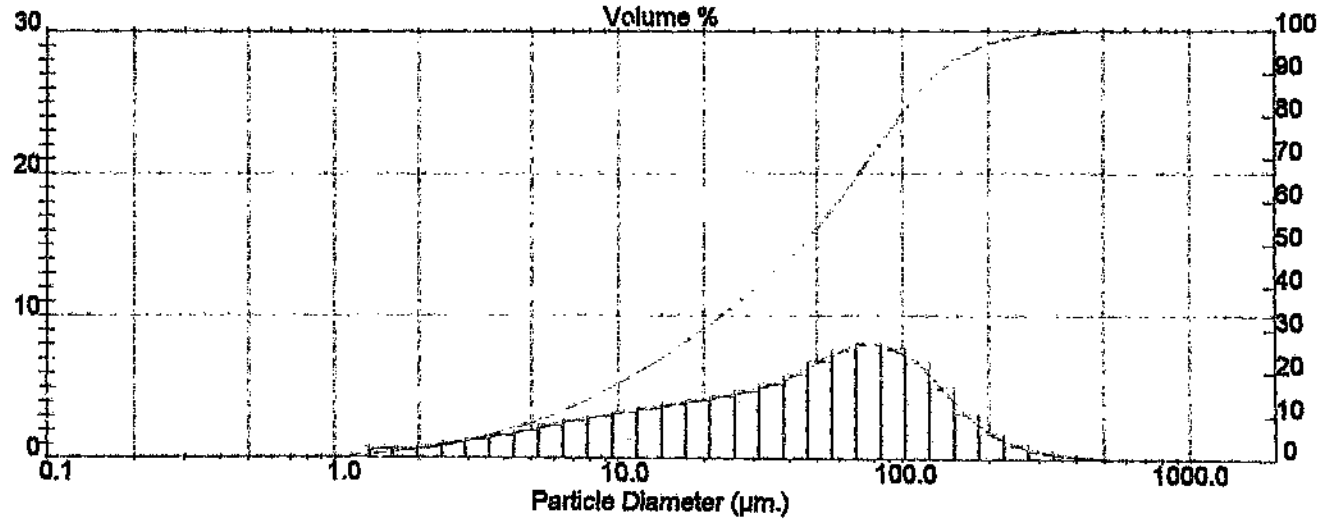

PF SAMPLES :Run Number 10

9AP1 - 4
31/01/96

Sample File Name: GENWATER, Record: 42 Source: Analysed
Measured on: Mon, Apr 01, 1996 9:17AM Last saved on: Mon, Apr 01, 1996 9:18AM

Presentation: 2$$D
Very Polydisperse model

Volume Result

Focus = 300 mm.

Residual = 0.397 %
d (0.5) = 24.77 µm
D [4, 3] = 37.22 µm
Sauter Mean (D[3,2]) = 10.15 µm
Specific Surface Area = 0.5910 sq. m. / gm

Concentration = 0.043 %
d (0.1) = 4.31 µm
Span = 3.42

Obscuration = 26.34 %
d (0.9) = 87.21 µm

Mode = 46.67 µm
Density = 1.00 gm. / c.c.

Size (Lo) µm	Result In %	Size (Hi) µm	Result Below %
0.50	1.13	1.32	1.13
1.32	0.89	1.60	2.02
1.60	0.89	1.95	2.90
1.95	1.19	2.38	4.10
2.38	1.55	2.90	5.64
2.90	1.94	3.53	7.58
3.53	2.38	4.30	9.96
4.30	2.88	5.24	12.84
5.24	3.42	6.39	16.26
6.39	3.93	7.78	20.20
7.78	4.35	9.48	24.54
9.48	4.71	11.55	29.26
11.55	5.06	14.06	34.32
14.06	5.42	17.15	39.74
17.15	5.73	20.90	45.47
20.90	6.03	25.46	51.49

Size (Lo) µm	Result In %	Size (Hi) µm	Result Below %
25.46	6.27	31.01	57.77
31.01	6.54	37.79	64.31
37.79	6.63	46.03	70.94
46.03	6.59	56.09	77.53
56.09	6.09	68.33	83.62
68.33	5.30	83.26	88.92
83.26	4.16	101.44	93.08
101.44	3.05	123.59	96.13
123.59	1.93	150.57	98.06
150.57	1.08	183.44	99.14
183.44	0.52	223.51	99.66
223.51	0.23	272.31	99.89
272.31	0.08	331.77	99.97
331.77	0.02	404.21	100.00
404.21	0.00	492.47	100.00
492.47	0.00	600.00	100.00

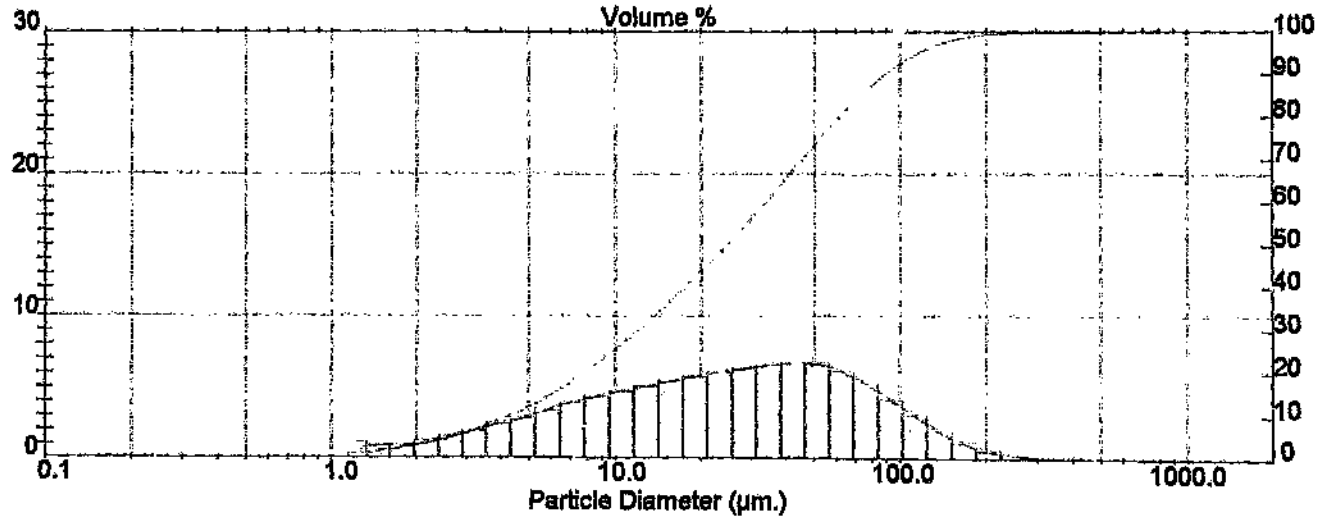

PF SAMPLES :Run Number 10

9 A P1 - 4 GRAP
02/02/96

Sample File Name: GENWATER, Record: 43 Source: Analysed
Measured on: Tue, Apr 02, 1996 7:19AM Last saved on: Tue, Apr 02, 1996 7:20AM

Presentation: 2$$D
Very Polydisperse model

Volume Result

Focus = 300 mm.

Residual = 0.136 %
d (0.5) = 76.64 µm
D [4, 3] = 88.56 µm
Sauter Mean (D[3,2]) = 29.59 µm
Specific Surface Area = 0.2028 sq. m. / gm

Concentration = 0.109 %
d (0.1) = 15.24 µm
Span = 2.01

Obscuration = 23.21 %
d (0.9) = 169.56 µm

Mode = 105.60 µm
Density = 1.00 gm. / c.c.

Size (Lo) µm	Result In %	Size (Hi) µm	Result Below %
0.50	0.21	1.32	0.21
1.32	0.17	1.60	0.38
1.60	0.17	1.95	0.55
1.95	0.24	2.38	0.80
2.38	0.33	2.90	1.13
2.90	0.44	3.53	1.57
3.53	0.57	4.30	2.14
4.30	0.71	5.24	2.85
5.24	0.87	6.39	3.71
6.39	1.03	7.78	4.75
7.78	1.24	9.48	5.98
9.48	1.47	11.55	7.46
11.55	1.75	14.08	9.21
14.08	2.06	17.15	11.29
17.15	2.47	20.90	13.76
20.90	2.90	25.46	16.66

Size (Lo) µm	Result In %	Size (Hi) µm	Result Below %
25.46	3.43	31.01	20.09
31.01	4.18	37.79	24.27
37.79	5.22	46.03	29.50
46.03	6.64	56.09	36.14
56.09	8.27	68.33	44.41
68.33	9.92	83.26	54.33
83.26	11.02	101.44	65.35
101.44	11.21	123.59	76.56
123.59	9.25	150.57	85.81
150.57	6.37	183.44	92.19
183.44	3.68	223.51	95.87
223.51	2.02	272.31	97.90
272.31	1.08	331.77	98.97
331.77	0.58	404.21	99.55
404.21	0.30	492.47	99.85
492.47	0.15	600.00	100.00

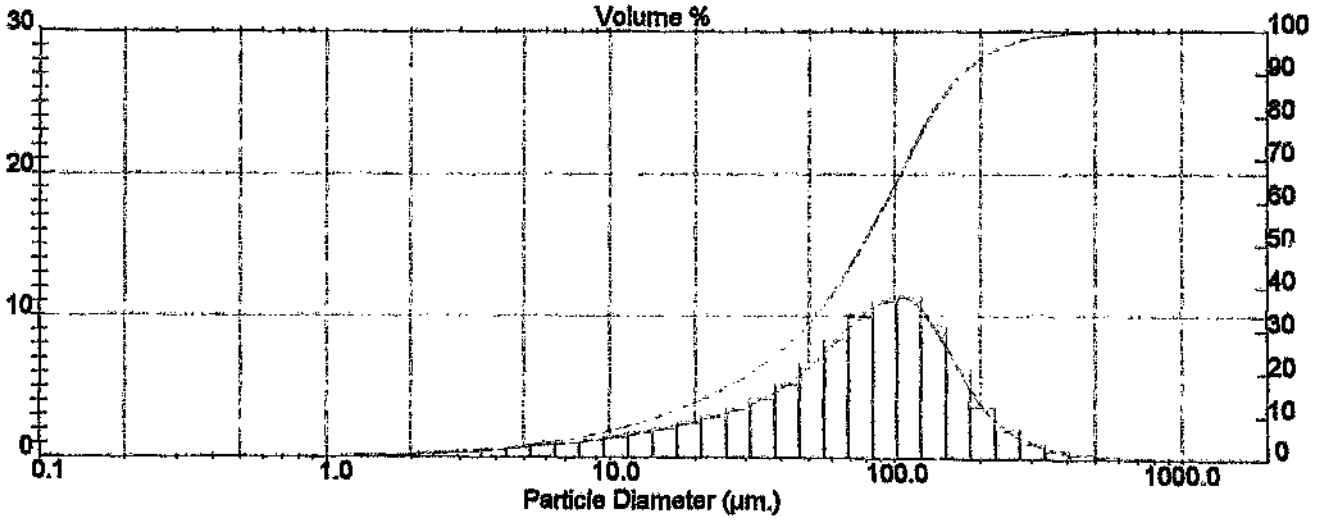

PF SAMPLES :Run Number 11

9 B P1 - 4
02/02/96

Sample File Name: GENWATER, Record: 44
Measured on: Tue, Apr 02, 1996 7:23AM Last saved on: Tue, Apr 02, 1996 7:24AM

Source: Analysed

Presentation: 2$$D
Very Polydisperse model

Volume Result

Residual = 0.302 %
D [3, 2] = 15.24 µm
D [4, 3] = 29.13 µm
Sauter Mean (D[3,2]) = 8.84 µm
Specific Surface Area = 0.6785 sq. m. / gm

Concentration = 0.040 %
d (0.1) = 3.87 µm
Span = 3.54

Focus = 300 mm.

Obscuration = 27.77 %
d (0.9) = 68.47 µm

Mode = 20.06 µm
Density = 1.00 gm. / c.c.

Size (Lo) µm	Result In %	Size (Hi) µm	Result Below %
0.50	1.30	1.32	1.30
1.32	1.02	1.60	2.33
1.60	1.02	1.95	3.35
1.95	1.37	2.38	4.72
2.38	1.79	2.90	6.51
2.90	2.25	3.53	8.76
3.53	2.78	4.30	11.54
4.30	3.39	5.24	14.93
5.24	4.09	6.39	19.02
6.39	4.78	7.78	23.80
7.78	5.37	9.48	29.16
9.48	5.87	11.55	35.03
11.55	6.28	14.08	41.31
14.08	6.59	17.15	47.90
17.15	6.75	20.90	54.65
20.90	6.71	25.46	61.36

Size (Lo) µm	Result In %	Size (Hi) µm	Result Below %
25.46	6.54	31.01	67.90
31.01	6.29	37.79	74.18
37.79	5.90	46.03	80.08
46.03	5.34	56.09	85.42
56.09	4.53	68.33	89.96
68.33	3.60	83.26	93.56
83.26	2.64	101.44	96.20
101.44	1.79	123.59	97.99
123.59	1.07	150.57	99.06
150.57	0.56	183.44	99.61
183.44	0.25	223.51	99.86
223.51	0.10	272.31	99.96
272.31	0.03	331.77	99.99
331.77	0.01	404.21	100.00
404.21	0.00	492.47	100.00
492.47	0.00	600.00	100.00

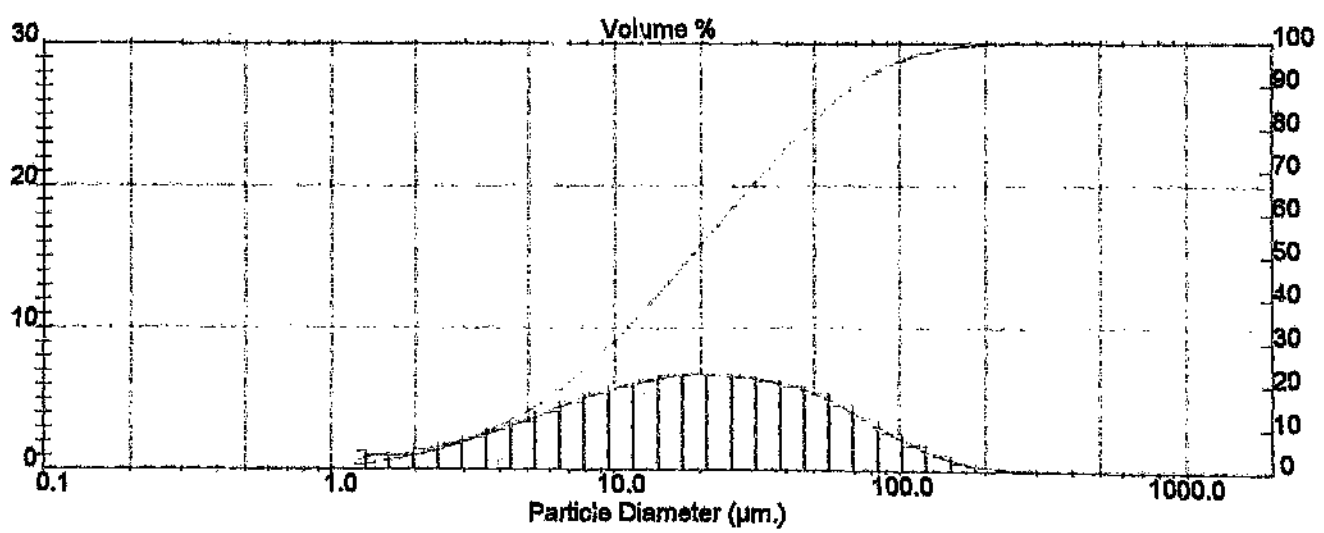

PF SAMPLES :Run Number 12

9 B P1 - 4 GRAP
02/02/96

Sample File Name: GENWATER, Record: 45 Source: Analysed
Measured on: Tue, Apr 02, 1996 7:28AM Last saved on: Tue, Apr 02, 1996 7:29AM

Presentation: 2$$D
Very Polydisperse model

Volume Result

Focus = 300 mm.

Residual = 0.167 %
d (0.5) = 55.65 µm
D [4, 3] = 97.46 µm
Sauter Mean (D[3,2]) = 35.70 µm
Specific Surface Area = 0.1681 sq. m. / gm

Concentration = 0.136 %
d (0.1) = 24.89 µm
Span = 1.85

Obscuration = 24.03 %
d (0.9) = 179.44 µm

Mode = 101.50 µm
Density = 1.00 gm. / c.c.

Size (Lo) µm	Result In %	Size (Hi) µm	Result Below %
0.50	0.27	1.32	0.27
1.32	0.20	1.60	0.47
1.60	0.19	1.95	0.66
1.95	0.22	2.38	0.88
2.38	0.25	2.90	1.14
2.90	0.28	3.53	1.42
3.53	0.31	4.30	1.72
4.30	0.35	5.24	2.07
5.24	0.41	6.39	2.48
6.39	0.50	7.78	2.99
7.78	0.61	9.48	3.60
9.48	0.76	11.55	4.36
11.55	0.96	14.08	5.33
14.08	1.24	17.15	6.57
17.15	1.61	20.90	8.17
20.90	2.10	25.46	10.27

Size (Lo) µm	Result In %	Size (Hi) µm	Result Below %
25.46	2.77	31.01	13.05
31.01	3.77	37.79	16.82
37.79	5.17	46.03	21.99
46.03	7.11	56.09	29.09
56.09	9.30	68.33	38.39
68.33	11.32	83.26	49.71
83.26	12.31	101.44	62.03
101.44	12.07	123.59	74.09
123.59	9.76	150.57	83.85
150.57	6.76	183.44	90.62
183.44	4.10	223.51	94.72
223.51	2.42	272.31	97.14
272.31	1.39	331.77	98.53
331.77	0.80	404.21	99.33
404.21	0.44	492.47	99.77
492.47	0.23	600.00	100.00

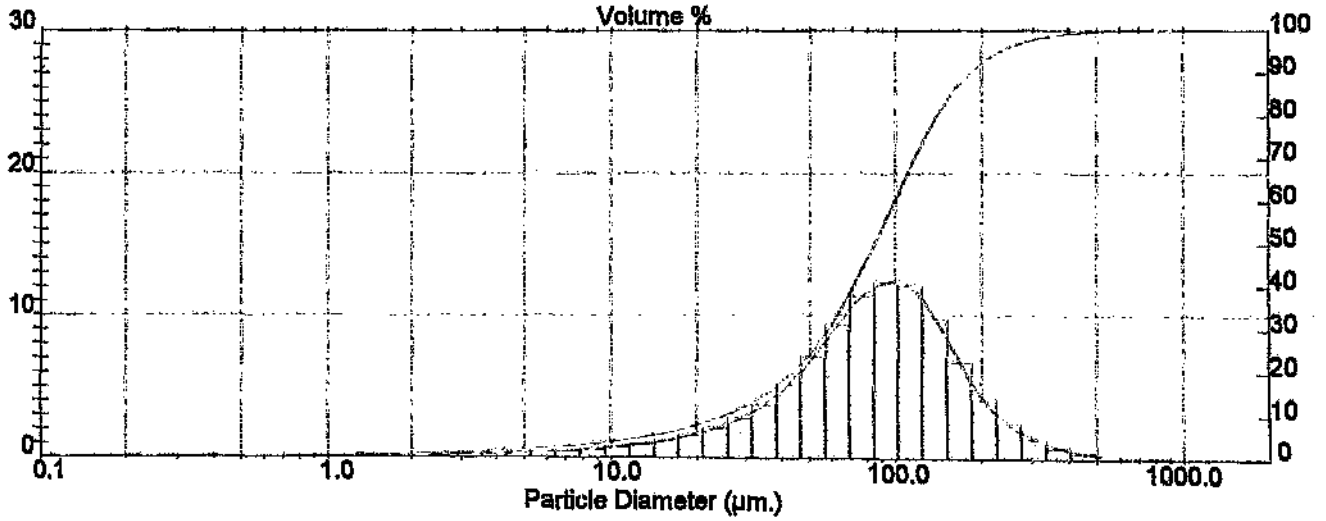

MALVERN MASTERSIZER X

Version 1.2b Tue, Apr 02, 1996 10:24AM

PF SAMPLES :Run Number 13

9 D P1 - 4
02/02/96

Sample File Name: GENWATER, Record: 46 Source: Analysed
Measured on: Tue, Apr 02, 1996 7:31AM Last saved on: Tue, Apr 02, 1996 7:33AM

Presentation: 2$$D
Very Polydisperse model

Volume Result

Focus = 300 mm.

Residual = 0.352 %
d (0.5) = 25.12 µm
D [4, 3] = 36.20 µm
Sauter Mean (D[3,2]) = 10.49 µm
Specific Surface Area = 0.5719 sq. m. / gm

Concentration = 0.041 %
d (0.1) = 4.50 µm
Span = 2.88

Obscuration = 24.38 %
d (0.9) = 79.84 µm

Mode = 37.09 µm
Density = 1.00 gm. / c.c.

Size (Lo) µm	Result In %	Size (Hi) µm	Result Below %
0.50	1.24	1.32	1.24
1.32	0.95	1.60	2.19
1.60	0.94	1.95	3.13
1.95	1.19	2.38	4.32
2.38	1.46	2.90	5.77
2.90	1.72	3.53	7.49
3.53	2.00	4.30	9.49
4.30	2.31	5.24	11.80
5.24	2.71	6.39	14.51
6.39	3.15	7.78	17.66
7.78	3.59	9.48	21.25
9.48	4.13	11.55	25.38
11.55	4.76	14.06	30.15
14.06	5.53	17.15	35.69
17.15	6.32	20.90	42.01
20.90	7.04	25.46	49.05

Size (Lo) µm	Result In %	Size (Hi) µm	Result Below %
25.46	7.60	31.01	56.64
31.01	7.96	37.79	64.60
37.79	7.88	46.03	72.48
46.03	7.32	56.09	79.80
56.09	6.22	68.33	86.02
68.33	4.91	83.26	90.93
83.26	3.58	101.44	94.51
101.44	2.47	123.59	96.98
123.59	1.52	150.57	98.51
150.57	0.84	183.44	99.35
183.44	0.40	223.51	99.75
223.51	0.17	272.31	99.92
272.31	0.06	331.77	99.98
331.77	0.02	404.21	100.00
404.21	0.00	492.47	100.00
492.47	0.00	600.00	100.00

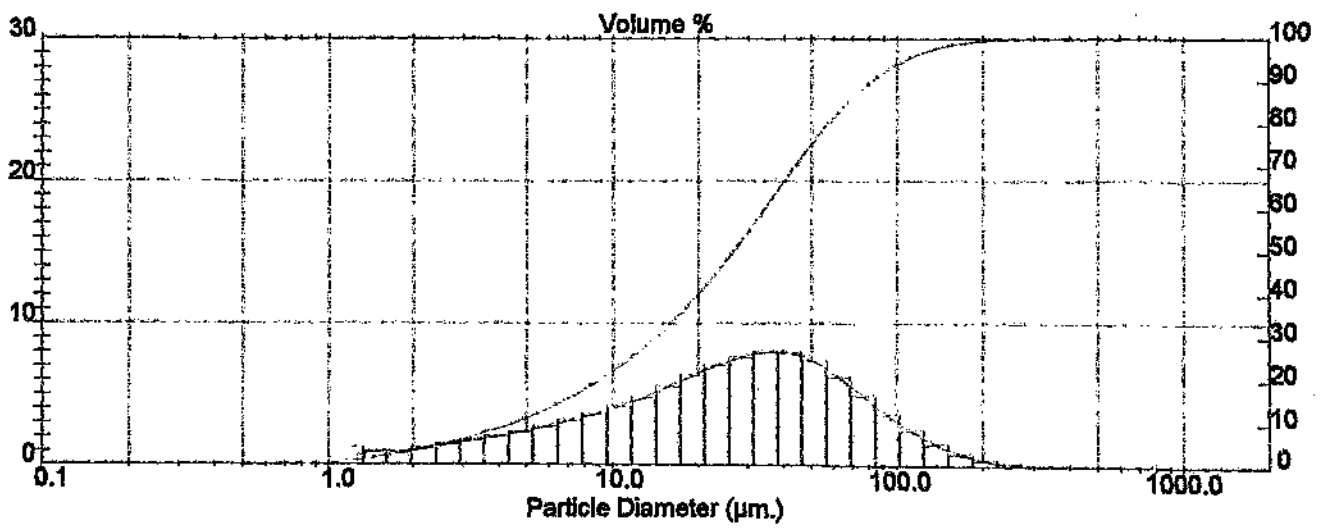

PF SAMPLES :Run Number 14

9 A P1 - 4
02/02/96

Sample File Name: GENWATER, Record: 47 Source: Analysed
Measured on: Tue, Apr 02, 1996 7:36AM Last saved on: Tue, Apr 02, 1996 7:37AM

Presentation: 2$$D
Very Polydisperse model

Volume Result

Focus = 300 mm.

Residual = 0.150 %
d (0.5) = 38.80 µm
D [4, 3] = 47.39 µm
Sauter Mean (D[3,2]) = 13.83 µm
Specific Surface Area = 0.4337 sq. m. / gm

Concentration = 0.062 %
d (0.1) = 5.85 µm
Span = 3.03

Obscuration = 27.57 %
d (0.9) = 106.65 µm

Mode = 58.57 µm
Density = 1.00 gm. / c.c.

Size (Lo) µm	Result In %	Size (Hi) µm	Result Below %
0.50	0.53	1.32	0.53
1.32	0.44	1.60	0.97
1.60	0.45	1.95	1.43
1.95	0.67	2.38	2.10
2.38	0.97	2.90	3.07
2.90	1.34	3.53	4.40
3.53	1.80	4.30	6.21
4.30	2.30	5.24	8.51
5.24	2.77	6.39	11.28
6.39	3.20	7.78	14.48
7.78	3.66	9.48	18.13
9.48	4.06	11.55	22.19
11.55	4.43	14.08	26.62
14.08	4.80	17.15	31.42
17.15	5.13	20.90	36.55
20.90	5.45	25.46	42.00

Size (Lo) µm	Result In %	Size (Hi) µm	Result Below %
25.46	5.80	31.01	47.80
31.01	6.28	37.79	54.09
37.79	6.82	46.03	60.90
46.03	7.32	56.09	68.22
56.09	7.41	68.33	75.62
68.33	7.01	83.26	82.64
83.26	6.03	101.44	88.66
101.44	4.73	123.59	93.40
123.59	3.12	150.57	96.52
150.57	1.79	183.44	98.31
183.44	0.89	223.51	99.20
223.51	0.43	272.31	99.63
272.31	0.20	331.77	99.83
331.77	0.10	404.21	99.93
404.21	0.05	492.47	99.98
492.47	0.02	600.00	100.00

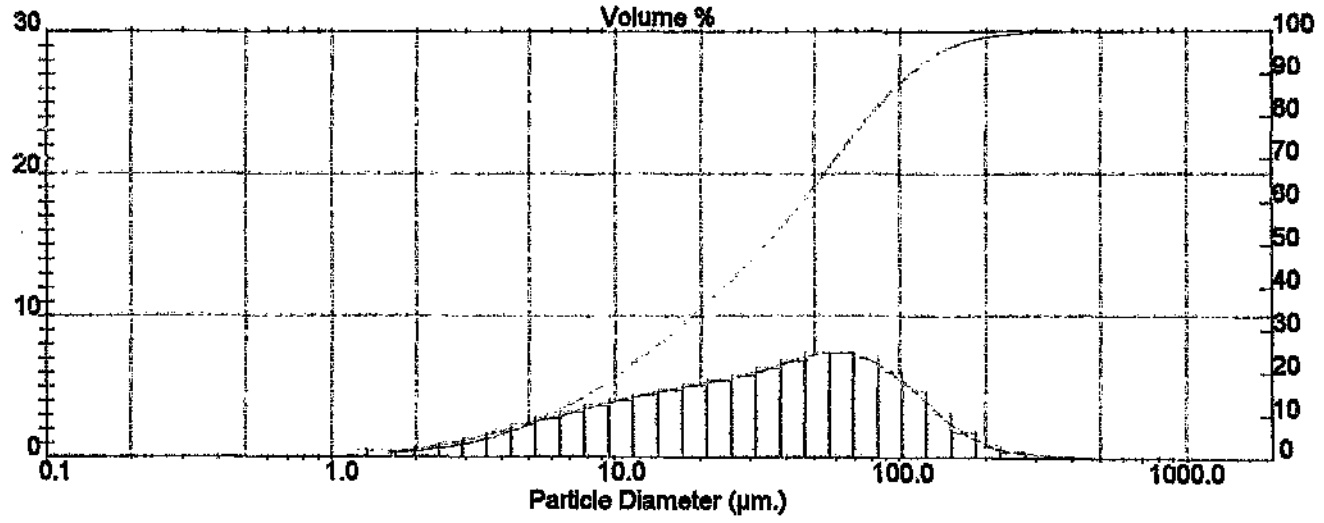

PF SAMPLES :Run Number 15

9 AP1 - 4
05/02/96

Sample File Name: GENWATER, Record: 43
Measured on: Tue, Apr 02, 1996 7:39AM Last saved on: Tue, Apr 02, 1996 7:39AM

Source: Analysed

Presentation: 2$$D
Very Polydisperse model

Volume Result

Focus = 300 mm.

Residual = 0.144 %
d (0.5) = 25.93 µm
D [4, 3] = 38.65 µm
Sauter Mean (D[3,2]) = 11.29 µm
Specific Surface Area = 0.5313 sq. m. / gm

Concentration = 0.049 %
d (0.1) = 4.94 µm
Span = 3.18

Obscuration = 26.68 %
d (0.9) = 87.38 µm

Mode = 47.23 µm
Density = 1.00 gm. / c.c.

Size (Lo) µm	Result In %	Size (Hi) µm	Result Below %
0.50	0.89	1.32	0.89
1.32	0.70	1.60	1.60
1.60	0.71	1.95	2.30
1.95	0.97	2.38	3.27
2.38	1.29	2.90	4.56
2.90	1.64	3.53	6.20
3.53	2.07	4.30	8.27
4.30	2.55	5.24	10.82
5.24	3.10	6.39	13.92
6.39	3.67	7.78	17.58
7.78	4.19	9.48	21.78
9.48	4.69	11.55	26.47
11.55	5.14	14.06	31.61
14.06	5.60	17.15	37.21
17.15	5.97	20.90	43.18
20.90	6.24	25.46	49.42

Size (Lo) µm	Result In %	Size (Hi) µm	Result Below %
25.46	6.46	31.01	55.88
31.01	6.76	37.79	62.64
37.79	7.00	46.03	69.64
46.03	7.03	56.09	76.66
56.09	6.55	68.33	83.22
68.33	5.60	83.26	88.82
83.26	4.30	101.44	93.13
101.44	3.03	123.59	96.15
123.59	1.84	150.57	97.99
150.57	1.01	183.44	99.00
183.44	0.50	223.51	99.50
223.51	0.26	272.31	99.76
272.31	0.13	331.77	99.89
331.77	0.07	404.21	99.95
404.21	0.03	492.47	99.99
492.47	0.01	600.00	100.00

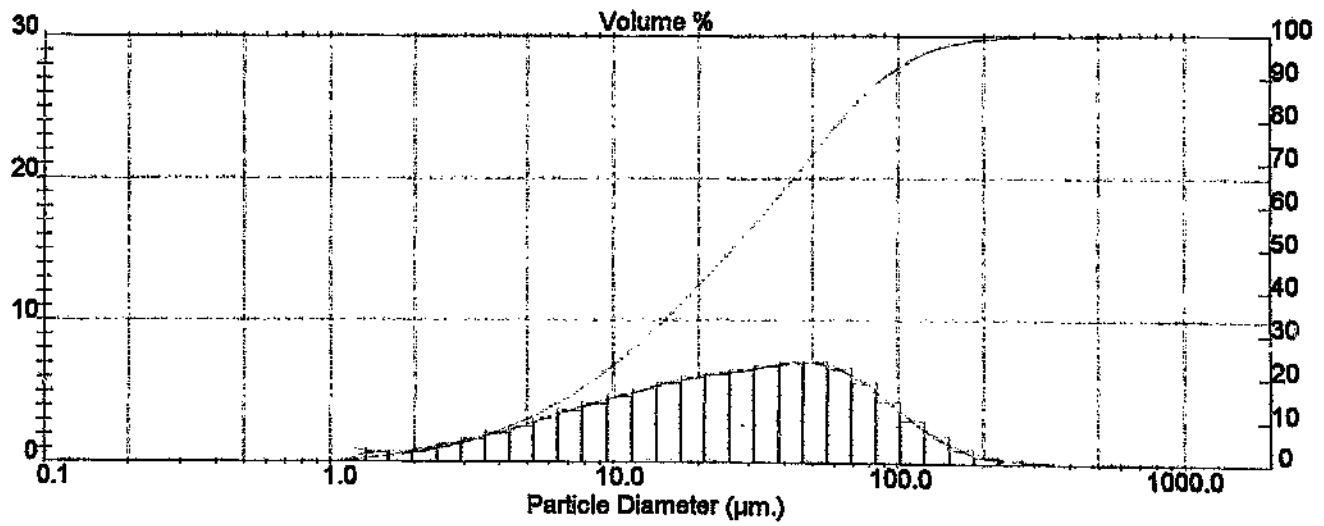

MALVERN

MASTERSIZER X

Version 1.2b

Tue, Apr 02, 1996 10:32AM

PF SAMPLES **:Run Number 16**

9 B P1 - 4
05/02/96

Sample File Name: GENWATER, Record: 49
Measured on: Tue, Apr 02, 1996 7:41AM Last saved on: Tue, Apr 02, 1996 7:42AM

Source: Analysed

Presentation: 2$$D
Very Polydisperse model

Volume Result

Focus = 300 mm.

Residual = 0.198 %
d (0.5) = 57.97 µm
D [4, 3] = 71.23 µm
Sauter Mean (D[3,2]) = 31.26 µm
Specific Surface Area = 0.1918 sq. m. / gm

Concentration = 0.129 %
d (0.1) = 15.29 µm
Span = 2.13

Obscuration = 25.73 %
d (0.9) = 136.54 µm

Mode = 69.10 µm
Density = 1.00 gm. / c.c.

Size (Lo) µm	Result In %	Size (Hi) µm	Result Below %
0.50	0.03	1.32	0.03
1.32	0.03	1.60	0.06
1.60	0.04	1.95	0.09
1.95	0.07	2.38	0.17
2.38	0.15	2.90	0.32
2.90	0.30	3.53	0.61
3.53	0.55	4.30	1.17
4.30	0.83	5.24	2.00
5.24	0.98	6.39	2.98
6.39	1.08	7.78	4.06
7.78	1.33	9.48	5.39
9.48	1.61	11.55	7.00
11.55	2.01	14.08	9.01
14.08	2.54	17.15	11.55
17.15	3.23	20.90	14.78
20.90	4.09	25.46	18.87

Size (Lo) µm	Result In %	Size (Hi) µm	Result Below %
25.46	5.15	31.01	24.02
31.01	6.53	37.79	30.55
37.79	8.08	46.03	38.63
46.03	9.64	56.09	48.27
56.09	10.56	68.33	58.84
68.33	10.56	83.26	69.40
83.26	9.40	101.44	78.80
101.44	7.74	123.59	86.54
123.59	5.51	150.57	92.06
150.57	3.53	183.44	95.59
183.44	2.02	223.51	97.60
223.51	1.14	272.31	98.75
272.31	0.63	331.77	99.38
331.77	0.35	404.21	99.73
404.21	0.18	492.47	99.91
492.47	0.09	600.00	100.00

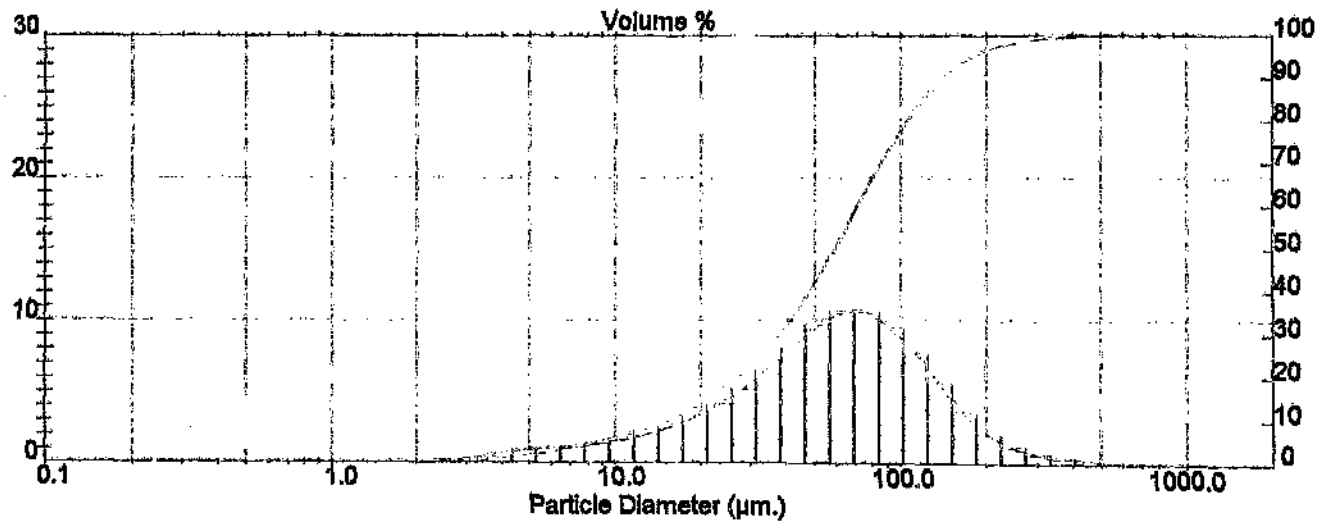

PF SAMPLES :Run Number 17

9 D P1 - 4
05/02/96

Sample File Name: GENWATER, Record: 50 Source: Analysed
Measured on: Tue, Apr 02, 1996 7:44AM Last saved on: Tue, Apr 02, 1996 7:45AM

Presentation: 2$$D
Very Polydisperse model

Volume Result

Focus = 300 mm.

Residual = 0.187 %
d (0.5) = 52.09 µm
D [4, 3] = 66.72 µm
Sauter Mean (D[3,2]) = 18.46 µm
Specific Surface Area = 0.3251 sq. m. / gm

Concentration = 0.063 %
d (0.1) = 8.34 µm
Span = 2.55

Obscuration = 21.93 %
d (0.9) = 141.00 µm

Mode = 75.40 µm
Density = 1.00 gm. / c.c.

Size (Lo) µm	Result In %	Size (Hi) µm	Result Below %
0.50	0.48	1.32	0.48
1.32	0.38	1.60	0.86
1.60	0.38	1.95	1.24
1.95	0.53	2.38	1.77
2.38	0.70	2.90	2.46
2.90	0.89	3.53	3.36
3.53	1.12	4.30	4.47
4.30	1.35	5.24	5.83
5.24	1.60	6.39	7.43
6.39	1.86	7.78	9.29
7.78	2.14	9.48	11.43
9.48	2.48	11.55	13.91
11.55	2.86	14.08	16.78
14.08	3.31	17.15	20.09
17.15	3.79	20.90	23.88
20.90	4.31	25.46	28.19

Size (Lo) µm	Result In %	Size (Hi) µm	Result Below %
25.46	4.90	31.01	33.09
31.01	5.68	37.79	38.77
37.79	6.58	46.03	45.35
46.03	7.60	56.09	52.95
56.09	8.37	68.33	61.32
68.33	8.75	83.26	70.07
83.26	8.38	101.44	78.46
101.44	7.50	123.59	85.96
123.59	5.73	150.57	91.68
150.57	3.82	183.44	95.50
183.44	2.18	223.51	97.69
223.51	1.19	272.31	98.88
272.31	0.61	331.77	99.48
331.77	0.30	404.21	99.79
404.21	0.15	492.47	99.93
492.47	0.07	600.00	100.00

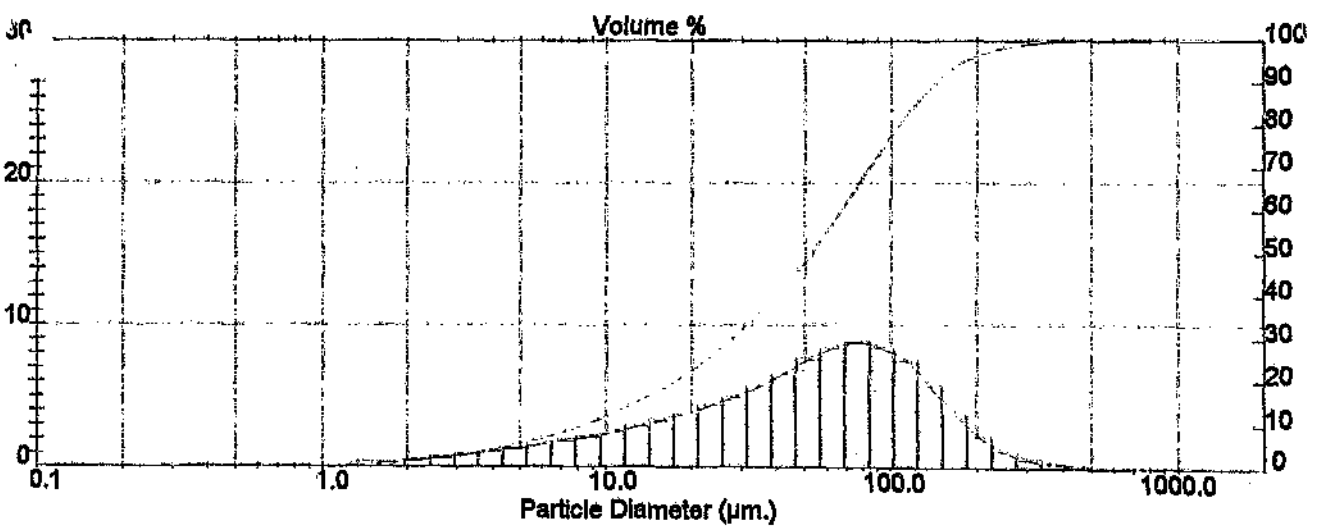

PF SAMPLES :Run Number 18

9 E P1 - 4
05/02/96

Sample File Name: GENWATER, Record: 51 Source: Analysed
Measured on: Tue, Apr 02, 1996 7:47AM Last saved on: Tue, Apr 02, 1996 7:48AM

Presentation: 2$$D
Very Polydisperse model

Volume Result

Focus = 300 mm.

Residual = 0.193 %
d (v, 50) = 50.46 µm
D [4, 3] = 65.20 µm
Sauter Mean (D[3,2]) = 17.23 µm
Specific Surface Area = 0.3483 sq. m. / gm

Concentration = 0.062 %
d (0.1) = 7.82 µm
Span = 2.58

Obscuration = 22.62 %
d (0.9) = 137.97 µm

Mode = 73.79 µm
Density = 1.00 gm. / c.c.

Size (Lo) µm	Result In %	Size (Hi) µm	Result Below %
0.50	0.59	1.32	0.59
1.32	0.46	1.60	1.06
1.60	0.46	1.95	1.51
1.95	0.60	2.38	2.11
2.38	0.77	2.90	2.88
2.90	0.94	3.53	3.82
3.53	1.14	4.30	4.97
4.30	1.37	5.24	6.34
5.24	1.65	6.39	7.99
6.39	1.95	7.78	9.94
7.78	2.25	9.48	12.19
9.48	2.60	11.55	14.79
11.55	2.96	14.06	17.75
14.06	3.39	17.15	21.15
17.15	3.84	20.90	24.99
20.90	4.34	25.46	29.33

Size (Lo) µm	Result In %	Size (Hi) µm	Result Below %
25.46	4.91	31.01	34.24
31.01	5.71	37.79	39.95
37.79	6.64	46.03	46.59
46.03	7.69	56.09	54.28
56.09	8.44	68.33	62.72
68.33	8.75	83.26	71.47
83.26	8.21	101.44	79.67
101.44	7.13	123.59	86.81
123.59	5.30	150.57	92.10
150.57	3.49	183.44	95.59
183.44	2.02	223.51	97.61
223.51	1.16	272.31	98.77
272.31	0.64	331.77	99.41
331.77	0.34	404.21	99.76
404.21	0.17	492.47	99.93
492.47	0.07	600.00	100.00

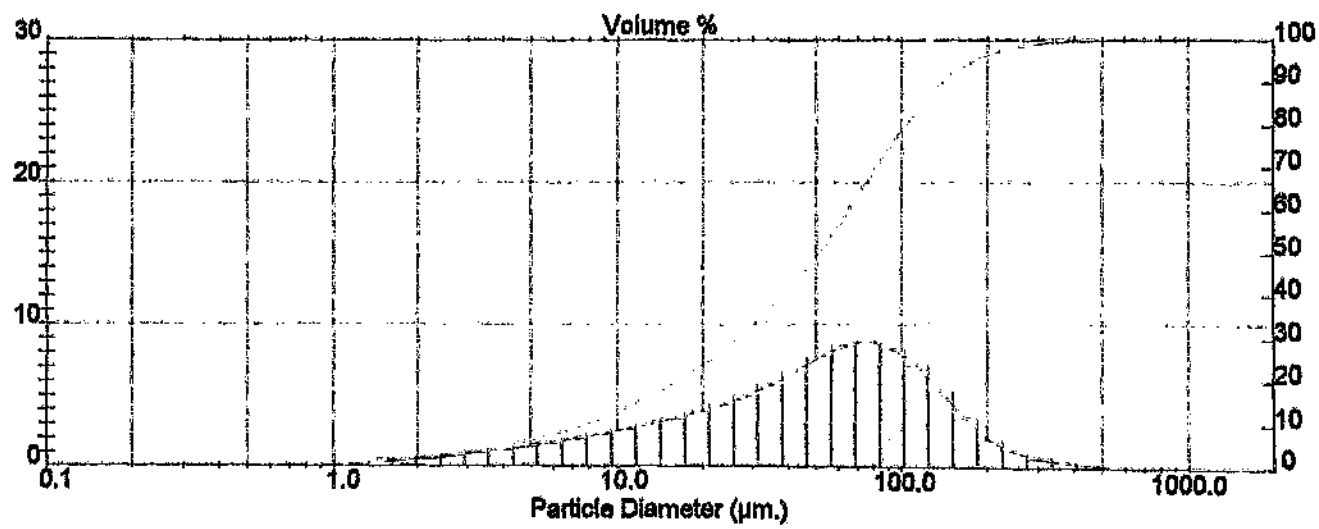

PF SAMPLES :Run Number 19

9 A P1 - 4
07/02/96

Sample File Name: GENWATER, Record: 52 Source: Analysed
Measured on: Tue, Apr 02, 1996 7:50AM Last saved on: Tue, Apr 02, 1996 7:51AM

Presentation: 2$$D
Very Polydisperse model

Volume Result

Focus = 300 mm.

Residual = 0.364 %
d (0.5) = 32.82 µm
D [4, 3] = 40.72 µm
Sauter Mean (D[2,2]) = 9.15 µm
Specific Surface Area = 0.6561 sq. m. / gm

Concentration = 0.038 %
d (0.1) = 3.75 µm
Span = 4.45

Obscuration = 25.91 %
d (0.9) = 103.08 µm

Mode = 55.42 µm
Density = 1.00 gm. / c.c.

Size (Lo) µm	Result In %	Size (Hi) µm	Result Below %
0.50	1.34	1.32	1.34
1.32	1.06	1.60	2.40
1.60	1.08	1.95	3.48
1.95	1.45	2.38	4.92
2.38	1.88	2.90	6.81
2.90	2.36	3.53	9.16
3.53	2.89	4.30	12.06
4.30	3.44	5.24	15.50
5.24	3.97	6.39	19.47
6.39	4.41	7.78	23.89
7.78	4.70	9.48	28.59
9.48	4.86	11.55	33.45
11.55	4.94	14.06	38.39
14.06	4.99	17.15	43.37
17.15	4.98	20.90	48.35
20.90	4.95	25.46	53.30

Size (Lo) µm	Result In %	Size (Hi) µm	Result Below %
25.46	4.96	31.01	58.25
31.01	5.10	37.79	63.36
37.79	5.29	46.03	68.64
46.03	5.50	56.09	74.14
56.09	5.49	68.33	79.63
68.33	5.30	83.26	84.93
83.26	4.72	101.44	89.65
101.44	3.94	123.59	93.58
123.59	2.84	150.57	96.43
150.57	1.81	183.44	98.24
183.44	0.98	223.51	99.22
223.51	0.49	272.31	99.71
272.31	0.21	331.77	99.92
331.77	0.07	404.21	99.98
404.21	0.01	492.47	100.00
492.47	0.00	600.00	100.00

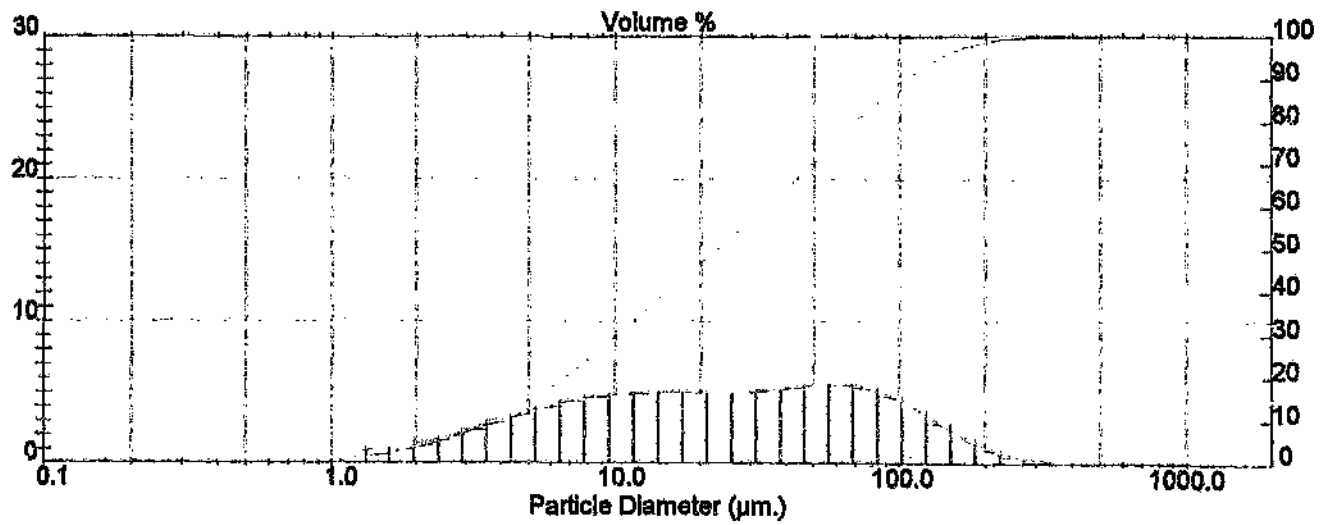

PF SAMPLES :Run Number 20

9 B P1 - 4
07/02/96

Sample File Name: GENWATER, Record: 53 Source: Analysed
Measured on: Tue, Apr 02, 1996 7:53AM Last saved on: Tue, Apr 02, 1996 7:54AM

Presentation: 2$$D
Very Polydisperse model

Volume Result

Focus = 300 mm.

Residual = 0.277 %
d (0.5) = 15.96 µm
D [4, 3] = 26.19 µm
Sauter Mean (D[3,2]) = 7.83 µm
Specific Surface Area = 0.7662 sq. m. / gm

Concentration = 0.032 %
d (0.1) = 3.37 µm
Span = 3.66

Obscuration = 25.73 %
d (0.9) = 61.77 µm

Mode = 16.80 µm
Density = 1.00 gm. / c.c.

Size (Lo) µm	Result In %	Size (Hi) µm	Result Below %
0.50	1.62	1.32	1.62
1.32	1.27	1.60	2.90
1.60	1.27	1.95	4.17
1.95	1.68	2.38	5.85
2.38	2.15	2.90	8.00
2.90	2.65	3.53	10.65
3.53	3.22	4.30	13.87
4.30	3.84	5.24	17.71
5.24	4.53	6.39	22.24
6.39	5.19	7.78	27.43
7.78	5.72	9.48	33.14
9.48	6.16	11.55	39.30
11.55	6.46	14.08	45.76
14.08	6.68	17.15	52.44
17.15	6.71	20.90	59.15
20.90	6.55	25.46	65.70
25.46	6.25	31.01	71.95
31.01	5.90	37.79	77.85
37.79	5.40	46.03	83.25
46.03	4.74	56.09	87.99
56.09	3.88	68.33	91.88
68.33	2.98	83.26	94.86
83.26	2.12	101.44	96.98
101.44	1.41	123.59	98.39
123.59	0.84	150.57	99.22
150.57	0.45	183.44	99.67
183.44	0.20	223.51	99.87
223.51	0.09	272.31	99.96
272.31	0.03	331.77	99.99
331.77	0.01	404.21	100.00
404.21	0.00	492.47	100.00
492.47	0.00	600.00	100.00

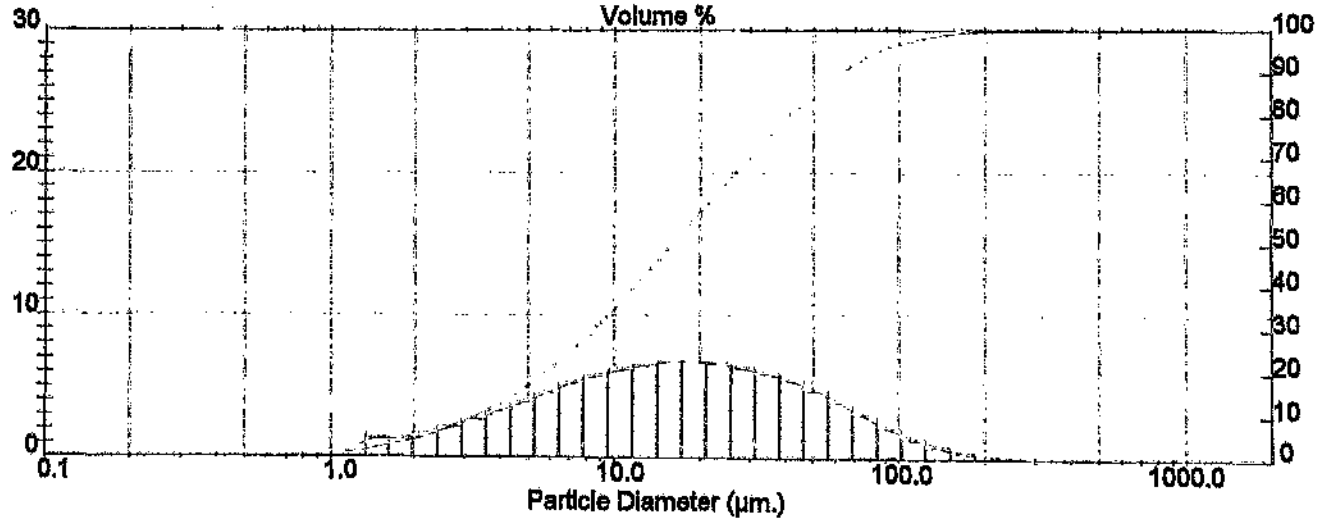

PF SAMPLES :Run Number 21

9 D P1 - 4
07/02/96

Sample File Name: GENWATER, Record: 54 Source: Analysed
Measured on: Tue, Apr 02, 1996 7:56AM Last saved on: Tue, Apr 02, 1996 7:57AM

Presentation: 2$$D
Very Polydisperse model

Volume Result

Focus = 300 mm.

Residual = 0.282 %
d (0.5) = 17.07 µm
D [4, 3] = 25.32 µm
Sauter Mean (D[3,2]) = 7.97 µm
Specific Surface Area = 0.7526 sq. m. / gm

Concentration = 0.037 %
d (0.1) = 3.41 µm
Span = 3.17

Obscuration = 28.24 %
d (0.9) = 57.47 µm

Mode = 24.42 µm
Density = 1.00 gm. / c.c.

Size (Lo) µm	Result In %	Size (Hi) µm	Result Below %
0.50	1.65	1.32	1.65
1.32	1.28	1.60	2.93
1.60	1.27	1.95	4.20
1.95	1.66	2.38	5.86
2.38	2.09	2.90	7.96
2.90	2.54	3.53	10.50
3.53	3.05	4.30	13.55
4.30	3.59	5.24	17.14
5.24	4.23	6.39	21.37
6.39	4.85	7.78	26.22
7.78	5.35	9.48	31.56
9.48	5.81	11.55	37.39
11.55	6.20	14.08	43.58
14.08	6.58	17.15	50.16
17.15	6.86	20.90	57.02
20.90	7.00	25.46	64.03

Size (Lo) µm	Result In %	Size (Hi) µm	Result Below %
25.46	6.97	31.01	71.00
31.01	6.79	37.79	77.79
37.79	6.27	46.03	84.05
46.03	5.37	56.09	89.43
56.09	4.10	68.33	93.53
68.33	2.83	83.26	96.36
83.26	1.75	101.44	98.11
101.44	1.01	123.59	99.12
123.59	0.51	150.57	99.63
150.57	0.24	183.44	99.87
183.44	0.09	223.51	99.96
223.51	0.03	272.31	99.99
272.31	0.01	331.77	100.00
331.77	0.00	404.21	100.00
404.21	0.00	492.47	100.00
492.47	0.00	600.00	100.00

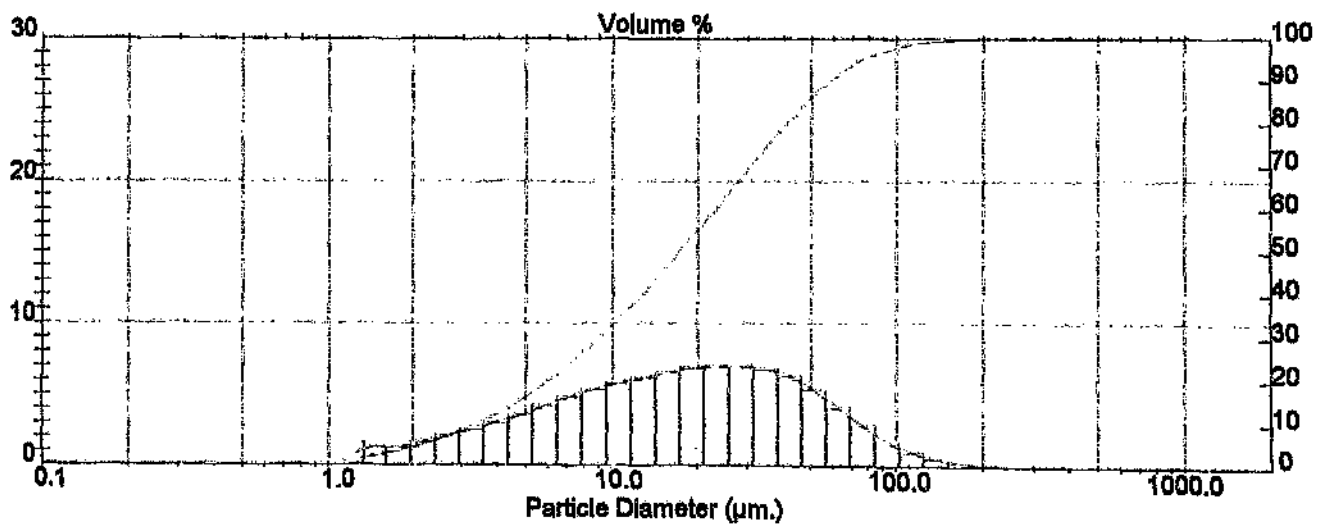

PF SAMPLES :Run Number 22

9 E P1 - 4
07/02/96

Sample File Name: GENWATER, Record: 55 Source: Analysed
Measured on: Tue, Apr 02, 1996 7:58AM Last saved on: Tue, Apr 02, 1996 8:00AM

Presentation: 2$$D
Very Polydisperse model

Volume Result

Focus = 300 mm.

Residual = 0.191 %
d (0.5) = 45.65 µm
D [4, 3] = 58.90 µm
Sauter Mean (D[3,2]) = 14.12 µm
Specific Surface Area = 0.4250 sq. m. / gm

Concentration = 0.065 %
d (0.1) = 5.79 µm
Span = 2.66

Obscuration = 28.05 %
d (0.9) = 127.38 µm

Mode = 75.12 µm
Density = 1.00 gm. / c.c.

Size (Lo) µm	Result In %	Size (Hi) µm	Result Below %
0.50	0.78	1.32	0.78
1.32	0.62	1.60	1.40
1.60	0.63	1.95	2.03
1.95	0.84	2.38	2.86
2.38	1.09	2.90	3.95
2.90	1.35	3.53	5.30
3.53	1.65	4.30	6.95
4.30	1.95	5.24	8.90
5.24	2.24	6.39	11.14
6.39	2.51	7.78	13.65
7.78	2.75	9.48	16.40
9.48	2.99	11.55	19.39
11.55	3.23	14.06	22.62
14.06	3.52	17.15	26.13
17.15	3.82	20.90	29.96
20.90	4.18	25.46	34.14

Size (Lo) µm	Result In %	Size (Hi) µm	Result Below %
25.46	4.62	31.01	38.76
31.01	5.32	37.79	44.08
37.79	6.19	46.03	50.27
46.03	7.26	56.09	57.53
56.09	8.11	68.33	65.65
68.33	8.54	83.26	74.19
83.26	8.05	101.44	82.24
101.44	6.87	123.59	89.11
123.59	4.86	150.57	93.97
150.57	2.96	183.44	96.93
183.44	1.55	223.51	98.48
223.51	0.80	272.31	99.28
272.31	0.39	331.77	99.67
331.77	0.20	404.21	99.87
404.21	0.09	492.47	99.96
492.47	0.04	600.00	100.00

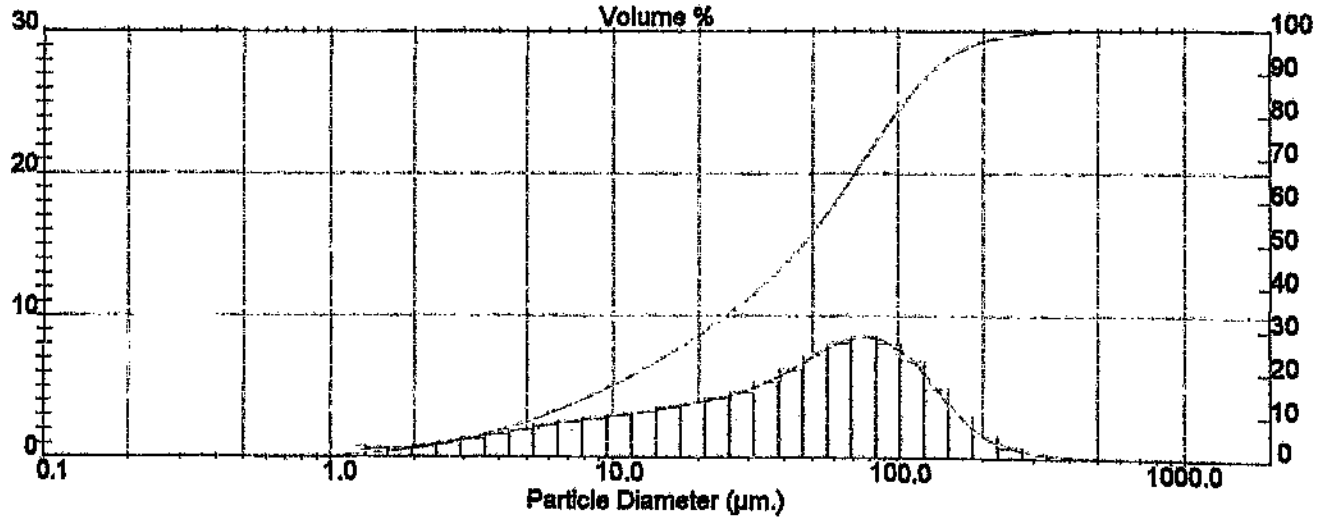

PF SAMPLES :Run Number 23

9 F P1 - 4
07/02/96

Sample File Name: GENWATER, Record: 56 Source: Analysed
Measured on: Tue, Apr 02, 1996 8:01AM Last saved on: Tue, Apr 02, 1996 8:02AM

Presentation: 2$$D
Very Polydisperse model

Volume Result

Residual = 0.302 %
d (0.5) = 17.94 µm
D [4, 3] = 30.83 µm
Sauter Mean (D[3,2]) = 8.72 µm
Specific Surface Area = 0.6884 sq. m. / gm

Concentration = 0.041 %
d (0.1) = 3.78 µm
Span = 3.91

Focus = 300 mm.
Obscuration = 28.83 %
d (0.9) = 73.98 µm
Mode = 20.27 µm
Density = 1.00 gm. / c.c.

Size (Lo) µm	Result In %	Size (Hi) µm	Result Below %
0.50	1.29	1.32	1.29
1.32	1.02	1.60	2.31
1.60	1.03	1.95	3.34
1.95	1.41	2.38	4.76
2.38	1.87	2.90	6.63
2.90	2.40	3.53	9.03
3.53	3.00	4.30	12.03
4.30	3.66	5.24	15.69
5.24	4.34	6.39	20.02
6.39	4.96	7.78	24.99
7.78	5.43	9.48	30.42
9.48	5.80	11.55	36.22
11.55	6.06	14.08	42.27
14.08	6.27	17.15	48.55
17.15	6.35	20.90	54.90
20.90	6.31	25.46	61.21
25.46	6.16	31.01	67.38
31.01	5.96	37.79	73.34
37.79	5.61	46.03	78.95
46.03	5.11	56.09	84.06
56.09	4.39	68.33	88.45
68.33	3.61	83.26	92.06
83.26	2.79	101.44	94.85
101.44	2.09	123.59	96.94
123.59	1.41	150.57	98.34
150.57	0.86	183.44	99.21
183.44	0.45	223.51	99.66
223.51	0.22	272.31	99.88
272.31	0.09	331.77	99.96
331.77	0.03	404.21	99.99
404.21	0.01	492.47	100.00
492.47	0.00	600.00	100.00

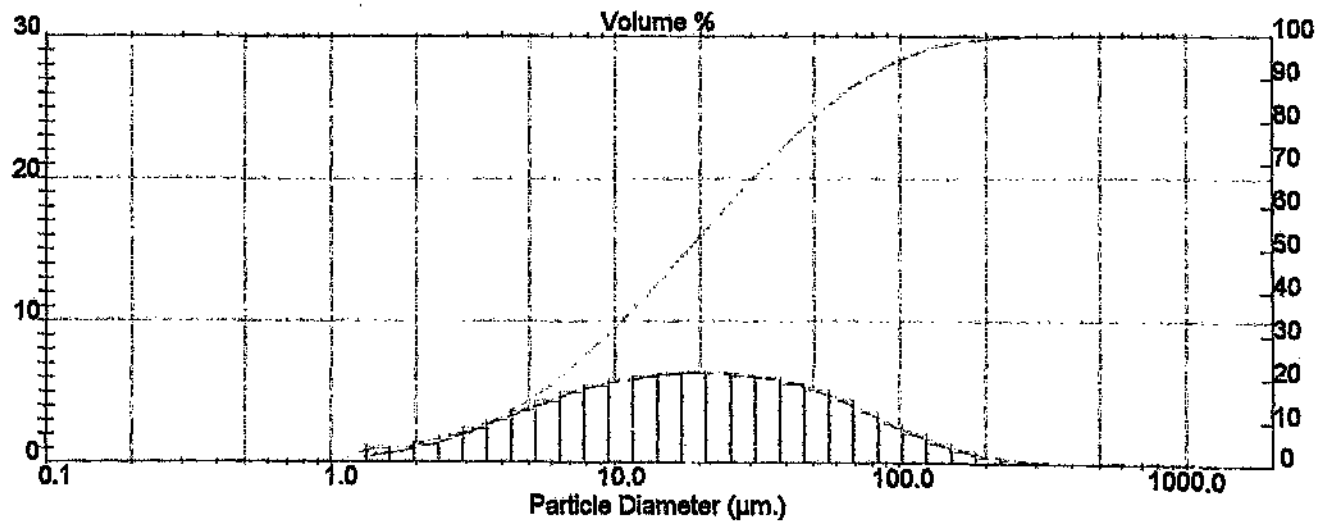

PF SAMPLES :Run Number 24

9 A P1 - 4
08/02/96

Sample File Name: GENWATER, Record: 57 Source: Analysed
Measured on: Tue, Apr 02, 1996 9:14AM Last saved on: Tue, Apr 02, 1996 9:18AM

Presentation: 2$$D
Very Polydisperse model

Volume Result

Focus = 300 mm.

Residual = 0.261 %
d (0.5) = 44.45 µm
D [4, 3] = 55.03 µm
Sauter Mean (D[3,2]) = 18.35 µm
Specific Surface Area = 0.3271 sq. m. / gm

Concentration = 0.067 %
d (0.1) = 8.74 µm
Span = 2.31

Obscuration = 23.12 %
d (0.9) = 111.64 µm

Mode = 58.80 µm
Density = 1.00 gm. / c.c.

Size (Lo) µm	Result In %	Size (Hi) µm	Result Below %
0.50	0.44	1.32	0.44
1.32	0.35	1.60	0.79
1.60	0.34	1.95	1.13
1.95	0.47	2.38	1.61
2.38	0.63	2.90	2.23
2.90	0.81	3.53	3.04
3.53	1.02	4.30	4.06
4.30	1.26	5.24	5.32
5.24	1.55	6.39	6.87
6.39	1.87	7.78	8.74
7.78	2.21	9.48	10.95
9.48	2.61	11.55	13.57
11.55	3.07	14.08	16.63
14.08	3.66	17.15	20.29
17.15	4.34	20.90	24.64
20.90	5.17	25.46	29.81

Size (Lo) µm	Result In %	Size (Hi) µm	Result Below %
25.46	6.09	31.01	35.90
31.01	7.26	37.79	43.16
37.79	8.41	46.03	51.57
46.03	9.46	56.09	61.03
56.09	9.67	68.33	70.70
68.33	9.01	83.26	79.72
83.26	7.37	101.44	87.09
101.44	5.49	123.59	92.58
123.59	3.47	150.57	96.05
150.57	1.96	183.44	98.01
183.44	0.99	223.51	99.00
223.51	0.51	272.31	99.51
272.31	0.26	331.77	99.77
331.77	0.13	404.21	99.90
404.21	0.07	492.47	99.97
492.47	0.03	600.00	100.00

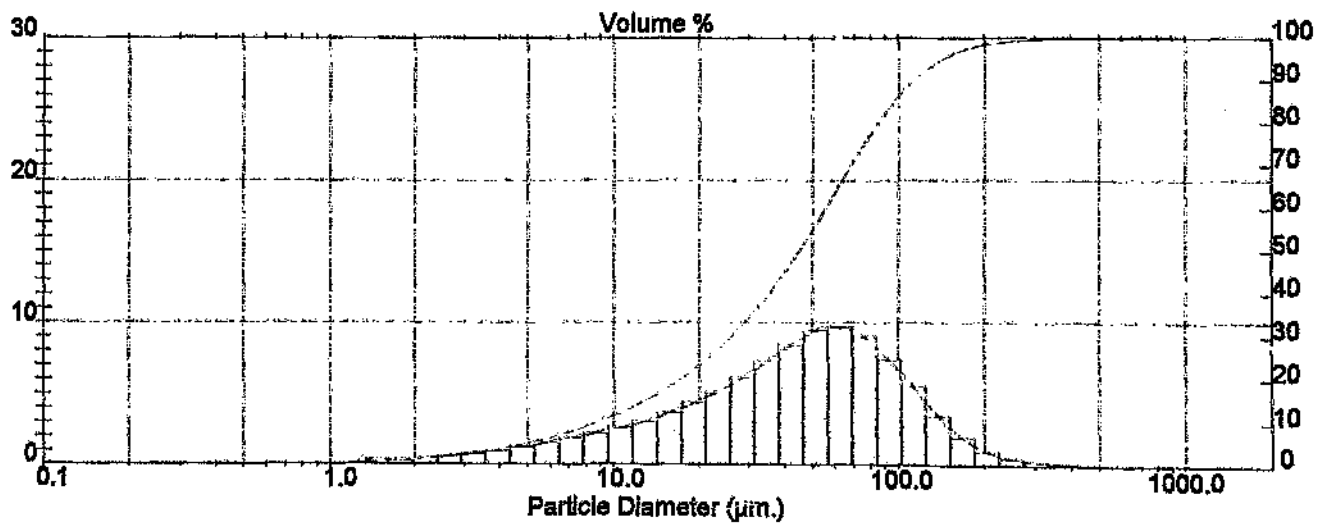

PF SAMPLES :Run Number 25

9 C P1 - 4
09/02/96

Sample File Name: GENWATER, Record: 58 Source: Analysed
Measured on: Tue, Apr 02, 1996 9:20AM Last saved on: Tue, Apr 02, 1996 9:20AM

Presentation: 2$$D
Very Polydisperse model

Volume Result

Focus = 300 mm.

Residual = 0.226 %
d (0.5) = 44.20 µm
D [4, 3] = 56.23 µm
Sauter Mean (D[3,2]) = 17.87 µm
Specific Surface Area = 0.3357 sq. m. / gm

Concentration = 0.068 %
d (0.1) = 7.87 µm
Span = 2.47

Obscuration = 23.92 %
d (0.9) = 117.03 µm

Mode = 59.02 µm
Density = 1.00 gm. / c.c.

Size (Lo) µm	Result In %	Size (Hi) µm	Result Below %
0.50	0.39	1.32	0.39
1.32	0.32	1.60	0.70
1.60	0.33	1.95	1.03
1.95	0.48	2.38	1.52
2.38	0.69	2.90	2.20
2.90	0.94	3.53	3.14
3.53	1.24	4.30	4.38
4.30	1.56	5.24	5.94
5.24	1.84	6.39	7.78
6.39	2.09	7.78	9.87
7.78	2.37	9.48	12.24
9.48	2.70	11.55	14.94
11.55	3.09	14.08	18.03
14.08	3.62	17.15	21.65
17.15	4.24	20.90	25.89
20.90	5.00	25.46	30.89

Size (Lo) µm	Result In %	Size (Hi) µm	Result Below %
25.46	5.87	31.01	36.76
31.01	6.96	37.79	43.72
37.79	8.02	46.03	51.74
46.03	8.95	56.09	60.69
56.09	9.14	68.33	69.83
68.33	8.62	83.26	78.45
83.26	7.26	101.44	85.71
101.44	5.68	123.59	91.39
123.59	3.83	150.57	95.22
150.57	2.30	183.44	97.52
183.44	1.22	223.51	98.74
223.51	0.65	272.31	99.39
272.31	0.33	331.77	99.71
331.77	0.17	404.21	99.88
404.21	0.08	492.47	99.96
492.47	0.04	600.00	100.00

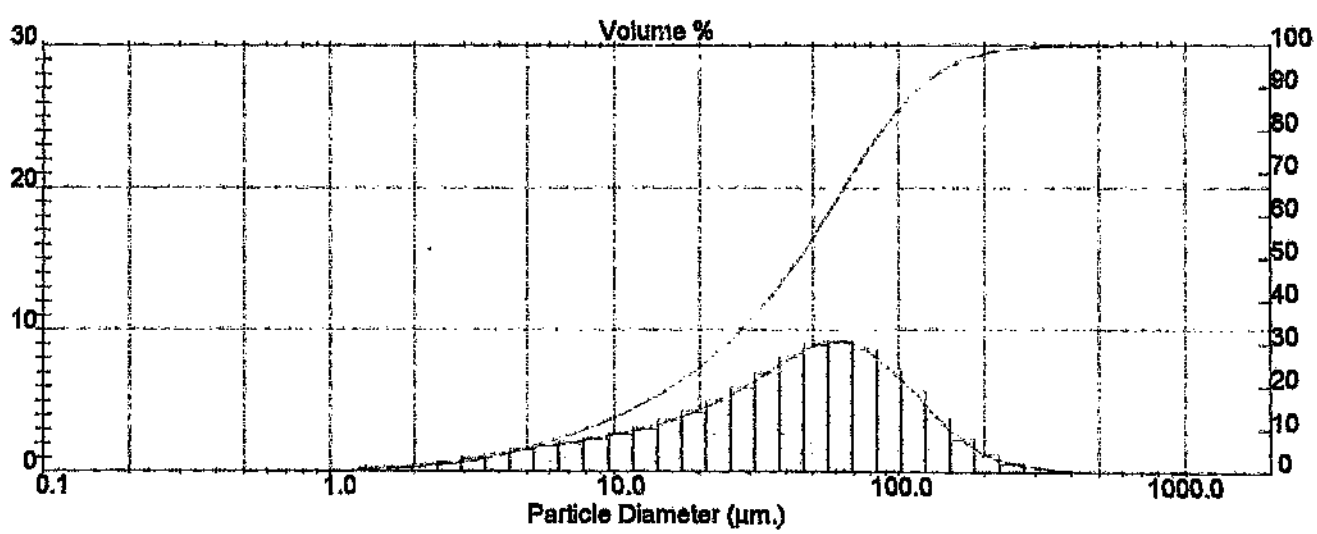

MALVERN MASTERSIZER X

Version 1.2b

Tue, Apr 02, 1996 10:57AM

PF SAMPLES :Run Number 26

9 D P1 - 4
08/02/96

Sample File Name: GENWATER, Record: 59
Measured on: Tue, Apr 02, 1996 9:22AM Last saved on: Tue, Apr 02, 1996 9:23AM

Source: Analysed

Presentation: 2$$D
Very Polydisperse model

Volume Result

Focus = 300 mm.

Residual = 0.304 %
d (0.5) = 16.20 µm
D [4, 3] = 34.22 µm
Sauter Mean (D[3,2]) = 7.63 µm
Specific Surface Area = 0.7859 sq. m. / gm

Concentration = 0.033 %
d (0.1) = 3.18 µm
Span = 5.32

Obscuration = 27.02 %
d (0.9) = 69.45 µm

Mode = 14.94 µm
Density = 1.00 gm. / c.c.

Size (Lo) µm	Result In %	Size (Hi) µm	Result Below %
0.50	1.75	1.32	1.75
1.32	1.38	1.60	3.13
1.60	1.40	1.95	4.53
1.95	1.84	2.38	6.37
2.38	2.36	2.90	8.73
2.90	2.91	3.53	11.64
3.53	3.52	4.30	15.16
4.30	4.12	5.24	19.28
5.24	4.71	6.39	23.99
6.39	5.18	7.78	29.17
7.78	5.47	9.48	34.64
9.48	5.64	11.55	40.28
11.55	5.68	14.08	45.95
14.08	5.67	17.15	51.62
17.15	5.53	20.90	57.16
20.90	5.32	25.46	62.47

Size (Lo) µm	Result In %	Size (Hi) µm	Result Below %
25.46	5.05	31.01	67.52
31.01	4.83	37.79	72.35
37.79	4.58	46.03	76.93
46.03	4.33	56.09	81.26
56.09	3.96	68.33	85.22
68.33	3.59	83.26	88.81
83.26	3.12	101.44	91.93
101.44	2.66	123.59	94.59
123.59	2.06	150.57	96.65
150.57	1.47	183.44	98.12
183.44	0.91	223.51	99.03
223.51	0.54	272.31	99.56
272.31	0.27	331.77	99.84
331.77	0.12	404.21	99.95
404.21	0.04	492.47	99.99
492.47	0.01	600.00	100.00

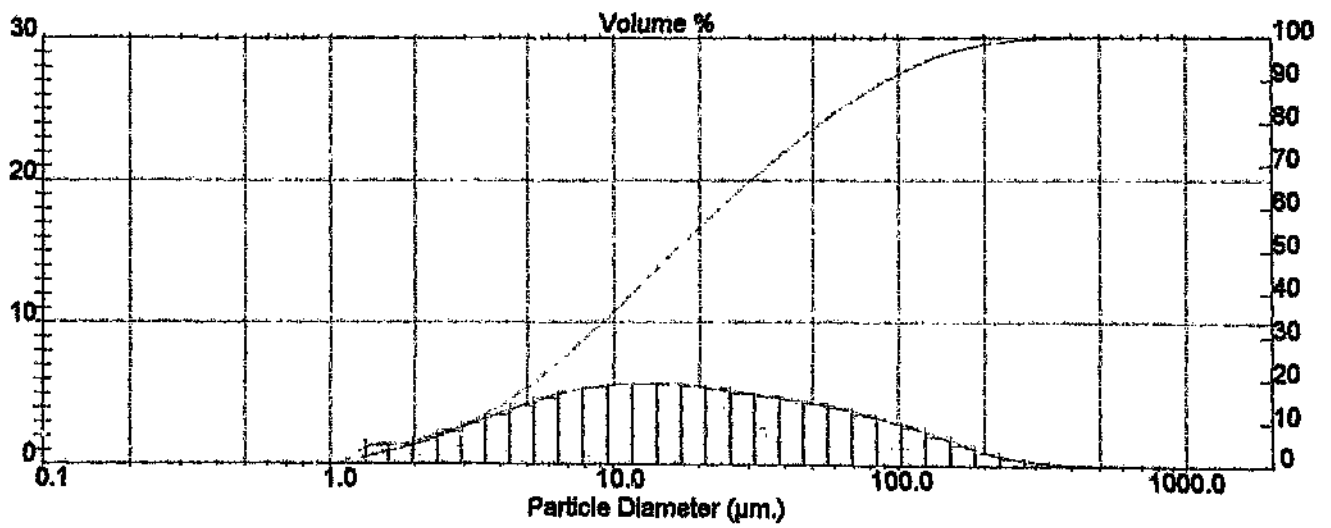

P/ SAMPLES :Run Number 27

9 E P1 - 4
08/02/96

Sample File Name: GENWATER, Record: 60 Source: Analysed
Measured on: Tue, Apr 02, 1996 9:24AM Last saved on: Tue, Apr 02, 1996 9:25AM

Presentation: 2$$D
Very Polydisperse model

Volume Result

Focus = 300 mm.

Residual = 0.251 %
d (0.5) = 48.93 µm
D [4, 3] = 62.83 µm
Sauter Mean (D[3,2]) = 19.12 µm
Specific Surface Area = 0.3138 sq. m. / gm

Concentration = 0.072 %
d (0.1) = 7.89 µm
Span = 2.55

Obscuration = 23.87 %
d (0.9) = 132.53 µm

Mode = 75.37 µm
Density = 1.00 gm. / c.c.

Size (Lo) µm	Result In %	Size (Hi) µm	Result Below %
0.50	0.26	1.32	0.26
1.32	0.22	1.60	0.48
1.60	0.24	1.95	0.72
1.95	0.38	2.36	1.09
2.36	0.59	2.90	1.68
2.90	0.88	3.53	2.57
3.53	1.28	4.30	3.84
4.30	1.69	5.24	5.53
5.24	2.01	6.39	7.54
6.39	2.28	7.78	9.83
7.78	2.61	9.48	12.44
9.48	2.92	11.55	15.36
11.55	3.23	14.08	18.59
14.08	3.61	17.15	22.21
17.15	3.99	20.90	26.20
20.90	4.44	25.46	30.64

Size (Lo) µm	Result In %	Size (Hi) µm	Result Below %
25.46	4.94	31.01	35.57
31.01	5.67	37.79	41.25
37.79	6.52	46.03	47.77
46.03	7.55	56.09	55.32
56.09	8.31	68.33	63.63
68.33	8.74	83.26	72.37
83.26	8.29	101.44	80.66
101.44	7.23	123.59	87.89
123.59	5.26	150.57	93.15
150.57	3.28	183.44	96.43
183.44	1.74	223.51	98.17
223.51	0.90	272.31	99.07
272.31	0.45	331.77	99.53
331.77	0.25	404.21	99.77
404.21	0.14	492.47	99.91
492.47	0.09	600.00	100.00

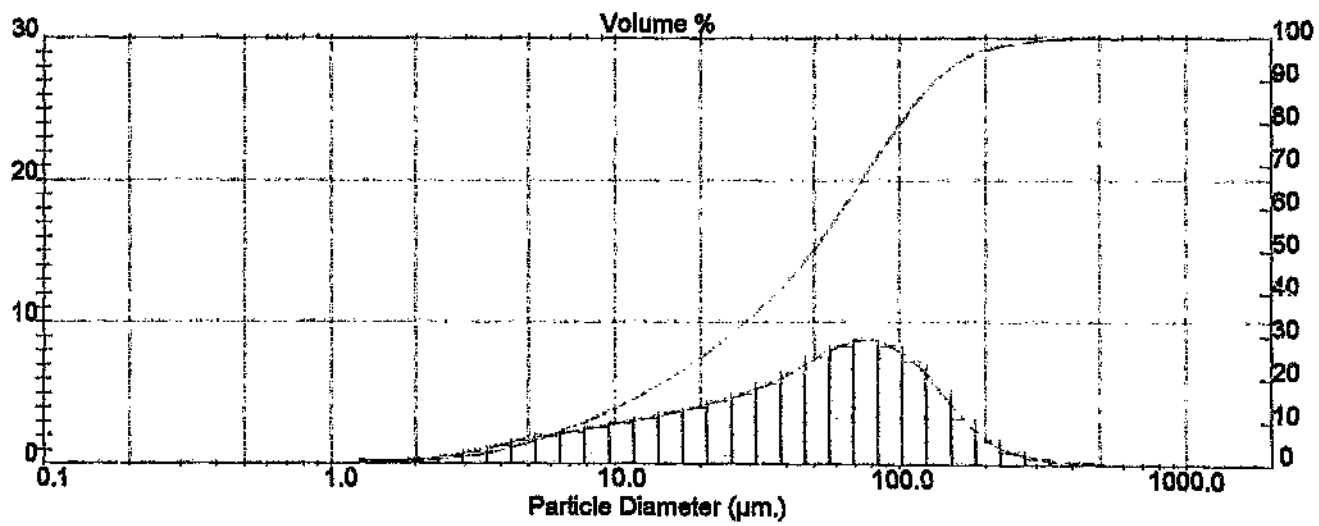

PF SAMPLES :Run Number 28

9 F P1 - 4
08/02/96

Sample File Name: GENWATER, Record: 61 Source: Analysed
Measured on: Tue, Apr 02, 1996 9:27AM Last saved on: Tue, Apr 02, 1996 9:28AM

Presentation: 2$$D
Very Polydisperse model

Volume Result

Focus = 300 mm.

Residual = 0.211 %
d (0.5) = 36.65 µm
D [4, 3] = 58 µm
Sauter Mean D[3,2] = 14.39 µm
Specific Surface Area = 0.4170 sq. m. / gm

Concentration = 0.060 %
d (0.1) = 6.02 µm
Span = 3.03

Obscuration = 25.97 %
d (0.9) = 123.20 µm

Mode = 71.83 µm
Density = 1.00 gm. / c.c.

Size (Lo) µm	Result In %	Size (Hi) µm	Result Below %
0.50	0.57	1.32	0.57
1.32	0.46	1.60	1.04
1.60	0.48	1.95	1.51
1.95	0.68	2.38	2.20
2.38	0.95	2.90	3.15
2.90	1.28	3.53	4.43
3.53	1.69	4.30	6.12
4.30	2.13	5.24	8.25
5.24	2.57	6.39	10.82
6.39	2.99	7.78	13.80
7.78	3.38	9.48	17.18
9.48	3.72	11.55	20.91
11.55	4.01	14.08	24.92
14.08	4.31	17.15	29.23
17.15	4.55	20.90	33.77
20.90	4.81	25.46	38.58

Size (Lo) µm	Result In %	Size (Hi) µm	Result Below %
25.46	5.11	31.01	43.69
31.01	5.63	37.79	49.32
37.79	6.22	46.03	55.53
46.03	6.92	56.09	62.45
56.09	7.34	68.33	69.79
68.33	7.45	83.26	77.24
83.26	6.89	101.44	84.13
101.44	5.95	123.59	90.08
123.59	4.34	150.57	94.42
150.57	2.74	183.44	97.15
183.44	1.46	223.51	98.61
223.51	0.74	272.31	99.36
272.31	0.36	331.77	99.71
331.77	0.17	404.21	99.88
404.21	0.08	492.47	99.96
492.47	0.04	600.00	100.00

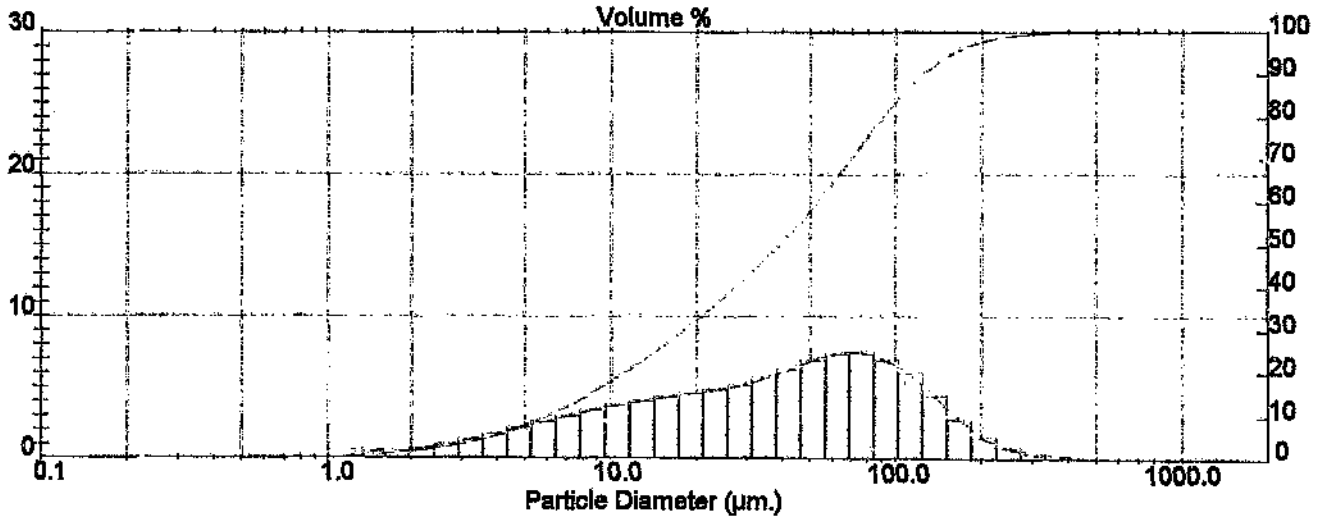

PF SAMPLES :Run Number 29

9 C
08/02/96

Sample File Name: GENWATER, Record: 62 Source: Analysed
Measured on: Tue, Apr 02, 1996 9:30AM Last saved on: Tue, Apr 02, 1996 9:31AM

Presentation: 2$$D
Very Polydisperse model

Volume Result

Focus = 300 mm.

Residual = 0.219 %
d (0.5) = 36.25 µm
D [4, 3] = 50.98 µm
Sauter Mean (D[3,2]) = 12.65 µm
Specific Surface Area = 0.4743 sq. m. / gm

Concentration = 0.048 %
d (0.1) = 5.18 µm
Span = 2.95

Obscuration = 23.82 %
d (0.9) = 113.96 µm

Mode = 64.24 µm
Density = 1.00 gm. / c.c.

Size (Lo) µm	Result In %	Size (Hi) µm	Result Below %
0.50	0.83	1.32	0.83
1.32	0.66	1.60	1.50
1.60	0.67	1.95	2.17
1.95	0.92	2.38	3.09
2.38	1.22	2.90	4.31
2.90	1.56	3.53	5.87
3.53	1.94	4.30	7.82
4.30	2.34	5.24	10.15
5.24	2.71	6.39	12.87
6.39	3.05	7.78	15.91
7.78	3.31	9.48	19.23
9.48	3.55	11.55	22.78
11.55	3.76	14.08	26.54
14.08	4.05	17.15	30.60
17.15	4.35	20.90	34.94
20.90	4.73	25.46	39.67
25.46	5.19	31.01	44.86
31.01	5.90	37.79	50.77
37.79	6.67	46.03	57.44
46.03	7.47	56.09	64.91
56.09	7.77	68.33	72.67
68.33	7.54	83.26	80.21
83.26	6.53	101.44	86.74
101.44	5.22	123.59	91.96
123.59	3.57	150.57	95.53
150.57	2.17	183.44	97.70
183.44	1.15	223.51	98.85
223.51	0.60	272.31	99.45
272.31	0.30	331.77	99.75
331.77	0.15	404.21	99.90
404.21	0.07	492.47	99.97
492.47	0.03	600.00	100.00

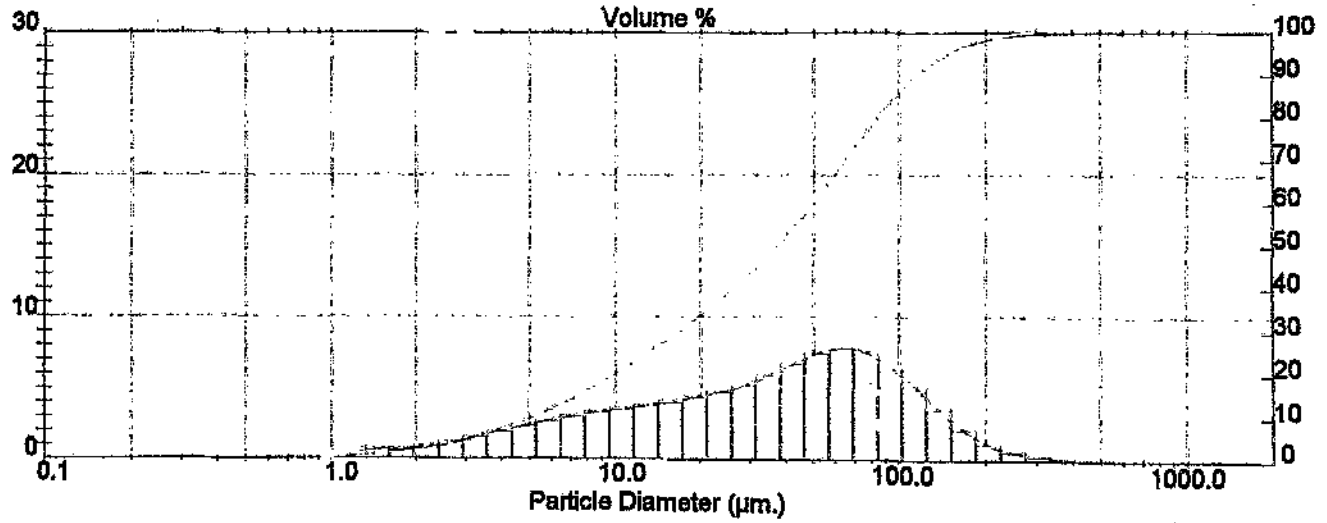

PF SAMPLES :Run Number 36

9FP2-4 GRAP
07/02/96

Sample File Name: GENWATER, Record: 68 Source: Analysed
Measured on: Tue, Apr 02, 1996 9:47AM Last saved on: Tue, Apr 02, 1996 9:48AM

Presentation: 2$$D
Very Polydisperse model

Volume Result

Focus = 300 mm.

Residual = 0.292 %
d (0.5) = 16.57 µm
D [4, 3] = 30.46 µm
Sauter Mean (D[3,2]) = 8.25 µm
Specific Surface Area = 0.7276 sq. m. / gm

Concentration = 0.033 %
d (0.1) = 3.55 µm
Span = 4.14

Obscuration = 24.80 %
d (0.9) = 73.79 µm

Mode = 16.52 µm
Density = 1.00 gm. / c.c.

Size (Lo) µm	Result In %	Size (Hi) µm	Result Below %
0.50	1.45	1.32	1.45
1.32	1.15	1.60	2.60
1.60	1.16	1.95	3.76
1.95	1.56	2.38	5.32
2.38	2.04	2.90	7.36
2.90	2.57	3.53	9.93
3.53	3.18	4.30	13.11
4.30	3.83	5.24	16.94
5.24	4.51	6.39	21.45
6.39	5.12	7.78	26.57
7.78	5.57	9.48	32.14
9.48	5.89	11.55	38.02
11.55	6.09	14.08	44.11
14.08	6.24	17.15	50.34
17.15	6.25	20.90	56.59
20.90	6.14	25.46	62.73

Size (Lo) µm	Result In %	Size (Hi) µm	Result Below %
25.46	5.92	31.01	68.65
31.01	5.67	37.79	74.32
37.79	5.29	46.03	79.62
46.03	4.82	56.09	84.44
56.09	4.14	68.33	88.58
68.33	3.43	83.26	92.01
83.26	2.68	101.44	94.69
101.44	2.04	123.59	96.72
123.59	1.41	150.57	98.13
150.57	0.91	183.44	99.04
183.44	0.51	223.51	99.55
223.51	0.27	272.31	99.82
272.31	0.12	331.77	99.94
331.77	0.05	404.21	99.99
404.21	0.01	492.47	100.00
492.47	0.00	600.00	100.00

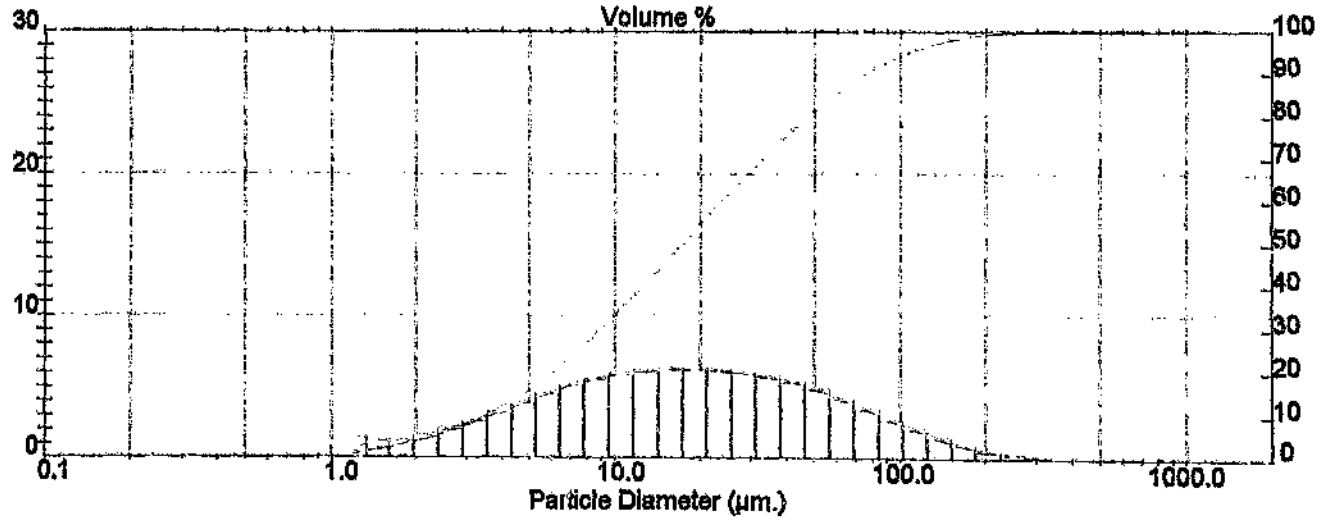

APPENDIX 3

Appendix 3.1

Grid discretisation file: Hen9b.dat

FILE: HEN9B.DAT
Grid Discretisation File

========== Text zur Beschreibung des Gitters ==========

HEN9 - FILE fuer Gittererzeugung

========== Daten zur Gittererzeugung ==========

HEN9 - FILE
LZYL kennzeichnet Zylinderkoordinaten
.FALSE. .FALSE.
IN=Anzahl der Gitterlinien in x-Richtung
77
JN=Anzahl der Gitterlinen in y-Richtung
48
KN=Anzahl der Gitterlinien in z-Richtung
101
Gitterlinien in x-Richtung [m]
0.0000
0.3697
0.6697
0.9697
1.2197
1.5297
1.7797
1.9397
2.0697
2.1761
2.2665
2.4375
2.6085
2.6989
2.8053
2.9353
3.0953
3.3950
3.6947
4.0047
4.2547
4.4147
4.5447
4.6511
4.7415
4.9125
5.0835
5.1739
5.2803
5.4103
5.5703
5.8203
6.1303
6.3803
6.6803
6.9803
7.1803
7.3620
7.3875
7.4130
7.5947
7.7947
8.0947
8.3947
8.6447
8.9547
9.2047
9.3647

9.4947
9.6011
9.6915
9.8625
10.0335
10.1239
10.2303
10.3603
10.5203
10.8200
11.1197
11.4297
11.6797
11.8397
11.9697
12.0761
12.1665
12.3375
12.5085
12.5989
12.7053
12.8353
12.9953
13.2453
13.5553
13.8053
14.1053
14.4053
14.7750

Gitterlinien in y-Richtung [m]

0.0000
0.0900
0.1880
0.2880
0.3880
0.5080
0.6580
0.8380
1.0380
1.2680
1.5280
1.8280
2.1780
2.5780
2.9780
3.3780
3.7280
4.0780
4.3780
4.6780
4.9780
5.2780
5.6125
5.8755
6.1755
6.4385
6.7730
7.0730
7.3730
7.6730
7.9730
8.3230
8.6730
9.0730
9.4730
9.8730
10.2230
10.5230

10.7835
11.0130
11.2130
11.3930
11.5430
11.6630
11.7630
11.8630
11.9610
12.0510

Gitterlinien in z-Richtung [m]

0.0000
0.5000
1.0000
1.5000
2.0000
2.5000
3.0000
3.5000
4.0000
4.5000
5.0000
5.5000
6.0000
6.5000
7.0660
7.2000
7.4000
7.7000
8.0500
8.3000
8.4500
8.6072
8.7136
8.8040
8.9750
9.1461
9.2365
9.3428
9.4500
9.5600
9.7600
10.1780
10.5960
11.0140
11.4320
11.8500
12.2000
12.4000
12.5000
12.6072
12.7136
12.8040
12.9750
13.1461
13.2365
13.3428
13.4500
13.5500
13.7500
14.1000
14.4500
14.8000
15.1500
15.5000
15.8500
16.2000
16.4000

16.5000
16.6072
16.7136
16.8040
16.9750
17.1461
17.2365
17.3428
17.4428
17.5628
17.6928
17.8228
18.1428
18.6428
19.1428
19.6428
20.1428
20.6428
21.1428
21.6428
22.1428
22.6428
23.1428
23.6428
24.1428
24.6428
25.1428
25.6428
26.1428
26.6428
27.1428
27.6428
28.1428
28.6428

29.1428
29.6428
30.1428
30.6428
31.0230
31.5000
32.0000
33.0000
34.0000
35.0000
******* Anzahl Einlaesse in xy-Ebenen 1 (neg. z) und 2 (pos.z)*********
0 0
******* Anzahl Auslaesse in xy-Ebenen 1 (neg. z) und 2 (pos.z)*********
0 1
Auslassnummer i,j,k - Koordinaten der Auslaesse in der xy-Ebene 2
1 2 77 2 48 101 101
******* Anzahl Einlaesse in xz-Ebenen 1 (neg. y) und 2 (pos. y)*********
96 96
Einlassnummer i,j,k - Koordinaten der Einlaesse in der xz-Ebene 1
101 11 11 2 2 24 27
101 12 13 2 2 24 24
101 14 14 2 2 24 27
101 12 13 2 2 27 27
401 10 10 2 2 23 28
401 11 14 2 2 23 23
401 15 15 2 2 23 28
401 11 14 2 2 28 28
402 29 29 2 2 23 28
402 24 24 2 2 23 28
102 28 28 2 2 24 27
102 25 25 2 2 24 27
402 25 28 2 2 23 23
102 26 27 2 2 24 24
402 25 28 2 2 28 28

102	26	27	2	2	27	27
403	55	55	2	2	23	28
403	50	50	2	2	23	28
103	54	54	2	2	24	27
103	51	51	2	2	24	27
403	51	54	2	2	23	23
103	52	53	2	2	24	24
403	51	54	2	2	28	28
103	52	53	2	2	27	27
404	69	69	2	2	23	28
404	64	64	2	2	23	28
104	68	68	2	2	24	27
104	65	65	2	2	24	27
404	65	68	2	2	23	23
104	66	67	2	2	24	24
404	65	68	2	2	28	28
104	66	67	2	2	27	27
204	65	65	2	2	42	45
204	68	68	2	2	42	45
504	64	64	2	2	41	46
504	69	69	2	2	41	46
203	51	51	2	2	42	45
203	54	54	2	2	42	45
503	50	50	2	2	41	46
503	55	55	2	2	41	46
202	25	25	2	2	42	45
202	28	28	2	2	42	45
502	24	24	2	2	41	46
502	29	29	2	2	41	46
501	15	15	2	2	41	46
501	10	10	2	2	41	46
201	14	14	2	2	42	45
201	11	11	2	2	42	45
202	26	27	2	2	42	42

502	25	28	2	2	41	41
501	11	14	2	2	41	41
201	12	13	2	2	42	42
204	66	67	2	2	42	42
504	65	68	2	2	41	41
203	52	53	2	2	42	42
503	51	54	2	2	41	41
202	26	27	2	2	45	45
502	25	28	2	2	46	46
501	11	14	2	2	46	46
201	12	13	2	2	45	45
204	66	67	2	2	45	45
504	65	68	2	2	46	46
203	52	53	2	2	45	45
503	51	54	2	2	46	46
304	65	65	2	2	61	64
304	68	68	2	2	61	64
604	64	64	2	2	60	65
604	69	69	2	2	60	65
303	51	51	2	2	61	64
303	54	54	2	2	61	64
603	50	50	2	2	60	65
603	55	55	2	2	60	65
302	25	25	2	2	61	64
302	28	28	2	2	61	64
602	24	24	2	2	60	65
602	29	29	2	2	60	65
601	15	15	2	2	60	65
601	10	10	2	2	60	65
301	14	14	2	2	61	64
301	11	11	2	2	61	64
302	26	27	2	2	61	61
602	25	28	2	2	60	60
601	11	14	2	2	60	60

301	12	13	2	2	61	61
304	66	67	2	2	61	61
604	65	68	2	2	60	60
303	52	53	2	2	61	61
603	51	54	2	2	60	60
302	26	27	2	2	64	64
602	25	28	2	2	65	65
601	11	14	2	2	65	65
301	12	13	2	2	64	64
304	66	67	2	2	64	64
604	65	68	2	2	65	65
303	52	53	2	2	64	64
603	51	54	2	2	65	65

Einlassnummer i,j,k - Koordinaten der Einlaesse in der xz-Ebene 2

307	26	27	48	48	61	61
307	28	28	48	48	61	64
307	26	27	48	48	64	64
307	25	25	48	48	61	64
308	14	14	48	48	6[illegible]	64
308	12	13	48	48	6[illegible]	61
308	12	13	48	48	64	64
308	11	11	48	48	61	64
207	28	28	48	48	42	45
207	26	27	48	48	42	42
207	25	25	48	48	42	45
207	26	27	48	48	45	45
208	14	14	48	48	42	45
208	12	13	48	48	42	42
208	11	11	48	48	42	45
208	12	13	48	48	45	45
107	28	28	48	48	24	27
107	26	27	48	48	24	24
107	26	27	48	48	27	27
107	25	25	48	48	24	27
108	12	13	48	48	27	27
108	12	13	48	48	24	24
108	14	14	48	48	24	27
108	11	11	48	48	24	27
305	68	68	48	48	61	64
305	66	67	48	48	61	61
305	65	65	48	48	61	64
305	66	67	48	48	64	64
306	52	53	48	48	61	61
306	54	54	48	48	61	64
306	51	51	48	48	61	64
306	52	53	48	48	64	64
205	68	68	48	48	42	45
205	66	67	48	48	42	42
205	65	65	48	48	42	45
205	66	67	48	48	45	45
206	54	54	48	48	42	45
206	52	53	48	48	42	42
206	52	53	48	48	45	45
206	51	51	48	48	42	45
105	68	68	48	48	24	27
105	66	67	48	48	24	24
105	65	65	48	48	24	27
105	66	67	48	48	27	27
106	52	53	48	48	24	24
106	54	54	48	48	24	27
106	51	51	48	48	24	27
106	52	53	48	48	27	27
405	69	69	48	48	23	28
405	64	64	48	48	23	28
406	50	50	48	48	23	28
406	55	55	48	48	23	28
407	24	24	48	48	23	28
407	29	29	48	48	23	28

```
408  15 15  48 48  23 28
408  10 10  48 48  23 28
407  25 28  48 48  23 23
408  11 14  48 48  23 23
405  65 68  48 48  23 23
406  51 54  48 48  23 23
407  25 28  48 48  28 28
408  11 14  48 48  28 28
405  65 68  48 48  28 28
406  51 54  48 48  28 28
505  64 64  48 48  41 46
505  69 69  48 48  41 46
506  50 50  48 48  41 46
506  55 55  48 48  41 46
508  10 10  48 48  41 46
508  15 15  48 48  41 46
508  11 14  48 48  41 41
505  65 68  48 48  41 41
506  51 54  48 48  41 41
508  11 14  48 48  46 46
505  65 68  48 48  46 46
506  51 54  48 48  46 46
605  64 64  48 48  60 65
605  69 69  48 48  60 65
606  50 50  48 48  60 65
606  55 55  48 48  60 65
607  29 29  48 48  60 65
607  24 24  48 48  60 65
608  10 10  48 48  60 65
608  15 15  48 48  60 65
607  25 28  48 48  60 60
608  11 14  48 48  60 60
605  65 68  48 48  60 60
606  51 54  48 48  60 60
605  65 68  48 48  65 65
606  51 54  48 48  65 65
607  25 28  48 48  65 65
608  11 14  48 48  65 65
507  24 24  48 48  41 46
507  29 29  48 48  41 46
507  25 28  48 48  41 41
507  25 28  48 48  46 46
******* Anzahl Auslaesse in xz-Ebenen 1 (neg. y) und 2 (pos.y)*********
 0   0
******* Anzahl Einlaesse in yz-Ebenen 1 (neg. x) und 2 (pos. x)*********
 0   0
******* Anzahl Auslaesse in yz-Ebenen 1 (neg. x) und 2 (pos.x)*********
 0   0
******* Anzahl period. Raender in xy-Ebene 1 (neg.y) und 2 (pos.y) **
 0   0
******* Anzahl period. Raender in xz-Ebene 1 (neg.y) und 2 (pos.y) **
 0   0
******* Anzahl period. Raender in yz-Ebene 1 (neg.x) und 2 (pos x) **
 0   0
******* min/max-Grenzen: Z-Linie, xmin, xmax, ymin, ymax
**************
 1  2 77  24 26
 2  2 77  24 26
 3  2 77  23 27
 4  2 77  22 28
 5  2 77  20 30
 6  2 77  19 31
 7  2 77  18 32
 8  2 77  17 33
 9  2 77  16 34
 10 2 77  15 35
 11 2 77  14 36
 12 2 77  13 37
```

```
 13  2 77  11 39
 14  2 77   8 42
 15  2 77   2 48
USW
WEITER
******** Ausblockierte Bereiche (0/1) = (nein/ja)
 1
 Ausblockierte Bereiche: x/y/z-Grenzen /xm...zpwas
(0=wand,1=einlass,2=auslass)
 999  2 77   2  4  15  22  0  0  0  0  0  0
 999  2 77   2  4  29  40  0  0  0  0  0  0
 999  2 77   2  4  47  59  0  0  0  0  0  0
 999  2 77   2  4  66 101  0  0  0  0  0  0
 999  2 77  46 48  15  22  0  0  0  0  0  0
 999  2 77  46 48  29  40  0  0  0  0  0  0
 999  2 77  46 48  47  59  0  0  0  0  0  0
 999  2 77  46 48  66 101  0  0  0  0  0  0
 999  2  9   2  4  15 101  0  0  0  0  0  0
 999 16 23   2  4  15 101  0  0  0  0  0  0
 999 30 49   2  4  15 101  0  0  0  0  0  0
 999 56 63   2  4  15 101  0  0  0  0  0  0
 999 70 77   2  4  15 101  0  0  0  0  0  0
 999  2  9  46 48  15 101  0  0  0  0  0  0
 999 16 23  46 48  15 101  0  0  0  0  0  0
 999 30 49  46 48  15 101  0  0  0  0  0  0
 999 56 63  46 48  15 101  0  0  0  0  0  0
 999 70 77  46 48  15 101  0  0  0  0  0  0
 999 39 40   2 48  15 101  0  0  0  0  0  0
 999  2 77   2  8  98 101  0  0  0  0  0  0
 999  2 77  12 14  98 101  0  0  0  0  0  0
 999  2 77  18 20  98 101  0  0  0  0  0  0
 999  2 77  24 26  98 101  0  0  0  0  0  0
 999  2 77  30 32  98 101  0  0  0  0  0  0
 999  2 77  36 38  98 101  0  0  0  0  0  0
 999  2 77  42 48  98 101  0  0  0  0  0  0
 999 38 41   2 48  98 101  0  0  0  0  0  0
ENDE
******** Einblockierte Bereiche (0/1) = (nein/ja)
 0
 Einblockierte Bereiche: x/y/z-Grenzen /xm...zpwas
(0=wand,1=einlass,2=auslass)
 6 13  8 11  3 21  0  0  0  0  0  0
 2  2  2  2  2 21  0  0  0  0  0  0
ENDE
 NUR 1 GITTER:DDM=0 ,GRUNDGITTER: DDM=GITTERANZAHL.
SUBDOMAIN: DDM = GITTERNR.
 0
```

Appendix 3.2

Definition of inlet conditions: margbl.f

FILE: margb1.f
Defines Inlet Conditions

```
C   I-------------------------------------------------------------------I
C   I       I                                I
C   I SR MARGB1  I Besetzt Brenner mit Eintrittswerten          I
C   I       I                                I
C   I-------------------------------------------------------------------I

      SUBROUTINE MARGB1 (U,V,W,TE,ED,VIS,RHO,F,H,T,G,CONC,SF  ',ZONC,RST
     &            ,GX,GY,GZ,PX,PY,PZ,PDX,PDY,PDZ,GDX,GDY,GDZ
     &            ,INLETS,NBCS,INLETSR)

C   I-----------------------------------------I
C   I  INPUT  : I
C   I  OUTPUT : I
C   I-----------------------------------------I
C   I              AUFRUF DURCH:               I
C   I-----------------------------------------I
C   I usrinp                                   I
C   I-----------------------------------------I

      INCLUDE 'CSDD.CMN'
      INCLUDE 'CARRAY.CMN'
      INCLUDE 'CBLANC.CMN'
      INCLUDE 'CCOMB.CMN'
      INCLUDE 'CDATA.CMN'
      INCLUDE 'CDECOL.CMN'
      INCLUDE 'CDIM.CMN'
      INCLUDE 'CGEO.CMN'
      INCLUDE 'COFFSET.CMN'
      INCLUDE 'CPCEG.CMN'
      INCLUDE 'CRADADD.CMN'
      INCLUDE 'CRADGEO.CMN'
      INCLUDE 'CSTEUER.CMN'


      DIMENSION U(INPD,JNPD,KNPD),V(INPD,JNPD,KNPD),W(INPD,JNPD,KNPD)
      DIMENSION TE(INPD,JNPD,KNPD),ED(INPD JNPD,KNPD)
     &     ,VIS(INPD,JNPD,KNPD)
      DIMENSION RHO(INPD,JNPD,KNPD),F(INPD,JNPD,KNPD),G(INPD,JNPD,KNPD)
      DIMENSION H(INPD,JNPD,KNPD),T(INPD,JNPD,KNPD)
      DIMENSION CONC(INPD,JNPD,KNPD,*),SKAI (INPD,JNPD,KNPD,9)
     &     ,ZONC(INPD,JNPD,KNPD,4)
     &     ,RST(INPD,JNPD,KNPD,6)

      DIMENSION GX(0:INPD),GY(0:JNPD),GZ(0:KNPD)
     &     ,PX(INPD-2),PY(JNPD-2),PZ(KNPD-2)
      DIMENSION PDX(INPD,JNPD,KNPD),PDY(INPD,JNPD,KNPD)
     &     ,PDZ(INPD,JNPD,KNPD)
      DIMENSION GDX(INPD,JNPD,KNPD),GDY(INPD,JNPD,KNPD)
     &     ,GDZ(INPD,JNPD,KNPD)

      DIMENSION INLETS(NBCS),INLETSR(NBCSR)

      PARAMETER (MAXDAT=999)

      DIMENSION UDAT(MAXDAT),VDAT(MAXDAT),WDAT(MAXDAT)
      DIMENSION RHODAT(MAXDAT),FDAT(MAXDAT),TDAT(MAXDAT)
      DIMENSION CDAT(MAXDAT,15)
      DIMENSION DHYD(MAXDAT),TURINL(MAXDAT)
      DIMENSION DRALL(MAXDAT)


      IDEBUG = 0

      NIJ = INPD*JNPD

      N_BRENNER = 24


      PI = 4. * ATAN(1.)


      GMPRK = 27.103/20  ! Gesamt-Massenstrom Brennstoff
      GMPPL = 48.659/20  ! Gesamt-Massenstrom Primaerluft
      GMPSL = 178.775/20 ! Gesamt-Massenstrom Sekundearluft

      BEDARF  = SUMLB * GMPRK * 0.233
      ANGEBOT = (GMPPL + GMPSL)*0.233
      QUOTE   = ANGEBOT/BEDARF

      AREASL = 0.2677  ! Sekundaerluft Eintrittsflaeche pro Ringspalt
      AREAPL = 0.1564  ! Primaerluft " "


       TPL =  80. + TREF
       TSL =  248. + TREF
       TWAND = 670. + TREF
```

```
      RHOSL = PREF/(288.*TSL)

CNE   Alle Groessen (ausser C) aller Einlaesse nullen
      DO I=1,MAXDAT
       UDAT(I)  = 0.0
       VDAT(I)  = 0.0
       WDAT(I)  = 0.0
       FDAT(I)  = 0.0
       TDAT(I)  = 0.0
       DHYD(I)  = 0.0
       TURINL(I) = 0.0
      ENDDO

CNE   Alle Einlasszellen mit Luft belegen
      DO I=1,MAXDAT
       CDAT(I,ISCOAL) = 0.
       CDAT(I,ISCHAR) = 0.
       CDAT(I,ISCH)  = 0.
       CDAT(I,ISO2)  = 0.233
       CDAT(I,ISCO2) = 0.
       CDAT(I,ISH2O) = 0.
       CDAT(I,ISCO)  = 0.
       CDAT(I,ISASH) = 0.
       CDAT(I,ISN2)  = 1.0 - CDAT(I,ISCOAL) - CDAT(I,ISCHAR)
     &               - CDAT(I,ISCH) - CDAT(I,ISO2) - CDAT(I,ISCO2)
     &               - CDAT(I,ISH2O) - CDAT(I,ISCO)
     &               - CDAT(I,ISASH)
      ENDDO

CNE   Brenner Primaereinlaesse in Betrieb
CNE   ====================================

      DO J=1,N_BRENNER

            IF (J.EQ.1) I = 101
       IF (J.EQ.2) I = 102
       IF (J.EQ.3) I = 103
       IF (J.EQ.4) I = 104
       IF (J.EQ.5) I = 201
       IF (J.EQ.6) I = 202
       IF (J.EQ.7) I = 203
       IF (J.EQ.8) I = 204
       IF (J.EQ.9) I = 301
       IF (J.EQ.10) I = 302
       IF (J.EQ.11) I = 303
       IF (J.EQ.12) I = 304
       IF (J.EQ.13) I = 105
       IF (J.EQ.14) I = 106
       IF (J.EQ.15) I = 107
       IF (J.EQ.16) I = 108
       IF (J.EQ.17) I = 205
       IF (J.EQ.18) I = 206
       IF (J.EQ.19) I = 207
       IF (J.EQ.20) I = 208
       IF (J.EQ.21) I = 305
       IF (J.EQ.22) I = 306
       IF (J.EQ.23) I = 307
       IF (J.EQ.24) I = 308

       FAKON = 1.        !definiert ob Brenner in Betrieb sind

       IF (J.GT.20) FAKON = 0.0


       CDAT(I,ISCOAL) = FAKON*GMPRK/(GMPRK+GMPPL)*BCUB
       CDAT(I,ISCHAR) = 0.
       CDAT(I,ISCH)  = 0.
       CDAT(I,ISO2)  = FAKON*GMPPL/(GMPRK+GMPPL)*0.233
       CDAT(I,ISCO2) = 0.
       CDAT(I,ISH2O) = FAKON*GMPRK/(GMPRK+GMPPL)*XSIF
       CDAT(I,ISCO)  = 0.
       CDAT(I,ISASH) = FAKON*GMPRK/(GMPRK+GMPPL)*XSIA
       CDAT(I,ISN2)  = FAKON*(1.0 - CDAT(I,ISCOAL) - CDAT(I,ISCHAR)
     &               - CDAT(I,ISCH) - CDAT(I,ISO2) - CDAT(I,ISCO2)
     &               - CDAT(I,ISH2O) - CDAT(I,ISCO)
     &               - CDAT(I,ISASH))

       FAK = 1.
       IF (J.GT.12) FAK = -1.

       UDAT(I) = 0.
       VDAT(I) = FAKON*FAK*(GMPPL*288.0+GMPRK*XSIF*RALLG/WMH2O)*TPL
     &         / (FREE*AREAPL)
       WDAT(I) = 0.
       IF (J.LE.20) RHODAT(I) = FAKON*(GMPRK + GMPPL)
     &                / (ABS(VDAT(I)) * AREAPL)
       FDAT(I)  = FAKON*1.0
       IF (FAKON.EQ.1.0) THEN
        TDAT(I) = TPL
       ELSE
```

```
      TDAT(I)  = TWAND
     ENDIF
     DHYD(I)  = FAKON*0.1808
     TURINL(I) = FAKON * 0.07
     VANEP = 0.       ! 'Schaufelstellung Primaerluft'
     DP   = 0.90      ! 'Druckverlust' Drallschaufeln bis Muffel
     DRALL(I) = DP * TAN(VANEP*PI/180)
    ENDDO

CNE    BRENNER SEKUNDAEREINLAESSE
CNE    ========================== ===
     DO J=1,N_BRENNER
      IF (J.EQ. 1) I = 401
      IF (J.EQ. 2) I = 402
      IF (J.EQ. 3) I = 403
      IF (J.EQ. 4) I = 404
      IF (J.EQ. 5) I = 501
      IF (J.EQ. 6) I = 502
      IF (J.EQ. 7) I = 503
      IF (J.EQ. 8) I = 504
      IF (J.EQ. 9) I = 601
      IF (J.EQ.10) I = 602
      IF (J.EQ.11) I = 603
      IF (J.EQ.12) I = 604
      IF (J.EQ.13) I = 405
      IF (J.EQ.14) I = 406
      IF (J.EQ.15) I = 407
      IF (J.EQ.16) I = 408
      IF (J.EQ.17) I = 505
      IF (J.EQ.18) I = 506
      IF (J.EQ.19) I = 507
      IF (J.EQ.20) I = 508
      IF (J.EQ.21) I = 605
      IF (J.EQ.22) I = 606
      IF (J.EQ.23) I = 607
      IF (J.EQ.24) I = 608

      FAKON = 1.          !definiert ob Brenner in Betrieb sind

      IF (J.GT.20) FAKON = 0.0


     FAK = 1.
     IF (J.GT.12) FAK = -1.

      UDAT(I) = 0.
      VDAT(I) = FAKON * FAK * GMPSL /(RHOSL*AREASL)
      WDAT(I) = 0.
      RHODAT(I) = FAKON * RHOSL
      FDAT(I) = 0.
      IF (FAKON.EQ.1.0) THEN
       TDAT(I) = TSL
      ELSE
       TDAT(I) = TWAND
      ENDIF
      DHYD(I) = FAKON* 0.2127
      TURINL(I) = FAKON * 0.07
      VANEM = 45.      ! 'Schaufelstellung Mantelluft
      DP   = 0.90      ! 'Druckverlust' Drallschaufeln bis Muffel
      DRALL(I) = DP * TAN(VANEM*PI/180)

     ENDDO



    NR = 0



    DO JDO=7,12
CDIRS JVDEP
     DO IDO=IPTD(JDO),IPTD(JDO+1)-1
      INC = JA(IDXBCSD+IDO-1)
      INC = INC + NND(JDO)
      K  = INT((INC-1)/NIJ)+1
      J  = INT((INC-1-(K-1)*NIJ)/NPD)+1
      I  = INC-(J-1)*INPD-(K-1)*NIJ


      NR  = NR +1
      NGRP = INLETS(NR)
      V(I,J,K)  =  VDAT(NGRP) ! fuer Brenner in der i-Ebene

      IF (K.LT.29.AND.ISDD.EQ.1) THEN
      ZMITTE = 8.9750
      ELSEIF (K.LT.51.AND.ISDD.EQ.1) THEN
       ZMITTE = 12.9750
      ELSEIF (ISDD.EQ.1) THEN
       ZMITTE = 16.9750
      ENDIF
```

```
IF (ISDD.EQ.2) THEN
 ZMITTE = 8.9750
ELSEIF (ISDD.EQ.3) THEN
 ZMITTE = 12.9750
ELSEIF (ISDD.EQ.4) THEN
 ZMITTE = 16.9750
ENDIF
BDZ = GZ(K) - ZMITTE - GDZ(I,J,K)/2

IF (I.LT.20.AND.ISDD.EQ.1) THEN
 XMITTE = 2.4375
 FAK = 1
ELSEIF (I.LT.30.AND.ISDD.EQ.1) THEN
 XMITTE = 4.9125
 FAK = -1
ELSEIF (I.LT.60.AND.ISDD.EQ.1) THEN
 XMITTE = 9.8625
 FAK = 1
ELSEIF (ISDD.EQ.1) THEN
 XMITTE = 12.3375
 FAK = -1
ENDIF
IF (I.LT.30.AND.ISDD.GT.1) THEN
 XMITTE = 2.4375
 FAK = 1
ELSEIF (ISDD.GT.1) THEN
 XMITTE = 4.9125
 FAK = -1
ENDIF
BDX = GX(I) - XMITTE - GDX(I,J,K)/2

BETA = ATAN2 (BDX,BDZ)
U(I,J,K)  =  ABS(V(I,J,K)) * COS(BETA) * DRALL(NGRP) * FAK
W(I,J,K)  = -ABS(V(I,J,K)) * SIN(BETA) * DRALL(NGRP) * FAK

VEL = SQRT( U(I,J,K)**2 + V(I,J,K)**2 + W(I,J,K)**2 )


RHO(I,J,K) =  RHODAT(NGRP)
T(I,J,K)   =  TDAT(NGRP)
IF(LOCD(FF)) F(I,J,K) = FDAT(NGRP)

IF(LPROP) THEN
 CONC(I,J,K,ISCOAL) = CDAT(NGRP,ISCOAL)
 CONC(I,J,K,ISCHAR) = CDAT(NGRP,ISCHAR)
 DO JC = 1,NCHAR
  CONC(I,J,K,ISCHAR+JC) = WSIZE(JC)*CDAT(NGRP,ISCHAR)
 ENDDO
 CONC(I,J,K,ISCH)  = CDAT(NGRP,ISCH)
 CONC(I,J,K,ISO2)  = CDAT(NGRP,ISO2)
 CONC(I,J,K,ISCO2) = CDAT(NGRP,ISCO2)
 CONC(I,J,K,ISH2O) = CDAT(NGRP,ISH2O)
 CONC(I,J,K,ISN2)  = CDAT(NGRP,ISN2)
 CONC(I,J,K,ISH2)  = CDAT(NGRP,ISH2)
 CONC(I,J,K,ISCO)  = CDAT(NGRP,ISCO)
 CONC(I,J,K,ISASH) = CDAT(NGRP,ISASH)
 CALL STOFAK(INC,T(I,J,K),CONC,CP,CP0)
 H(I,J,K) = CP*T(I,J,K) - CP0*TREF
ENDIF


IF(LOCD(KK).AND.(VEL.GT.0.)) THEN
 TEDUM     = 1.5*(TURINI(NGRP) * VEL)**2
 EDDUM     = (CMUE*34*TEDUM**1.5)/(0.03*DHYD(NGRP)/2.)
 TE(I,J,K)  = TEDUM
 ED(I,J,K)  = EDDUM
 VIS(I,J,K) = CMUE*RHO(I,J,K)*TEDUM**2/EDDUM + RMUE
 IF (NTURBD.GE.2) THEN
  RST(I,J,K,1) = 2./3.*TE(I,J,K)
  RST(I,J,K,2) = 2./3.*TE(I,J,K)
  RST(I,J,K,3) = 2./3.*TE(I,J,K)
  RST(I,J,K,4) = 0.
  RST(I,J,K,5) = 0.
  RST(I,J,K,6) = 0.
 ENDIF
ELSE
 VIS(I,J,K) = 7.3E-03
ENDIF

 ENDDO
ENDDO


CBR ------------------------
CBR  Einlasstemperatur im Strahlungsgitter
CBR ------------------------
   IF (ISDD.EQ.1.AND.LDD) THEN
C  .AND.LRAYD) THEN
    NR = 0
```

```
      DO JDO=7,12
CDIR$ IVDEP
        DO IDO=IPTR(JDO),IPTR(JDO+1)-1
         INC = JA(IDXBCSR+IDO-1)
         INC = INC + NNR(JDO)
         K   = INT((INC-1)/NIJ)+1
         J   = INT((INC-1-(K-1)*NIJ)/INPD)+1
         I   = INC-(J-1)*INPD-(K-1)*NIJ


         NR  = NR +1
         NGRP = INLETSR(NR)

         T(I,J,K)  = TDAT(NGRP)
        ENDDO
       ENDDO
      ENDIF



      IF(IDEBUG.EQ.1)THEN
       WRITE(31,10) ( (U(I,1,K) ,I=2,20) ,K=7,21 )
       WRITE(32,10) ( (U(I,1,K) ,I=21,39) ,K=7,21 )
       WRITE(33,10) ( (W(I,1,K) ,I=2,20) ,K=7,21 )
       WRITE(34,10) ( (W(I,1,K) ,I=21,39) ,K=7,21 )
   10  FORMAT(19(F6.2,2X))
      ENDIF


      END
```

Appendix 3.3

Coal parameters: Composition, pyrolysis and combustion kinetics: combdat.f

FILE: combdat.f

Coal Parameters (compasition, pyrolysis and combustion kinetics)

```
C  I=============================================================I
C  I      I                          I
C  I SR COMBDAT I Parameter der Kohleverbrennung          I
C  I      I                          I
C  I=============================================================I

   SUBROUTINE COMBDAT

C  I-------------------------------------I
C  I            AUFRUF DURCH:            I
C  I-------------------------------------I
C  I  usrinp                            I
C  I-------------------------------------I

   INCLUDE 'CSDD.CMN'
   INCLUDE 'CARRAY.CMN'
   INCLUDE 'CCOMB.CMN'
   INCLUDE 'CSTEUER.CMN'



C  ---------------------
CCM  Berechnung der Fluechtigenzusammensetzung
C  ---------------------

CCM  Formel des Kohlenwasserstoffes
CNE  Chemical Formula of hydrocarbon
CCM  ---------------
   DATA  RNCX  / 1.0 /
   DATA  RNHY  / 2.0 /

   WMCXHY = RNCX*WMC + RNHY*WMH2/2.


   IF (LCOAL) THEN

CRS  Heizwerte [J/kg]
CNE      Calorific Value (daf - derive from gross cal. value)
CRS  ---------------------
     DATA      HUDAF
    &      / 32188782. /
```

```
CRS  Fluechtige laut Analyse (waf)
CNE      Volatile Matter Content (daf) according to DTF Analysis
CRS  ---------------------
     VMDAFA = 0.356725*1.226

CCM  Elementaranalyse (roh : ! ! )
CNE      Elemental Analysis (as received)
C  ---------------
     XSIC = 0.5247
     XSIO = 0.0601                    !O
     XSIH = 0.0312                    !H
     XSIS = 0.0078                    !S
     XSIN = 0.0131                    !N
     XSIA = 0.2762          !Ash
     XSIF = 0.08696                   !total Moisture

   ELSE
     VMDAFA = 1.0

     XSIC = WMC/WMCXHY
     XSIO = 0.
     XSIH = 2.*WMH2/WMCXHY
     xSIS = 0.
     XSIN = 0.
     XSIA = 0.                  ! Asche
     XSIF = 0.                  ! Feuchte

   ENDIF

   CHK  =  XSIC + XSIO + XSIH + XSIS + XSIN + XSIA + XSIF



   IF(CHK.NE.1.)THEN
    WRITE(*,*) ' >>> COMBDAT <<< '
    WRITE(*,*) ' Summation der Elementaranalyse ungleich 1 '
    WRITE(*,*) ' Summe :',CHK
    WRITE(*,*) ''
   ENDIF


CRS  Bezug auf System ohne Schwefel und Stickstoff
CNE  Recalc of Ultimate Elemental Analysis on a N and S free basis
CRS  ---------------------
```

```
      XSIC = XSIC + XSIS + XSIN
      XSIH = XSIH
      XSIA = XSIA
      XSIF = XSIF
      XSIO = XSIO


CRS   brennbare Substanz
CNE   combustible matter
CRS   ----------
      BSUB = 1. - XSIA - XSIF


CCM   Umrechnung der Elementaranalyse auf DAF (entspricht waf)
CNE   Recalc of Ultimate/Elemental on an daf basis
C     ----------
      SUMVM  = XSIC + XSIH + XSIO
      XSICDAF = XSIC / SUMVM
      XSIHDAF = XSIH / SUMVM
      XSIODAF = XSIO / SUMVM


CCM   minimal bzw maximal moeglicher Fluechtigenanteil (waf)
CNE   possible max/min volatile matter contents on daf basis
CCM       !!  ggf. Anpassung vom VMDAF  !!
CCM   ----------
      VMCH4 = XSIODAF + XSIHDAF
     &      + ( WMC/(0.5*WMO2) ) * XSIODAF
     &      - ( WMC/WMH2 ) * XSIHDAF

      VMCO  = VMCH4
     &      - ( WMH2/(0.5*WMO2) * XSIODAF - XSIHDAF )
     &        * WMC/(0.5*WMH2)*(RNCX + RNHY/2.)/RNHY

      VMH2O = VMCH4
     &      - ( WMC/(0.5*WMH2) ) * XSIHDAF * (RNCX + RNHY/2.)/RNHY

      VMMIN = MAX(VMCH4,VMCO)
      VMMAX = VMH2O

      VMDAF = MAX(VMMIN,VMDAFA)
      VMDAF = MIN(VMMAX,VMDAF)


CCM   C, H, O in Fluechtigen
CNE   C, H, O contant in volatile matter
CCM   ----------
      XSICVM = ( VMDAF - XSIHDAF - XSIODAF ) / VMDAF
      XSIHVM = XSIHDAF / VMDAF
      XSIOVM = XSIODAF / VMDAF


      IF (LCOAL) THEN
       CXHYNU1 = ( XSICVM/WMC - XSIOVM/(0.5*WMO2) + XSIHVM/WMH2 )
     &         * ( WMCXHY / (RNCX + RNHY/2.) )

       H2ONU1  = ( XSIHVM/WMH2 - (RNHY/2.)*(CXHYNU1/WMCXHY) ) * WMH2O

       CONU1   = 1.0 - CXHYNU1 - H2ONU1


       RN1RK   = -1.0
       RN1C    = 1. - VMDAF
       RN1CO   = CONU1 * VMDAF
       RN1H2O  = H2ONU1 * VMDAF
       RN1CH4  = CXHYNU1 * VMDAF

       RN1VM   = VMDAF


CRS   ----------
CRS   massenbezogene stoechiometrische Koeffizienten
CNE   mass related stoichiometric coefficients
CRS   ----------
      DATA  RN2C  , RN2O2 , RN2CO
     &    / -0.42857 , -0.57143 ,  1. /
      DATA  RN4CO , RN4O2 , RN4CO2
     &    / -0.63636 , -0.36364 ,  1. /
      DATA  RN5H2 , RN5O2 , RN5H2O
     &    / -0.1119 , -0.8881 ,  1. /

CNE   Kinetics of Devolatilisation
c_standard_ivd      DATA RK01,E1R     / 1.5E05 , 8900. /
      DATA RK01,E1R     / 1.5E05 , 8900. /
cNE         Kinetics of Char Combustion
c_standard_ivd      DATA RK02,E2R     /  208. , 9553. /
      DATA RK02,E2R     /  271. , 12817. /
CNE         Diffusion Constant
```

```
      DATA DO2REF       / 3.49E-04 /
      DATA FMP          / 0.875 /
      DATA RHOS0        / 1609. /

CCM   NCHAR Einfuehrung
      PHO_CA0 = RHOS0*(RN1C*(1.-XSIA-XSIF)+XSIA)
CSR   Faktor fuer Koksmodell (vgl.combcoal.f)
      RKASH = BSUB/XSIA

      DATA NCHAR   /3/
      DATA WSIZE(1) /0.3/
      DATA WSIZE(2) /0.4/
      DATA WSIZE(3) /0.3/
      DATA DPJJ(1)  /50.E-06/
      DATA DPJJ(2)  /50.E-06/
      DATA DPJJ(3)  /50.E-06/


      IF(NCHAR.GT.3) STOP 'NCHAR > 3 !!!!!! COMBDAT STOP'

CCM   Kohleparameter
CRS   ----------
      DATA RN_B   /0.67/ ! Ausbrandexponent (1-Bca)**n_B


CRS   ----------
CRS   Heizwerte [J/kg]
CRS   ----------
      HUCH4 = HUDAF - RN1CO*HUCO
     &      - (XSICDAF - (VMDAF-XSIHDAF-XSIODAF))*HUKOKS
      HUCH4 = HUCH4/RN1CH4
      HUR2  = HUKOKS - HUCO*WMCO/WMC
      HUR3  = HUCH4 - HUCO*RNCX*WMCO/WMCXHY
      HUR4  = HUCO


    ELSE
      RN1RK  = 0.
      RN1C   = 0.
      RN1CO  = 0.
      RN1H2O = 0.
      RN1CH4 = 0.

      RN2C   = 0.
      RN2O2  = 0.
      RN2CO  = 0.

CRS   ----------
CRS   Heizwerte [J/kg]
CRS   ----------
      HUR2  = 0.
      HUR3  = HUCH4-HUCO*RNCX*WMCO/WMCXHY  ! HUCH4 - HUCO*28/16
      HUR4  = HUCO

    ENDIF



cRS   ----------
CRS   spezifischer Luftbedarf (nur Info)
CRS   ----------
      CBO2 = XSIC * WMO2/WMC
      HBO2 = XSIH * WMO2/(2.*WMH2)

      SUMBO2 = CBO2 + HBO2 - XSIO
      SUMLB = SUMBO2 / 0.233


CCM   ----------
CCM   EDC-Modell
CCM   ----------

CCM   FUEL/AIR RATIO Reaktion von CxHy,CO,H2
CRS   ----------

CRS   stoech. Koeff. fuer CxHy vollstaendig bis zu CO2 + H2O
      ZAE3   =  WMCXHY + (RNCX+RNHY/4.)*WMO2
      RN3CXHYVOLL = - WMCXHY / ZAE3
      RN3O2VOLL  = -(RNCX+RNHY/4.)*WMO2 / ZAE3

      RFU3 = ABS(RN3O2VOLL/RN3CXHYVOLL)
      RFU4 = ABS(RN4O2/RN4CO)
      RFU5 = ABS(RN5O2/RN5H2)


      END
```

```
      XSIC = XSI
      XSIH = XSI
      XSIA = XSI
      XSIF = XSI
      XSIO = XSI

CRS  brennbare
CNE  combustil
CRS  ----------
      BSUB = 1.-

CCM  Umrechn
CNE  Recale of
C    ----------
      SUMVM  =
      XSICDAF =
      XSIHDAF =
      XSIODAF =

CCM  minimal
CNE  possible n
CCM       ! f  g
CCM  ----------
      VMCH4 = X
     &    +( WM
     &    -( WM

      VMCO = V
     &    -( WM
     &     * WM

      VMH2O = V
     &    +( WM

      VM
      VM

      VMDA
      VMD
```

```
      DATA DO2REF      / 3.49E-04 /
      DATA FMP         / 0.875 /
      DATA RHOS0       / 1609. /

CCM   NCHAR Einfuehrung
      RHO_CA0 = RHOS0*(RN1C*(1.-XSIA-XSIF)+XSIA)
CSR   Faktor fuer Koksmodell (vgl.combcoal.f)
      RKASH = BSUB/XSIA

      DATA NCHAR   /3/
      DATA WSIZE(1) /0.3/
      DATA WSIZE(2) /0.4/
      DATA WSIZE(3) /0.3/
      DATA DPJJ(1)  /30.E-06/
      DATA DPJJ(2)  /50.E-06/
      DATA DPJJ(3)  /50.E-06

      IF(NCHAR.GT.3) STOP 'NCHAR > 3 !!!!!! COMBDAT STOP'

CCM   Kohleparameter
CRS   ----------
      DATA  RN_B   /0.67/ ! Ausbrandexponent (1-Bu)**n_B

CRS   ----------
CRS   Heizwerte [J/kg]
CRS   ----------
      HUCH4 = HUDAF - RN1CO*HUCO
     &      - (XSICDAF - (VMDAF-XSIHDAF-XSIODAF))*HUKOKS
      HUCH4 = HUCH4/RN1CH4
      HUR2  = HUKOKS - HUCO*WMCO/WMC
      HUR3  = HUCH4 - HUCO*RNCX*WMCO/WMCXHY
      HUR4  = HUCO


    ELSE
      RN1RK  = 0.
      RN1C   = 0.
      RN1CO  = 0.
      RN1H2O = 0.
      RN1CH4 = 0.

      RN2C   = 0.
      RN2O2  = 0.
      RN2CO  = 0.

CRS   ----------
CRS   Heizwerte [J/kg]
CRS   ----------
      HUR2 = 0.
      HUR3  = HUCH4-HUCO*RNCX*WMCO/WMCXE  ' ! HUCH4 - HUCO*28/16
      HUR4  = HUCO

    ENDIF


cRS   ----------
CRS   spezifischer Luftbedarf (nur Info)
CRS   ----------
      CBO2 = XSIC * WMO2/WMC
      HBO2 = XSIH * WMO2/(2.*WMH2)

      SUMBO2 = CBO2 + HBO2 - XSIO
      SUMLB = SUMBO2 / 0.233


CCM   ----------
CCM   EDC-Modell
CCM   ----------

CCM   FUEL/AIR RATIO Reaktion von CxHy,CO,H2
CRS   ----------

CRS   stoech. Koeff. fuer CxHy vollstaendig bis zu CO2 + H2O
      ZAE3   =  WMCXHY + (RNCX+RNHY/4.)*WMO2
      RN3CXHYVOLL = - WMCXHY / ZAE3
      RN3O2VOLL  = -(RNCX+RNHY/4.)*WMO2 / ZAE3

      RFU3 = ABS(RN3O2VOLL/RN3CXHYVOLL)
      RFU4 = ABS(RN4O2/RN4CO)
      RFU5 = ABS(RN5O2/RN5H2)


      END
```

Appendix 3.4

Specification for the NOx model: nodat. f

FILE: nodat.f
Specifications for the NOx model

```
C  I=================================================================I
C  I      I                              I
C  I SR NODAT  I Parameter der Kohleverbrennung          I
C  I      I                              I
C  I=================================================================I

   SUBROUTINE NODAT

C  I-------------------------------------I
C  I          AUFRUF DURCH:              I
C  I-------------------------------------I
C  I usrinp                              I
C  I-------------------------------------I

   INCLUDE 'CSDD.CMN'
   INCLUDE 'CARRAY.CMN'
   INCLUDE 'CCOMB.CMN'
   INCLUDE 'CSTEUER.CMN'


CCM ***************************************************
CCM            NO-Modell
CCM ***************************************************
CCM  --------
CCM  NO Parameter
CCM  --------
     DATA  XSINDAF  ! N-Gehalt der Kohle
    &    / 0.0199 /

CCM  Anteil der Kohle-N Freisetzung
CCM       Pyrolyse , Koksabbrand , nicht verwendet/
     DATA  RL1HCN   , RL2HCN    , RL3HCN   ! %N von Nges als HCN ueber
    &    / 0.54   , 0.46    , 0.00  / ! RLx austretend


CCM  ------------------------------------
CCM  1 = orginal DeSoete- Modell nach Schnell
CCM  2 = neues Reburn-NO-Modell von C. Magel
CCM  ------------------------------------
     NO_MODEL = 1

CCM  ------------------------------------
CCM  Berechnung von NO Konstanten fuer Quellentermbestimmung
CCM  ------------------------------------
CCM  XSINDAF schon von Kohle daf
     RN1HCN =  1.0      *RL1HCN*XSINDAF/ 1.0      *27./14.
     RN2HCN = ABS(RN2C)  *RL2HCN*XSINDAF/ABS(RN1C)  *27./14.
     RN3HCN = 0.0 !ABS(RN3CH4) *RL3HCN*XSINDAF/ABS(RN1CH4)*27./14.


CCM  ----------
CCM  Felder ausnullen
CCM  ----------
     DO NMF=1,NCNOMAX
      DO NRL=1,NRLNOMAX
       VNO(NMF,NRL,1)=0.0
       VNO(NMF,NRL,2)=0.0
      ENDDO
      DO NRL=1,6
       VNOSRC(NMF,NRL)=0.0
      ENDDO
     ENDDO

CCM  ------------------------
     IF(NO_MODEL.EQ. 1 )THEN
CCM  ------------------------
CCM  ------------------------
CCM  orginal DeSoete- Modell nach Schnell
CCM  Z2 = HCN
CCM  Z3 = NO gesamt
CCM  Z4 = NO thermisch  Kontrollgroesse
CCM  ------------------------
     VNOSRC(1,1) = RN1HCN
CCM  KOKS-N
     VNOSRC(1,2) = RN2HCN * 1.0          ! als HCN
     VNOSRC(2,2) = RN2HCN * 0.0  *30./27.  ! als NO


     VNO(1,2,2) = -1.
     VNO(1,3,2) = -1.
     VNO(2,2,1) =  30./27.
     VNO(2,3,2) =  -30./27.
     VNO(2,4,1) =  1.
     VNO(3,4,1) =  1.
```

```
      ELSEIF(NO_MODEL.EQ.2)THEN
CCM   neues Rebum-Modell C. Mügel
CCM   /2  HCN
CCM   /3  NO gesamt
CCM   /4
CCM   ------------------------
      VNOSRC(1,1)  RN1HCN
      VNOSRC(1,2)  RN2HCN*0.3
      VNOSRC(2,2)  RN2HCN*0.2*30./27.

CCM   -- HCN ------
      VNO(1,1,2)  -1.   !! Oxidation Mitchell
      VNO(1,4,1) = 1.   !! Reburning Wei Rate
C     VNO(1,6,1) = 27./30.!! Reburning proportional zu RI.3 (C. Mügel)

CCM   -- NO --------
      VNO(2,2,1)  30./17.  !! Oxidation
      VNO(2,3,2) = -30./17  !! Reduktion
      VNO(2,4,2)  -30./27.  !! Reburning Wei Rate
      VNO(2,6,2)  -1.       !! Reburning proportional zu RI.3 (C. Mügel)
      VNO(2,5,2)  -1.       !! Charreduktion Levy Rate

CCM   -- NH3 --------
      VNO(3,1,1)  17./27.
      VNO(3,2,2) = -1
      VNO(3,3,2)  -1

      ENDIF

      RETURN
      END
```

Author: Eichhorn, Niels Wilhelm.
Name of thesis: Combustion modelling of pulverised coal boiler furnaces fuelled with Eskom Coals.

PUBLISHER:
University of the Witwatersrand, Johannesburg
©2015

LEGALNOTICES:

Copyright Notice: All materials on the University of the Witwatersrand, Johannesburg Library website are protected by South African copyright law and may not be distributed, transmitted, displayed or otherwise published in any format, without the prior written permission of the copyright owner.

Disclaimer and Terms of Use: Provided that you maintain all copyright and other notices contained therein, you may download material (one machine readable copy and one print copy per page)for your personal and/or educational non-commercial use only.

The University of the Witwatersrand, Johannesburg, is not responsible for any errors or omissions and excludes any and all liability for any errors in or omissions from the information on the Library website.